2024 Neutron Scattering Principal Investigator's Meeting

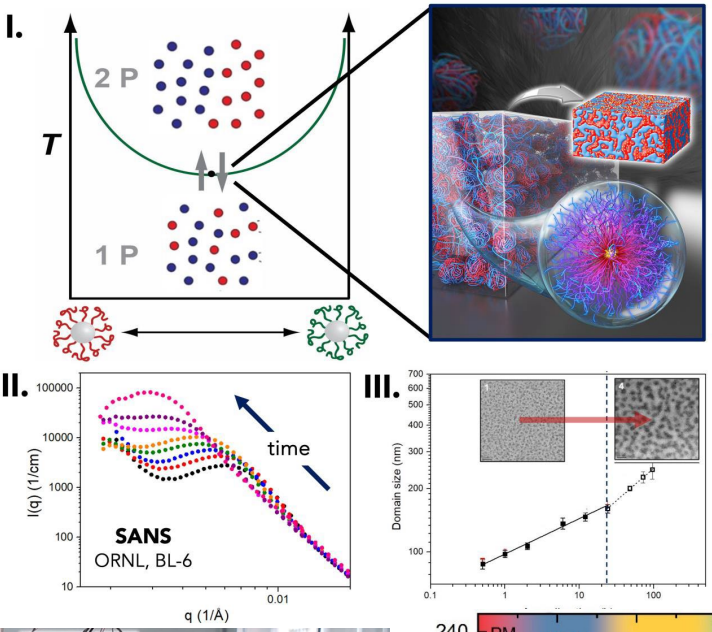

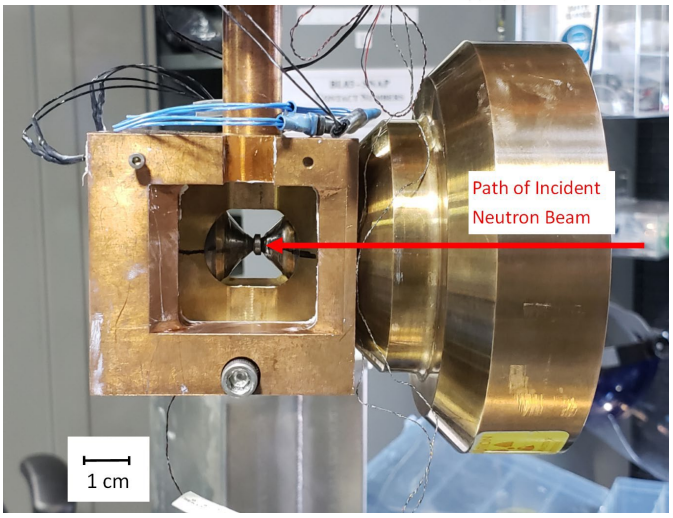

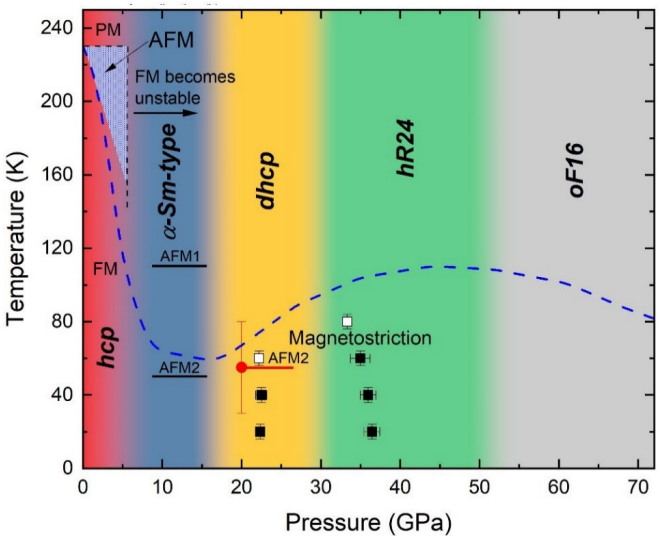

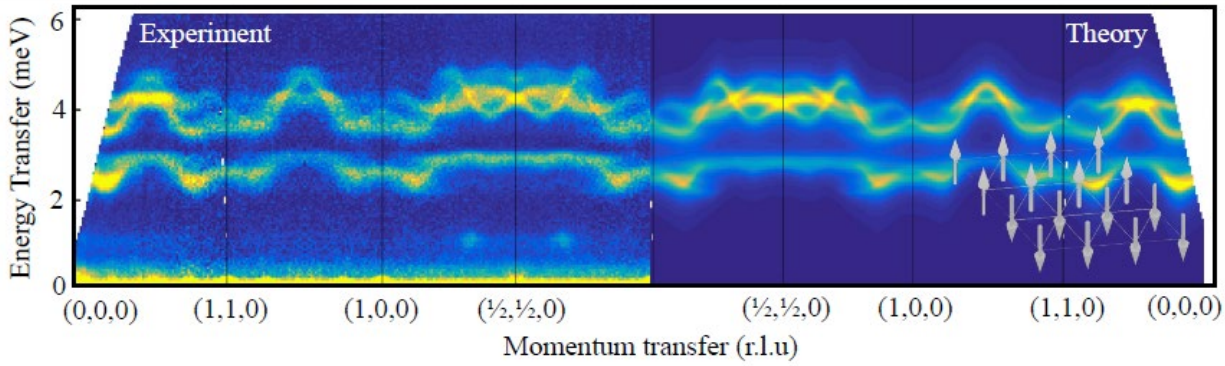

Top:
Autonomous organization of nanoparticle superlattice structures features anomalous diffusion behavior (I) Illustration of mixture of polymer-modified (aka 'brush') nanoparticles undergoing autonomous organization into microdomain structure. Interactions between polymer ligands at T > LCST drives autonomous self-assembly into bicontinuous superstructure. (II) Small angle neutron scattering (SANS) curves at distinct time of self-assembly. Peak position indicates characteristic length-scale of domain superstructure. (III) Plot of domain growth kinetics. Change in slope (i.e., scaling coefficients) reveal that initial separation follows anomalous growth kinetics.
Figure courtesy of M.R. Bockstaller, K. Matyjaszewski and A. Karim

Middle:
(Left) Large volume diamond anvil cell for ultrahigh pressure and low temperatures studies at the SNAP beamline at the Spallation Neutron Source, Oak Ridge National Laboratory. (Right) Magnetic phase diagram of heavy lanthanide element Terbium (Tb) based on neutron diffraction studies. Crystal structures and magnetic phases are indicated in this Pressure-Temperature diagram. Results published in the Journal of Magnetism and Magnetic Materials 580, 170935 (2023). https://doi.org/10.1016/j.jmmm.2023.170935 .
Figure courtesy of Y.K. Vohra

Bottom:
Model of high-resolution inelastic neutron scattering data collected on the spin-anisotropic magnet FeI_2 using the SEQUOIA time-of-flight spectrometer at ORNL. Despite conventional magnetic ordering, the excitations of this quantum magnet display bands of hybridized dipolar and quadrupolar spin excitations. A theory was developed to explain the behavior of these excitations and their precise momentum-energy dispersion [Bai *et al.* Nature Physics **17**, 467–472 (2021)]. The experiment motivated the development of a generalized spin-wave theory framework using coherent states of SU(N) applicable to many magnets with spin S greater than 1/2 [Zhang and Batista, Phys. Rev. B **104**, 104409 (2021)].
Figure courtesy of M. Mourigal.

Forward

This abstract book is a compilation of scientific content presented at the 2024 Neutron Scattering Principal Investigators' (PI) Meeting sponsored by the Division of Materials Sciences and Engineering in the U.S. Department of Energy Office of Basic Energy Sciences (BES).

The first principal investigators meeting of the neutron scattering (NS) core research program since the COVID pandemic was held in-person January 10-12, 2024 at the Rockville, Maryland Hilton Hotel. The purpose of the meeting was to promote discussions and foster collaborations among the PIs to fulfill the strategic goals of the NS program, to alert PIs to opportunities outside the program and to identify emerging trends. The Oak Ridge Institute for Science and Education (ORISE) staff and T. Crocket (DOE-BES) are gratefully acknowledged for their exceptional assistance, ranging from planning to execution of the meeting. Special thanks to the 2024 Meeting Chairs, Xiaodan Gu (U. of Southern Mississippi) and Dmitry Reznik (U. of Colorado) for developing the meeting agenda and organizing a very productive meeting. Introductory remarks by Michael Fitzsimmons, NS program manager, and Andrew Schwartz, MSE division director, described program and divisional strategic goals. After these remarks, the morning talks featured aspirational goals and first results of newly funded programs spanning the gambit of hard to soft matter, quantum information science and materials science. During lunch, Dr. William Ratcliff (NIST) discussed the 2023 UMD workshop on *Artificial Intelligence and Machine Learning Applications for Scattering*. The first day of talks concluded with progress reports from the DOE-funded labs and the University of Minnesota Center for Quantum Materials. During the afternoon half of more than two dozen posters were presented. At dinner, Dr. Jon Taylor (ORNL) provided a progress report on ORNL's strategic vision of the three-source strategy, encompassing the SNS, HFIR and STS. The presentation described many exciting opportunities for the future neutron community, including the current power upgrade at the SNS, and upcoming beamlines at the STS, enabled by DOE funding.

The second day began with a series of flash talks related to data science and neutron scattering. The talks were followed by a panel discussion with panelists selected based on their roles in developing data analysis and simulation software. The panel discussed challenges and opportunities afforded by data science to neutron scattering, as well as the community's need for beamline operation and data reduction and analysis software. The discussion benefited from lively audience participation. The panel was followed by more talks, an update on the ESS facility provided by Dr. Mikhail Feygenson (ESS) during lunch, and the second poster session. The day concluded with an update on the NIST/NCNR facility by Dr. Ron Jones (NIST).

The meeting concluded before lunch on the third day with oral sessions on soft and hard matter, followed by closing remarks from the program manager.

Selected topics of emerging trends elucidated at the meeting:

- Importance for projects to ensure the vitality and growth of the neutron scattering community.
    - Reinforce passion to align projects to achieve the goal.
    - Consider a virtual career fair for students, postdocs and future faculty candidates.
    - Consider topical virtual meetings/workshops to broadly engage BES-MSE programs.
    - Promote neutron scattering workshop(s) to ensure continuous supply of future talent.
- More powerful instruments produce more nuanced data that require more accurate theories and analysis.
    - Intentionally target problems that require new theories to be disruptive.
- Competency and exploitation of data science is compulsory for next generation neutron scattering.
    - *Operando* experiments producing copious data, "materials are alive", once rare are becoming essential (to move from pictures to movies).
    - Applications of AI (e.g., neutral networks, deep learning) to analyze data are increasingly common.
    - Challenges seen to promote data sharing, archiving, and cataloguing are paramount.
    - AI/ML enables disruptive research based on closed loop materials discovery.
    - Several examples of PI-led data analysis software development being ported via GitHub to the user community.

Many of the experimental, theoretical and data analysis developments presented at the PI meeting will provide a foundation facilitating science of next generation users of neutron scattering and enable disruptive research. Examples include: observation of changes of structure/properties revealed in real time as complex environments are changed, or identifying theories once thought adequate that are woefully lacking. Opportunities afforded by more powerful instruments and data science are heralding a bright and vibrant future for the field of neutron scattering.

Michael Fitzsimmons
BES-MSE, Office of Science
U.S. Department of Energy

Table of Contents

Table of Contents ..... **v**

Agenda ..... **ix**

Abstracts **1**

Seeking Quasiparticles in Perturbed Matter using Low-Energy Spin Dynamics **2**

Arnab Banerjee

Real materials in action: Data analysis developments for real materials doing real things **6**

Simon J. L. Billinge

University of Minnesota Center for Quantum Materials **8**

Turan Birol, Rafael Fernandes, Martin Greven, and Chris Leighton

University of Minnesota Center for Quantum Materials: CQM Research on Heteroepitaxial Strain Tuning of Perovskite Cobaltites **14**

Turan Birol, Rafael Fernandes, Martin Greven, and Chris Leighton

University of Minnesota Center for Quantum Materials: CQM Research on Metallic Delafossites **18**

Turan Birol, Rafael Fernandes, Martin Greven, and Chris Leighton

Dynamic Modulation of Structure and Phase Transformations in Asymmetric Crystalline Colloidal Brush Alloys **21**

Michael R. Bockstaller, Krzysztof Matyjaszewski, and Alamgir Karim

Probing nano-structured quantum magnetism with neutrons **26**

Collin Broholm and Satoru Nakatsuji

Nonreciprocity and Light-controlled Phenomena in Low-symmetry Antiferromagnets: Neutron and Optical Vortex Beam Studies **27**

Sang-Wook Cheong, Valery Kiryukhin, and Andrei Sirenko

Understanding Quantum Matter Beyond the Unit Cell **32**

Andrew Christianson

Using neutron as a probe to study magnetic excitations in strongly correlated electron materials **37**

Pengcheng Dai

Dynamic atomistic processes of sodium-ion conduction in solid-state electrolytes **42**

Olivier Delaire

Neutron scattering studies of phonon anharmonicity and coupling with spin, charge and disorder **45**

Olivier Delaire

Equilibrium and Non-Equilibrium Skyrmion and Vortex Lattices 49

Morten R. Eskildsen

Probing Short-Range Structure and Magnetism in Next-Generation Energy Conversion Materials 54

Benjamin Frandsen

Inelastic Neutron Scattering Studies of Quantum Anharmonicity and Nonlinear Phonons 58

Brent Fultz

Exotic Uses of Neutrons an X-rays as Probes for Chiral Magnets 63

Dustin A. Gilbert

University of Minnesota Center for Quantum Materials (CQM): Structural and Electronic Properties of Titanates 68

Martin Greven, Turan Birol, Rafael Fernandes, and Chris Leighton

University of Minnesota Center for Quantum Materials (CQM): Structural and Electronic Properties of Bismuthate and Cuprate Superconductors 72

Martin Greven and Chris Leighton

Precise Chain Conformation and Dynamics Control For Conjugated Polymers In Organic Electronic Thin Film Devices 77

Xiaodan Gu

Investigating Possible Emergence of Quantum Spin Liquid State in Triangular Lattice Compounds 82

Sara Haravifard

Understanding the role of polymer topology on molecular deformation and scission under extreme shear using *in situ* neutron scattering 83

Matthew E. Helgeson

Neutron Scattering Studies of Hybrid Excitations 88

R. P. Hermann and M. E. Manley

Topological magnons and topological electronic properties in metallic Kagome magnets .. 93

Xianglin Ke

Hybrid Organic-Inorganic Nanosheets with Emergent Properties 97

Seung-Hun Lee and Joshua J. Choi

Scattering and Spectroscopic Studies of Quantum Materials 100

Young Lee

Neutron Scattering Study of Spin-Lattice Interactions 103

Chen Li

Machine learning on neutron scattering 108

Mingda Li

Neutron Scattering on Topological Quantum Materials 113

Mingda Li

Chain Exchange in Block Copolymer Nanoparticles..... 118

Timothy P. Lodge and Frank S. Bates

Topological Quantum States Probed by Neutron Scattering..... 123

Despina Louca

Using phonon mode analysis to study optoelectronic organic materials 132

Adam Moulé

Quantum multipolar fluctuations in spin-orbit magnets 136

Martin Mourigal

Designing Novel Nanostructures Using Sequence-Defined Biopolymers..... 141

Bradley D. Olsen

Designing an *in situ* tribometer for neutron reflectivity measurements of soft gels 146

Angela Pitenis

Deciphering Low Energy Spin and Orbital Dynamics in Frustrated Quantum Magnets . 147

Kemp Plumb

Neutron and X-ray Scattering Analysis of Organic Mixed Ionic Conducting (OMIEC) Composite Formulations from Blends of Conjugated Polymers and Block-Copolymers.. 150

Lilo D. Pozzo

Neutron scattering investigation of novel phases created by application of electric field.. 154

Dmitry Reznik

Process-Structure Relationships of Lithium-Ion Battery Cathodes..... 158

Jeffrey J. Richards

Magnetic Structure and In-Situ Synthesis of van der Waals Metal Chalcophosphates with Neutron and X-ray Diffraction 163

Efrain E. Rodriguez

National School on Neutron and X-ray Scattering 166

Stephan Rosenkranz, Jessica McChesney, and Chengjun Sun

Neutron and x-ray scattering investigations of the impact of short-range correlations on properties of energy and quantum materials 170

Stephan Rosenkranz, Omar Chmaissem, Raymond Osborn, and Daniel Phelan

Dynamics of Bottlebrush Polymers by Neutron Scattering 175

Gerald J. Schneider

Small Angle Neutron Scattering (SANS) Insight into Deconstruction Reaction of Complex Polymer Systems 180

Manjula Senanayake, Jialiang Zhang, Jingwen Luo, Anand Narani, Snehasish Mondal, Sai Venkatesh Pingali, and Marcus Foston.

Study of Magnetic Charge Dynamics and Correlation in Artificial Magnetic Honeycomb Lattice..... 185

Deepak Kumar Singh

Inelastic and Quasielastic Neutron Scattering Studies of Dynamics and Relaxations in Glasses..... 189

Hillary Smith

Neutron Scattering Studies of Non-Linear Quantum Hydrodynamics and Backscattering in Low-Dimensional Systems..... 193

Paul Sokol

Revealing the molecular origin of interactions between nanocrystals..... 196

James Swan

Neutron Scattering Studies of Magnetic Quantum Materials..... 200

John M. Tranquada, Genda Gu, and Igor A. Zaliznyak

Diffuse Neutron Scattering Studies of Far-from-equilibrium Topological Defects..... 205

Priya Vashishta

Neutron Diffraction Study of Magnetic Structures in Heavy Lanthanides under Extreme Conditions..... 211

Yogesh K. Vohra

Orbitally-Active Platforms for Novel Magnetism and Entangled Electronic States..... 215

Stephen D. Wilson

Unraveling Emergent Quantum States in Magnetic Topological Materials using High Pressure Neutron Scattering..... 221

Weiwei Xie

Exotic Magnetic Orders and Dynamics in Chiral Magnets..... 226

Junjie Yang

Universality of Collective Density Fluctuations in Liquids at and away from Equilibrium – An Integrated Inelastic Neutron Scattering, Theoretical, and Computational Study..... 231

Yang Zhang

Author Index..... 235

Participant List..... 237

Agenda

2024 DOE-BES Neutron Scattering and Instrumentation Principal Investigators' Meeting

Meeting Chairs: Xiaodan Gu (University of Southern Mississippi) and Dmitry Reznik (University of Colorado)

Wednesday, January 10, 2024	
8:00-8:50 AM	**Breakfast**
8:50-9:05 AM	**Michael Fitzsimmons**, NS Program Manager, DOE-BES *Welcome and Introductory Remarks*
9:05-9:20 AM	**Andrew Schwartz**, MSE Division Director, DOE-BES *Materials Science and Engineering Division Update*
New Projects 1	Session Chair: **Xiaodan Gu** (University of Southern Mississippi)
9:20-9:40 AM	**Paul Sokol**, Indiana University *Neutron Scattering Studies of Non-Linear Quantum Hydrodynamics and Backscattering in Low-Dimensional Systems*
9:40-10:00 AM	**Simon Billinge,** Columbia University *Real materials in action: Data analysis developments for real materials doing real things*
10:00-10:20 AM	**Collin Broholm**, John Hopkins University *Probing nano-structured quantum magnetism with neutrons*
10:20-10:40 AM	**Dmitry Reznik,** University of Colorado *Neutron scattering investigation of novel phases created by application of electric field*
10:40-11:10 AM	**Break**
New Projects 2	Session Chair: **Dmitry Reznik** (University of Colorado)
11:10-11:30 AM	**Chen Li**, UC Riverside *Neutron Scattering Study of Spin-Lattice Interactions*
11:30-11:50 AM	**Steve May**, Drexel University *Controlling magnetism via charge modifications in quantum material heterostructures*
11:50-12:10 PM	**Angela Pitenis**, UCSB *Designing an in situ tribometer for neutron reflectivity measurements of soft gels*
12:10-12:30 PM	**Hillary Smith**, Swarthmore College *Inelastic and Quasielastic Neutron Scattering Studies of Dynamics and Relaxations in Glasses*
12:30-2:00 PM	**Working Lunch and Concurrent Keynote Presentation**
12:50-1:30 PM	**William Ratcliff,** NIST *Report on the UMD workshop on AI/ML for scattering* Session Chair: **Mingda Li** (MIT)

Hard Matter 1	Session Chair: **Dustin Gilbert,** University of Tennessee
2:00-2:20 PM	**John Tranquada,** BNL *Neutron Scattering Studies of Magnetic Quantum Materials*
2:20-2:40 PM	**Martin Greven,** UMN *University of Minnesota Center for Quantum Materials (CQM)*
2:40-3:00 PM	**Stephan Rosenkranz**, ANL *Neutron and x-ray scattering investigations of the impact of short-range correlations on properties of energy and quantum materials*
3:00-3:30 PM	**Break**
Hard Matter 2	Session Chair: **Chris Leighton,** UMN
3:30-3:50 PM	**Andrew Christianson**, ORNL *Understanding Quantum Matter Beyond The Unit Cell*
3:50-4:10 PM	**Young Lee**, SLAC *Scattering And Spectroscopic Studies Of Quantum Materials*
4:10-4:30 PM	**Raphael Hermann**, ORNL *Neutron Scattering Studies of Hybrid Excitations*
4:30-6:30 PM	**Poster Session (Odd numbered posters)**
6:30-8:00 PM	**Working Dinner and Concurrent Keynote Presentation**
7:00-7:30 PM	**Jon Taylor,** ORNL *SNS and HFIR facility update* Session Chair: **Xiaodan Gu** (U. So. Mississippi)

Thursday, January 11, 2024	
8:00–9:00am	**Breakfast**
Panel Discussion	Software for Neutrons, Moderator: **Dmitry Reznik** (University of Colorado)
9:00-9:40AM	**10 minute flash talks by Mingda Li** (MIT), **Lilo Pozzo** (University of Washington), **Kipton Barros** (LANL), **Yang Zhang** (University of Michigan)
9:40-10:30 AM	**Panelists: Li, Pozzo, Barros, Zhang, Ratcliff, Taylor**
10:30-10:50 AM	**Break**
Soft Matter 1	Session Chair: **Gerald Schneider**, Louisiana State University
10:50-11:10 AM	**Lilo Pozzo,** University of Washington *Neutron and X-ray Scattering Analysis of Organic Mixed Ionic Conducting (OMIEC) Composite Formulations from Blends of Conjugated Polymers and Block-Copolymers*
11:10-11:30 AM	**Adam Moule**, UC-Davis *Using phonon mode analysis to study optoelectronic organic materials*
11:30-11:50 AM	**Xiaodan Gu,** U. of Southern Mississippi *Synthesis and Scattering of Deuterated Conjugated Polymers And Their Application For Optoelectronics*
11:50-12:10 AM	**Manjula Senanayake, Marcus Foston**, Washington University *Small Angle Neutron Scattering (SANS) Insight into Deconstruction Reaction of Complex Polymer Systems*
12:10-1:40PM **12:50-1:30pm** **Virtual**	**Working Lunch and Concurrent Keynote Presentation** Mikhail Feygenson**, ESS** ***ESS Facility update*** **Session Chair: Dmitry Reznik** (University of Colorado)
Hard Matter 3	Session Chair: **Arnab Banerjee**, Purdue University
1:40-2:00 PM	**Xianglin Ke,** Michigan State University *Topological magnons and topological electronic properties in metallic Kagome magnets*
2:00-2:20 PM	**Deepak Singh**, U. of Missouri *Study of Magnetic Charge Dynamics and Correlation in Artificial Magnetic Honeycomb Lattice*
2:20-2:40 PM	**Brent Fultz**, Caltech *Inelastic Neutron Scattering Studies of Quantum Anharmonicity and Nonlinear Phonons*
2:40-3:00 PM	**Weiwei Xie**, Michigan State University *Unraveling Emergent Quantum States in Magnetic Topological Materials using High Pressure Neutron Scattering*

3:00-3:30 PM	**Break**
Hard Matter 4	Session Chair: **Adrian Del Maestro**, University of Tennessee
3:30-3:50 PM	**Olivier Delaire**, Duke *Neutron scattering studies of phonon anharmonicity and coupling with spin, charge and disorder*
3:50-4:10 PM	**Despina Louca**, University of Virginia *Topological Quantum States Probed by Neutron Scattering*
4:10-4:30 PM	**Mingda Li**, MIT *Neutron Scattering on Topological Quantum Materials*
4:30-6:30 PM	**Poster Session 2 (Even numbered posters)**
6:30-8:00 PM	**Working Dinner and Concurrent Keynote Presentation**
6:50-7:30 PM	**Ron Jones,** NIST *NIST facility update* Session Chair: **Michael Fitzsimmons** (DOE-BES)

Friday, January 12, 2024	
8:00–8:40am	**Breakfast**
Soft Matter 2	Session Chair: **Jeff Richards**, Northwestern University
8:40-9:00 AM	**Yang Zhang**, University of Michigan *Universality of Collective Density Fluctuations in Liquids at and away from Equilibrium – An Integrated Inelastic Neutron Scattering, Theoretical, and Computational Study*
9:00-9:20 AM	**Tim Lodge**, UMN *Chain Exchange in Block Copolymer Nanoparticles*
9:20-9:40 AM	**Matthew Helgeson**, UCSB / Patrick Underhill, RPI *Understanding the role of polymer topology on molecular deformation and scission under extreme shear using in situ neutron scattering*
9:40-10:00 AM	**Gerald Schneider**, Louisiana State University *Dynamics of Bottlebrush Polymers by Neutron Scattering*
10:00-10:30 AM	**Break**
Hard Matter 5	Session Chair: **Collin Broholm**, Johns Hopkins University
10:30-10:50 AM	**Steve Wilson**, UCSB *Orbitally-Active Platforms for Novel Magnetism and Entangled Electronic States*
10:50-11:10 AM	**Pengcheng Dai**, Rice University *Using neutron as a probe to study magnetic excitations in strongly correlated electron materials*
11:10-11:30 AM	**Valery Kiryukhin**, Rutgers University *Nonreciprocity and Light-controlled Phenomena in Low-symmetry Antiferromagnets: Neutron and Optical Vortex Beam Studies*
11:30-11:50 AM **Virtual**	**Martin Mourigal**, Georgia Tech University *Quantum multipolar fluctuations in spin-orbit magnets*
11:50-12:00 PM	**Concluding Remarks, M. Fitzsimmons (DOE-BES)**

Wednesday and Thursday
4:30-6:30 PM

Poster Session

Poster	Presenter	Institution	Title
1	Banerjee	Purdue	*Seeking Quasiparticles in Perturbed Matter using Low-Energy Spin Dynamics*
2	Bockstaller / Karim	CMU/U of Houston	*Dynamic Modulation of Structure and Phase Transformations in Asymmetric Crystalline Colloidal Brush Alloys*
3	Delaire	Duke	*Dynamic Atomistic Processes of Sodium-Ion Conduction in Solid-State Electrolytes,*
4	Eskildsen	U of Notre Dame	*Equilibrium and Non-Equilibrium Skyrmion and Vortex Lattices*
5	Frandsen	BYU	*Probing Short-Range Structure and Magnetism in Next-Generation Energy Conversion Materials*
6	Gilbert	UTK	*Exotic Uses of Neutrons an X-rays as Probes for Chiral Magnets*
7	Haravifard	Duke	*Investigating Possible Emergence of Quantum Spin Liquid State in Triangular Lattice Compounds*
8	Lee, S	U of Virginia	*Hybrid Organic-Inorganic Nanosheets with Emergent Properties*
9	Li, Mingda	MIT	*Machine Learning on Neutron Scattering*
10	Olsen	MIT	*Designing Novel Nanostructures Using Sequence-Defined Biopolymers*
11	Plumb	Brown University	*Deciphering Low Energy Spin and Orbital Dynamics in Frustrated Quantum Magnets*
12	Richards	Northwestern	*Process-Structure Relationships of Lithium-Ion Battery Cathodes*
13	Rodriguez	UMD	*Magnetic Structure and In-Situ Synthesis of van der Waals Metal Chalcophosphates with Neutron and X-ray Diffraction*
14	Tisdale	MIT	*Revealing the Molecular Origin of Interactions Between Nanocrystals*
15	Vashista	APS	*Diffuse Neutron Scattering Studies of Far-from-equilibrium Topological Defects*
16	Vohra	NAS	*Neutron Diffraction Study of Magnetic Structures in Heavy Lanthanides under Extreme Conditions*
17	Yang, Junjie	New Jersey Institute of Technology	*Exotic Magnetic Orders and Dynamics in Chiral Magnets*
18	Schneider	LSU	*Compact Neutron Source Concept*
19	Greven	UMN	*University of Minnesota Center for Quantum Materials: CQM Research on Metallic Delafossites*
20	Leighton	UMN	*University of Minnesota Center for Quantum Materials: CQM Research on Heteroepitaxial Strain Tuning of Perovskite Cobaltites*

21	Leighton	UMN	*University of Minnesota Center for Quantum Materials (CQM): Structural and Electronic Properties of Titanates*
22	Greven	UMN	*University of Minnesota Center for Quantum Materials (CQM): Structural and Electronic Properties of Bismuthate and Cuprate Superconductors*

Abstracts

Seeking Quasiparticles in Perturbed Matter using Low-Energy Spin Dynamics

PI Name: Arnab Banerjee, Asst. Prof., Phys. and Astron., Purdue Univ., West Lafayette IN.

Keywords: Neutron Spin Echo, Polarized neutron, Quantum Spin Liquids, Topological Insulators

The primary objective of this proposal is to identify, measure, and control new quantum and topological states in magnetic materials through the analysis of their low-energy dynamical properties, utilizing innovative polarized neutron scattering techniques. The pursuit of emergent phases of matter stands as a crucial goal in condensed matter physics, not only for its scientific significance but also due to its immense potential in advancing solid-state quantum electronics beyond the limitations of Moore's law. Consequently, the quest for these states must be accompanied by the development of specialized detection techniques, preferably applicable in device-ready configurations. Numerous significant many-body quantum phenomena remain elusive to conventional detection techniques, presenting a considerable challenge. These phenomena encompass conclusive evidence of quantum spin liquids, small topological quantum gaps, in-gap bound-states, Landau levels in quantum spin liquids, as well as spin-polarized surface currents in highly spin-orbit-coupled topological insulators exhibiting anomalous spin Hall effects. In this study, we aim to extend the utilization of polarized neutron scattering techniques to highly spin-orbit-coupled quantum materials, such as topological semimetals, disordered quantum materials, paramagnets, and quantum spin liquids. Our objective is to employ neutron spin echo (NSE) to measure low-energy excitations in quantum magnets, employing both paramagnetic and ferromagnetic echoes, in order to identify distinct signatures, quantum gaps, and excitations associated with bound quasiparticle states and flat bands. Additionally, we intend to elucidate the interactions between polarized neutrons and the spin Hall effect in topological insulators (TIs). This research introduces new avenues to interrogate spin-orbit coupled materials which hold great promise for advancing topological quantum logic and sensor technologies**.**

Research Scope:

Thrust 1: Search for new quantum materials: An important part of the project is the in-house co-development of new quantum magnets with interesting ground states. Two main classes of materials are explored – (i) *Quantum spin liquid (QSL)s:* Geometrically or bond-frustrated QSL candidates (such as the triangular, and the Kitaev honeycomb) are particularly interesting as the motion of the entangled spins can embody an emergent topological order and fractionalization that leads to highly non-linear low-energy dynamical states. In this project we undertake the development and conventional characterization (both using bulk techniques and neutrons) of new QSL candidates and (eventually) dilute them to induce defect and bound states, or to examine the robustness of spin states. (ii) *Topological insulators and Anomalous Spin Hall Effect (ASHE) materials:* Topological insulators (TI) are novel class of electronic materials where combination of charge order and spin-orbit coupling (SOC) gives rise to an insulating bulk and topological surface conduction states which feature spin-polarized Dirac Fermionic excitations. Here we propose the experiment to study polarized surface states using polarization of incident polarized neutron beam. We develop/obtain materials high SOC which can show anomalous spin Hall effect (ASHE), including Bi_2Se_3, Bi_2Te_3 single crystals and Pt single crystals for the project.

Thrust 2: Paramagnetic and Ferromagnetic NSE at moderate fields**:** The measurement of the low-energy excitations of magnetic quantum materials remains a grand challenge. In this proposal, we develop low temperature paramagnetic (PM) and ferromagnetic (FM) NSE expanding the capabilities

at ORNL (BL-15). With higher resolution compared to Raman and Inelastic X-Ray Spectroscopy, this technique also supersedes NMR with ability to resolve momentum-transfer.

The project is a major hardware upgrade undertaking by adding flipper coils, phase coils around the shorty, install a magnet to fit the instrument, and design Q-compensation coils around the magnet to guide the polarization – much of which we plan to perform during the SNS outage. Initially, we perform *paramagnetic spin* in zero field using XYZ polarization analysis measurements providing valuable insight on the topology of the magnetic moments. Next we explore *ferromagnetic spin echo* configuration, which allows for applying high magnetic fields at the sample indicating a new capability for ORNL. To design or find a horizontal field cryomagnet which is capable of high fields and He^3 environment, but with very low fringe fields is a challenge.

Thrust 3: Spin Hall effect using polarized neutrons: We aim to demonstrate if polarized neutrons are indeed affected by spin polarization of the surface conduction. We answer whether polarized surface states in TI have the requisite spin density to affect incident neutron beam polarization. The goal of the program is to perform an idea of "Mott Skew Scattering" [1] that polarized neutron beam would interact electronic spins in TI and exchange angular momentum which would manifest into incident neutron polarization dependent spin Hall voltage, that would be picked up in anomalous spin Hall effect (ASHE), when longitudinal current is passed through the sample. Also, a change in neutron polarization will be observed through (current and temperature dependent) polarization tensor that would carry the information of the effect of TI on the neutron beam. If discovered, polarized neutrons would become a probe for TI-s and AQHE effects broadly, including in doped samples, opening a new realm of measurements of several other TI candidates.

Recent progress (2023): *Personnel:* The project started in Sept 2022, and my first post-doc, Gavin Hester, got a tenure-track faculty position in Brock University in Canada in Dec 2022. While that was a setback, he successfully trained two graduate students, Guga Khundzakishvili (GK), and Bishnu Belbase (BB) in polarized neutron techniques and crystal growth respectively.

Thrust 1: Material synthesis and characterization: BB has grown several new (and known old) crystals for the project. These included the Bi_2Se_3 (TI candidate), ErI_3 (Kitaev QSL candidate, Tc = 0.3 K), $GdTe_3$ (competing CDW/SDW close to criticality), $BaCo_2(AsO_4)_2$ (Kitaev QSL candidate, Hc = 0.5 T), $YbCr_6Ge_6$ (triangular QSL candidate with broad hump) using flux growth techniques. We were also successful in making powder of well-studied Kitaev candidate $Na_2Co_2TeO_6$, new Kitaev candidate $Li_2Co_2TeO_6$, and delaffosite $TlYbS_2$ (Tc=3 K, Hc=3 T, working with PD of Athena Safa Sefat). We are also attempting to grow HfI_3, and $ErCl_3$. We have access to $RuCl_3$, $MoCl_3$ through Jiaqiang Yan at ORNL. In order to obtain high-quality single-crystal mono- and poly-layers of $RuCl_3$ and other 2D Kitaev halides, GK is working with Dr. Matt Brahlek (CNMS) to device a MBE chamber capable of $RuCl_3$ and other 2D chloride thin-films (Fig 1 Dn).

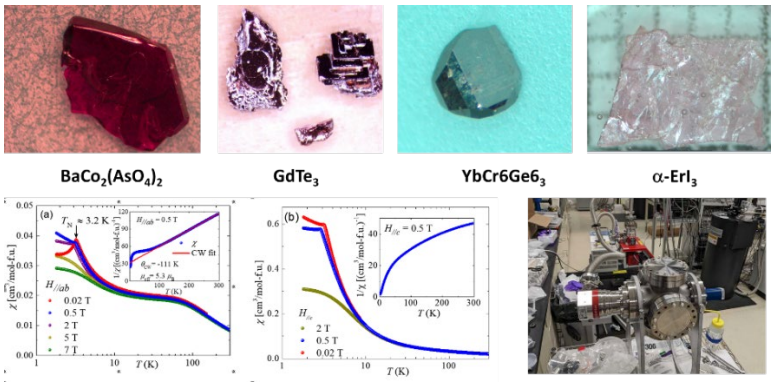

Fig 1:(Top) Crystals grown by us, (Dn left) Susceptibility of $YbCr_6Ge_6$ with field direction showing suppression of order (Dn right) MBE chamber for $RuCl_3$ co-developing with CNMS.

***Thrust 2: Installation of flippers, cryostats and magnets*:** One shortcoming at the NSE instrument at ORNL is the absence of the π/2 MEZEI flippers which preclude the use of a magnetic field at the sample location as required for both PM-NSE and FM-NSE. In February 2023, with Katiya Pappas, we have already solved this shortcoming with additional π/2 MEZEI flippers around the sample, which we already tested and installed for this project (see Fig. 9). We have identified, designed and tested the WAND^2 cryostat at BL-15, down to 300 mK from the existing 4 K, at zero field, indicating an expansion of capabilities for ORNL.

Having magnetic field around the sample causes uncontrollable Larmor precession in the system, it's also crucial for transporting polarization. We have begun work in two areas: (i) Testing of 5 T Mag-H horizontal field and 5 T Mag-E vertical field magnets for transporting polarization (upcoming beamtime at HFIR HB-2 station in Jan-Feb with Fankang Li. (ii) Design (COMSOL), build and test XYZ Q-coils capable to ~5-100 G to ensure an adiabatic rotation of the magnetic field (and thus of the beam polarization), from the longitudinal (parallel to $\vec{k}_i$) to a transverse (parallel to $\vec{q}$) field at the sample position.

Thrust 3: Seeking surface polarized modes with neutrons: GK, Fankang Li and Peter Jiang, used 1.5 days of awarded beamtime to achieve promising results on a polarized neutron + ASHE measurement single crystal Bi_2Se_3 sample which was grown at Purdue University and cut into the correct dimensions. We had successfully mounted a single crystal on Si substrate with e-beam patterned gold pads, (Fig. 2 left) and performed the experiment described in Fig. 2 (middle). We used a combination of specially designed chopper (running at 17 Hz) paired to a Keithley 6220 current source and a SR-830 Lock-in Amplifier with a SR-554 transformer pre-amplifier, as we used in the previous measurement. In quantum spin hall voltage analysis, we found existing correlation between Hall signal (refers to 2nd harmonic measurement through lock-in amplifier SR-830) and incident neutron beam polarization (Figure 2a) as well as dependence of non-diagonal element(s) (elements responsible for the change of neutron polarization direction) of polarization tensor on current and temperature. Additionally, the current affects the neutron polarization in non-trivial ways in TI-s, where the neutron polarization is slightly altered between 5K (TI regime) and 200K (non-TI regime). We additionally tracked the polarization matrices for the [105] Bragg peak and observed a change of neutron polarization beyond what is simply expected from Biot-Savart law. If confirmed, this is a discovery of an interaction between polarized neutrons and the TI surface currents, which leads to a discernable signal in the Hall voltage measured on the TI – a new phenomenon.

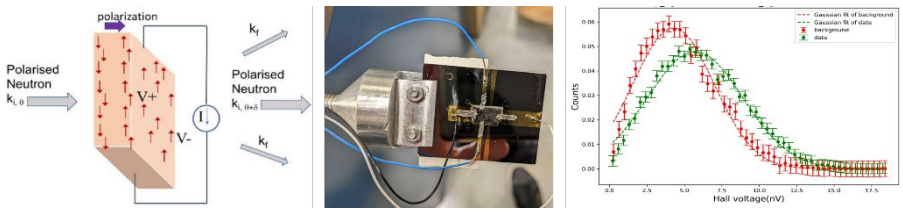

Fig. 2 (left) Geometry of the anomalous spin-Hall (ASHE) interaction with polarized neutrons. (middle) ASHE measured on sample of Bi2Se3 cut and placed on a Si/SiO2 substrate with e-beam gold leads. (right) difference in with change in pol. neutron flux.

Future plans (2024-2025):

Thrust 1: Expanding to newer materials: Future plans include, (i) the synthesis and characterization of triangular lattice $TlYbSe_2$ (iso-structural to $TlYbS_2$), spin-chain compounds $A_2R(PO_4)(XO_4)$ (A= alkali metal, R= rare-earth, X= W, Mo), honeycomb lattice systems $A_2M_2TeO_6$ (A= alkali metal, M= Co^{2+}, Ni^{2+}). Additionally, we are dedicating some effort to synthesis of $CeBr_3$, $CeCl_3$ and $TbCl_3$ Kitaev candidates with possibly S=1/2 moments. (ii) All the above materials, including ErI_3, $YbCr_6Ge_6$ will be characterized for bulk magnetic properties (C_p, χ) using 1.8 K, 9 T PPMS at Birck

Nano Center and using neutrons at SNS/HFIR (some beamtimes are already obtained). (iii) We are still testing the feasibility of the MBE growth of $RuCl_3$, and the conversion of Ru-sputtered films into $RuCl_3$, which if successful, would be tested in Magnetic Reflectometry, NSE, besides the array of nano-science characterization techniques and Raman.

***Thrust 2: Seeking low-energy features in QSL with high-resolution*:** *With neutrons in June 2024,* we plan to: (1) Install and test the XYZ flippers and Q-coils and the transport of polarization, (2) Design/Configure a cryomagnet which can produce Tesla (horizontal?) fields at the sample location for FM Spin Echo, (3) Install new flippers or phase coils on the current NSE coils which can help to correct phases arising from the fields and magnetic samples. Revamping and testing the instrument, with the help of NSE team at SNS and Crow's team at HFIR, is an important task to allow fully new capabilities for ORNL. In this way, we hope to expand capabilities of transduction of magnetic materials in the ~1 micro-eV energy scales, and k-vectors of ~0.2 – 1.5$Å^{-1}$, where no other q-resolved techniques exist for material science at this moment, required to tease apart the Hamiltonian and quantum quasiparticle bound-states and possible Landau levels for several disordered quantum magnets. Possible first systems to explore PM-NSE are in doped $RuCl_3$, Transverse-field Ising $LiXF_4$ (X = Ho, Er, which has a walker mode at 500 mK, 0-5 T, crystals obtained from Impex GmbH), $BaCo_2(AsO_4)_2$ or α-ErI_3 (as they require low magnetic fields).

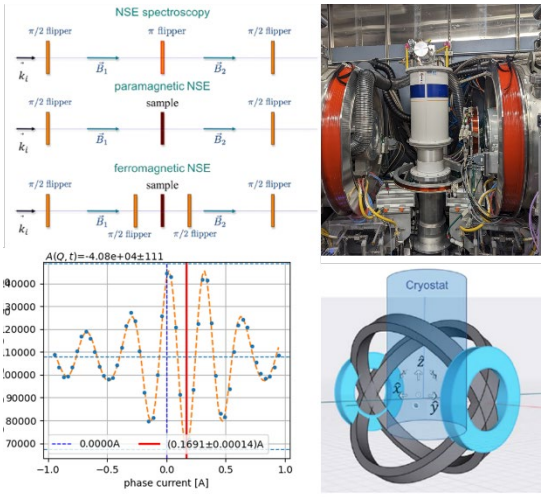

Fig. 3 (top left) Geometry of NSE, PM and FM-NSE (bottom left) Echo after installation of pi/2 flippers for FM-NSE (top right) Installation of He3 cryostat at ORNL NSE for first time. (bottom right) design of Q-coils going ahead.

Thrust 3: Confirmation and expansion to newer TI-s: (i) In April 2024 we will confirm our previous findings. Our goal is to eliminate possible sources of interference and collect enough statistics to understand the size of the effect and its origin in Bi_2Se_3. We are improving the LabView program to simultaneously obtain phase data. and adding a 5th voltage lead to a carbon-fiber dipstick custom-built for this experiment (Fig. 2) and a second SR-830 for longitudinal resistance measurement to fully understand the resistivity tensor. These hardware improvements, supposed to be complete soon, we aim to confirm the existence / observation of the effect through three systematic analyses. We aim to perform a systematic *current vs polarization analysis* by changing the current flowing through the sample to observe a current-dependent effect on the [105] Bragg peaks followed by a *systematic temperature dependance.* This goal relies on the effects of SO coupling in Bi_2Se_3 vanishing over 100 K and hence would lead to a confirmatory temperature dependent effect. We also seek to eliminate any possible extraneous effects by using an *addendum measurement,* which is a simple copper block with no SO coupling, but with everything else remaining the same. If successful, we propose to extend the findings to doped TI BiSeTe, and other promising candidates such as Pt crystals, WTe_2 and others.

Publications:

Norhan M. Eassa, Joe Gibbs, Zoe Holmes, Andrew Sornborger, Lukasz Cincio, Gavin Hester, Paul Kairys, Mario Motta, Jeffrey Cohn, and Arnab Banerjee, *High-fidelity dimer excitations using quantum hardware,* arxiv:2304.06146 (2023). [Preprint]
Note: [BES Secondary – only GH supported by BES for helping to interpret and re-plot the neutron spectrum].

Real materials in action: Data analysis developments for real materials doing real things

Simon J. L. Billinge, Department of Applied Physics and Applied Mathematics, Columbia University

Keywords: PDF, powder diffraction, *in situ*, *operando*, data analysis, machine learning, ML

Research Scope

Modern materials under study for next generation technologies, such as for energy conversion and storage, environmental remediation and health, are highly complex, often heterogeneous and nanostructured. In real applications the materials can undergo dramatic changes that are at the heart of the property that we are trying to exploit. For example, ions move around under electrochemical potentials in batteries and catalysts temporarily undergo chemical changes during the catalysis process. We therefore seek to understand materials not just in their thermodynamically stable state, but also changes that occur as they are driven by external forces. Neutron diffraction is a powerful tool for doing this.

To fully understand these processes requires making the structural and spectroscopic measurements in actual operating devices. In general, such devices are highly heterogeneous, made up of different components in complex arrangements on micron and millimeter lengths-scales. A fundamental challenge in such *operando* experiments is to separate the signals from the different components in the device, so the signal of interest can be extracted and successfully analyzed.
This project will develop data analysis tools that take advantage of developments in artificial intelligence and machine learning to separate signals from heterogeneous devices for the case of time of flight (tof) neutron data.

We plan to address two challenges, (1) heterogeneity, requiring the separation and interpretation of overlapping signals, (2) sample non-ideality, where experimental geometries make data non-ideal, for example bad powder averages (spotty data) due to the inability to spin a battery. Other aspects of the problem are the existence of sets of time-series data and occasionally the need to extract tiny signals from large backgrounds.

For these experiments data handling and knowledge extraction is currently a major bottleneck. Algorithmic and computational developments are needed that can help us to overcome this challenge of heterogeneity and this is the focus of our proposal. The goal is to develop the software and computational tools that will allow the community to study complex heterogeneous samples with neutrons. This will help to prize open the door to a wider range of neutron *operando* measurements on operating devices in the future.

The general approach is based on the following hypothesis:
It is possible to separate overlapping signals from heterogeneous samples in time of flight neutron experiments by exploiting the high dimensionality of the "experiment parameter space" and using modern algorithms.

For the tof data we envisage taking advantage of the very high dimensionality of the data acquisition space in time of flight neutron diffraction experiments. The high dimensionality comes from the fact that there is large solid angle coverage of pixelated, 2D detectors, but furthermore, in each detector

there is a time-of-flight dimension. Modern algorithms (such as ML) coupled with advances in high performance computing are, in principle, able to explore the "event mode" data directly in the full high dimensional space in which it was collected. We aim to exploit this in our goal of signal separation from heterogeneous samples. The scope of the project is to develop, test and validated novel algorithms, methods and software for signal separation from heterogeneous samples in tof data. We will also look for opportunities to develop signal extraction protocols of cw neutron data.

Such tools can be expected to have broad application by domain scientists interested in carrying out *in situ* and *operando* measurements at neutron beamlines in the future applied to a broad range of scientific and technological problems.

Recent Progress

The project was funded in October and we are in the process of recriting staff.

Future Plans

Please see above.

Publications

None

University of Minnesota Center for Quantum Materials (CQM)

Turan Birol[1], Rafael Fernandes[2], Martin Greven (PI)[2], Chris Leighton[1]

[1]Department of Chemical Engineering and Materials Science, University of Minnesota

[2]School of Physics and Astronomy, University of Minnesota

Keywords: Quantum materials, oxides, neutron scattering, x-ray scattering, strain

Research Scope

The University of Minnesota Center for Quantum Materials (CQM), founded in 2016, is comprised of an inter-disciplinary team of four faculty and more than a dozen Ph.D. students and post-docs. The team investigates the structural, electronic, and magnetic properties of select quantum materials, particularly complex oxides, which embody many of the most fundamental questions regarding quantum behavior of interacting electrons and are relevant to important technologies, including data storage, spintronics, catalysis, and fuel cells. *The CQM vision is to substantially advance the understanding of quantum electronic phases and phase transitions in these materials, thereby addressing multiple BES grand challenges.* This is being achieved through the synthesis of exceptional quality model materials in both bulk and thin-film form, the application of cutting-edge neutron, x-ray, and other probes, the exploration of novel material control paradigms, and tight coupling to first-principles and analytical theory. The current focus is primarily on perovskite titanates, cobaltites and bismuthates, and on lamellar cuprates and metallic delafossites. Exciting new directions include strain control (both elastic *and* plastic), an increased emphasis on advancing the science and application of neutron scattering methods and instrumentation, and yet further focus on unique and enabling materials synthesis and processing.

Recent Progress

Field-leading synthesis efforts, broad application of state-of-the-art neutron and x-ray techniques, and the pursuit of new opportunities such as elastic and plastic deformation control, have enabled significant recent CQM advances [1-34].

Examples of recent CQM progress – strain tuning and strain engineering. The high level of synergy within the CQM is exemplified by recent advances with strain tuning and engineering (Fig. 1), such as pioneering work on enhanced superconductivity and ferroelectricity in *plastically* deformed $SrTiO_3$ [1]. This breakthrough result involved three CQM investigators (*Fernandes, Greven, Leighton*), state-of-the-art diffuse neutron and x-ray scattering at ORNL and ANL (Fig. 1(a)), novel uniaxial strain techniques (which induce self-organization of dislocation structures), and theoretical modeling. Bulk superconductivity is enhanced by about a factor of two with plastic deformation, with tantalizing initial transport evidence for a minority volume fraction with a *hundredfold* T_c increase (30-40 K *vs.* 300-400 mK). This work appeared in *Nature Materials* [1] and as a *2023 DOE BES Highlight*. It initiated further collaborative work on plastically deformed $SrTiO_3$, *e.g.,* micro-SQUID data (by B. Kalisky, Bar Ilan, Israel) led to the discovery of magnetism [30]. A robust theoretical framework on quantum critical phenomena promoted by ferroelectricity in metals and semimetals has also been developed by *Fernandes* and collaborators [14,18].

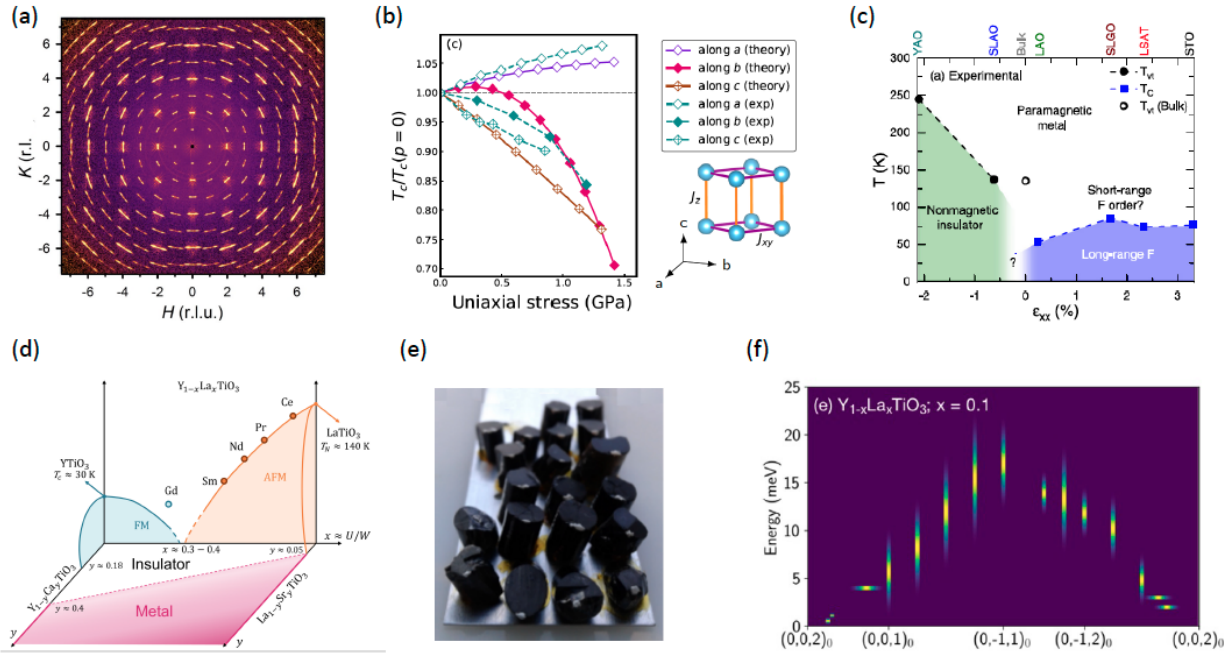

Figure 1: (a) Diffuse neutron scattering (CORELLI, SNS) for lightly-doped $SrTiO_3$, *plastically* deformed by 4.5% along [010]. The scattering is arc-like, with a fine pattern indicative of periodic dislocation walls, near which superconductivity and ferroelectricity are substantially enhanced [1]. (b) Comparison of *elastic* stress dependence of the Curie temperature of $YTiO_3$ from ac susceptibility with mean-field results from DFT [5]. (c) Experimental temperature *vs.* "in-plane strain" phase diagram for $(Pr_{0.85}Y_{0.15})_{0.7}Ca_{0.3}CoO_{3-\delta}$ [15]. (d) Phase diagram of $RETiO_3$ compounds. (e) Successful growth of large high-quality crystals for neutron scattering [22]. (f) Detailed spin-wave measurements (HB-3, HFIR) and theoretical modeling give fresh insight into the spin-dynamics of $Y_{1-x}La_xTiO_3$ [22].

A related example of CQM synergy is the demonstration of strain-tuned Curie temperature (T_C) in ferromagnetic (FM) rare-earth (RE) titanate crystals ($RETiO_3$), understood theoretically using a combination of first-principles and phenomenological calculations (*Birol*, *Fernandes, Greven*) (Fig. 1(b)) [5]. Complementary theoretical work (*Birol*, *Fernandes*) led to new insights into the strain-tunable metamagnetic critical endpoint in Mott insulating rare-earth titanates [3].

CQM efforts also involve strain-tuning *via* heteroepitaxy. *Leighton*, *Birol*, and *Fernandes* used strain to completely manipulate the electronic ground state of $(Pr_{1-y}Y_y)_{1-x}Ca_xCoO_{3-\delta}$. This system exhibits a unique Pr valence transition, triggering spin-state/structural/metal-insulator transitions, originally discovered at 90 K in bulk. In epitaxial films, however, tensile strain stabilizes a FM metallic state, while, remarkably, compressive strain drives large enhancement of the metal-insulator transition to ambient temperatures (Fig. 1(c)) [15]. Following this discovery, the CQM went on to elucidate an extraordinary mechanism of strain relaxation in this system [17] and to explore a potential spin-state quantum critical point in the strain phase diagram [33].

Examples of recent CQM progress – rare-earth titanates. The RE titanates $RETiO_3$ exhibit fascinating Mott-insulating states, non-trivial magnetic transitions/crossovers, and lattice/charge/spin/orbital coupling (Fig. 1(d)). Synthesis efforts have resulted in sizable single crystals for neutron scattering work (Fig. 1(e)). In addition to the demonstration of a strain-tuned T_C noted above (*Birol*, *Fernandes, Greven*) [5], CQM work has explored the effects of random antiferromagnetic exchange on the spin waves (*Birol*, *Fernandes, Greven*) (Fig. 1(f)) [22]. This effort established $Y_{1-x}La_xTiO_3$ as a model system for the study of antiferromagnetic spin-exchange disorder in a three-dimensional Heisenberg ferromagnet. *Greven* and former CQM postdoc D. Pelc (U. Zagreb, Croatia) pursued an electron spin resonance/nuclear magnetic resonance study that provided key

insight into the spin-orbital interplay and indicated that full orbital degeneracy lifting is associated with FM order [28]. For her outstanding Ph.D. work on RE titanates and plastically deformed strontium titanate, former CQM graduate student Sajna Hameed received the 2022 Neutron Scattering Society of America (NSSA) Prize for Outstanding Student Research.

Examples of recent CQM progress – metallic delafossites. Delafossite compounds such as $PdCoO_2$ have only recently been understood to be *the most conductive oxides known*. $PtCoO_2$ has resistivity lower than Au at 300 K, while $PdCoO_2$ achieves 8 nΩcm residual resistivity and a staggering 20 μm mean-free-path. *Leighton*, with *Birol* and *Fernandes,* is now leading research to understand two key aspects of this behavior: What is special about electron-phonon scattering to enable such low 300-K resistivity, and how can crystals be sufficiently perfect to enable these low-temperature resistivities? A new crystal growth method has been developed, using chemical vapor transport to achieve the highest structural qualities yet in $PdCoO_2$, in addition to a 500X increase in size [12,34]. These crystals were used in wide-temperature-range x-ray diffraction and calorimetry studies, establishing a *R*-3*m* structure, thermal expansion in agreement with DFT, and unusual phonon DOS [12]. Moreover, the first detailed defect study was performed, establishing that, contrary to the prevailing narrative, these materials are *not* ultrapure [34]. Due to their crystal chemistry, however, most impurities are forced to occupy BO_6 octahedra, leaving the conductive Pd sheets ultrapure, explaining the ultrahigh conductivity of these materials [34].

Examples of recent CQM progress – cobaltites. Perovskite cobaltites have been a mainstay of CQM research. The majority of recent CQM research on these materials has morphed into strain-tuning studies, as detailed above for the Pr-based perovskite cobaltite films. In addition, *Leighton* recently published on the first understanding of the importance of magnetic frustration in archetypal $La_{1-x}Sr_xCoO_3$ [7]. The evolution from spin-state polarons at low doping to ferromagnetism at high doping was shown to be profoundly impacted by magnetic frustration, delaying the onset of percolation, and providing the first explanation for a puzzling aspect of these foundational materials [7]. This work developed a theory of frustration of spin-state polarons, explaining results from small-angle neutron scattering (SANS) in particular [7].

***Examples of recent CQM progress – cuprates and bismuthates*.** The doped perovskite $BaBiO_3$ was the first high-T_c oxide to be discovered, yet pivotal questions regarding the nature of both the metallic and superconducting states remain unresolved. In a diffuse x-ray scattering study, *Greven* uncovered nanoscale structural correlations that break inversion symmetry, with far-reaching implications for the electronic physics [16]. Somewhat related neutron and x-ray diffuse scattering work (by *Greven* and ORNL and ANL collaborators) on two cuprates revealed highly unusual yet universal structural fluctuations consistent with the notion that structural and electronic properties of perovskites in general, and the cuprates in particular are affected or even governed by inherent 'hidden' inhomogeneity [13]. In a combined neutron and x-ray scattering study, *Greven* collaborated with D. Reznik (U. Colorado) to unravel the effects of electric currents (a process referred to as 'flash') on the structural properties of the cuprate parent compound Pr_2CuO_4 [21].

Examples of recent CQM progress – other projects. CQM researchers are active in a number of additional opportunistic and collaborative projects. For example, *Leighton* is collaboratively exploring the prototypical antiferromagnetic Mott insulator NiS_2. Recent work on 2D flakes [19] and bulk crystals [23] provided substantial advances through the first elucidation of the low-temperature magnetoresistive behavior of this system, including large, field-asymmetric magnetoresistance due to a novel surface spin reorientation. As part of an effort to bring the tools of polarized SANS to the CQM, *Leighton* has applied this method to ferromagnetic Ni nanoparticle assemblies, resulting in the first direct observation of nanometric magnetic dead shells arising due to chemical reactions with

ligands [9]. On the theory front, *Fernandes* and collaborators elucidated the behavior of the thermal pseudogap generated by spin fluctuations [29] and the properties of the spin-resonance mode, which can be observed via neutron scattering, in unconventional superconductors with weak out-of-plane anisotropy [8].

Future Plans

Elastic and plastic deformation of STO and other bulk quantum materials will be pursued *via in situ* scattering experiments involving new strain cells; one of these cells is being tested and refined through a collaborative beam time proposal at ORNL. This will be complemented by in-house strain studies of electronic properties. Strain engineering work on cobaltites will further tune the balance between the spin-state and magnetic ordering temperatures, pursuing the spin-state quantum critical point, as well as studying fascinating heterostructures of these materials. CQM's ability to grow the largest available delafossite single crystals will enable inelastic scattering experiments to study phonons, to be compared with DFT, and neutron diffraction and spectroscopy studies of complex frustrated magnetism in the analogous $PdCrO_2$. Comprehensive studies of the model cuprate $HgBa_2CuO_{4+\delta}$, including cutting-edge diffuse scattering and ΔPDF analysis, will be extended to ever lower doping levels. Work on the bismuthates will be extended to inelastic scattering measurements of phonons, and to transport and thermodynamic measurements. Work on NiS_2 will be extended to hole/electron doping and involve neutron powder diffraction and SANS. In May 2024, CQM and the University of Minnesota Fine Theoretical Physics Institute (FTPI) plan to co-host a workshop on *New Insights into Quantum Materials: Scattering, Other Probes, and Theory.*

Publications

1. S. Hameed, D. Pelc, Z. W. Anderson, A. Klein, R. J. Spieker, L. Yue, B. Das, J. Ramberger, M. Lukas, Y. Liu, M. J. Krogstad, R. Osborn, Y. Li, **C. Leighton**, **R. M. Fernandes**, and **M. Greven**, *Enhanced superconductivity and ferroelectric quantum criticality in plastically deformed strontium titanate*, Nat. Mater. **21**, 54 (2022).
2. R. A. Gnabasik, P. K. Suri, J. Chen, and D. J. Flannigan, *Imaging coherent phonons and precursor dynamics in LaFeAsO with 4D ultrafast electron microscopy*, Phys. Rev. Mater. **6**, 024802 (2022).
3. Z. Wang, D. Gautreau, **T. Birol**, and **R. M. Fernandes**, Strain-tunable metamagnetic critical endpoint in Mott insulating rare-earth titanates, Phys. Rev. B **105**, 144404 (2022).
4. J. Chen, and D. J. Flannigan, *A quantitative method for in situ pump-beam metrology in 4D ultrafast electron microscopy*, Ultramicroscopy **234**, 113485 (2022).
5. A. Najev, S. Hameed, D. Gautreau, Z. Wang, J. Joe, M. Požek, **T. Birol**, **R. M. Fernandes**, **M. Greven**, and D. Pelc, *Uniaxial Strain Control of Bulk Ferromagnetism in Rare-Earth Titanates*, Phys. Rev. Lett. **128**, 167201 (2022).
6. J. Yue, Y. Ayino, T. K. Truttmann, M. N. Gastiasoro, E. Persky, A. Khanukov, D. Lee, L. R. Thoutam, B. Kalisky, **R. M. Fernandes**, V. S. Pribiag, and B. Jalan, *Anomalous transport in high-mobility superconducting $SrTiO_3$ thin films*, Sci. Adv. **8**, 21 (2022).
7. P. P. Orth, D. Phelan, J. Zhao, H. Zheng, J. F. Mitchell, **C. Leighton**, and R. M. Fernandes, *Essential role of magnetic frustration in the phase diagrams of doped cobaltites*, Phys. Rev. Mater. **6**, L071402 (2022).
8. F. Chen, **R. M. Fernandes**, and M. H. Christensen, *Hot-lines topology and the fate of the spin resonance mode in three-dimensional unconventional superconductors*, Phys. Rev. B **106**, 014511 (2022).
9. B. Das, J. Batley, C. Korostynski, M. Nguyen, I. Kamboj, K. Krycka, P. Quarterman, J. Borchers, E.S. Aydil, and **C. Leighton**, *Chemically Induced Magnetic Dead Shells in Superparamagnetic Ni Nanoparticles Deduced from Polarized Small-Angle Neutron Scattering*, ACS. Appl. Mater. Interf. **14**, 33491 (2022).
10. C. Naya, D. Schubring, M. Shifman, and Z. Wang, *Skyrmions and hopfions in three-dimensional frustrated magnets*, Phys. Rev. B **106**, 094434 (2022).

11. T. D. C. Hobson, H. Shiel, C. N. Savory, J. E. N. Swallow, L. A. H. Jones, T. J. Featherstone, M. J. Smiles, P. K. Thakur, T.-L. Lee, B. Das, **C. Leighton**, G. Zoppi, V. R. Dhanak, D. O. Scanlon, K. Durose, J. D. Major, and T. D. Veal, *P-type conductivity in Sn-doped Sb_2Se_3*, J. Phys. Energy **4**, 045006 (2022).
12. Y. Zhang, A. Saha, F. Tutt, V. Chaturvedi, B. Voigt, W. Moore, J. Garcia-Barriocanal, **T. Birol**, and **C. Leighton**, *Thermal properties of the metallic delafossite $PdCoO_2$: A combined experimental and first-principles study*, Phys. Rev. Mater. **6**, 115004 (2022).
13. D. Pelc, R. J. Spieker, Z. W. Anderson, M. J. Krogstad, N. Biniskos, N. G. Bielinski, B. Yu, T. Sasagawa, L. Chauviere, P. Dosanjh, R. Liang, D. A. Bonn, A. Damascelli, S. Chi, Y. Liu, R. Osborn, and **M. Greven**, *Unconventional short-range structural fluctuations in cuprate superconductors*, Sci. Rep. **12**, 20483 (2022).
14. V. Kozii, A. Klein, **R. M. Fernandes**, and J. Ruhman, *Synergetic Ferroelectricity and Superconductivity in Zero-Density Dirac Semimetals near Quantum Criticality*, Phys. Rev. Lett. **129**, 237001 (2022).
15. V. Chaturvedi, S. Ghosh, D. Gautreau, P. Quarterman, P. P. Balakrishnan, B. J. Kirby, H. Zhou, H. Cheng, A. Huon, T. Charlton, M. R. Fitzsimmons, W. M. Postiglione, A. Jacobson, C. Korostynki, J. E. Dewey, J. G. Barriocanal, **T. Birol**, K. A. Mkhoyan, and **C. Leighton**, *Room-temperature valence transition in a strain-tuned perovskite oxide*, Nat. Commun. **13**, 7774 (2022).
16. S. Griffitt, M. Spaić, J. Joe, Z. Anderson, D. Zhai, M. J. Krogstad, R. Osborn, D. Pelc, **M. Greven**, *Local inversion-symmetry breaking in a bismuthate high-T_c superconductor*, Nat. Commun. **14**, 845 (2023).
17. J. E. Dewey, S. Ghosh, V. Chaturvedi, W. M. Postiglione, L. Figari, A. Jacobson, C. Korostynski, T. R. Charlton, K. A. Mkhoyan, and **C. Leighton**, *Anomalous strain relaxation and its impact on the valence-driven spin-state/metal-insulator transition in epitaxial $(Pr_{1-y}Y_y)_{1-x}Ca_xCoO_{3-\delta}$*, Phys. Rev. Mater. **7**, 024415 (2023).
18. A. Klein, V. Kozii, J. Ruhman, and **R. M. Fernandes**, *Theory of criticality for quantum ferroelectric metals*, Phys. Rev. B **107**, 165110 (2023).
19. R. Hartmann, M. Hogen, D. Lignon, A. K. C. Tan, M. Amado, S. El-Khatib, M. Egilmez, B. Das, **C. Leighton**, M. Atature, E. Scheer, and A. Di Bernardo, *Intrinsic giant magnetoresistance due to exchange-bias-type effects at the surface of single-crystalline NiS_2 nanoflakes*, Nanoscale **15**, 10277 (2023).
20. H. Zhang, Z. Wang, D. Dahlbom, K. Barros, C. D. Batista, *CP^2 skyrmions and skyrmion crystals in realistic quantum magnets*, Nat. Commun. **14**, 3626 (2023).
21. S. Roy, F. Ye, Z. Morgan, K. Mathur, A. Parulekar, S. I. A. Jalali, Y. Zhang, G. Cao, N.-H. Kaneko, **M. Greven**, R. Raj, and D. Reznik, *Structural changes induced by electric currents in a single crystal of Pr_2CuO_4*, Phys. Rev. Materials **7**, 083803 (2023).
22. S. Hameed, Z. Wang, D. M. Gautreau, J. Joe, K. P. Olson, S. Chi, P. M. Gehring, T. Hong, D. M. Pajerowski, T. J. Williams, Z. Xu, M. Matsuda, **T. Birol**, **R. M. Fernandes**, and **M. Greven**, *Effect of random antiferromagnetic exchange on the spin waves in a three-dimensional Heisenberg ferromagnet*, Phys. Rev. B **108**, 134406 (2023).
23. S. El-Khatib, F. Mustafa, M. Egilmez, B. Das, Y. Tao, M. Maiti, Y. Lee, and **C. Leighton**, *Exotic surface magnetotransport phenomena in the antiferromagnetic Mott insulator NiS_2*, Phys. Rev. Mater. **7**, 104401 (2023).
24. Z. Wang, and C. D. Batista, *Skyrmion crystals in the triangular Kondo lattice model*, SciPost Phys. **15**, 161 (2023).
25. K. Currier, C.Y. Lin, K. Gotlieb, R. Mori, H. Eisaki, **M. Greven**, A. Fedorov, Z. Hussain, A. Lanzara, *Driving Spin Texture in High-Temperature Cuprate Superconductors via Local Structural Fluctuations*, (preprint).
26. W. Tabiś, P. Popčević, B. Klebel-Knobloch, I. Biało, C. M. N. Kumar, B. Vignolle, **M. Greven**, N. Barišić, *Arc-to-pocket transition and quantitative understanding of transport properties in cuprate superconductors*, (arXiv:2106.07457).
27. W. Simeth, Z. Wang, E. A. Ghioldi, D. M. Fobes, A. Podlesnyak, N. H. Sung, E. D. Bauer, J. Lass, J. Vonka, D. G. Mazzone, C. Niedermayer, Yusuke Nomura, Ryotaro Arita, C. D. Batista, F. Ronning, M. Janoschek, *A microscopic Kondo lattice model for the heavy fermion antiferromagnet $CeIn_3$*, (arXiv:2208.02211).
28. A. Najev, S. Hameed, A. Alfonsov, J. Joe, V. Kataev, **M. Greven**, M. Požek, D. Pelc, *Magnetic resonance study of rare-earth titanates*, (arXiv:2211.12387).
29. M. Ye, Z. Wang, **R. M Fernandes**, and A. V Chubukov, *Location and thermal evolution of the pseudogap due to spin fluctuations*, Phys. Rev. B **108**, 115156 (2023).
30. X. Wang, A. Kundu, B. Xu, S. Hameed, I. Sochnikov, D. Pelc, **M. Greven**, A. Klein, B. Kalisky, *Multiferroicity in plastically deformed $SrTiO_3$*, (arXiv:2308.14801).

31. T. E. Glier, M. Rerrer, L. Westphal, G. Lüllau, L. Feng, S. Tian, R. Haenel, M. Zonno, H. Eisaki, **M. Greven**, A. Damascelli, S. Kaiser, D. Manske, M. Rübhausen, *Direct observation of the Higgs mode in a superconductor by non-equilibrium Raman scattering*, (arXiv:2310.08162).
32. A. Montanaro, E. Maria Rigoni, F. Giusti, L. Barba, G. Chita, F. Glerean, G. Jarc, S. Y. Mathengattil, F. Boschini, H. Eisaki, **M. Greven**, A. Damascelli, C. Giannetti, D. Mihailovic, V. Kabanov, D. Fausti, *Dynamics of non-thermal states in optimally-doped $Bi_2Sr_2Ca_{0.92}Y_{0.08}Cu_2O_{8+\delta}$ revealed by mid-infrared three-pulse spectroscopy*, (arXiv:2310.10279).
33. J. E. Dewey, V. Chaturvedi, T. A. Webb, P. Sharma, W. M. Postiglione, P. Quarterman, P. P. Balakrishnan, B. J. Kirby, L. Figari, C. Korostynski, A. Jacobson, **T. Birol**, **R. M. Fernandes**, A. N. Pasupathy, **C. Leighton**, *First-order phase transition vs. spin-state quantum-critical scenarios in strain-tuned epitaxial cobaltite thin films*, (arxiv:2311.06127).
34. Y. Zhang, F. Tutt, G. N. Evans, P. Sharma, G. Haugstad, B. Kaiser, J. Ramberger, S. Bayliff, Y. Tao, M. Manno, J. Garcia-Barriocanal, V. Chaturvedi, **R. M. Fernandes**, **T. Birol**, W. E. Seyfried Jr., **C. Leighton**, *Crystal-Chemical Origins of the Ultrahigh Conductivity of Metallic Delafossites*, (arxiv:2308.14257).

University of Minnesota Center for Quantum Materials: CQM Research on Heteroepitaxial Strain Tuning of Perovskite Cobaltites

Turan Birol[1], Rafael Fernandes[2], Martin Greven (PI)[2], Chris Leighton[1]

[1]Department of Chemical Engineering and Materials Science, University of Minnesota

[2]School of Physics and Astronomy, University of Minnesota

Keywords: Complex oxides, perovskites, cobaltites, strain, neutron scattering

Research Scope

The University of Minnesota Center for Quantum Materials (CQM), founded in 2016, investigates the structural, electronic, and magnetic properties of select quantum materials, particularly complex oxides, which embody many of the most fundamental questions regarding quantum behavior of interacting electrons and are relevant to important technologies, including data storage, spintronics, catalysis, and fuel cells. *This abstract complements the main CQM abstract, focusing on the center's work on heteroepitaxial strain tuning of perovskite cobaltite materials*. This work involves all four CQM faculty (*Leighton*, *Birol*, *Fernandes*, and *Greven*), and relies heavily on both neutron and x-ray scattering.

As described in the main CQM abstract, strain tuning, through both elastic and plastic deformation, is a central unifying theme in the center's work. Thin films play directly into this, as high quality pseudomorphic epitaxy enables wide-ranging control of heteroepitaxial biaxial strain through substrate selection. Perovskite oxides are ideal for this approach, and perovskite cobaltites provide an excellent specific model system due to high sensitivity of their lattice/spin-state/electronic degrees of freedom to strain. Building on a history of prior work with bulk crystals and thin films of systems such as $La_{1-x}Sr_xCoO_3$ (as in our recent work elucidating magnetic frustration effects [1]), current CQM cobaltite efforts are focused on *Pr-containing* cobaltites. This is because systems such as $Pr_{1-x}Ca_xCoO_3$ and $(Pr_{1-y}Y_y)_{1-x}Ca_xCoO_3$ (PYCCO) exhibit remarkable, coupled first-order spin-state/structural/metal-insulator transitions, triggered by a Pr valence shift mechanism. In essence, Pr shifts from 3+ toward 4+ at a specific temperature in these materials (~90 K in bulk $Pr_{1-x}Ca_xCoO_3$), inducing a change in Co hole density and thus electronic and magnetic properties. This transition is stabilized by chemical pressure in $(Pr_{1-y}Y_y)_{1-x}Ca_xCoO_3$ (PYCCO), rendering this a model system for the study of these phenomena, which have strong parallels with anomalous valence tendencies in other rare-earth based compounds, particularly the $RBa_2Cu_3O_{7-x}$ series (in which Pr is the only non-superconducting member). Recent CQM work (by *Leighton* and *Birol*) thus used heteroepitaxial strain in thin films of the PYCCO system, seeking strain control over the electronic ground state [2-4].

Recent Progress

As shown in Fig. 1(a), epitaxy of thin films of PYCCO (~30-unit-cell-thick) on complex oxide substrates such as YAO, SLAO, LAO, and LSAT, results in biaxial in-plane strains (ε_{xx}) from -2.1% (compressive) to +2.3% (tensile), generating spectacular changes in electronic and magnetic properties [2]. In particular, tensile strain induces a ferromagnetic metallic state that does not exist in bulk at this composition, while compressive strain promotes the metal-insulator transition that takes place on cooling. The ferromagnetism under tension is indeed essentially depth-wise uniform, as verified by the polarized neutron reflectometry data in Fig. 1(b), for which refinements reveal ~1 μ_B/Co saturation magnetization throughout the film interior [2]. Most significantly, the enhancement

of the metal-insulator transition under compression is to ~250 K (Fig. 1(a)), double the bulk value at this composition ($(Pr_{0.85}Y_{0.15})_{0.7}Ca_{0.3}CoO_3$). That this is indeed a valence-driven spin-state/structural/metal-insulator transition was explicitly verified through temperature-dependent synchrotron x-ray diffraction and electron energy loss spectroscopy [2]. Moreover, compositional fine tuning to $(Pr_{0.75}Y_{0.25})_{0.7}Ca_{0.3}CoO_3$ was then performed, increasing the transition temperature to 291 K, *i.e.*, ambient temperature, realizing the first room-temperature valence transition in any perovskite oxide, with substantial device potential [2].

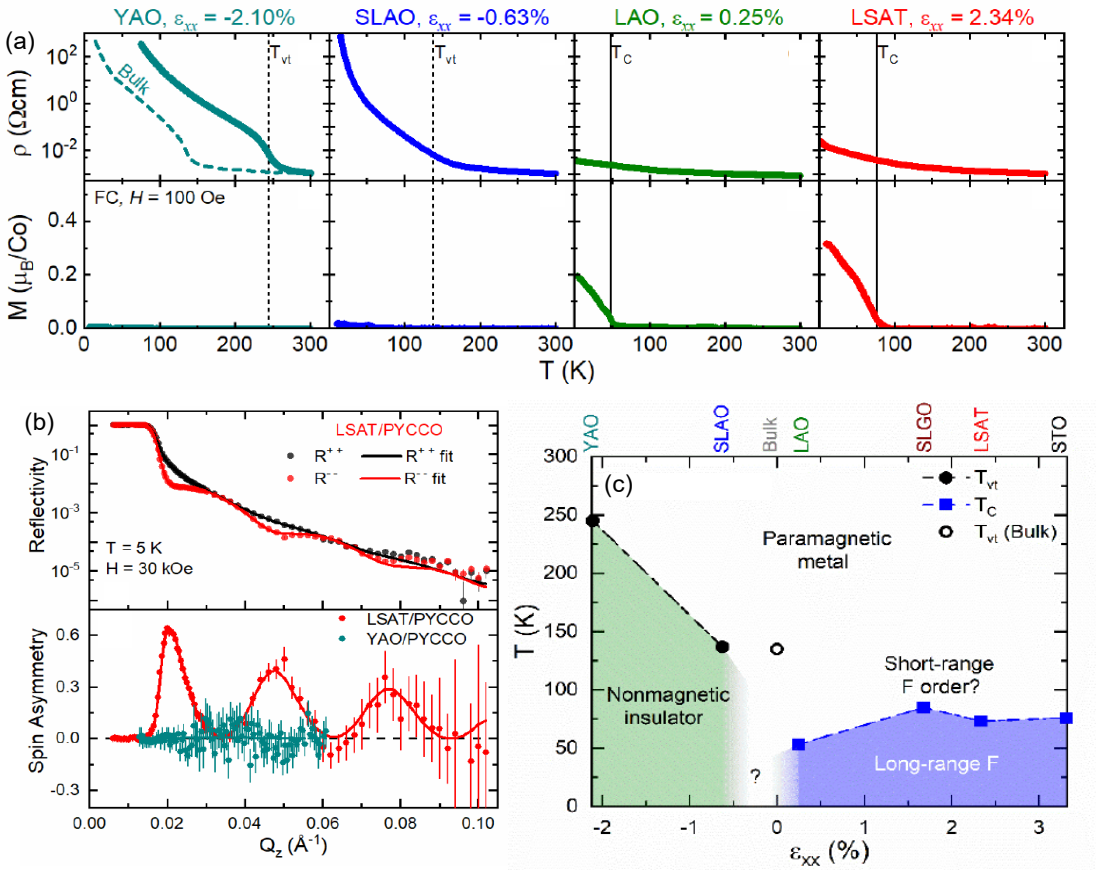

Fig. 1. (a) Temperature-dependence of the resistivity (top) and magnetization (bottom) of fully-strained PYCCO films grown on YAO, SLAO, LAO, and LSAT substrates. (b) Polarized neutron reflectometry data from a ferromagnetic film on LSAT, compared to a non-ferromagnetic film on YAO. (c) Resulting strain phase diagram.

The above behavior results in the strain phase diagram shown in Fig. 1(c), capturing the complete control over the electronic ground state of this system, from nonmagnetic insulator under compression to ferromagnetic metal under tension. This behavior was also semi-quantitatively reproduced by model density functional theory calculations by *Birol* [2]. Such phase diagrams pose obvious additional questions, particularly what occurs in the white region labeled "?" between the two phases. Exactly this issue was addressed in the most recent CQM work of *Leighton*, *Fernandes* and *Birol* [3], using the relaxation of strain with increasing thickness on substrates such as SLAO to quasi-continuously traverse the region between the phases in Fig. 1(c). This resulted in the more detailed electronic/magnetic phase diagram shown in Fig. 2(a), revealing a clear mixed-phase regime in the central region, where nonmagnetic insulator and ferromagnetic metal domains spatially coexist [3]. This coexistence was not only inferred from magnetometry and electronic transport measurements, but also directly probed *via* polarized neutron reflectometry coupled with magnetic force microscopy. In particular, magnetic force microscopy directly unveiled nanometric spatial coexistence of the two electronic phases [3]. With the aid of theory by *Fernandes* and *Birol*, this was

directly interpreted in terms of a first-order phase transition as a function of strain. The significance of this result is that it lies in stark contrast with the previously discussed possibility of a spin-state quantum critical point in such a scenario, where the spin gap decreases to zero followed by the emergence of a magnetic ordering temperature. The theory of *Fernandes* and *Birol* points to a means to further pursue such a unique quantum critical point, however, specifically through compositional tuning to decrease the spin-state transition temperature of the employed PYCCO films [3].

Finally, similar strain relaxation was also explored on other substrates, including YAO [4]. What evolves in that case is a remarkable situation where the strain relaxation mechanism is of completely different character to the standard Matthews-Blakeslee picture. As shown in Fig. 2(b), at higher thicknesses, a defect-free region remains at the bottom of the film, followed by an abrupt transition to a defective upper region that hosts a strikingly periodic dislocation array with accompanying top-surface modulation [4]. Such a mechanism has rarely, if ever, been reported in oxides. In our recent work, this was characterized in detail, connecting atomic-resolution cross-sectional transmission electron microscopy with extensive x-ray scattering characterization, and transport and magnetic measurements, to provide a complete picture of this unusual phenomenon [4].

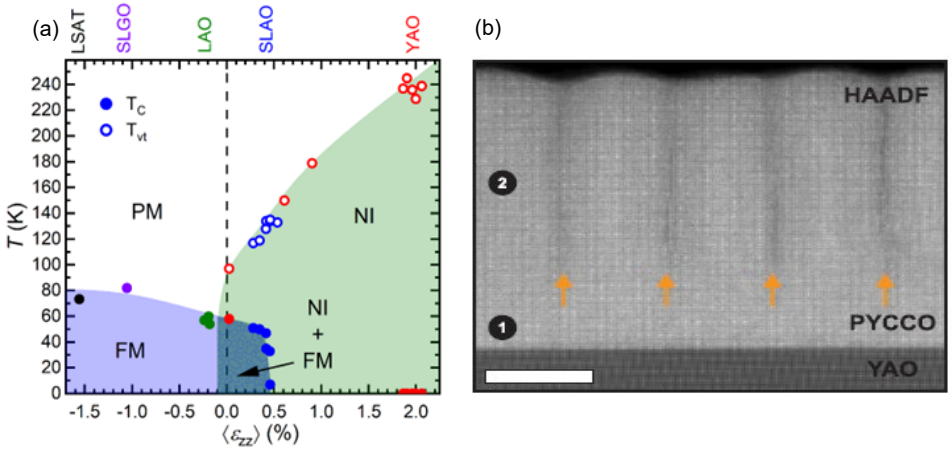

Fig. 2. (a) More detailed strain phase diagram of PYCCO revealing the dark green phase coexistence regime. (b) Cross-sectional transmission electron microscopy image of a YAO/PYCCO film revealing a periodic dislocation array (orange arrows) terminating in the central region of the film.

Future Plans

As already noted, the alluring spin-state quantum critical point remains a viable possibility in this system, provided that the spin state transition temperature can be suppressed. Experiments are currently underway to pursue exactly this, guided by theory by *Birol* and *Fernandes*, using composition control of the starting PYCCO as a tuning mechanism. *Greven* and *Leighton* are also pursuing uniaxial pressure control over this system, combining fixed heteroepitaxial biaxial strain with variable uniaxial pressure achieved through *Greven*'s recently developed pneumatic strain cells. The CQM's ability to plastically deform materials such as $SrTiO_3$ to generate periodic dislocation arrays is also being pursued to imprint periodic defect arrays into overgrown cobaltite films, using deformed $SrTiO_3$ and related materials as substrates. Finally, the controllable, temperature-dependent structural/metal insulator transition in PYCCO films also presents some unique opportunities in more complex heterostructures. In experiments initially designed to explore if such transitions couple in PYCO bilayers with different transition temperatures, it was recently discovered that the interfaces between such films are unexpectedly metallic, suggesting the extraordinary possibility of a two-dimensional electron gas at the interface (in a non-titanate oxide heterostructure). This is currently

being explored through a combination of careful epitaxy, electronic transport measurements, and scattering characterization.

Publications (this abstract only; see the main CQM abstract for a full listing)

35. P. P. Orth, D. Phelan, J. Zhao, H. Zheng, J. F. Mitchell, **C. Leighton**, and R. M. Fernandes, *Essential role of magnetic frustration in the phase diagrams of doped cobaltites*, Phys. Rev. Mater. **6**, L071402 (2022).
36. V. Chaturvedi, S. Ghosh, D. Gautreau, P. Quarterman, P. P. Balakrishnan, B. J. Kirby, H. Zhou, H. Cheng, A. Huon, T. Charlton, M. R. Fitzsimmons, W. M. Postiglione, A. Jacobson, C. Korostynki, J. E. Dewey, J. G. Barriocanal, **T. Birol**, K. A. Mkhoyan, and **C. Leighton**, *Room-temperature valence transition in a strain-tuned perovskite oxide*, Nat. Commun. **13**, 7774 (2022).
37. J. E. Dewey, V. Chaturvedi, T. A. Webb, P. Sharma, W. M. Postiglione, P. Quarterman, P. P. Balakrishnan, B. J. Kirby, L. Figari, C. Korostynski, A. Jacobson, **T. Birol**, **R. M. Fernandes**, A. N. Pasupathy, **C. Leighton**, *First-order phase transition vs. spin-state quantum-critical scenarios in strain-tuned epitaxial cobaltite thin films*, (arxiv:2311.06127).
38. J. E. Dewey, S. Ghosh, V. Chaturvedi, W. M. Postiglione, L. Figari, A. Jacobson, C. Korostynski, T. R. Charlton, K. A. Mkhoyan, and **C. Leighton**, *Anomalous strain relaxation and its impact on the valence-driven spin-state/metal-insulator transition in epitaxial* $(Pr_{1-y}Y_y)_{1-x}Ca_xCoO_{3-\delta}$, Phys. Rev. Mater. **7**, 024415 (2023).
39. N. Nandakumaran, W. Postiglione, V. Chaturvedi, and **C. Leighton**, in preparation.

University of Minnesota Center for Quantum Materials: CQM Research on Metallic Delafossites

Turan Birol[1], Rafael Fernandes[2], Martin Greven (PI)[2], Chris Leighton[1]

[1]Department of Chemical Engineering and Materials Science, University of Minnesota

[2]School of Physics and Astronomy, University of Minnesota

Keywords: Complex oxides, delafossites, electronic transport, neutron scattering, x-ray scattering

Research Scope

The University of Minnesota Center for Quantum Materials (CQM), founded in 2016, investigates the structural, electronic, and magnetic properties of select quantum materials, particularly complex oxides, which embody many of the most fundamental questions regarding quantum behavior of interacting electrons and are relevant to important technologies, including data storage, spintronics, catalysis, and fuel cells. *This abstract complements the main CQM abstract, focusing on the center's work on metallic delafossite materials*. This involves all four CQM faculty (*Leighton*, *Birol*, *Fernandes*, and *Greven*), and both neutron and x-ray scattering.

The delafossites are a family of complex oxides with general formula ABO_2 that have been available synthetically since 1971. A subset of the delafossites are metallic, where conductive triangular sheets of A^{1+} ions are interspersed with insulating $B^{3+}O_6$ edge-sharing octahedral layers, generating a remarkably simple electronic structure at the Fermi level. Only in the last 10 years, however, was it understood that despite their highly anisotropic complex-oxidic nature, metallic delafossites (particularly $PdCoO_2$ and $PtCoO_2$) are the *most conductive oxides known*, for reasons that are poorly understood. In particular, their room-temperature resistivity can be lower than that of Au and their low-temperature resistivity is as low as 8 nΩ cm, implying mean-free-paths of a staggering 20 μm. These extraordinary values have led to a slew of recent advances, spanning ballistic electron transport, claims of hydrodynamic transport, discoveries of new quantum oscillations, *etc*. To reach such striking low-temperature resistivities and mean-free-paths, it is widely accepted that these materials must be ultrapure and ultraperfect, although the methods for their bulk growth (which produce only small crystals) are not typically capable of such. This is the stimulus for CQM research in this area, seeking to understand: What is special about the electron-phonon scattering in such systems to enable such low room-temperature resistivity, and how crystals of these systems attain the perfection needed for such extraordinary residual resistivities.

Recent Progress

The first CQM advance in this area, driven by *Leighton*, was a new approach to crystal growth of the model metallic delafossite $PdCoO_2$, attempting to overcome limitations of the current metathesis/flux method. A novel chemical vapor transport (CVT) method was developed, leading to an immediate 500-fold enhancement in crystal mass (Fig. 1(a,b)) [1,2]. Critically, this opens up a variety of measurements that were not previously viable, including various types of scattering. These crystals were then employed in a wide-temperature-range study of thermal properties by *Leighton* and *Birol* [1]. The *R*-3*m* structure was found stable from 10-1000 K, with thermal expansion in remarkable agreement with density functional theory (DFT) [1]. Detailed analysis also shed light on the stability of the low-spin ($S = 0$, $t_{2g}^6 e_g^0$) state of Co^{3+}, which derives from the short Co-O bond length and hence large crystal-field splitting; strong metallic bonds in the Pd sheets are the ultimate source of this effect.

Specific heat was also found to be in agreement with DFT, which was traced to a simple description in terms of a Debye model augmented with an Einstein oscillator [1]. This was rationalized based on the DFT phonon band structure, which revealed high-frequency, two-dimensional, oxygen-related optical modes, separated from the remaining Pd-, Co-, and O-based modes [1]. This work thus brought the thermal properties of metallic delafossites to a level comparable to that of the electronic properties, for the first time.

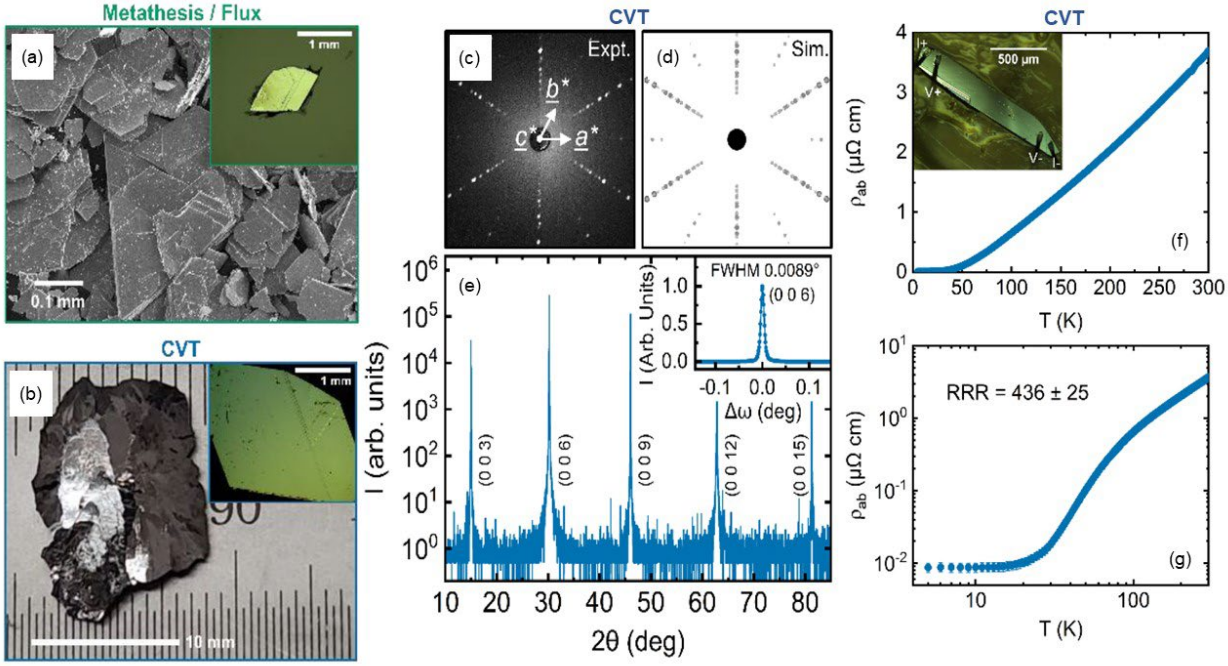

Fig. 1. (a,b) Comparison of standard metathesis/flux-grown $PdCoO_2$ crystals and new CVT-grown crystals. (c-e) Laue and high-resolution single-crystal x-ray diffraction characterization of CVT-grown $PdCoO_2$. The rocking curve width is a record for metallic delafossites. (d,e,) *a*-*b* plane resistivity of CVT-grown $PdCoO_2$, showing record RRR.

More significantly, the most recent CQM work, by *Leighton*, *Birol* and *Fernandes*, demonstrated that CVT-grown crystals of $PdCoO_2$ have the highest structural qualities yet reported (Fig. 1(a-e)), and record residual resistivity ratios ($440 < RRR < 760$, Fig. 1(f,g)) [2]. Nevertheless, the first detailed mass spectrometry measurements revealed, in contrast to the prevailing narrative, that they are *not* ultrapure, typically harboring 100s-of-part-per-million impurity levels [2]. Through detailed crystal-chemical analyses, we resolved this apparent dichotomy, showing that the vast majority of impurities are forced to reside in insulating Co-O octahedral layers, leaving the conductive Pd sheets highly pure. These purities were then shown to be in *quantitative agreement* with measured residual resistivites [2]. We thus concluded that a "sublattice purification" mechanism is essential to the ultrahigh low-temperature conductivity and mean-free-path of metallic delafossites [2], opening up many exciting possibilities.

Future Plans

Building on the above, the CQM is currently expanding its study of metallic delafossites, taking advantage of the newly available large single crystals. Magnetically-doped $PdCo_{1-x}Cr_xO_2$ has been synthesized, realizing near-deal non-interacting paramagnetism up to ~5% Cr [3]. Remarkably, such crystals have 1000-fold higher Cr concentration than undoped crystals, but only 3-fold higher residual resistivity, validating our sublattice purification picture [3]. In addition, prominent magnetic specific heat and Kondo minima arise, suggesting a Kondo effect from Pd *s* – Cr *d* exchange between layers, of high interest [3]. Pure $PdCrO_2$ has also been synthesized, to study the unresolved non-collinear, non-coplanar antiferromagnetic spin structure in this geometrically frustrated triangular lattice system. Neutron diffraction and SANS are planned, and will be coupled with transport, seeking to understand the unconventional anomalous Hall effect in this antiferromagnet. Preliminary work shows the absence of a previously reported weak ferromagnetic signal, which is likely due to phase impurities eliminated in CVT growth. Anomalous thermal expansion has also been detected in $PdCrO_2$ [4].

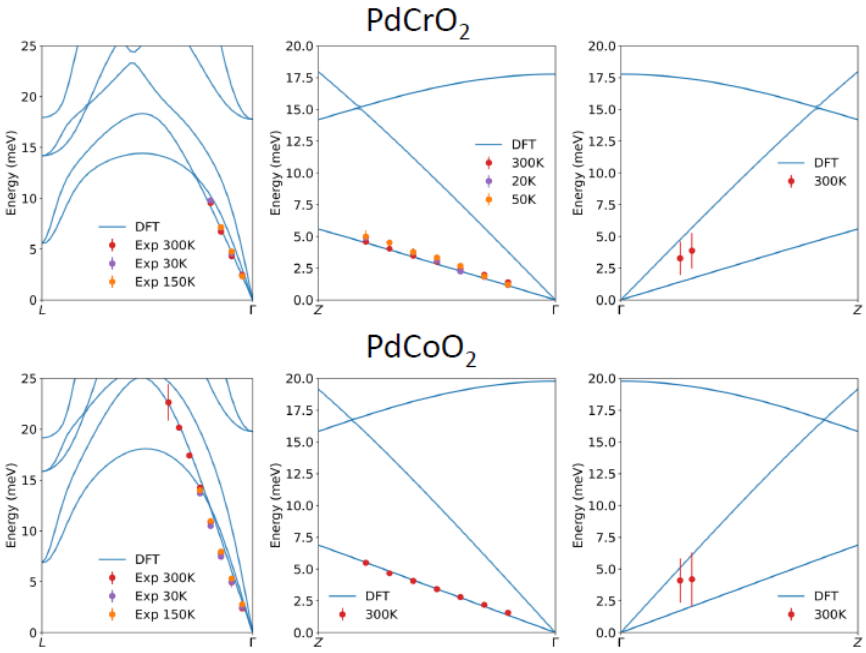

Fig. 2. DFT (solid lines) and measured (points) phonon dispersions in $PdCrO_2$ (top) and $PdCoO_2$ (bottom) at various temperatures.

Finally, directed at improved understanding of the critical electron-phonon interactions and scattering in these compounds, initial inelastic x-ray scattering measurements have been performed by *Leighton* and *Greven*, and will be expanded to inelastic neutron scattering. Initial measurements of dispersion of acoustic modes (Fig. 2) reveals good agreement with DFT by *Birol*. $PdCoO_2$ and $PdCrO_2$ have also been compared, leading to the insight that some temperature-dependent mode softening occurs in $PdCrO_2$. This work is close to publication, likely along with thermal expansion measurements by temperature-dependent diffraction [4].

Publications (this abstract only; see main CQM abstract for a full listing)

40. Y. Zhang, A. Saha, F. Tutt, V. Chaturvedi, B. Voigt, W. Moore, J. Garcia-Barriocanal, **T. Birol**, and **C. Leighton**, *Thermal properties of the metallic delafossite $PdCoO_2$: A combined experimental and first-principles study*, Phys. Rev. Mater. **6**, 115004 (2022).
41. Y. Zhang, F. Tutt, G. N. Evans, P. Sharma, G. Haugstad, B. Kaiser, J. Ramberger, S. Bayliff, Y. Tao, M. Manno, J. Garcia-Barriocanal, V. Chaturvedi, **R. M. Fernandes**, **T. Birol**, W. E. Seyfried Jr., and **C. Leighton**, *Crystal-Chemical Origins of the Ultrahigh Conductivity of Metallic Delafossites*, (arxiv:2308.14257).
42. Y. Zhang, F. Tutt, B. Kaiser, R. Raj, A. Mkhoyan, and **C. Leighton**, in preparation.
43. Y. Tao, Y. Zhang, F. Tutt, E. Ritz, X. He, D. Zhai, J. Garcia-Barriocanal, **T. Birol**, **M. Greven**, and **C. Leighton**, in preparation.

Dynamic Modulation of Structure and Phase Transformations in Asymmetric Crystalline Colloidal Brush Alloys

Michael R. Bockstaller, Krzysztof Matyjaszewski, Alamgir Karim

Keywords: brush colloid, phase separation, SANS, neutron reflection, hyperuniformity

Research Scope

Progress in the chemistry and physics underlying the organization of surfactant-modified particles now provides a framework for the controlled assembly of multi-component particle systems into a range of superlattice structures that mimic atomic crystals. The opportunities for property engineering that are afforded by these processes have instigated a new era for both the fundamental science and engineering of particle-based materials. Polymeric ligands present new opportunities to smoothly vary interparticle potentials, to selectively vary relevant material characteristics or to reversibly switch from attractive to repulsive interactions between constituents that could advance the development of a generalized physics framework for interpreting structure formation in particle-based materials [1]. *The overarching scope of this collaborative research program is to elucidate the governing parameters that control the structure formation in systems of mixed polymer-modified colloids and to demonstrate that interactions between polymer ligands can drive the reversible transition between distinct ordered and disordered structural (and property) states.* The research is devided into three research thrusts that focus on (1) the synthesis of model brush particles with polymer composition suitable for instigating LCST transitions in mixed brush particle systems and in which the neutron scattering length density (SLD) of particle core and polymer shell can be varied independently; (2) the elucidation of the role of brush architecture on temperature-dependent structure formation and transitions in mixed brush particle systems using SANS, SAXS, and electron as well as scanning probe microscopy; and (3) the characterization of the dynamical properties of brush particles using NR and the evaluation of the effect of dynamic constraints on the kinetics of phase transformations in LCST brush particle alloys.

Recent Progress

The polymer ligand chemistry to instigate *T*-induced phase transitions was developed as part of the previous funding period and is based on poly(methyl methacrylate) (PMMA) and poly(styrene-*r*-acrylonitrile) (PSAN) polymer grafts [2]. The polymers are amorphous with high glass transition temperature ($T_g \sim 115$ °C) and, upon mixing, feature a lower critical solution temperature (*LCST*) at ~ 160°C. This allows tuning of the Flory interaction parameter $\chi(T)$ from negative to positive by variation of temperature in the range $120°C < T < 180°C$ [3]. The use of deuterated monomers allows variation of SLD across the range $SLD_{PMMA} = 1.06 – 6.46\times10^{10}$ cm^{-2}; $SLD_{PSAN} = 1.56 – 5.64 \times10^{10}$ cm^{-2}, respectively. Two particle core chemistries are being pursued as platform for brush colloid model systems: First, as part of the previous funding period, a novel organo silica ($oSiO_2$) precursor

was developed that enables the one-step synthesis of ATRP-initiator modified $oSiO_2$ particles with narrow size dispersity (<3%) [4]. Variation of the degree of deuteration of the organo-constituent enables control of SLD in the range 1.09 – 2.81×10^{10} cm^{-2}. Limitations of this approach are the small particle diameter (1.5 nm – 5 nm) due to self-limiting particle growth as well as dilute grafting densities (~ 0.1 nm^{-2}). To overcome these limitations, research in the current funding period was focused on the development of a novel miniemulsion technique using a mixed surfactant system that enables the synthesis of crosslinked organoparticles with size 10 nm – 35 nm and narrow size dispersity (< 2%) [P2, P7]. The use of initiator-modified monomers (i.e., 'inimers') enables dense crosslinking and high density of initiating sites (>1 nm^{-2}) for subsequent surface polymerization (Figure 1). Advantages of this new particle chemistry entail a more narrow size dispersity as compared to established sol-gel chemistries, a wider accessible range of SLD (1.23 – 4.47 $\times10^{10}$ cm^{-2}) by variation of deuterated inimers as well as the tunability of the elastic modulus of particles by variation of the crosslink density across the range 1 – 3.8 GPa. The versatility of this material system renders inimer-organoparticles a unique model system to elucidate the governing paramters controlling the assembly of brush particle systems and, in particular, the formation of hyperuniform structures that will be the subject of our future research.

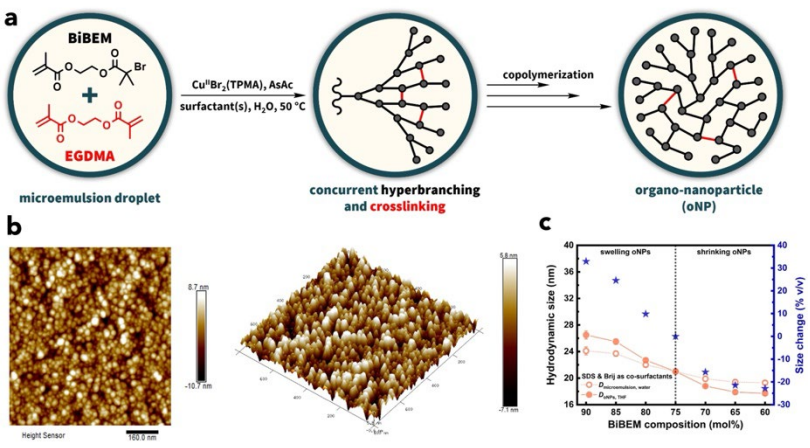

			SLD ($\times10^{-10}$ cm^{-2}) ; $X_D = 0 \rightarrow 1$
B90E10	90	10	1.24 - 3.97
B75E25	75	25	1.23 - 4.22
B60E40	60	40	1.22 - 4.47

Figure 1. Panel a-c : Illustration of mixed surfactant miniemulsion process (a) for synthesis of inimer-organoparticles with narrow (<2%) size dispersity (b) and tunable diameter (c). Panel d shows accessible SLD range variation of degree of deuteration of inimer.

Ligand-induced phase separation of binary brush particle blends was evaluated for the example of equimolar $oSiO_2$-PMMA/$oSiO_2$-PSAN (d = 3.5 nm, $N_{PMMA} \sim N_{PSAN} \sim 250$) by quenching of systems at 180 °C > LCST = 165 °C for t = 0.5, 1, 2, 6, 12, 24, 48, and 72h and subsequent vitrification. Electron imaging confirmed the phase separation of blends by spinodal decomposition (Fig. 2a, b). SANS experiments performed at SNS (EQ-SANS, BL-6, Fig. 2c) revealed two distinct domain growth regimes featureing scaling coefficients ($\xi \sim t^x$) of x = 0.18 and 0.3, respectively (inset of Fig. 2c). The result was rationalized as consequence of dynamical constraints due to caging of brush particles in the melt state that causes the initial domain growth to proceed through *sub diffusion* (x < 0.3) [in preparation].

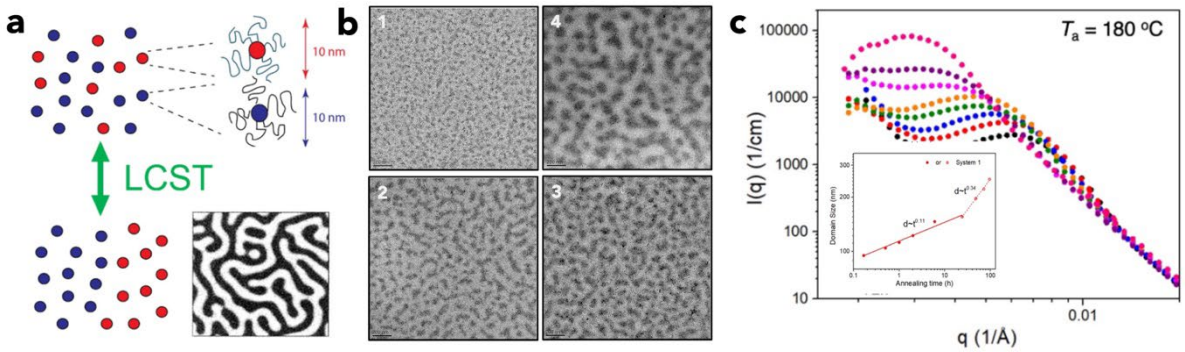

Figure 2. Panel a: Illustration of ligand-induced spinodal decomposition in symmetric LCST brush particle blend. Panel b: TEM of SiO_2-PSAN/SiO_2-PMMA (50/50) blends after 0.5 h (1), 1h (2), 3h (3) and 6h (4) of thermal annealing at 180 C°. Image shows formation of bicontinuous spinodal structure. Scale bar is 400 nm. Panel c: SANS curves of oSiO_2-PMMA/oSiO_2-PSAN blends as a function of annealing time at 180°C. Peak at low-q indicates domain size. Inset shows domain growth kinetics depicting anomalous ($t^{0.1}$) and normal ($t^{0.3}$) growth regimes.

Numerical simulations have shown the ratio between the characteristic timescale of cage confinement and self diffusion to be $\tau_{cage}/\tau_R \sim 12$ for typical colloidal systems near the glass transition. The characteristic timescale for particle brush self diffusion τ_R was determined from layer interdiffusion experiments. A bilayer stack (2 ×100 nm thickness) of fully deuterated and hydrogenated oSiO_2-PMMA was annealed at 140 ºC and the SLD profile was monitored using NR (SNS, BL-4). Analysis of the interfacial width revealed a brush particle self-diffusionet coefficient of $D = 6.87\times10^{-16}$ cm^2/s (Figure 3). The characteristic timescale for self diffusion follows as $\tau = R^2/2D \sim 1500$ s where R = 15 nm is the diameter of a brush particle (i.e., sum of particle diameter and twice the brush height) and diffusion along z-axis has been assumed. Thus, bilayer interdiffusion experiments suggest the transition from anomalous to regular domain growth to occur after about 6h, in reasonable agreement with the experimental value (~9.5h).

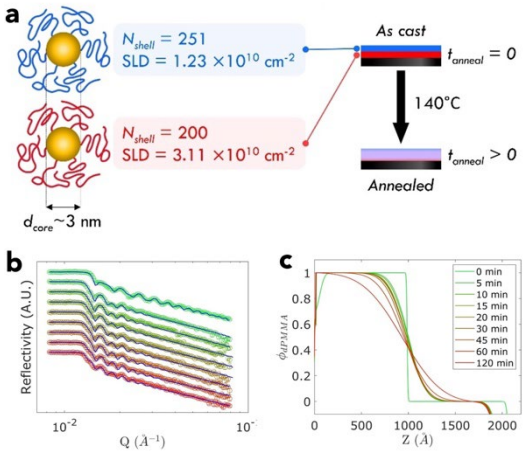

Figure 3. Panel a: Illustration of bilayer interdiffusion experiment to determine particle self diffusion coefficient. Panel b and c: Neutron reflectivity curves (b) and computed SLD profiles in z-direciton (c) as function of annealing time at T = 140

To better understand the role of sequence structure on the interaction of bursh particle-based materials, a series of poly(butyl acrylate-*co*-methyl methacrylate) copolymers with alternating, statistical and gradient sequence structure was synthesized. This copolymer system has attracted interest as platform for engineering polymers with self-heal ability [P1-P5]. SANS analysis revealed the formation of hetereogeneities in gradient sequence structures that can be harnessed to increase the Young's modulus of self healing polymer systems [P4]. Control of sequence structure was subsequently used to demonstrate brush particle hybrid materials featureing dual self-healing and shape memory properties [P3].

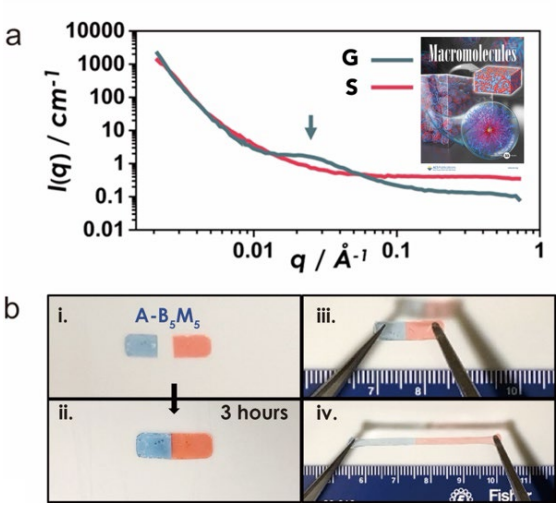

Figure 4. Panel a: SANS (BL-6, SNS) curves of gradient (G) and statistical (S) P(BA-co-MMA) films reveaing MMA cluster formation. Panel b demonstrates self-healing of films at 21 ºC.

Future Plans

Disordered hyperuniform materials represent an 'exotic' class of disordered materials that are characterized by the suppression of long-wavelength fluctuations and the absence of long-range order. Koch first hypothesized that the grafting of polymer chains to the surface of colloidal particles reduces density fluctuations in assembly structures [5]. However, hyperuniformity (H) could not be demonstrated. We hypothesize that this was due to a lack of control over chain and core dispersity. Preliminary results of the PIs support the feasibility of hyperuniform hybrid materials based on brush particle materials (Figure 5). The material chemistry developed as part of DE-SC0018784 thus sets the stage for a collaborative approach to elucidate the molecular parameters that govern H in self-assembled brush particle materials. This will be accomplished through chemistry-enabled control of particle size and stiffness, and the select control of the SLD of particle and polymer constituents to enable the synergistic application of X-ray and neutron scattering to elucidate the role of core size and stiffness as well as packing density, length and dispersity of tethered chains.

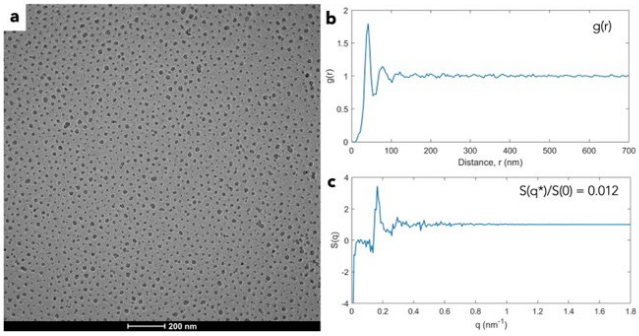

Figure 5. oSiO$_2$-PMMA particle brush monolayer revealing reduction of long wavelength fluctuations of particle density. Panel a shows TEM image. Panel b and c show pair distribution function $g(r)$ and structure factor $S(q)$.

References

1. T. W. Odom and M. -. Pileni, Nanoscience. Accounts of Chemical Research, 41, 1565–1565 (2008).
2. J. Yan, M. Bockstaller, and K. Matyjaszewski, Brush-modified materials Progr. Polym. Sci. 100, 101180, (2020).
3. K. Hahn, B. J. Schmitt, M. Kirschey, R. G. Kirste, H. Salie, and S. Schmitt-Strecker, Structure and thermodynamics in polymer blends. Polymer, 33, 5150-5166, (1992).
4. Y. Zhai, J. Han, Y. Zhao, K. Matyjaszewski, and M. R. Bockstaller. Processable Sub-5 Nanometer Organosilica Hybrid Particles for Dye Stabilization. ACS Appl. Polym. Mater. 3, 3631–3635, (2021).
5. H.-Y. Yu, S. Srivastava, L. A. Archer, and D. L. Koch Soft Matter, 10, 9120, (2014).

Publications

(P1) Y. Zhao, H. Wu, R. Yin, K. Matyjaszewski, and M. R. Bockstaller, The Importance of Bulk Viscoelastic Properties in "Self-Healing" of Acrylate-Based Copolymer Materials. ACS Macro Lett. (2023), ASAP, https://doi.org/10.1021/acsmacrolett.3c00626

(P2) R. Yin, Y. Zhao, J. Jeong, J. Tarnsangpradit, T. Liu, S. Y. An, Y. Zhai, X. Hu, M. R. Bockstaller, and K. Matyjaszewski, Composition-Orientation Induced Mechanical Synergy in Nanoparticle Brushes with Grafted Gradient Copolymers. Macromolecules (2023), ASAP, https://doi.org/10.1021/acs.macromol.3c01799

(P3) Y. Zhao, H. Wu, R. Yin, C. Yu, K. Matyjaszewski, and M. R. Bockstaller, Copolymer Brush Particle Hybrid Materials with "Recall-and-Repair" Capability. Chem. Mater. 35, 6990–6997, (2023)

(P4) Y. Zhao, R. Yin, H. Wu, Z. Wang, Y. Zhai, K. Kim, C. Do, K. Matyjaszewski, and M. R. Bockstaller, Sequence-Enhanced Self-Healing in “Lock-and-Key” Copolymers. ACS Macro Lett. 12, 475–480, (2023).
(P5) R. Yin, Y. Zhao, A. Gorczyński, G. Szczepaniak, M. Sun, L. Fu, K. Kim, H. Wu, M. R. Bockstaller, and K. Matyjaszewski, Alternating Methyl Methacrylate/n-Butyl Acrylate Copolymer Prepared by Atom Transfer Radical Polymerization. ACS Macro Lett. 11, 1217–1223, (2022).
(P6) W. Wu, M. Singh, Y. Zhai, A. Masud, W. Tonny, C. Yuan, R. Yin, A. M. Al-Enizi, M. R Bockstaller, K. Matyjaszewski, J. F. Douglas, A. Karim, Facile Entropy-Driven Segregation of Imprinted Polymer-Grafted Nanoparticle Brush Blends by Solvent Vapor Annealing Soft Lithography. ACS Appl. Mater. Interfaces, 14, 45765–45774, (2022).
(P7) R. Yin, P. Chmielarz, I. Zaborniak, Y. Zhao, G. Szczepaniak, Z. Wang, T. Liu, Y. Wang, M. Sun, H. Wu, J. Tarnsangpradit, M. R. Bockstaller, and K. Matyjaszewski, Miniemulsion SI-ATRP by Interfacial and Ion-Pair Catalysis for the Synthesis of Nanoparticle Brushes. Macromolecules, 55, 6332–6340, (2022).
(P8) M. Singh, A. Agrawal, W. Wu, A. Masud, E. Armijo, D. Gonzalez, S. Zhou, T. Terlier, C. Zhu, J. Strzalka, K. Matyjaszewski, M. Bockstaller, J. F. Douglas, and A. Karim, Soft-Shear-Aligned Vertically Oriented Lamellar Block Copolymers for Template-Free Sub-10 nm Patterning and Hybrid Nanostructures. ACS Appl. Mater. Interfaces, 14, 12824–12835, (2022).

Probing nano-structured quantum magnetism with neutrons

Collin Broholm and Satoru Nakatsuji, Institute for Quantum Matter and Department of Physics and Astronomy, Johns Hopkins University, Baltimore, MD.

Keywords: nano-wires, thin films, spin chains, Weyl magnetism, AFM domain switching

Research Scope

Neutron scattering sources and instrumentation have improved dramatically in recent decades and there are continued prospects for major advances. This opens the possibility to apply neutron scattering methods to explore dynamic aspects of nano-structured magnetic materials. In this project we focus on probing magnetic excitations and domain switching in such engineered magnetic materials using neutrons.

Recent Progress and Future plans

We have started several projects aimed at synthesizing nano-structured magnetic materials in sufficient quantities for inelastic neutron scattering experiments. A nano-molding technique will be used to form assemblies of single crystalline nano-wires of cubic ferro- and anti-ferromagnet model systems. Pulsed laser deposition is being explored as a method to form a mono-disperse assembly of Haldane spin chains in sufficient quantity for neutron scattering experiments. This should allow directly probing the collective magnetism of topologically protected spin-1/2 edge states. Finally, we are using magnetron sputtering to form thin films of the topological magnetic semi-metal Mn_3Sn. Here the goal is to probe electrical domain switching first statically and then dynamically using magnetic neutron scattering. All of these samples will be characterized by multiple other experimental techniques including x-ray diffraction and a range of thermo-magnetic measurements.

In this talk we shall discuss the feasibility of the proposed experiments and our progress towards developing the various forms of nano-structured samples.

Nonreciprocity and Light-controlled Phenomena in Low-symmetry Antiferromagnets: Neutron and Optical Vortex Beam Studies

Sang-Wook Cheong and Valery Kiryukhin (Rutgers U.) and Andrei Sirenko (NJIT)

Keywords: (Antiferro-)alter-magnetism, Nonreciprocity, Chiral excitations, Optical vortex beams.

Research Scope

Effects lacking symmetry under the exchange of source and detector are called nonreciprocal. They are well-known in optics and transport, but can occur for any (quasi)particles, including neutrons, spin waves etc. Numerous applications for these effects are in all-optics computing, quantum cryptography, and spintronics. While the nonreciprocal effects involving various quasiparticles are important for both fundamental and applied science, they are little studied, e.g., those for phonons, spin waves, electromagnons. Neutron scattering is an ideal probe for lattice/magnetic excitations. Our goal is to understand nonreciprocal effects utilizing inelastic neutron scattering, advanced crystal growth, and optical spectroscopy. We focus on studies of polar magnets, magnets with structural chirality, and ferrorotational magnets. Among these compounds are magneto-toroidal magnets, spin liquid systems, and unconventional magnetoelectrics. In these systems, combinations of absent inversion, time-reversal, and mirror symmetries can lead to nonreciprocal effects revealed, for example, in non-equivalent magnon/electromagnon spectra for the opposite propagation directions and as frequency-dependent directional dichroism (difference in the light absorption) in the optical spectra. The high-quality monodomain single crystals synthesized under this Project are crucial for the studies of nonreciprocal and magnetoelectric effects. Spectroscopic studies utilize vortex beams, which we recently developed as a new probe of magnetism in matter. Combined neutron and optical studies will reveal the physical mechanisms responsible for the exotic nonreciprocal properties in low symmetry materials and help identify prospective quantum materials for novel computational techniques.

Recent Progress

Magnetic structure of pyroelectric honeycomb antiferromagnet $Ni_2Mo_3O_8$ (NMO)**.** NMO belongs to the compound family exhibiting tunable magnetoelectricity (ME), optical diode effect, and nonreciprocal light propagation. It is a promising platform for studies of nonreciprocal magnons, as well as for control of magnetic domain populations with light. These properties are defined by the magnetic order and its underlying symmetries. Using neutron diffraction,[1] we have determined the complicated noncollinear magnetic order in NMO, see Fig. 1. The obtained symmetries of the ME tensor allowed to rationalize the complex ME properties of this compound. Our work also shows that the DM interaction cannot be responsible for the spin canting, as was assumed before, indicating the importance of anisotropic interactions. NMO can be grown as single structural/magnetic domain. Studies of nonreciprocal effects in NMO are planned.

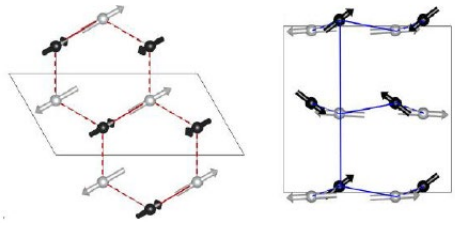

Fig 1. Magnetic structure of $Ni_2Mo_3O_8$

Dynamic Imaging of AFM domains. To observe many of the effects described in this project, monodomain (structural or magnetic) samples are essential. Imaging antiferromagnetic (AFM) domains is a nontrivial task. For some domain types, such as antiphase AFM domains in collinear magnets, there were no practical imaging approaches. We have recently invented a new imaging technique which is applicable to AFM phase domains. It is based on magnetic diffraction of coherent soft x-rays. We have now improved[2] the sensitivity of the method, making possible observation of AFM domain dynamics, including thermal fluctuations and directional motion of the domain walls under thermal gradients, see Fig 2. This is the first observation of this kind in real space and time. In addition to the scientific interest, these experiments open new possibilities for the studies of AFM spintronic devices in real time/space.

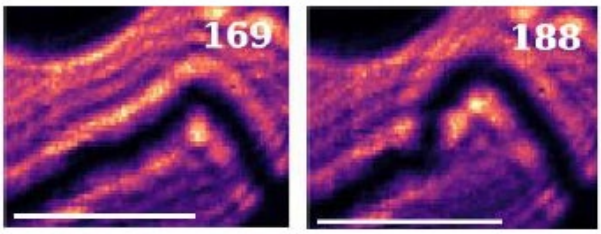

Fig 2. Moving AFM domain boundary under the thermal gradient created by beam heating. Scale bar is 10 μm, time difference between the images is 3.7 s.

Symmetric exchanges and helicoidal magnetism in $MnSb_2O_6$ (MSO). MSO is a noncentrosymmetric magnet with Mn^{2+} (S = 5/2, L ≈ 0) spins arranged on a triangular motif. The spins form a cycloidal structure which was believed to be tilted away from the *c* axis. We show that all elastic and inelastic neutron scattering results are consistent with an untilted cycloid. This structure originates from seven nearest-neighbor Heisenberg exchange constants. It is coupled to the underlying crystallographic chirality, in which polar domain switching has been reported. We apply neutron spectroscopy[3] to extract the magnetic exchange constants. The exchange network is complex. Thus, we use multiplexed neutron instrumentation and the first moment sum rule of neutron scattering. This fixes six constants. The last parameter is determined from the magnon dispersion near the zone boundary. We use the obtained symmetric exchange constants to calculate the low energy spin waves (previously analyzed using asymmetric coupling) and find agreement with experiments, see, *eg.*, Fig 3. Our results reveal the coupling between crystallographic and magnetic chirality through predominantly symmetric exchange, without any need for antisymmetric exchange paths.

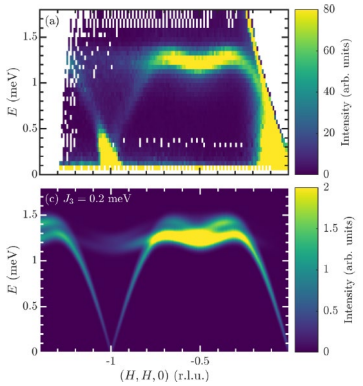

Fig 3. Spin wave dispersions. (top) Measured at MACS, and (bottom) calculated using linear spin-wave theory.

Directional nonreciprocity vs. Circular nonreciprocity. To establish the basis for exploring nonreciprocity in low-symmetry materials, we have performed a comprehensive symmetry analysis for directional nonreciprocity (nonreciprocal directional dichroism) as well as circular nonreciprocity (circular dichroism).[4] Numerous cases of directional nonreciprocity and circular nonreciprocity are illustrated in Fig. 4. All cases of Figs. 4(a-h) has the similar symmetry with a constant velocity (or linear momentum, $\boldsymbol{k}$). Circular nonreciprocity in Fig. 4(i,j) is directionally nonreciprocal (i.e. related to the Faraday effect in the case of dissipationless transmission), but circular nonreciprocity in Figs. (k-q) are directionally reciprocal (i.e. related to natural optical activity

in the case of dissipationless transmission). Some of the predicted exotic properties have been recently observed. We are using these results for planning future experiments.

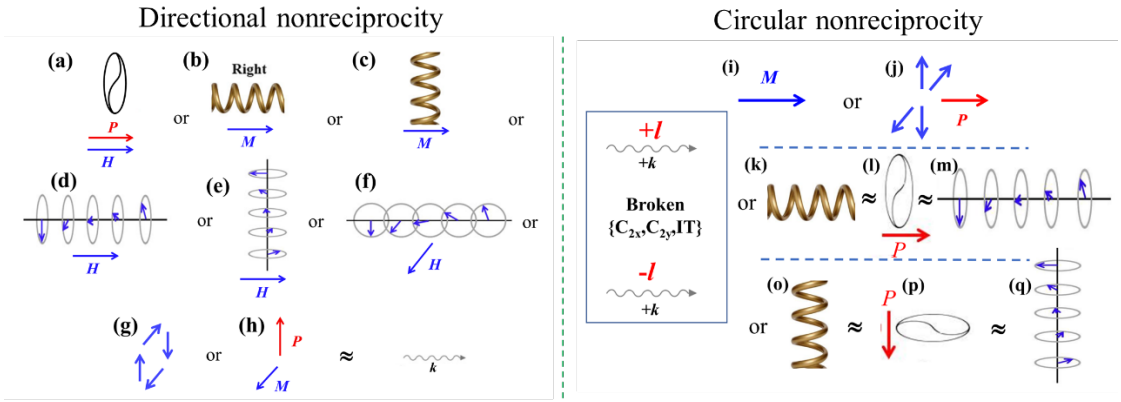

Fig 4. Various cases of directional nonreciprocity and circular nonreciprocity Yin-yang symbol and golden-color springs represent ferro-rotation and chirality, respectively. Blue arrows are spins or magnetic fields, and red arrows are electric fields or polarizations. (a-f) directional nonreciprocity due to magnetochiral effects. (g,h) directional nonreciprocity due to magnetic toroidal moments. (i) circular dichroism of the Faraday effect. (j) circular dichroism of magnetic monopole with electric field. (k-m) circular dichroism due to chirality. (o-q) transverse circular dichroism due to chirality.

Kibbe-Zurek mechanism (KZM) of Ising domains. KZM provides insight into the universal behavior of topological defect formation in systems undergoing nonequilibrium dynamics during symmetry-breaking phase transitions. KZM was observed in various condensed matter systems. However, it was unclear if it also applies to topologically trivial cases, such as those involving regular Ising domains. We demonstrate that it does,[5] by studying BiTeI with 3D Ising polar domains and $NiTiO_3$ with ferro-rotational domains (also Ising type), see Fig. 5. Our results demonstrate the validity of KZM for Ising domains and reveal an enhancement of the power-law exponent for transitions of non-topological quantities with long-range interactions. We are considering neutron scattering experiments, such as SANS, to extend these studies.

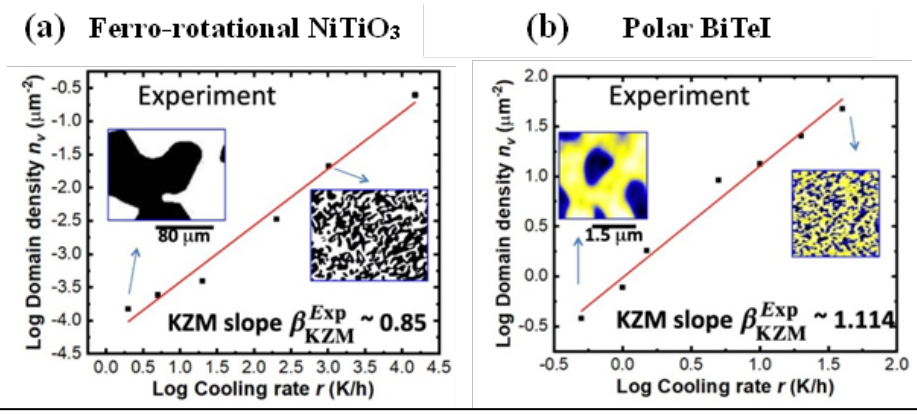

Fig 5. KZM exponents of (a) 3D Ising ferro-rotational domains in NiTiO3, and (b) 3D Ising polar domains in BiTeI.

Nonreciprocal effects in polar/toroidal h-(Lu,Sc)FeO_3 (*h*-LSFO). This compound has ferroelectric polarization along the *c* axis and $T_C \sim$ 1200 K. The Fe ions form a trimerized triangular lattice. The Fe spins order in the 120° structure below $T \sim$160 K. INS studies have been done in multidomain *h*-LSFO crystals of the A_1 type, where nonreciprocal effects cancel. We have studied single crystals using THz optical spectroscopy (Fig. 6). An electromagnon was found at 0.6 THz and a magnon was found at ~0.85 THz. The latter splits due to spontaneous magnetization and then further splits in an external magnetic field applied along the *c*-axis. Due to the combination of the electric polarization and spontaneous magnetization along the *c*-axis, we observed a strong vortex dichroism of THz beams with orbital angular momentum $l=\pm1$ at the resonance with the magnon.

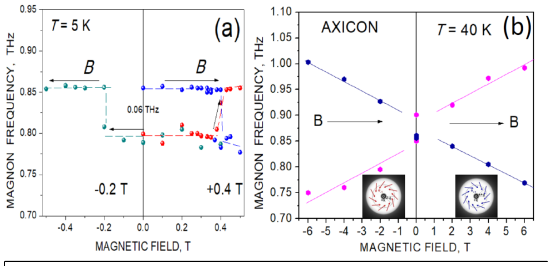

Fig 6. (a) Nonreciprocal changes of the selection rules for the magnon absorption due to the spontaneous magnetization of the sample. (b) Magnetic field dependence of the magnon doublet measured with vortex beams with OAM $l=\pm1$.

Future Plans

Continuing sample-growth optimization, especially for crystals with homo polar/chiral domain. Neutron scattering on chiral $BaCoSiO_4$ and polar/chiral Ni_3TeO_6, especially to explore their chiral excitations. Inelastic neutrons on altermagnetic $(Fe,Mn)_2Mo_3O_8$, to demonstrate their split spin/orbital nature. Monitoring the most promising lattice/magnetic excitations for the INS studies by optical spectroscopy. Continuing development of the vortex-beam spectroscopy and vortex dichroism of magnetic materials in the x-ray and THz energy ranges. Design of an optical setup for *in situ* pump-probe neutron experiments using high-power near-IR lasers.

References

1. P. Yadav, S. Lee, G.L. Pascut, J. Kim, M.J. Gutmann, X.H. Xu, B. Gao, S.W. Cheong, V. Kiryukhin, S. Choi, *Noncollinear magnetic order, in-plane anisotropy, and magnetoelectric coupling in the pyroelectric honeycomb antiferromagnet $Ni_2Mo_3O_8$*. Phys. Rev. Res. **5** (3), 22 (2023).

2. M.G. Kim, A. Barbour, W. Hu, S.B. Wilkins, I.K. Robinson, M.P.M. Dean, J.J. Yang, C. Won, S.W. Cheong, C. Mazzoli, V. Kiryukhin, *Real-space observation of fluctuating antiferromagnetic domains*. Sci. Adv. **8** (21), 6 (2022).

3. E. Chan, H. Lane, J. Pásztorová, M. Songvilay, R. D. Johnson, R. Downie, J. W. G. Bos, J. A. Rodriguez-Rivera, S. W. Cheong, R. A. Ewings, N. Qureshi, C. Stock, *Neutron scattering sum rules, symmetric exchanges, and helicoidal magnetism in $MnSb_2O_6$.* Phys. Rev. B **107** (14), 21 (2023).

4. 2. S. W. Cheong and X. H. Xu, *Magnetic chirality*. npj Quantum Mater. **7** (1), 40 (2022).

5. K. Du, X. C. Fang, C. Won, C. D. De, F. T. Huang, W. Q. Xu, H. Y. You, F. J. Gómez-Ruiz, A. Del Campo, and S. W. Cheong. *Kibble–Zurek mechanism of Ising domains*. Nat. Phys. **19**, 1495–1501 (2023).

Publications

(10 out of 25 total for 2022-2023)

1. P. Yadav, S. Lee, G. L. Pascut, J. Kim, M. J. Gutmann, X. H. Xu, B. Gao, S. W. Cheong, V. Kiryukhin, and S. Choi, *Noncollinear magnetic order, in-plane anisotropy, and magnetoelectric coupling in the pyroelectric honeycomb antiferromagnet $Ni_2Mo_3O_8$*. Phys. Rev. Res. **5** (3), 22 (2023).

2. X. Y. Guo, R. Owen, A. Kaczmarek, X. C. Fang, C. D. De, Y. Ahn, W. Hu, N. Agarwal, S. H. Sung, R. Hovden, S. W. Cheong, and L. Y. Zhao, *Ferrorotational domain walls revealed by electric quadrupole second harmonic generation microscopy.* Phys. Rev. B **107** (18), 8 (2023).

3. T. S. Jung, X. Xu, J. Kim, B. H. Kim, H. J. Shin, Y. J. Choi, E. G. Moon, S. W. Cheong, and J. H. Kim, *Unconventional room-temperature carriers in the triangular-lattice Mott insulator $TbInO_3$*. Nat. Phys., **11** (2023).

4. K. Du, X. C. Fang, C. Won, C. D. De, F. T. Huang, W. Q. Xu, H. Y. You, F. J. Gómez-Ruiz, A. del Campo, and S. W. Cheong, *Kibble-Zurek mechanism of Ising domains*. Nat. Phys., **16** (2023).
5. E. Chan, H. Lane, J. Pásztorová, M. Songvilay, R. D. Johnson, R. Downie, J. W. G. Bos, J. A. Rodriguez-Rivera, S. W. Cheong, R. A. Ewings, N. Qureshi, and C. Stock, *Neutron scattering sum rules, symmetric exchanges, and helicoidal magnetism in $MnSb_2O_6$.* Phys. Rev. B **107** (14), 21 (2023).
6. S. W. Cheong and X. H. Xu, *Magnetic chirality*. npj Quantum Mater. **7** (1), 40 (2022).
7. M. G. Kim, A. Barbour, W. Hu, S. B. Wilkins, I. K. Robinson, M. P. M. Dean, J. J. Yang, C. Won, S. W. Cheong, C. Mazzoli, and V. Kiryukhin, *Real-space observation of fluctuating antiferromagnetic domains*. Sci. Adv. **8** (21), 6 (2022).
8. A. Nag, A. Nocera, S. Agrestini, M. Garcia-Fernandez, A. C. Walters, S. W. Cheong, S. Johnston, and K. J. Zhou, *Quadrupolar magnetic excitations in an isotropic spin-1 antiferromagnet*. Nat. Commun. **13** (1), 7 (2022).
9. L. Ponet, S. Artyukhin, T. Kain, J. Wettstein, A. Pimenov, A. Shuvaev, X. Wang, S. W. Cheong, M. Mostovoy, and A. Pimenov, *Topologically protected magnetoelectric switching in a multiferroic*. Nature **607** (7917), 81 (2022).
10. X. H. Xu, F. T. Huang, A. S. Admasu, M. Kratochvílová, M. W. Chu, J. G. Park, and S. W. Cheong, *Multiple ferroic orders and toroidal magnetoelectricity in the chiral magnet $BaCoSiO_4$.* Phys. Rev. B **105** (18), 12 (2022).

Understanding Quantum Matter Beyond the Unit Cell

Andrew Christianson, Materials Science & Technology Division, Oak Ridge National Laboratory, Oak Ridge, TN 37831.

Andrew May, Materials Science & Technology Division, Oak Ridge National Laboratory, Oak Ridge, TN 37831.

Joseph Paddison, Materials Science & Technology Division, Oak Ridge National Laboratory, Oak Ridge, TN 37831.

Gábor Halász, Materials Science & Technology Division, Oak Ridge National Laboratory, Oak Ridge, TN 37831.

David Mandrus, Materials Science & Technology Division, Oak Ridge National Laboratory, Oak Ridge, TN 37831; Department of Physics & Astronomy, University of Tennessee, Knoxville, TN 37996; Department of Material Science & Engineering, University of Tennessee, Knoxville, TN 37996.

Keywords: Quantum Magnetism, Spin Textures, Higher order spin systems, Spiral spin liquids

Research Scope

Advances in understanding and manipulating quantum magnetism, entanglement, coherence, and topology are critical for driving innovation in advanced computation, information, and energy technologies. The broadly appreciated vision for fundamental research in this area is to provide the basis to accelerate discovery, selection, and materials realization of quantum phenomena perfected for device applications. Progress in this direction is a prerequisite for the co-design paradigm envisioned in the BES Basic Research Needs report on Microelectronics and similarly to address the need to control and exploit quantum mechanical behaviors for novel functionalities as a priority research direction described in the BES BRN on Quantum Materials. The Overarching Goal of this project is to achieve a fundamental understanding of how anisotropy, frustration, and topology acting in concert produce collective quantum phenomena. To achieve this goal, the Specific Aims of the project are: (1) Reveal the quantum mechanical origins of magnetic continua and how multi-magnon interactions both impact and reveal the nature of quantum magnetism; (2) Understand and tune topologically nontrivial character reflected in the excited states of quantum magnets; (3) Unravel the formation and properties of multi-$\boldsymbol{Q}$ magnetism with an emphasis on novel spin textures. These topics are pursued by employing sophisticated theoretical modeling and simulation to exploit the multi-faceted information available from various neutron scattering techniques. The principal outcomes will be the construction of physical models that describe how quantum magnetism and topology together influence macroscopic properties and guidelines for identifying and manipulating systems to produce specific, quantum phenomena.

Recent Progress

Field-tuned quantum renormalization of spin dynamics in the honeycomb lattice Heisenberg antiferromagnet $YbCl_3$: In quantum magnets, magnetic moments fluctuate heavily and are strongly entangled with each other, a fundamental distinction from classical magnetism. Models of quantum magnetism for Archimedean tessellations of two dimensions such as square, triangular, and honeycomb lattices have proven instrumental to achieve our current understanding of collective

quantum phenomena. However, despite serving as one of the prototype models of quantum magnetism in two dimensions, determining and understanding the collective behavior of quantum spins decorating the honeycomb lattice remains an open challenge.

We have used inelastic neutron scattering measurements with applied magnetic field in tandem with linear and nonlinear spin wave theory calculations to demonstrate and explain quantum effects for the honeycomb lattice through a comprehensive study of the model quantum magnet $YbCl_3$ [1]. By examining the spin excitation spectrum above the saturation field where the physical behavior is explicitly classical and linear spin-wave theory is essentially exact, we accurately determined the dominant nearest-neighbor Heisenberg interaction. Below the saturation field, we revealed a field-dependent energy renormalization of the entire magnetic spectrum -- the sharp spin-wave modes as well as the multimagnon continuum [**Fig. 1**]. This renormalization is a quantum effect that can be accurately captured by the first 1/S correction in nonlinear spin-wave theory. Furthermore, we find that the application of a magnetic field induces a qualitatively new yet sharp feature inside the multimagnon continuum. This result demonstrates that structures within the multimagnon continuum can occur over a wide experimental parameter space and can be used as an additional means of identifying and distinguishing quantum phenomena from more mundane effects such as disorder.

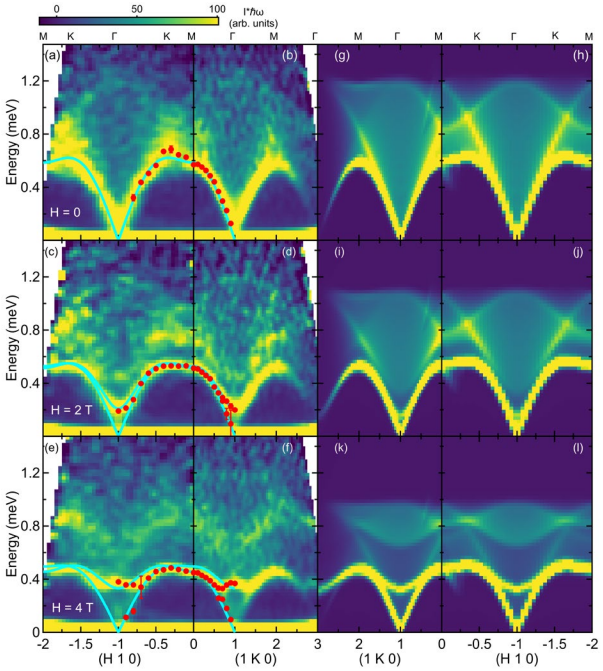

Figure 1: Inelastic neutron scattering of $YbCl_3$ under applied field ($\mu_0 H \| c$). Measured ((a)-(f)) and calculated ((g)-(i)) scattering intensity times energy transfer ($I\hbar\omega$) as a function of wave-vector transfer. The calculated intensities are obtained from a nonlinear spin-wave theory. Red points are the fitted peak positions of the transverse spin waves as a function of energy and wave-vector transfer plotted in a reduced zone scheme. Solid blue lines are the fitted field-dependent linear spin-wave dispersions. [1]

Understanding quantum magnets with spin S > 1/2: The computation of dynamical correlation functions at finite temperature is one of the most challenging problems of modern quantum many-body physics. These functions are not only crucial to test models against different spectroscopic techniques but are also critical to the development of fast machine learning tools aimed at accelerating and enhancing our understanding of problems at the forefront of condensed matter physics.

We addressed this problem by using inelastic neutron scattering to measure the temperature dependent spin dynamics of the effective spin-one quantum antiferromagnet $Ba_2FeSi_2O_7$ [2]. More than one classical limit can be taken for quantum magnets, and a key insight of our work is that higher order spin (N-level (N=2S+1)) systems with strong single-ion anisotropy are best described by a classical limit employing SU(N) spins. The measured dynamic structure factor of $Ba_2FeSi_2O_7$ is calculated with a generalized Landau-Lifshitz dynamics for SU(3) coherent states. In contrast to the traditional classical limit employing SU(2) coherent states, our results with SU(3) coherent states are in good agreement with the measured temperature dependent spectrum. The SU(3) approach applied here is part of a more general framework and provides a basis to move toward understanding the broad class

of materials comprising weakly coupled antiferromagnetic dimers, trimers, or tetramers, and magnets with strong single-ion anisotropy. In addition, it provides an efficient methodology enabling applications to machine learning algorithms that will accelerate understanding of quantum magnets.

New routes to spiral spin liquids: Competition among exchange interactions can induce novel spin correlations on a bipartite lattice without geometrical frustration. Spiral spin-liquids are correlated *paramagnetic* states with degenerate propagation vectors forming a continuous ring or surface in reciprocal space. On the honeycomb lattice, spiral spin-liquids present a novel route to realize emergent fracton excitations, quantum spin liquids, and topological spin textures, yet experimental realizations remained elusive. Using neutron scattering experiments, we showed that a spiral spin-liquid is realized in the van der Waals honeycomb magnet $FeCl_3$ [3]. A continuous ring of scattering is directly observed at T = 10 K (T_N=8 K), which indicates the emergence of an approximate U(1) symmetry in momentum space. Our work demonstrates that spiral spin-liquids can be achieved in two-dimensional systems and provides a promising platform to study the fracton physics and novel spin textures in a new class of materials with the potential to impact the next generation of materials for QIS applications.

The limitation of spiral spin liquids to bipartite lattices has hindered progress due to the limited number of materials found thus far. To overcome this limit, we have demonstrated that nonbipartite lattices can serve as hosts to spiral spin liquids [4]. Together this work and the work described in the preceding paragraph represent a significant advance in the study of spiral spin liquids by greatly expanding the space of candidate materials that can be used to harness the unique characteristics of these spin liquids for next generation device applications.

Stabilization mechanism of a skyrmion lattice in Gd_2PdSi_3: Magnetic skyrmions are topological spin textures with potentially transformative applications in quantum computing and information storage. Skyrmions usually emerge in crystals without a center of inversion symmetry. In some cases, however, skyrmions also occur in centrosymmetric crystals, offering exciting prospects of higher skyrmion densities and manipulating chiral degrees of freedom with external fields. Extracting the magnetic interactions that stabilize such spin textures remains a key challenge, and addressing this challenge is necessary for designing and manipulating skyrmion-based devices.

To address this problem, we used neutron-scattering measurements of the centrosymmetric skyrmion hosting material Gd_2PdSi_3 to quantify the interactions that drive skyrmion formation [5]. Our analysis of magnetic diffuse and inelastic scattering data revealed large ferromagnetic inter-planar interactions that are modulated by the Pd/Si crystallographic superstructure, and extended exchange interactions in triangular planes that are likely consistent with RKKY interactions. To achieve this, we synthesized an isotopically enriched sample to minimize the impact of neutron absorption that hinders scattering experiments on Gd-containing materials. Our refinements also reveal that the skyrmion phase emerges from a zero-field helical magnetic order with magnetic moments perpendicular to the magnetic propagation vector, suggesting that the magnetic dipolar interaction plays an important role. Monte Carlo simulations then demonstrated that our model explained key features of the observed magnetic field *vs*. temperature phase diagram, including the skyrmion phase observed at small fields. Notably, our effective spin Hamiltonian explains key aspects of the experimental behavior without invoking biquadratic or higher order spin interactions. However, the spin dynamics can only be understood by accounting for the Pd/Si crystallographic superstructure. In summary, our experimental results establish an interaction space that can promote skyrmion formation, facilitating identification and design of centrosymmetric skyrmion materials.

Future Plans

Novel spin textures and multi-Q magnetism

- Understand the energy scales driving the manifestation of different types of magnetism including noncoplanar structures on a face-centered cubic (FCC) lattice.
- Understand the origin of spin textures in centrosymmetric materials through the use and analysis of neutron diffraction, diffuse scattering, and inelastic neutron scattering measurements.
- Use neutron scattering measurements to probe the magnetic topological properties of a new class of topological materials and explore connections between electronic topology and magnetism.

Quantum magnetism and topological excitations

- Investigate the connection between field-dependent phases and topological Hall effects in pyrochlore materials.
- Understand the anomalous magnon broadening and subtle magnetic structures and/or spin textures in transition metal halide materials.
- Tune and understand mode interactions and resulting mode decays of various types in quantum magnets.
- Study novel structural motifs that exhibit strong frustration effects in three dimensions.
- Identify model systems to study quantum magnetism on square lattices

References

1. G. Sala, M. B. Stone, Gabor B. Halasz, M. D. Lumsden, A. F. May, D. M. Pajerowski, S. Ohira-Kawamura, K. Kaneko, D. G. Mazzone, G. Simutis, J. Lass, Yasuyuki Kato, Seung-Hwan Do, J. Y. Y. Lin, and A. D. Christianson, *Field-tuned quantum renormalization of spin dynamics in the honeycomb lattice Heisenberg antiferromagnet $YbCl_3$*, Communications Physics **6**, 234 (2023).

2. Seung-Hwan Do, Hao Zhang, David A. Dahlbom, Travis J. Williams, V. Ovidiu Garlea, Tao Hong, Tae-Hwan Jang, Sang-Wook Cheong, Jae-Hoon Park, Kipton Barros, Cristian D. Batista, and Andrew D. Christianson, *Understanding temperature-dependent SU(3) spin dynamics in the S = 1 antiferromagnet $Ba_2FeSi_2O_7$*, npj Quantum Mater. **8**, 5 (2023).

3. S. Gao, M. A. McGuire, Y. Liu, D. L. Abernathy, C. dela Cruz, M. Frontzek, M. B. Stone, and A. D. Christianson, *Spiral spin-liquid on a honeycomb lattice*, Phys. Rev. Lett. **128**, 227201 (2022).

4. Shang Gao, Ganesh Pokharel, Andrew F. May, Joseph A. M. Paddison, Chris Pasco, Yaohua Liu, Keith M. Taddei, Stuart Calder, David G. Mandrus, Matthew B. Stone, and Andrew D. Christianson, *Line-Graph Approach to Spiral Spin Liquids*, Phys. Rev. Lett. **129**, 237202 (2022).

5. J. A. M. Paddison, B. K. Rai, A. F. May, S. A. Calder, M. B. Stone, M. D. Frontzek, and A. D. Christianson, *Magnetic interactions of the centrosymmetric skyrmion material Gd_2PdSi_3*, Phys. Rev. Lett. **129**, 137202 (2022).

Publications

1. G. Pokharel, H. Suriya Arachchige, S. Gao, S.-H. Do, R. S. Fishman, G. Ehlers, Y. Qiu, J. A. Rodriguez-Rivera, M. B. Stone, H. Zhang, S. D. Wilson, D. Mandrus, and A. D. Christianson, *Spin dynamics in the skyrmion-host lacunar spinel GaV_4S_8*, Phys. Rev. B **104**, 224425 (2021).

2. S. Gao, M. A. McGuire, Y. Liu, D. L. Abernathy, C. dela Cruz, M. Frontzek, M. B. Stone, and A. D. Christianson, *Spiral spin-liquid on a honeycomb lattice*, Phys. Rev. Lett. **128**, 227201 (2022).

3. S.-H. Do, K. Kaneko, R. Kajimoto, K. Kamazawa, M. B. Stone, S. Itoh, T. Masuda, G. D. Samolyuk, E. Dagotto, W. R. Meier, B. C. Sales, H. Miao, and A. D. Christianson, *Damped Dirac magnon in a metallic kagome antiferromagnet FeSn*, Phys. Rev. B **105**, L180403 (2022).

4. J. A. M. Paddison, B. K. Rai, A. F. May, S. A. Calder, M. B. Stone, M. D. Frontzek, and A. D. Christianson, *Magnetic interactions of the centrosymmetric skyrmion material Gd_2PdSi_3*, Phys. Rev. Lett. **129**, 137202 (2022).

5. S.-H. Do, J. A. M. Paddison, G. Sala, T. J. Williams, K. Kaneko, K. Kuwahara, A. F. May, J.-Q. Yan, M. A. McGuire, M. B. Stone, M. D. Lumsden, and A. D. Christianson, *Gaps in topological magnon spectra: intrinsic vs. extrinsic effects*, Phys. Rev. B **106**, L060408 (2022). (Editors' suggestion)

6. Shang Gao, Ganesh Pokharel, Andrew F. May, Joseph A. M. Paddison, Chris Pasco, Yaohua Liu, Keith M. Taddei, Stuart Calder, David G. Mandrus, Matthew B. Stone, and Andrew D. Christianson, *Line-Graph Approach to Spiral Spin Liquids*, Phys. Rev. Lett. **129**, 237202 (2022).

7. Joseph A M Paddison, Li Yin, Keith M Taddei, Malcolm J Cochran, Stuart Calder, David S Parker, Andrew F May, *Multiple Incommensurate States in the Kagome Antiferromagnet $Na_2Mn_3Cl_8$*, Phys. Rev. B **108**, 054423 (2023).

8. G. Sala, M. B. Stone, Gabor B. Halasz, M. D. Lumsden, A. F. May, D. M. Pajerowski, S. Ohira-Kawamura, K. Kaneko, D. G. Mazzone, G. Simutis, J. Lass, Yasuyuki Kato, Seung-Hwan Do, J. Y. Y. Lin, and A. D. Christianson, *Field-tuned quantum renormalization of spin dynamics in the honeycomb lattice Heisenberg antiferromagnet $YbCl_3$*, Communications Physics **6**, 234 (2023).

9. Seung-Hwan Do, Hao Zhang, David A. Dahlbom, Travis J. Williams, V. Ovidiu Garlea, Tao Hong, Tae-Hwan Jang, Sang-Wook Cheong, Jae-Hoon Park, Kipton Barros, Cristian D. Batista, and Andrew D. Christianson, *Understanding temperature-dependent SU(3) spin dynamics in the S = 1 antiferromagnet $Ba_2FeSi_2O_7$*, npj Quantum Mater. **8**, 5 (2023).

10. C. M. Pasco, B. K. Rai, M. Frontzek, G. Sala, M. B. Stone, B. C. Chakoumakos, V. Ovidiu Garlea, A. D. Christianson, and A. F. May, *Anisotropic magnetism of the Shastry-Sutherland lattice material $BaNd_2PtO_5$*, Phys. Rev. Mater. **7**, 074407 (2023). Editor's suggestion.

Using neutron as a probe to study magnetic excitations in strongly correlated electron materials

Pengcheng Dai (pdai@rice.edu)

Department of Physics and Astronomy, Rice University, Houston, Texas 77005

Program Scope

A quantum spin liquid (QSL) is a state of matter in which the spins of unpaired electrons in a solid are quantum entangled, but do not show magnetic order in the zero-temperature limit. Because such a state may be important to the microscopic origin of high-Tc superconductivity and useful for quantum computation, experimental realization of QSL is a long-sought goal in modern condensed matter physics. Models supporting QSLs for 2D spin-1/2 Kagome, triangular, honeycomb, and 3D pyrochlore lattice systems indicate that all QSLs share the presence of deconfined spinons. Spinons are elementary excitations from the entangled ground state which carry spin S = ½ and thus, are fractionalized quasiparticles, fundamentally different from the S = 1 spin waves in conventional 3D ordered magnets. This research program describes our efforts to study different families of QSL materials, focusing on triangular lattice and pyrochlore lattice families of materials. In the field of superconductors, we have made two major discoveries over the past two years. First, we showed that superconductivity in spin triplet superconductivity could be driven by antiferromagnetic, instead of the long-believed ferromagnetic spin fluctuations. Second, we found that electronic nematic phase in iron based superconductor FeSe is driven by spin fluctuations. Here we describe our recent progresses in these two directions.

Recent Progress

Resonance from antiferromagnetic spin fluctuations for superconductivity in UTe_2

Superconductivity originates from the formation of bound (Cooper) pairs of electrons that can move through the lattice without resistance below the superconducting transition temperature T_c. While electron Cooper pairs in most superconductors form anti-parallel spin-singlets with total spin S = 0, they can also form parallel spin-triplet Cooper pairs with S = 1 and an odd parity wavefunction. Spin-triplet pairing is important because it can host topological states and Majorana fermions relevant for quantum computation. Since spin-triplet pairing is usually mediated by ferromagnetic (FM) spin fluctuations, uranium based materials near a FM instability are considered ideal candidates for realizing spin-triplet superconductivity. Indeed, UTe_2, which has a T_c=1.6 K, has been identified as a candidate for chiral spin-triplet topological superconductor near a FM instability, although it also has antiferromagnetic (AF) spin fluctuations. Here we use inelastic neutron scattering (INS) to show that superconductivity in

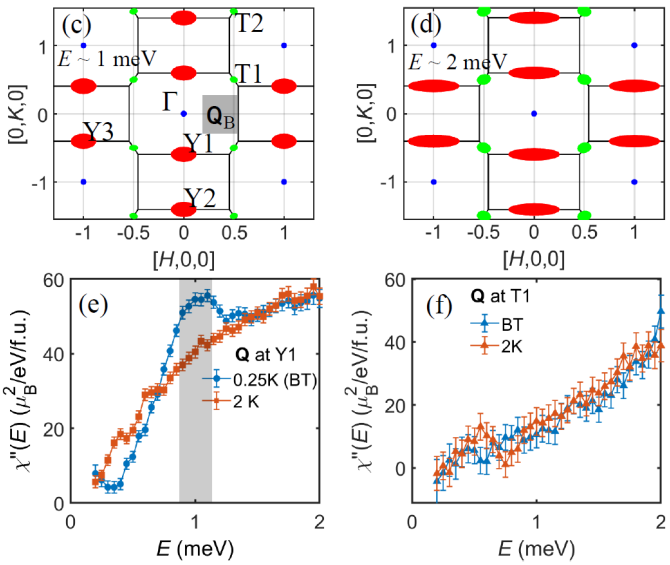

Fig. 1 (c,d) Schematics of the energy dependence of spin fluctuations in UTe2. (e,f) Temperature dependence of the spin fluctuations across T_c at Y1 and T1 points, respectively.

UTe_2 is coupled with a sharp magnetic excitation, termed resonance, at the Brillouin zone (BZ) boundary near AF order. Since the resonance has only been636 found in spin-singlet unconventional superconductors near an AF instability, its discovery in UTe_2 suggests that AF spin fluctuations may also induce spin-triplet pairing or that electron pairing in UTe_2 has a spin-singlet component. [C. R. Dun *et al.*, *Nature* ***600****,636-640 (2021)*].

Diffusive Excitonic Bands from Frustrated Triangular Sublattice in a Singlet-Ground-State System

Magnetic order in most materials occurs when magnetic ions with finite moments arrange in a particular pattern below the ordering temperature. Intriguingly, if the crystal electric field (CEF) effect results in a spin-singlet ground state, a magnetic order can still occur due to the exchange interactions between neighboring ions admixing the excited CEF levels. The magnetic excitations in such a state are spin excitons generally dispersionless in reciprocal space. Here we use neutron scattering to study stoichiometric $Ni_2Mo_3O_8$, where Ni^{2+} ions form a bipartite honeycomb lattice comprised of two triangular lattices, with ions subject to the tetrahedral and octahedral crystalline environment, respectively. We find that in both types of ions, the CEF excitations have nonmagnetic singlet ground states, yet the material has magnetic order. Furthermore, CEF spin excitons from the tetrahedral sites form a dispersive diffusive pattern around the Brillouin zone boundary, likely due to spin entanglement and geometric frustrations. [Bin Gao *et al.*, *Nature Communications* **14**, 2051 (2023)].

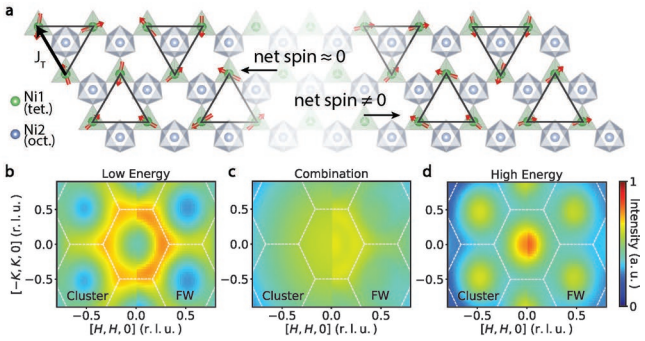

Fig. 2 a, Schematic of spin clusters used to calculate the structural factors. The 120° configurations with approximately zero net spin give rise to the pattern in which high intensity is near the zone boundary. The FM clusters lead to the pattern where high intensity is near the zone center. **b-d**, Comparison of the structural factors by the cluster and flavor wave calculations. Both methods reproduce the scattering in $Ni_2Mo_3O_8$ at 12-16 meV (**b**), 18-22 meV (**d**), and the sum of

Spin-excitation anisotropy in the nematic state of detwinned FeSe

The origin of the electronic nematicity in FeSe is one of the most important unresolved puzzles in the study of iron-based superconductors. In both spin- and orbital-nematic models, the intrinsic magnetic excitations at Q_1 = 1, 0) and Q_2 0, 1) of twin-free FeSe are expected to provide decisive criteria for clarifying this issue. Although a spin-fluctuation anisotropy below eV between Q_1 and Q_2 has been observed by

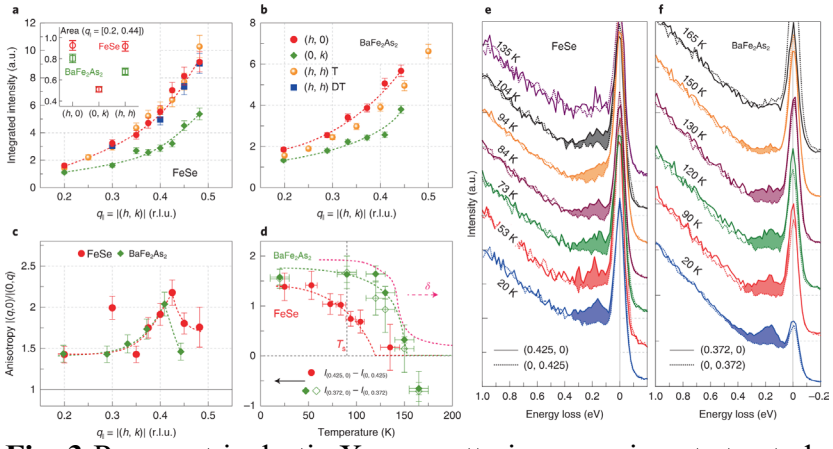

Fig. 3 Resonant inelastic X-ray scattering experiments to study evolution of high energy spin excitations of FeSe.

inelastic neutron scattering at low temperature, it remains unclear whether such an anisotropy also persists at higher energies and associates with the nematic transition T_s. Here we use resonant inelastic X-ray scattering to probe the high-energy magnetic excitations of detwinned FeSe. A prominent anisotropy between the magnetic excitations along the H and K directions is found to persist to $E \approx$ eV, which decreases gradually with increasing temperature and finally vanishes at a temperature around T_s. The measured high-energy spin excitations are dispersive and underdamped, which can be understood from a local-moment perspective.Taking together the large energy scale far beyond the d_{xz}/d_{yz} orbital splitting, we suggest that the nematicity in FeSe is probably spin-driven. [Xingye Lu *et al*., Nature Physics **18**, 806 (2022)].

Emergent photons and fractionalized excitations in a quantum spin liquid

A quantum spin liquid (QSL) arises from a highly entangled superposition of many degenerate classical ground states in a frustrated magnet, and is characterized by emergent gauge fields and deconfined fractionalized excitations (spinons). Because such a novel phase of matter is relevant to high-transition-temperature superconductivity and quantum computation, the microscopic understanding of QSL states is a long-sought goal in condensed matter physics. Although Kitaev QSL exists in an exactly solvable spin-1/2 ($S = 1/2$) model on a two-dimensional (2D) honeycomb lattice, there is currently no conclusive identification of a Kitaev QSL material. The 3D pyrochlore lattice of corner-sharing tetrahedra (Fig. 1a), on the other hand, can host a QSL with $U(1)$ gauge fields called quantum spin ice (QSI), which is a quantum (with effective $S = 1/2$) analog of the classical (with large effective moment) spin ice. The key difference between a QSI and classical spin ice is the predicted presence of the linearly dispersing collective excitations near zero energy, dubbed the "photons" arising from emergent quantum electrodynamics, in addition to the spinons at higher energies. Recently, 3D pyrochlore systems $Ce_2M_2O_7$ (M = Sn, Zr, Hf) have been suggested as effective $S = 1/2$ QSI candidates, but there has been no evidence of quasielastic magnetic scattering signals from photons, a key signature for a QSI. Here, we use polarized neutron scattering experiments on single crystals of $Ce_2Zr_2O_7$ to conclusively demonstrate the presence of magnetic excitations near zero energy at 50 mK in addition to the signatures of spinons at higher energies. By comparing the energy (E), wave vector (Q), and polarization dependence of the magnetic excitations

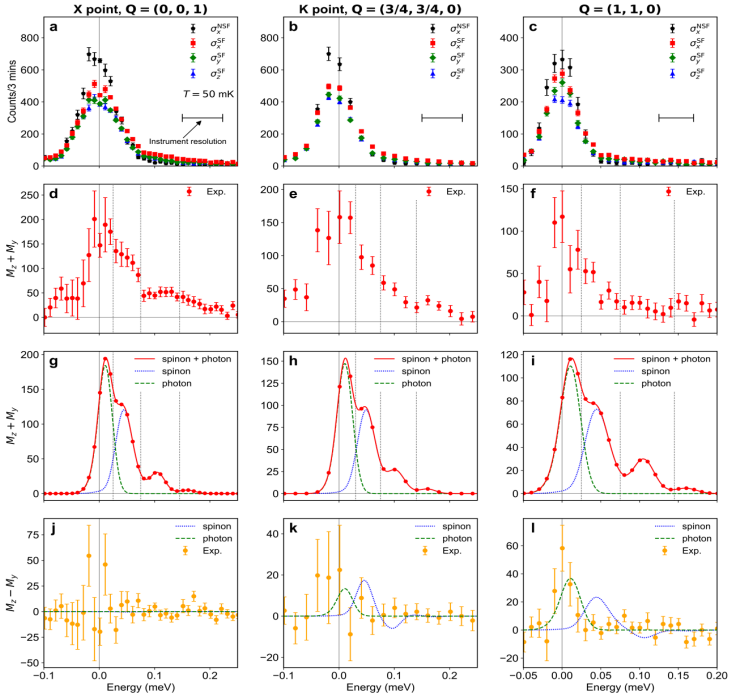

Fig. 4 Polarized neutron scattering measurements on $Ce_2Zr_2O_7$ reveal quasielastic magnetic scattering indicating the presence of photon scattering predicted 20 years ago.

with theoretical calculations, we conclude that $Ce_2Zr_2O_7$ is the first example of a dipolar-octupolar π-flux QSI with dominant dipolar Ising interactions, therefore identifying a microscopic Hamiltonian responsible for a QSL. [B. Gao *et al*., Nature (under review), Phys. Rev. B **106**, 094425 (2022)]

Future Plans

Our ultimate goal in this DOE supported project is to understand the microscopic origin of QSL and unconventional superconductivity in quantum materials. In particular, we will focus on spin dynamics in spin triplet candidate UTe_2, which reveal AF spin fluctuations coupled with superconductivity. In the coming months, we will determine magnetic field dependence of spin excitations UTe_2, and search for vortex lattice, and determine how hydrostatic pressure-induced AF order. Recently, we discovered photon scattering in $Ce_2Zr_2O_7$. We will investigate similar excitations in $Ce_2Hf_2O_7$ and sort out how disorder will affect the spin excitation continuum and photon scattering. Our goal is to determine microscopic Hamiltonian of QSL ground state and compare with Hamiltonian for these materials. We will also carrying out systematic doping study to understand how quantum coherence is established in triangular lattice system $Na(Yb,La)Se_2$. We have also carried out systematic neutron scattering experiments to determine how disorder can induce spinon like excitations in a spin-1/2 cobaltate on a triangular lattice in CoZnM3O8 [Bin Gao *et al*., Phys. Rev. B 108, 024431 (2023)]. During the current funding cycle, we started to work on CsV_3Sb_5 kagome lattice superconductor, and discovered that phonons are involved in the charge density wave order in the system [Y. Xie *et al*., Phys. Rev. B 105, L140501 (2022)]. In collaboration with other groups, we have made several important discoveries in the field, including the discovery of possible time-reversal symmetry breaking charge density wave in kagome lattice superconductor [Nature **602**, 245 (2022)]; the interplay between charge density and superconductivity in kagome lattice superconductors [Nature Communications **14**, 153 (2023)]. We will continue our collaborative projects with different groups working on the above mentioned projects.

Most relevant 10 Publications[1-10] from DOE support from December 1st, 2021 till Nov. 30, 2023

1. C. Duan, R.E. Baumbach, A. Podlesnyak, Y. Deng, C. Moir, A.J. Breindel, M.B. Maple, E.M. Nica, Q. Si, and P. Dai, "Resonance from antiferromagnetic spin fluctuations for superconductivity in UTe2", *Nature* **600**(7890), 636-640 (2021). https://doi.org/10.1038/s41586-021-04151-5.
2. C. Mielke, D. Das, J.-X. Yin, H. Liu, R. Gupta, C.N. Wang, Y.-X. JIang, M. Medarde, X. Wu, H.C. Lei, J.J. Chang, P.C. Dai, Q. Si, H. Miao, R. Thomale, T. Neupert, Y. Shi, R. Khasanov, M.Z. Hasan, H. Luetkens, and Z. Guguchia, "Time-reversal symmetry-breaking charge order in a correlated kagome superconductor", *Nature* **602**, 245-250 (2022). https://doi.org/10.1038/s41586-021-04327-z.
3. Y. Xie, Y. Li, P. Bourges, A. Ivanov, Z. Ye, J.-X. Yin, M.Z. Hasan, A. Luo, Y. Yao, Z. Wang, G. Xu, and P. Dai, "Electron-phonon coupling in the charge density wave state of ${\mathrm{CsV}}_{3}{\mathrm{Sb}}_{5}$", *Physical Review B* **105**(14), L140501 (2022). https://link.aps.org/doi/10.1103/PhysRevB.105.L140501.
4. X. Lu, W. Zhang, Y. Tseng, R. Liu, Z. Tao, E. Paris, P. Liu, T. Chen, V.N. Strocov, Y. Song, R. Yu, Q. Si, P. Dai, and T. Schmitt, "Spin-excitation anisotropy in the nematic state of detwinned FeSe", *Nature Physics* **18**(7), 806-812 (2022). https://doi.org/10.1038/s41567-022-01603-1.
5. B. Gao, T. Chen, H. Yan, C. Duan, C.-L. Huang, X.P. Yao, F. Ye, C. Balz, J.R. Stewart, K. Nakajima, S. Ohira-Kawamura, G. Xu, X. Xu, S.-W. Cheong, E. Morosan, A.H. Nevidomskyy, G. Chen, and P. Dai, "Magnetic field effects in an octupolar quantum spin liquid candidate", *Physical Review B* **106**(9), 094425 (2022). https://link.aps.org/doi/10.1103/PhysRevB.106.094425.
6. Z. Guguchia, C. Mielke, D. Das, R. Gupta, J.X. Yin, H. Liu, Q. Yin, M.H. Christensen, Z. Tu, C. Gong, N. Shumiya, M.S. Hossain, T. Gamsakhurdashvili, M. Elender, P. Dai, A. Amato, Y. Shi, H.C. Lei, R.M. Fernandes, M.Z. Hasan, H. Luetkens, and R. Khasanov, "Tunable unconventional kagome superconductivity in charge ordered RbV3Sb5 and KV3Sb5", *Nature Communications* **14**(1), 153 (2023). https://doi.org/10.1038/s41467-022-35718-z.
7. B. Gao, T. Chen, X.-C. Wu, M. Flynn, C. Duan, L. Chen, C.-L. Huang, J. Liebman, S. Li, F. Ye, M.B. Stone, A. Podlesnyak, D.L. Abernathy, D.T. Adroja, M. Duc Le, Q. Huang, A.H. Nevidomskyy, E. Morosan, L.

Balents, and P. Dai, “Diffusive excitonic bands from frustrated triangular sublattice in a singlet-ground-state system”, *Nature Communications* **14**(1), 2051 (2023). https://doi.org/10.1038/s41467-023-37669-5.

8. B. Gao, T. Chen, C.-L. Huang, Y. Qiu, G. Xu, J. Liebman, L. Chen, M.B. Stone, E. Feng, H. Cao, X. Wang, X. Xu, S.-W. Cheong, S.M. Winter, and P. Dai, “Disorder-induced excitation continuum in a spin-$\frac{1}{2}$ cobaltate on a triangular lattice”, *Physical Review B* **108**(2), 024431 (2023). https://link.aps.org/doi/10.1103/PhysRevB.108.024431.
9. B. Gao, T. Chen, C. Wang, L. Chen, R. Zhong, D.L. Abernathy, D. Xiao, and P. Dai, “Spin waves and Dirac magnons in a honeycomb-lattice zigzag antiferromagnet BaNi2(AsO4)2”, *Physical Review B* **104**(21), 214432 (2021). https://link.aps.org/doi/10.1103/PhysRevB.104.214432.
10. Y. Guo, M. Klemm, J.S. Oh, Y. Xie, B.-H. Lei, L. Moreschini, C. Chen, Z. Yue, S. Gorovikov, T. Pedersen, M. Michiardi, S. Zhdanovich, A. Damascelli, J. Denlinger, M. Hashimoto, D. Lu, C. Jozwiak, A. Bostwick, E. Rotenberg, S.-K. Mo, R.G. Moore, J. Kono, R.J. Birgeneau, D.J. Singh, P. Dai, and M. Yi, “Spectral evidence for unidirectional charge density wave in detwinned ${\mathrm{BaNi}}_{2}{\mathrm{As}}_{2}$”, *Physical Review B* **108**(8), L081104 (2023). https://link.aps.org/doi/10.1103/PhysRevB.108.L081104.

Dynamic atomistic processes of sodium-ion conduction in solid-state electrolytes, DOE award DE-SC0023286

Olivier Delaire (Duke University)

Keywords: ionic diffusion, solid-state electrolytes, sodium batteries, neutron, x-ray

Research Scope

Current rechargeable battery technology relies on liquid electrolytes with intrinsically limited chemical stability and detrimental flammability, which limit the achievable power density and thermal stability required for large-scale storage and faster charging. Concomitantly, supply challenges of mineral resources hinder mass development of lithium-based solutions for grid-scale energy storage and low-carbon distributed power. Addressing both these concerns, next-generation solid-state rechargeable batteries based on sodium-ion conducting materials could provide abundant and safe energy storage. All-solid Na-ion batteries will require novel solid materials capable of fast Na-ion conduction with high chemical and thermal stability. Recent breakthroughs in battery materials research uncovered solid Na-ion conductors achieving superionic conductivities rivaling those of conventional liquid electrolytes. Yet, limited understanding of atomistic mechanisms underlying superionic Na conduction and of thermal transport in the superionic state is precluding the rational design of high-performance and thermally safe Na-ion solid-state electrolytes. A clear understanding of how superionic Na conduction arises in structurally and chemically disparate compounds is still missing, a knowledge gap which is in part due to insufficient understanding of their atomic dynamics. Many parameters have been correlated with superionicity, but previously proposed descriptors typically do not consider the collective sublattice dynamics and flexibility of the framework, which modulate the local instantaneous environment felt by Na ions. Further, the strong anharmonicity and coupling of ionic diffusion with framework phonons are beyond our current understanding of thermal transport in normal solids, precluding rational thermal management for safe battery operation.

As part of this research project, the Delaire group at Duke is performing investigations of the atomic structure and atomic dynamics in sodium ion conductors of interest as candidate solid-state electrolytes for next-generation all-solid batteries. We hypothesize that fast diffusion of Na ions can be enabled by favorable structural dynamics of the host crystal lattice, boosting performance. Driven by this central hypothesis, the project is articulated around two complementary objectives to address the above knowledge gaps. This research project provides foundational knowledge to advance the Long Duration Storage Shot objective “to reduce the cost of grid-scale energy storage by 90% for systems that deliver 10+ hours of duration within the decade”. The Delaire group performs a combination of experimental measurements and computer simulations to gain new fundamental insights into the atomistic mechanisms underpinning fast sodium diffusion in Na-ion solid-state electrolyte compounds, and revealing their heat transport mechanisms. The experiments include x-ray and neutron scattering measurements, Raman spectroscopy, and transport / thermal characterization. The computer simulations include first-principles modeling of the atomic and electronic structure with density functional theory, and molecular dynamics simulations based on both ab-initio and surrogate neural net force-fields derived from machine-learning. The scattering measurements take advantage of DOE national user facilities for synchrotron x-ray scattering and neutron scattering. The new knowledge resulting from this research project will enable the more reliable prediction and design of Na-ion solid-state electrolytes, and quantitative thermal design for applications in sodium solid-state rechargeable batteries. These insights will also be relevant to other superionic conductor families, for instance for Li-batteries, fuel-cells, or thermoelectrics.

Recent Progress

Interplay of low-energy anharmonic phonons and superionic Na diffusion and ultralow thermal transport in Na_3PSe_4 solid-state electrolyte

We recently investigated the atomic dynamics in the related compound Na_3PS_4, including its quasielastic response and low-energy vibrational modes, using both neutron scattering experiments and large-scale MLMD simulations [1]. Over the past two years, we extend our prior results and investigated the atomic dynamics of the sister compound Na_3PSe_4, focusing on the interplay of Na diffusion with anharmonic low-energy phonons. We combined extensive neutron and x-ray scattering measurements and atomistic modeling to unravel the hybrid vibrational-diffusive atomic dynamics in Na_3PSe_4 (**Figure 1**). The high-resolution INS and QENS measurements, complemented with molecular dynamics (MD) based on both ab-initio and machine-learned potentials, provide critical insights into the role of anharmonic phonons underlying fast ion conduction. X-ray PDF measurements provide changes in the spatial correlation between various pairs of atoms on heating across the superionic phase transition. Our results reveal low-energy vibrational modes simultaneously involving motions of Na+ ions and framework polyanion subunits. We found that these modes become strongly overdamped in the superionic regime as they couple with the Na+ hopping process. In particular, the Na+ migration energy landscape is strongly modulated by low-energy phonons derived from a soft acoustic branch of the host lattice, which vary the diameter of the Na diffusion channel at the bottleneck. We find that an additional factor for the enhanced Na conductivity in Na_3PSe_4 is a significant concentration of Na-vacancies. Further, we investigate the origin of ultralow thermal conductivities in Na_3PSe_4 and Na_3PS_4 using Green-Kubo simulations. Our mode-resolved analysis shows that low-energy acoustic phonon modes of the overall crystal framework are a dominant contribution to the thermal conductivity. These results establish the importance of anharmonic low-energy modes in a soft crystal structure near a structural phase

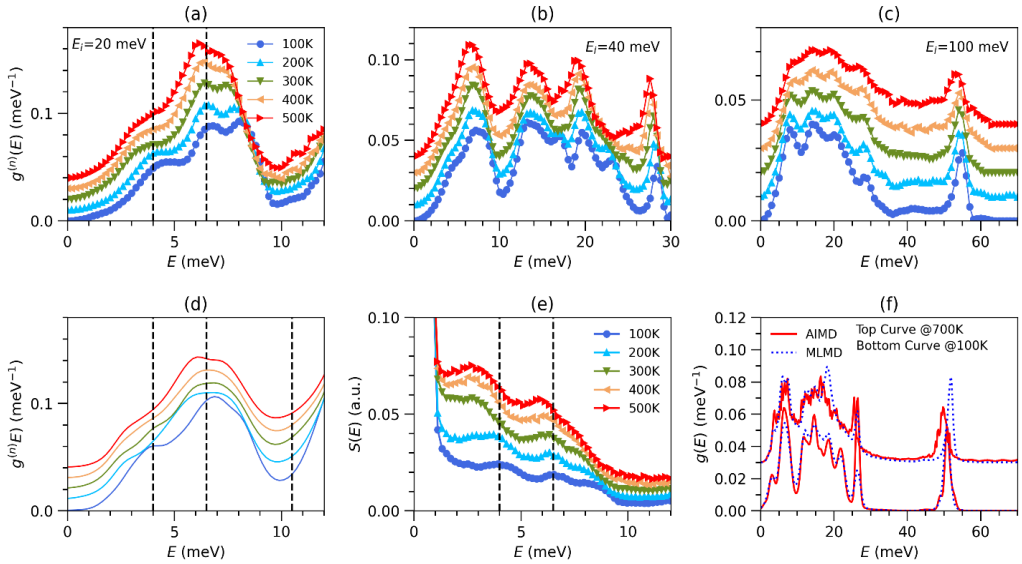

Figure 1 (a-c) Multiphonon corrected neutron-weighted DOS derived from S(Q, E) measured with INS with $E_i = 20$, 40 and 100 meV, respectively at ARCS. (d) Simulated neutron-weighted DOS obtained from MLMD trajectories at the temperatures measured with INS. Both measured (Fig 2a) and simulated DOS (Fig 2e) are normalized over the E range 0-15 meV. (e) T-dependent dynamical structure factor, S(E), of Na_3PSe_4 measured with INS with $E_i = 20$ meV using ARCS for Q-integrated data ($1.0\ Å^{-1} \leq Q \leq 4.0\ Å^{-1}$). (f) Validation of MLMD force-field (dashed blue line) against AIMD simulations (solid red line) by comparing the total phonon DOS at 100 K and 700 K.

transition to facilitate fast ion conduction, which provides a new type of descriptor in screening for future solid electrolyte candidates.

A manuscript was written, to be submitted for publication:

Mayanak K. Gupta, Jingxuan Ding, Zachary Hood, Naresh C. Osti, Douglas L. Abernathy, Andrey A. Yakovenko, Hui Wang and Olivier Delaire, "Interplay of low-energy anharmonic phonons and superionic Na diffusion and ultralow thermal transport in Na_3PSe_4 solid-state electrolyte", *to be submitted (2023)*

Ultrasoft host-phonons and fast Na-conduction in $Na_{11}PSn_2S_{12}$

This subproject comprehensively investigated the structure and dynamics of potential Na solid-electrolyte, $Na_{11}Sn_2PS_{12}$ and their role in fast Na diffusion using neutron scattering experiments and molecular dynamics simulations based on a surrogate force-field machine-learned from first-principles simulations. The compound $Na_{11}Sn_2PS_{12}$ (NSPS) was first synthesised by the Nazar group and Dehnen using Na_3PS_4 and Na_4SnS_4 precursors [2, 3]. The NSPS structure closely resembles its Li counterpart LGPS. However, ordering of Sn and P sites (Wyckoff sites 16*e* and 8*a*, respectively) leads to an enlarged unit-cell in NSPS. Further, the larger ionic size of Na^+ compared to Li^+ leads to a 30% volume increase in the equivalent unit cell [2]. We performed temperature-dependent INS to probe the anharmonic atomic dynamics to investigate the critical phonon modes across the superionic transition. Further, we investigated the Na-diffusion process with QENS. Neutron measurements are corroborated with large-scale AIMD and MLMD simulations, in order to assess the critical features in structure and dynamics controlling the fast Na-diffusion. A draft manuscript has been written on $Na_{11}PSn_2S_{12}$:

Mayanak K. Gupta, Jingxuan Ding, Naresh C. Osti, Douglas L. Abernathy, Linda F. Nazar, and Olivier Delaire, "Ultrasoft host-phonons and fast Na-conduction in $Na_{11}PSn_2S_{12}$" *to be submitted (2023).*

Future Plans

We plan to investigate diffusion and lattice dynamics in the promising superionic conductors Na_3SbSe_4 and Na_3SbS_4 by combining INS and QENS. We have already acquired preliminary neutron data on these compounds (ARCS and BASIS at SNS). We will be performing computational modeling to study the interplay between fast Na diffusion and host lattice dynamics. Na_3SbSe_4 crystallizes in a tetragonal phase at low temperature and transforms into cubic phase above 200 K, following the same crystal structures as Na_3PSe_4 described above. Its Na^+ ionic conductivity is on the order of 10^{-3} Scm^{-1} at room temperature, with activation energy for ion hopping of ~0.2 eV. Our INS measurements reveal a spectral weight transfer from low-energy phonons to diffusive dynamics upon warming, which also suggests that low-energy anharmonic phonons can be seen as precursors of ionic hopping. Further, we plan to study Na diffusion and lattice dynamics in NASICON type materials (including $Na_xZr_2Si_2PO_{12}$) that exhibit high Na conductivity.

References

1. M. K. Gupta, J. Ding, N.C. Osti, D.L. Abernathy, W. Arnold, H. Wang, Z. Hood, and O. Delaire, "Fast Na diffusion and anharmonic phonon dynamics in superionic Na3PS4". Energy & Environmental Science, **14**(12), 6554-6563 (2021).
2. Z. Zhang, E. Ramos, F. Lalère, A. Assoud, K. Kaup, P. Hartman, and L. F. Nazar, "Na11Sn2PS12: a new solid state sodium superionic conductor", Energy & Environmental Science, **11**(1), 87-93 (2018).
3. Duchardt, M., U. Ruschewitz, S. Adams, S. Dehnen, and B. Roling, "Vacancy-Controlled Na+ Superionic Conduction in Na11Sn2PS12", Angewandte Chemie International Edition, **57**(5),1351-1355 (2018).

Publications

Nothing to report (two manuscripts described above to be submitted).

Neutron scattering studies of phonon anharmonicity and coupling with spin, charge and disorder, DOE award DE-SC0019978

Olivier Delaire (Duke University)

Keywords: phonons, anharmonicity, disorder, electron-phonon and spin-phonon couplings

Research Scope

Understanding the microscopic processes involved in the transport and conversion of energy from the atomic scale to the mesoscale is critical for the development of next-generation materials for energy sustainability and quantum information sciences. The fundamental underpinnings of thermal transport in crystalline insulators and semiconductors is the propagation of phonon quasiparticles through the lattice. These phonon vibrations also critically modulate the interactions between orbitals and spins providing material functionalities. Significant progress has enabled a nanoscale understanding of heat transfer based on novel experimental techniques and first-principles modeling of Boltzmann transport for phonons. Yet, regimes of strong anharmonicity close to lattice instabilities reside beyond perturbation theories currently used to investigate phonon-phonon scattering rates. Further, the impacts of strong electron-phonon coupling and spin-phonon coupling on phase stability and transport phenomena remain insufficiently understood. Simultaneously, quantum effects involving coupled degrees-of-freedom may impact the properties of materials over wide ranges of compositions and temperatures. This project investigates the interaction of phonons in crystalline materials with other degrees of freedom (electronic, spin) and disorder, using a combination of neutron scattering, x-ray scattering, Raman spectroscopy, thermal and transport characterization, and first-principles simulations. Our approach is focused on mapping microscopic excitations (phonons, magnons) and their dependence on temperature or externally applied fields. In particular, we investigate strongly anharmonic effects near phase transitions, for example in halide perovskites and oxide perovskites, with the aim of better understanding their thermodynamics and transport properties, as well as the role of quantum fluctuations. The key role of soft phonon modes or hybrid-improper mechanisms involving multiple coupled modes is investigated in both canonical and novel materials, taking advantage of single-crystal measurements to map extended regions in wave-vector space and isolate critical interactions. We also investigate thermal transport properties using an integrative suite of measurements and simulations. To this end, the project utilizes inelastic neutron scattering beamlines, in particular at the Spallation Neutron Source at Oak Ridge National Laboratory. Neutron scattering measurements are analyzed with the help of density functional theory simulations, including ab-initio molecular dynamics and machine-learning augmented simulations. This research provides new insights into atomic dynamics in crystals that will enable the design of next-generation materials for both energy technologies and information processing.

Recent Progress

<u>Anharmonic overdamped phonons and 2D correlations of octahedral rotations in metal halide perovskites:</u>

Our inelastic neutron scattering (INS) and diffuse scattering studies have revealed the existence of strongly overdamped anharmonic phonons in $CsPbBr_3$, which are associated with dynamic 2D correlations of octahedral rotations [1]. These dynamic 2D fluctuations in a 3D cubic lattice are manifested as continuous diffuse scattering rods arising from overdamped low-energy Br-dominated phonon modes for wavevectors along the edge of the cubic Brillouin zone. Recently, we

extended our work to other halide perovskite systems including $CsSnBr_3$, $Cs_2AgBiBr_6$ and MAPI (INS and diffuse neutron/x-ray scattering measurements), whose compositions vary in A-site cation, B-cite cation and halide anion. Despite the composition differences, we find clear similarities across the halide perovskite family, indicating that the lattice anharmonicity mainly originates from the inorganic M-X_6 framework. Therefore, our discovery in $CsPbBr_3$ is likely to hold true also in the entire family of metal halide perovskites, with important implications for our understanding of excited carrier relaxation with the lattice (strongly anharmonic electron-phonon coupling), as well as the thermal and thermodynamic properties of these materials. We have performed additional INS studies with triple-axis spectrometry at HFIR and with LET at ISIS to further investigate the temperature dependence of anomalous dynamics across compositions, and over a wider temperature range than previously measured on CNCS at SNS.

Further, we have investigated the double-perovskite $Cs_2AgBiBr_6$ and its connection with soft phonon modes. Compared with $CsPbX_3$, $Cs_2AgBiBr_6$ adopts a double perovskite structure and shows lower toxicity and improved stability, thus is attracting interests in both optoelectronic and thermal applications. $Cs_2AgBiBr_6$ undergoes a second-order phase transition at T_c=122K to a tetragonal structure with space group *I*4/m, which was proposed to arise from the freezing of a zone-center soft mode (out-of-phase Br octahedra rotations about the *c* axis, $a^0a^0c^-$ in Glazer notation) which differs from single $CsMX_3$ perovskites. Our x-ray diffuse scattering and neutron diffractions experiments discovered satellite Bragg peaks in T<39K, which reveals a further low temperature phase transition not been previously discovered and suggests a complex modulated ground state structure in $Cs_2AgBiBr_6$. In order to clarify the low-T structure and phase transitions, we have performed single-crystal diffraction with TOPAZ at SNS. We also performed IXS measurements on small crystals using inelastic x-ray scattering (HERIX sector-30, at the APS).

A manuscript on $Cs_2AgBiBr_6$ was written and submitted for publication (under review revision).

Xing He, Matthew Krogstad, Mayanak K Gupta, Tyson Lanigan-Atkins, Chengjie Mao, Feng Ye, Yaohua Liu, Tao Hong, Songxue Chi, Haotong Wei, Jinsong Huang, Stephan Rosenkranz, Raymond Osborn, and Olivier Delaire, "Multiple lattice instabilities and complex ground state in Cs2AgBiBr6", submitted (2023).

<u>Anharmonic phonons near tunable ferroelectric quantum critical points in K(Ta,Nb)O_3:</u>

Driven by the search for novel quantum material functionalities, recent studies of quantum criticality (QC) in ferroelectric and multiferroic materials have identified the potential in tuning perovskite oxides, such as $SrTiO_3$ (STO) or $KTaO_3$ (KTO), toward or away from a ferroelectric quantum critical points (QCP). Further, strong interest has emerged over the past few years into the low-temperature thermal transport properties of STO and KTO. Importantly, many theoretical studies of the ferroelectric instability are still based on quasi-harmonic phonon simulations and thus miss the effects of anharmonic couplings that are prevalent in oxide perovskites. We have carefully investigated phonon anharmonicity and correlated disorder in K(Ta,Nb)O_3 (KTN). By alloying $KTaO_3$ with $KNbO_3$, a high temperature ferroelectric (T_C=700K), the Curie temperature and associated structural phase transitions can be controlled away from the QCP. In the past two years, we have conducted several INS measurements (ARCS, HYSPEC) and diffuse scattering measurements (CORELLI) and performed extensive first-principles simulations, including finite-temperature ab-initio molecular dynamics (AIMD) and simulations of S(Q,E) on large-scale MD with machine-learning interatomic

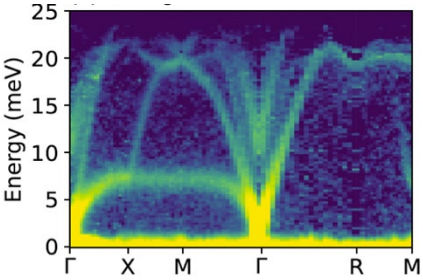

Figure 2 Inelastic neutron scattering measurement of phonon dynamical structure factor S(**Q**,E) in KTN performed with ARCS at the SNS.

potentials (simulations run at NERSC). Example data from our INS measurements are shown in Fig. 1.

A manuscript on $K(Ta,Nb)O_3$ (KTN) is under preparation:

Xing He, Douglas L Abernathy, Garrett Granroth, Feng Ye, Barry Winn, Lynn Boatner, and Olivier Delaire, "Dynamic correlated disorder in $KTa_{(1-x)}Nb_xO_3$"

BES funding has supported the research of several PhD students in the Delaire group at Duke University. Three BES-supported PhD theses were awarded in the past two years:

Xing He, "Phonon Anharmonicity and Phase Transitions in Perovskites", PhD dissertation, Duke University (2022).

Jingxuan Ding, "Phonon Anharmonicity and Ionic Diffusion in Emergent Energy Materials", PhD dissertation, Duke University (2022)

Shan Yang, "Lattice Dynamics in Temperature-driven and Photo-induced Phase Transitions", PhD dissertation, Duke University (2022)

Future Plans

We have secured beamtimes for further INS measurements of large single crystals of metal halide perovskites and will study the detailed wavevector and temperature dependence of the overdamped zone-boundary phonon modes to assess spatio-temporal correlation lengths and the nature of their phase transitions. We will also use our INS and x-ray diffuse scattering data on CsSnBr3 and $Cs_2AgBiBr_6$ to compare with our previous data on CsPbBr3 and evaluate the possibility of any dynamic off-centering of ions on the B-site, which has been widely suggested in the literature. We will perform extensive machine-learning accelerated simulations of atomic dynamics and correlations to rationalize our experimental results.

Building on our recent success at rationalizing anharmonic phonons in the quantum paralectric SrTiO3 [2], we plan to continue our investigations of phonons, anharmonicity and disorder near the QCP in KTaO3 and doped KTN compounds, using INS and anharmonic phonon simulations, including large-scale machine-learning accelerated MD simulations to treat effects of disorder explicitly. We also plan to extend our study to related transition metal oxides, combining INS, diffuse scattering and IXS measurements, together with detailed DFT and MD simulations to resolve anharmonicity and dynamic correlated disorder effects.

References

1. T. Lanigan-Atkins*, X. He*, M. J. Krogstad, D. M. Pajerowski, D. L. Abernathy, Guangyong NMN Xu, Zhijun Xu, D.-Y. Chung, M. G. Kanatzidis, S. Rosenkranz, R. Osborn, and O. Delaire, "Two-dimensional overdamped fluctuations of soft perovskite lattice in $CsPbBr_3$", Nature Materials **20**, 977–983 (2021)
2. X. He, D. Bansal, B. Winn, S. Chi, L. Boatner, and O. Delaire, "Anharmonic Eigenvectors and Acoustic Phonon Disappearance in Quantum Paraelectric SrTiO3", Phys. Rev. Letters **124**, 145901 (2020).
3. P. M. Gehring, H. Chou, S. M. Shapiro, J. A. Hriljac, D. H. Chen, J. Toulouse, D. Rytz, and L. A. Boatner, "Anomalous dispersion and thermal expansion in lightly-doped $KTa_{1-x}Nb_xO_3$", Ferroelectrics **150**, 47-58 (1993).
4. E. Farhi, A.K. Tagantsev, R. Currat, B. Hehlen, E. Courtens, and L. A. Boatner, "Low energy phonon spectrum and its parameterization in pure $KTaO_3$ below 80K", Eur. Phys. J. B **15**, 615 (2000).
5. A. Narayan, A. Cano, A. B. Balatsky, N. A. Spaldin, "Multiferroic quantum criticality", Nature Materials **18**, 223–228 (2019).

Publications

1. M. K. Gupta, S. Kumar, R. Mittal, S. K. Mishra, S. Rols, O. Delaire, A. Thamizhavel, P. U. Sastry and S. L. Chaplot, "Distinct anharmonic characteristics of phonons driven lattice thermal conductivity and thermal expansion in bulk MoSe2 and WSe2", J. Mater. Chem. A **11**, 21864-21873 (2023).
2. M. K. Gupta, J. Ding, D. Bansal, D. L. Abernathy, G. Ehlers, N. C. Osti, W. G. Zeier, O. Delaire, "Strongly Anharmonic Phonons and Their Role in Superionic Diffusion and Ultralow Thermal Conductivity of Cu_7PSe_6", Advanced Energy Materials **12**, 2200596 (2022),
3. J. Li, L. Wu, S. Yang, X. Jin, W. Wang, J. Tao, L. Boatner, M. Babzien, M. Fedurin, M. Palmer, W. Yin, O. Delaire, and Y. Zhu, "Direct detection of V-V atom dimerization and rotation dynamic pathways upon ultrafast photoexcitation in VO_2", Physical Review X **12**, 021032 (2022).
4. L. Chen, C. Mao, J-H Chung, M. B. Stone, A. I. Kolesnikov, X. Wang, K. Nakajima, S. Ohira-Kawamura, B. Gao, O. Delaire and P. Dai, "Anisotropic magnon damping by zero-temperature quantum fluctuations of the Cr atom in ferromagnetic $CrGeTe_3$", Nature Communications **13**, 4037 (2022).
5. G. A. de la Pena Munoz, A. A. Correa, S. Yang, O. Delaire, Y. Huang, A. S. Johnson, T. Katayama, V. Krapivin, E. Pastor, D A. Reis, S Teitelbaum, L Vidas, S Wall, and M Trigo, **"**Ultrafast lattice disordering accelerated by electronic collisional forces**",** Nature Physics **19**, 1489–1494 (2023).
6. Y Huang, S Teitelbaum, S Yang, G De la Peña, T Sato, M Chollet, D Zhu, J L. N, D Bansal, A F. May, A M. Lindenberg, O Delaire, M Trigo, and D A. Reis, "Nonthermal bonding origin of a novel photoexcited lattice instability in SnSe", Physical Review Letters **131**, 156902 (2023).
7. Y Huang, S Yang, S Teitelbaum, G De la Pena, T Sato, M Chollet, D Zhu, J L. Niedziela, D Bansal, A P. May, A M. Lindenberg, O Delaire, D A. Reis, M. Trigo, "Observation of a Novel Lattice Instability in Ultrafast Photoexcited SnSe", Physical Review X **12**, 011029 (2022).
8. G Sala, M Mourigal, C Boone, NP Butch, AD Christianson, O Delaire, AJ DeSantis, CL Hart, RP Hermann, T Huegle et al. "CHESS: The future direct geometry spectrometer at the second target station", Review of Scientific Instruments **93**, 6:065109 (2022).
9. M K. Gupta, J Ding, N C. Osti, D L. Abernathy, W Arnold, H Wang, Z Hood and O Delaire, "Fast Na diffusion and anharmonic phonon dynamics in superionic Na_3PS_4", Energy and Environmental Science **14**, 6554 - 6563 (2021)
10. T. Lanigan-Atkins*, X. He*, M. J. Krogstad, D. M. Pajerowski, D. L. Abernathy, Guangyong NMN Xu, Zhijun Xu, D.-Y. Chung, M. G. Kanatzidis, S. Rosenkranz, R. Osborn, and O. Delaire, "Two-dimensional overdamped fluctuations of soft perovskite lattice in $CsPbBr_3$", Nature Materials **20**, 977–983 (2021)

Equilibrium and Non-Equilibrium Skyrmion and Vortex Lattices

Morten R. Eskildsen, Department of Physics and Astronomy, University of Notre Dame

Keywords: small-angle neutron scattering, vortex lattice, skyrmion lattice

Research Scope

Skyrmions in chiral magnets and superconducting vortices possess particle-like characteristics, sharing many common features as well as similarities to liquid crystals, colloids, and granular materials. Due to this commonality and the comparable length scales for both skyrmion lattice (SkL) and vortex lattice (VL), they are well suited for investigation by small-angle neutron scattering (SANS). The manipulation of skyrmions and vortices by electrical and/or thermal currents is relevant for potential applications. In addition, vortices may serve as probes of the superconducting state in the host material. Finally, the SkL/VL present conceptually simple, two-dimensional model systems to study fundamental problems such as metastable states, nonequilibrium phase transitions and kinetics, and structural transformation at the mesoscopic scale.

Recent Progress

Skyrmion manipulation by electrical and thermal currents: Since SkL rotations (as opposed to translations) are easily observed by SANS we have adopted a Corbino geometry where current and/or heat is injected at the center of a disc shaped sample and extracted at the perimeter or *vice versa*. This generates a radial current that decreases as $1/r$, where r is the distance from the center. Both electric and thermal currents give rise to an r-dependent azimuthal force on the skyrmions and thus a net torque on the SkL. In our initial measurements on MnSi with an electrical current we found a non-monotonic response, with the SkL rotating in one direction for low currents and in the opposite direction for high currents, as shown in Fig. 1 [1]. Subtracting scattering from different current directions gives rise to an intensity "dipole" which switches polarity at an inflection point of ±3 A. Measurements at different sample locations shows that the SkL rotation depends on the local radial current density, Fig. 1(g). The SANS measurements were complemented by micromagnetic simulations, showing how the non-monotonic behavior is due to a competition between the effects of the electric current and thermal gradient due to joule heating.

Motivated by the initial measurement we recently performed SANS measurements on the SkL on insulating Cu_2OSeO_3 subject to a radial thermal current. Here, the azimuthal force is sufficient to cause continuous rotations of SkL domains, rather than the static reorientation discussed above. Moreover, the timescale for the SkL rotation is sufficiently slow that it can be solved in the SANS measurements (rotating diffraction patterns). These measurements are ongoing.

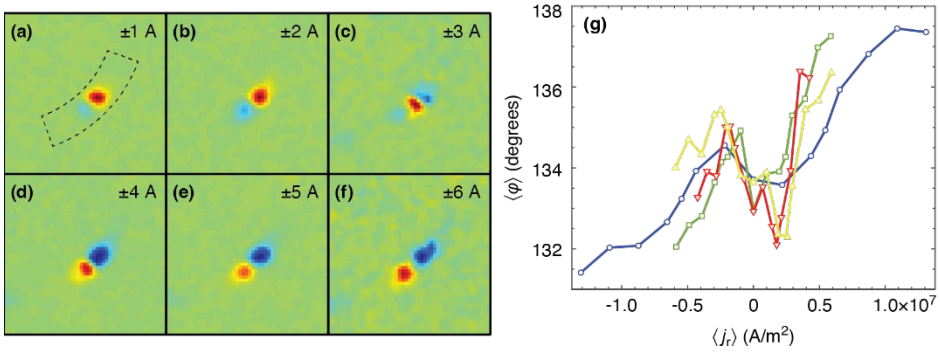

Fig. 1 (a)-(f) Subtraction of MnSi SkL diffraction patterns obtained at positive and negative currents of the same magnitude. Only one of the six SkL peaks is shown. (g) Azimuthal intensity distribution vs the local radial current density.

Order parameter symmetry in the topological superconductor UPt_3: With three distinct superconducting phases UPt_3 is the prototypical unconventional superconductor, and despite decades of experimental and theoretical studies the order parameter in this material is still not fully understood. A key component is the presence of a symmetry breaking field (SBF) that couples to the E_{2u} superconducting order parameter. The SBF lifts the degeneracy of the multi-dimensional representation, splitting the zero-field transition and leading to the multiple superconducting phases. We have demonstrated how the rotated VL phase at low temperatures and intermediate fields, summarized in Fig. 2, can be directly attributed to the SBF [2]. This is the first observation of such an effect at the microscopic level.

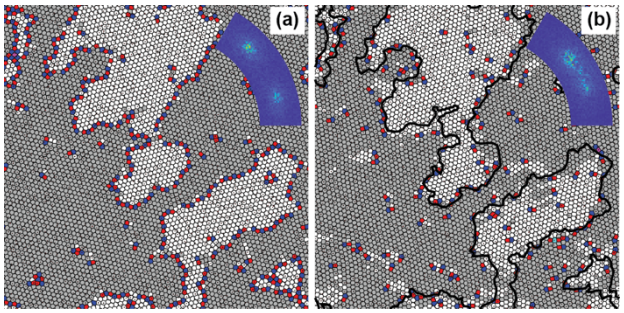

Fig. 4 Voronoi constructions of the VL in a superconductor with combined 6- and 12-fold anisotropic interactions. (a) Initial state. Grain boundaries are decorated by 5/7 dislocations (red/blue). (b) VL after the application of 1,000 penetration depth oscillations. Insets show the VL structure factor.

VL studies in Ta-doped CsV_3Sb_5: The AV_3Sb_5 (A = K, Rb, Cs) kagome family of superconductors continues to attract great attention, and a multitude of interesting properties have been reported for these materials. We have performed SANS studies of VL in CsV_3Sb_5 doped with Ta to suppress the Charge Density Wave (CDW) formation. Since the CDW may be responsible for some of the unconventional superconducting behavior, our measurements serve as a valuable reference. Our results provide bulk information about the VL morphology, flux quantization, and superconducting gap [3]. Altogether, this indicates a fully conventional superconducting state with conventional 2e-pairing, and a field dependence of the scattered intensity that is described by the London model. Furthermore, the temperature dependence of the superfluid density is consistent with a uniform s-wave gap as shown in Fig. 3. From this it is possible to determine the gap which confirms weak coupling superconductivity.

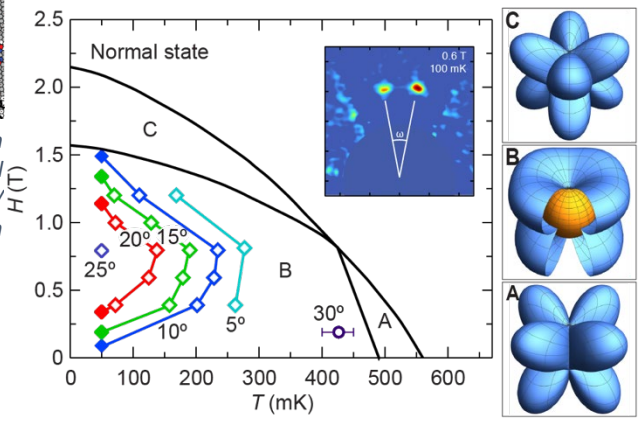

Fig. 2 VL peak splitting (ω) contours superimposed on the UPt_3 phase diagram. Schematics on the right shows the superconducting order parameter in the A, B and C phases.

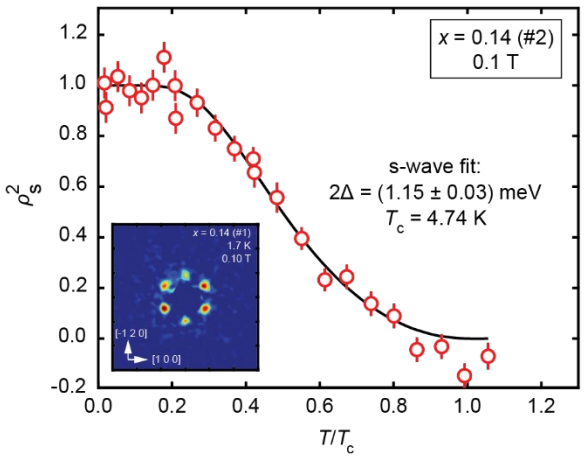

Fig. 3 Temperature dependence of the superfluid density for $Cs(V_{0.86}Ta_{0.14})_3Sb_5$. The line is a fit to an s-wave model. Inset shows a VL diffraction pattern.

Molecular dynamics simulations of skyrmion and vortex lattices: Skyrmion hosting materials and superconductors invariable possess a degree of anisotropy which is responsible for the preferred alignment of the SkL or VL relative to the crystalline axes. In driven skyrmion systems as discussed above, as well as superconductors with competing anisotropies on different Fermi surface sheets, this can rise to domain formation, metastability and other out-of-equilibrium configurations. To model such systems and obtain real space information that complement the SANS results, we have implemented

MD simulations with anisotropic interactions [4]. Applying a drive that mimics an oscillating magnetic field allows us to reproduce the behavior observed in MgB_2 where a metstable VL is driven towards the equilibrium state. This is illustrated in Fig. 4, where grain boundaries between metstable VL domains shift due to dislocation annihilation events and allows it to rotate towards the ground state.

Fig. 4 Assembled SANS scanning aperture stage.

Future Plans

Skyrmion manipulation by electrical and thermal currents: The SkL studies under the influence of a radial electrical and thermal currents will be continued, where a Corbino sample geometry has turned out to be highly useful. These will include high precision measurements, both in terms of the magnitude of the drive and the location within the sample. Measurements along the radial direction will also be carried out as both azimuthal and radial forces will decay with distance from the center. Focusing on smaller regions of the sample will also reduce effects of domain formation, greatly simplifying the modeling and interpretation of the data. In addition to a statistical analysis of the time averaged data, we will develop methods to process the diffraction pattern movies obtained on Cu_2OSeO_3.

VL studies in Ta-doped CsV_3Sb_5: VL studies $Cs(V_{1-x}Ta_x)_3Sb_5$ in will be continued. Experiments at high-flux sources such as HFIR will allow us to expand measurements to higher fields and explore a larger portion of the superconducting phase diagram. Furthermore, we will explore the VL as the applied field is rotated away from the crystalline *c*-axis. Such studies have in the past been used to provide direct bulk evidence for multiband superconductivity in MgB_2, KFe_2As_2 and Sr_2RuO_4. Finally, studies in samples with intermediate Ta-doping where a CDW is observed will allow us to study a connection between charge order and unconventional superconductivity.

Spatially resolved SANS measurements: The SkL state in chiral magnets arise due to a competition between different magnetic interactions. Due to the small free energy difference between the topological SkL state, with an associated activation barrier for skyrmion formation, and neighboring conical state, such systems will often exhibit phase coexistence. An example is Cu_2OSeO_3 where low temperature skyrmion and twisted conical phases coexist at low temperature and give rise to an inherently heterogenous state. This provides an opportunity to explore the spatial inhomogeneities and domain formations on a mesoscopic scale through spatially resolved SANS. We will use an actuated sample stage, shown in Fig. 5, that precisely translates a neutron aperture placed immediately adjacent to the sample, eliminating blurring providing a micron-level precision. In the longer term this approach may be combined with the Corbino experiments, although such an integration will provide a technical challenge.

SANS studies under strain: Strain has emerged as a powerful method for manipulating the Fermi surface of materials and thereby their electronic properties. Initial SANS measurements on niobium indicated that the superconducting state may be altered by strain, causing a transition into/out of the intermediate mixed state (IMS) where a local minimum in the vortex-vortex interaction gives rise to a field-independent VL periodicity. We have optimized the sample preparation for such measurements, which include cutting, etching and careful annealing to reduce vortex pinning in the niobium single crystals. This project will be continued.

References

1. N. Chalus, A. W. D. Leishman, G. Longbons, R. Menezes, M. V. Milošević, U. Welp, W.-K. Kwok, M. Bartkowiak, J. S. White, R. Cubitt, E. D. Bauer, M. Janoschek, and M. R. Eskildsen, *Skyrmion Lattice Manipulation with Electric Currents and Thermal Gradients in MnSi*, manuscript in preparation.

2. K. E. Avers, W. J. Gannon, A. W. D. Leishman, L. DeBeer-Schmitt, W. P. Halperin, and M. R. Eskildsen, *Effects of the order parameter anisotropy on the vortex lattice in UPt_3*, Front. Electron. Mater. **2**, 878308 (2022).

3 Y. Xie, N. Chalus, W. Yao, J. Liu, Y. Yao, Z. Wang, J. S. White, L. M. DeBeer-Schmitt, P. Dai, and M. R. Eskildsen, *Conventional s-Wave Superconductivity in $Cs(V_{0.86}Ta_{0.14})_3Sb_5$ Inferred from Vortex Lattice Studies*, manuscript in preparation.
4. D. Minogue, M. R. Eskildsen, C. Reichhardt, and C. J. O. Reichhardt, *Activated vortex lattice transition in a superconductor with combined sixfold and twelvefold anisotropic interactions*, New J. Phys. **25**, 113047 (2023).

Publications

1. A. W. D. Leishman, A. Sokolova, M. Bleuel, N. D. Zhigadlo, and M. R. Eskildsen, *Field-angle dependent vortex lattice phase diagram in MgB_2*, Phys. Rev. B **103**, 094516 (2021). DOI: 10.1103/PhysRevB.103.094516

2. K. E. Avers, W. J. Gannon, A. W. D. Leishman, L. DeBeer-Schmitt, W. P. Halperin, and M. R. Eskildsen, *Effects of the order parameter anisotropy on the vortex lattice in UPt_3*, Front. Electron. Mater. **2**, 878308 (2022). DOI: 10.3389/femat.2022.878308

3. K. E. Avers, S. J. Kuhn, A. W. D. Leishman, L. DeBeer-Schmitt, C. D. Dewhurst, D. Honecker, R. Cubitt, W. P. Halperin and M. R. Eskildsen, *Reversible ordering and disordering of the vortex lattice in UPt_3*, Phys. Rev. B **105**, 184512 (2022). DOI: 10.1103/PhysRevB.105.184512

4. E. R. Louden, S. Manni, J. E. Van Zandt, A. W. D. Leishman, V. Taufour, S. L. Bud'ko, L. DeBeer-Schmitt, D. Honecker, C. D. Dewhurst, P. C. Canfield, and M. R. Eskildsen, *Effects of magnetic and non-magnetic doping on the vortex lattice in MgB_2*, J. Appl. Cryst. **55**, 693-701 (2022). DOI: 10.1107/S160057672200468X

5. E. Roe, M. R. Eskildsen, C. Reichhardt, and C. J. O. Reichhardt, *Driven superconducting vortex dynamics in systems with twofold anisotropy in the presence of pinning*, New J. Phys. **24**, 073029 (2022). DOI: 10.1088/1367-2630/ac7d6c

6. D. Minogue, M. R. Eskildsen, C. Reichhardt, and C. J. O. Reichhardt, *Activated vortex lattice transition in a superconductor with combined sixfold and twelvefold anisotropic interactions*, New J. Phys. **25**, 113047 (2023). DOI: 10.1088/1367-2630/ad0c82

7. Y. Xie, N. Chalus, W. Yao, J. Liu, Y. Yao, Z. Wang, J. S. White, L. M. DeBeer-Schmitt, P. Dai, and M. R. Eskildsen, *Conventional s-Wave Superconductivity in $Cs(V_{0.86}Ta_{0.14})_3Sb_5$ Inferred from Vortex Lattice Studies*, manuscript in preparation.

8. N. Chalus, A. W. D. Leishman, G. Longbons, R. Menezes, M. V. Milošević, U. Welp, W.-K. Kwok, M. Bartkowiak, J. S. White, R. Cubitt, E. D. Bauer, M. Janoschek, and M. R. Eskildsen, *Skyrmion Lattice Manipulation with Electric Currents and Thermal Gradients in MnSi*, manuscript in preparation.

Probing Short-Range Structure and Magnetism in Next-Generation Energy Conversion Materials

Benjamin Frandsen, Department of Physics and Astronomy, Brigham Young University

Keywords: Magnetic pair distribution function, short-range magnetic correlations, magnetostructural coupling, magnetic semiconductors, multiferroics

Research Scope

This project employs advanced neutron scattering methods and other complementary techniques to study materials with significant technological potential for energy conversion applications and/or importance for fundamental understanding of magnetostructural coupling and short-range magnetism. Systems investigated as part of this project include magnetic thermoelectrics, multiferroics, magnetocalorics, magnetostructurally active antiferromagnets, and frustrated magnets. Given that the properties of functional and quantum materials often depend sensitively on the details of *local* structural and magnetic correlations, i.e. correlations that are well defined on length scales up to several unit cells but that average to zero on longer length scales, we utilize atomic and magnetic pair distribution function (PDF) analysis of neutron scattering data. The PDF reveals the local pairwise correlations directly in real space, providing an intuitive view of the relevant short-range correlations and allowing for quantitative refinements of models of the local structure. In addition to atomic and magnetic PDF analysis of neutron scattering data, we also utilize inelastic neutron scattering, x-ray total scattering, and muon spin relaxation (μSR) experiments to gain a comprehensive understanding of the local structure and dynamics of relevant materials.

Specific material systems under recent investigation include the antiferromagnetic semiconductor and high-performance thermoelectric material MnTe, the type-I multiferroic (Sr,Ba)MnO_3, and frustrated magnetic materials $NaYbO_2$ and (Zn,Mn)Te. In addition to establishing the influence of local atomic and magnetic correlations in these materials on their properties, this project aims to develop magnetic PDF methods further, from new experimental approaches (e.g. with polarized neutrons) to user-friendly software infrastructure with novel data visualization and modeling capabilities.

Recent Progress

MnTe: The hexagonal antiferromagnetic semiconductor MnTe has attracted intense recent interest as a magnetically enhanced high-performance thermoelectric material [1], a structural component of the magnetic topological insulator $MnBi_2Te_4$ [2], and a candidate altermagnetic material [3]. We have contributed to the understanding and potential applications of MnTe in two concrete ways. First, we used magnetic PDF to visualize and analyze short-range magnetic correlations that persist far into the paramagnetic phase and strongly affect the electronic thermopower. This study confirmed the picture of paramagnon drag posed in Ref. [1] and revealed previously unknown spatial anisotropies in the magnetic correlations that have implications for device design (Pub. 7). Our second contribution is the discovery that MnTe exhibits the largest known spontaneous magnetovolume

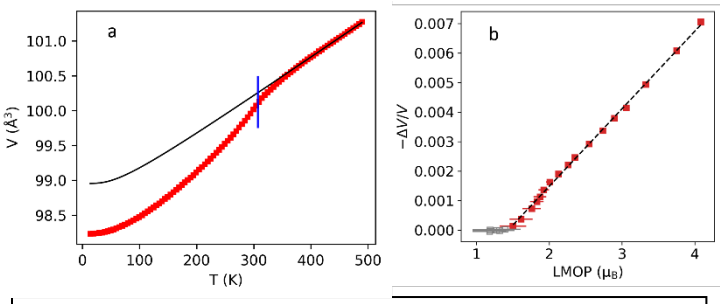

Fig. 1. (a) Unit cell volume of MnTe as a function of temperature, showing a strong decrease below the Neel temperature. (b) Plot of the fractional volume change versus the locally ordered magnetic moment, revealing a striking linear relationship that begins above T_N.

effect of any antiferromagnet (Pub. 3). The unit cell volume contracts nearly 1% due to the development of long-range magnetic order. Perhaps more surprisingly, the effect begins far above T_N due to the formation of short-range magnetic correlations, and the observed lattice response scales linearly with the locally ordered magnetic moment. Linear scaling would appear to violate time reversal symmetry of the free energy, suggesting a novel magnetostructural mechanism is at play. We explain these findings in terms of trilinear couplings between the strain and distinct short-range-ordered domains of the magnetic order parameter. These results highlight the influence of short-range magnetic correlations on macroscopic material properties.

(Sr,Ba)MnO_3: (Sr,Ba)MnO_3 is a promising type-I multiferroic system with unusually large magnetoelectric coupling compared to other type-I systems [4]. We have performed a comprehensive study of the local atomic and magnetic structure across several compositions of this system using atomic and magnetic PDF analysis, polarized neutron scattering, and muon spin relaxation (Pub. 1). We show that the atomic structure has locally broken symmetry at least 100 K above the long-range ferroelectric transition in the form of a tetragonal distortion on a ~2 nm length scale. Similarly, short-range antiferromagnetic correlations begin to develop about 100 K above the Neel temperature. Most significantly, we demonstrate that the short-range magnetic correlations facilitate magnetoelectric coupling and alter the electric polarization even when long-range magnetic order is absent (see Fig. 2), identifying the local magnetic structure as a key factor in this multiferroic system.

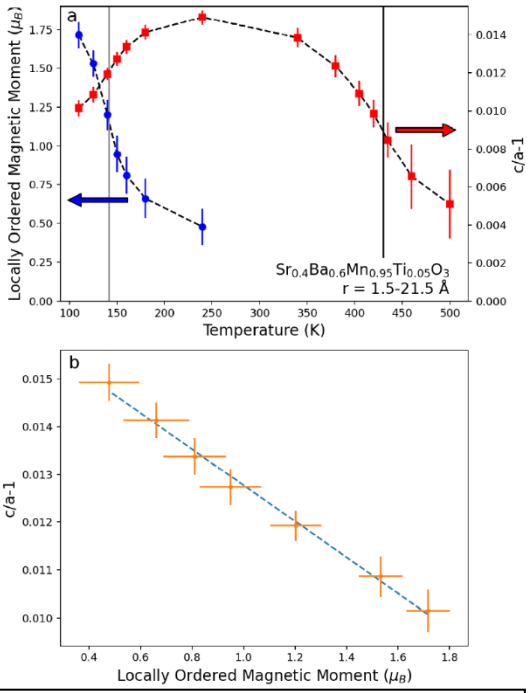

Fig. 2. Linear magnetoelectric coupling achieved in (Sr,Ba)MnO_3 via short-range magnetic correlations.

Systems with intrinsically disordered magnetic ground states: We used magnetic PDF to investigate the quantum spin liquid candidate $NaYbO_2$ [5] and the spin glass (Zn,Mn)Te, both of which are intrinsically disordered antiferromagnets. These systems were selected partially as valuable case studies for magnetic PDF technique development (see next section), but also because they are interesting materials in their own right. In both cases, we are able to visualize the local magnetic correlations directly in real space using magnetic PDF, which offers intuitive insights into the underlying magnetic interactions. Quantitative modeling in both real space and reciprocal space yields excellent fits to the data (Fig. 3), allowing us to track the development of the short-range correlations as the temperature is lowered. In the case of $NaYbO_2$ (Pub. 2), we demonstrated that the short-range magnetism is consistent with a quantum spin liquid ground state. In (Zn,Mn)Te (manuscript in preparation), we show that the spin glass state can

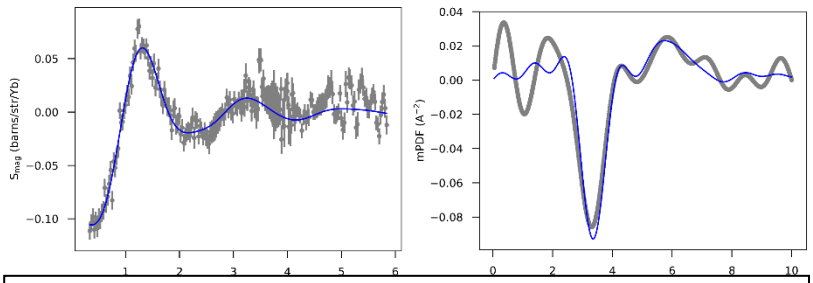

Fig. 3. Reciprocal space (left) and real space (right) modeling of short-range antiferromagnetic correlations in candidate quantum spin liquid material $NaYbO_2$, which has a triangular lattice of J_{eff}=1/2 moments.

be viewed as a short-range-ordered version of type-III antiferromagnetism on an fcc lattice.

Technique Development: Our recent work has resulted in several meaningful developments of the magnetic PDF technique. This includes releasing a comprehensive, open-source python package for mPDF analysis called diffpy.mpdf (Pub. 6); improving the mPDF data reduction using a new algorithm with *ad hoc* corrections and demonstrating the first successful application of mPDF using polarized neutrons (Pub. 5); implementing symmetry-mode analysis in fits of symmetry-broken local structures to atomic PDF data (Pub. 4); and demonstrating the advantages of combined reciprocal space and real space analysis when exploring disordered magnetic structures (Pub. 2). These developments make mPDF analysis easier to learn and implement while also providing new capabilities for gaining deeper insights into magnetic materials with mPDF.

Future Plans

We have collected a large amount of neutron, x-ray, and muon data on several additional materials that we have not yet had time to analyze fully. We plan to complete the data analysis for these materials and publish the results. We will first focus on MnSb, a metallic ferromagnet with applications as a magnetocaloric material and a potential permanent magnet. Preliminary neutron PDF analysis shows significant short-range magnetic correlations above T_C and a sizeable spontaneous magnetostriction, while x-ray PDF with an *in situ* magnetic field shows forced magnetostriction with a non-trivial temperature dependence of the magnetostriction coefficient. Related to this, we also have neutron PDF data for the solid solution of MnSb-CrSb which shows an interesting crossover from ferromagnet to antiferromagnet via multiple non-collinear magnetic phases. The data will allow us to investigate the nature of the short-range magnetic correlations above the long-range ordering temperature when multiple competing phases are proximate, which may have implications for paramagnon drag in magnetic semiconductors.

We will also investigate the influence of short-range magnetic correlations on spontaneous magnetostriction in the ilmenite compounds $NiTiO_3$, $MnTiO_3$, and $FeTiO_3$. We currently have neutron PDF, x-ray PDF, and μSR data on these compounds, with earlier results indicating the presence of robust short-range antiferromagnetic correlations in a large temperature window above T_N. We hypothesize that the trilinear coupling leading to an apparent linear scaling of the spontaneous magnetostriction with the local magnetic order parameter in MnTe will also be realized in these ilmenite systems. Further analysis will allow us to confirm or reject this hypothesis, leading to a deeper understanding of spontaneous magnetostriction in antiferromagnets.

Further, we will continue our studies of the giant magnetocaloric system $(Mn,Fe)_2(P,Si)$ using atomic and magnetic PDF analysis. The objective is to determine how the local structure dictates the behavior across the first-order magnetostructural/magnetoelastic transitions in this system. We have collected complementary neutron and x-ray PDF data on several compositions of this system, which will allow us to conduct a thorough and systematic investigation.

These future studies will complement the current and earlier studies conducted as part of this project, allowing us to gain a deeper understanding of the role played by short-range magnetic correlations and local structural features in determining macroscopic material properties. Already, our studies have demonstrated the decisive impact of short-range magnetism in magnetostructurally active systems such as MnTe and (Sr,Ba)MnO3. Extending our studies to the other systems mentioned in this section will allow us to draw broader conclusions about when to expect nontrivial effects of short-range structure and magnetism in a variety of systems, helping pave the way for the ultimate goal of utilizing short-range magnetism as a controllable knob to achieve desired material properties.

References

[1] Y. Zheng et al, “Paramagnon drag in the high thermoelectric figure of merit Li-doped MnTe”, *Sci. Adv.* **5** eaat9461 (2019).

[2] Yujun Deng, Yijun Yu, Meng Zhu Shi, Zhongxun Guo, Zihan Xu, Jing Wang, Xian Hui Chen, and Yuanbo Zhang, "Quantum anomalous Hall effect in intrinsic magnetic topological insulator $MnBi_2Te_4$", *Science* **367**, 895-900 (2020).
[3] I. I. Mazin, "Altermagnetism in MnTe: Origin, predicted manifestations, and routes to detwinning", *Phys. Rev. B* **107**, L100418 (2023).
[4] H. Somaily, S. Kolesnik, J. Mais, D. Brown, K. Chapagain, B. Dabrowski, and O. Chmaissem. "Strain-induced tetragonal distortions and multiferroic properties in polycrystalline Sr1-xBaxMnO3 (x=0.43-0.45) perovskites", *Phys. Rev. Mater.* **2**, 054408 (2018).
[5] Mitchell M. Bordelon, Eric Kenney, Chunxiao Liu, Tom Hogan, Lorenzo Posthuma, Marzieh Kavand, Yuanqi Lyu, Mark Sherwin, N. P. Butch, Craig Brown, M. J. Graf, Leon Balents, and Stephen D. Wilson. "Field-tunable quantum disordered ground state in the triangular-lattice antiferromagnet $NaYbO_2$", *Nature Physics* **15**, 1058-1064 (2019).

Publications

1. Braedon Jones, Christiana Z. Suggs, Elena Krivyakina, Daniel P. Phelan, Ovidiu Garlea, Omar Chmaissem, and Benjamin A. Frandsen. "Local atomic and magnetic structure of multiferroic $(Sr,Ba)(Mn,Ti)O_3$". Acceptance pending at *Phys. Rev. B*.
2. Kristina Michelle Nuttall, Christiana Z. Suggs, Henry E. Fischer, Mitchell M. Bordelon, Stephen D. Wilson, and Benjamin A. Frandsen. "Quantitative investigation of the short-range magnetic correlations in candidate quantum spin liquid $NaYbO_2$". *Phys. Rev. B* **108**, L140411 (2023).
3. Raju Baral, Milinda Abeykoon, Branton J. Campbell, and Benjamin A. Frandsen. "Giant spontaneous magnetostriction in MnTe driven by a novel magnetostructural coupling mechanism". *Advanced Functional Materials* **33**, 2305247 (2023).
4. Parker K. Hamilton, Jaime M. Moya, Alannah M. Hallas, E. Morosan, Raju Baral, and Benjamin A. Frandsen. "Symmetry-mode analysis for local structure investigations using pair distribution function data". *J. Appl. Cryst.* **56**, 1192 – 1199 (2023).
5. Benjamin A. Frandsen, Raju Baral, Barry Winn, and V. Ovidiu Garlea. "Magnetic pair distribution function data using polarized neutrons and *ad hoc* corrections". *J. Appl. Phys.* **132**, 223909 (2022).
6. Benjamin A. Frandsen, Parker K. Hamilton, Jacob A. Christensen, Eric Stubben, and Simon J. L. Billinge. "diffpy.mpdf: open-source software for magnetic pair distribution function analysis". *J. Appl. Cryst.* **55**, 1377 – 1382 (2022).
7. Raju Baral, Jacob Christensen, Parker Hamilton, Feng Ye, Karine Chesnel, Taylor D. Sparks, Rosa Ward, Jiaqiang Yan, Michael A. McGuire, Michael E. Manley, Julie B. Staunton, Raphael P. Hermann, and Benjamin A. Frandsen. "Real-space visualization of short-range antiferromagnetic correlations in a magnetically enhanced thermoelectric". *Matter* **5**, 1853 – 1864 (2022).

DE-FG02-03ER46055: Inelastic Neutron Scattering Studies of Quantum Anharmonicity and Nonlinear Phonons

Brent Fultz, Applied Physics and Materials Science, California Institute of Technology

Keywords: inelastic neutron scattering, anharmonic, nonlinear crystals, melting, liquids

Research Scope

This is an experimental program based on inelastic neutron scattering (INS) measurements of atom vibrations in materials. The emphasis is on highly nonlinear vibrations, and how they change with temperature. Results from work on single crystals and liquids are described in this abstract; other results are reported in some of the publications.

Recent Progress

If a crystal is harmonic, with potentials quadratic in atom displacements, a standard phonon picture is successful [1]. With cubic and quartic perturbations to the potentials, many-body perturbation theory [2] is useful for predicting the thermal shifts of phonons and phonon lifetimes, which are relevant for thermal conductivity and thermal expansion. This many body theory loses its predictive power when the crystal is highly anharmonic, as we find for NaBr, Zn, and Cu_2O. Our group has started using a different approach to interpret vibrational dynamics in highly anharmonic systems. We use the quantum Langevin equation, which has proved its worth in analyzing noise in quantum information systems. Our first project with NaBr was able to adapt methods from quantum optics of resonant cavities to predict the shapes of "intermodulation phonon sidebands" (IPS) in NaBr [3]. These sidebands are at approximately the sum and difference of the energies of flat transverse phonon dispersions (see band at 25 meV in Fig. 1, and intensity at 8 meV). It was fortunate that the strongly interacting phonons in NaBr have flat dispersions, so the sidebands were flat and we could ignore the Q-dependence. This is generally not the case, as we are finding for IPS features from a zinc crystal.

A second feature we found in NaBr is a second harmonic of fundamental phonon frequencies, which lies above the top of the optical modes of the conventional phonons (at 33 meV in Fig. 1). It is possible to treat both sidebands and second harmonics on the same footing with a semi-classical model of a

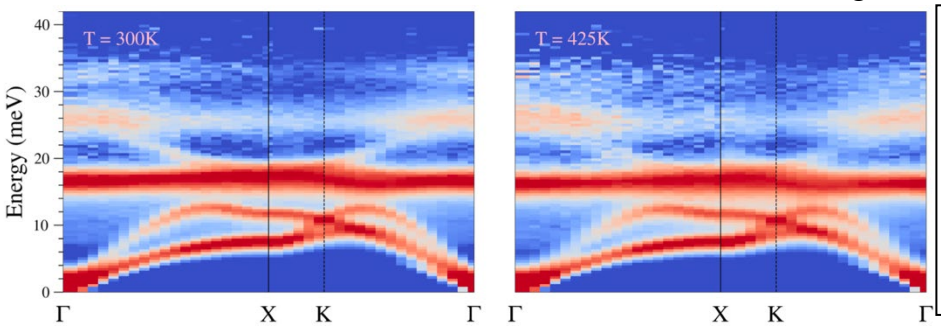

Fig. 1. Inelastic neutron scattering data from NaBr single crystal at 300 K and 425 K. Each panel is normalized with respect to its total inelastic intensity (data are on log scale).

nonlinear system. The system has a response to adding phonons as: $\psi_{out} = \eta\psi_{in} + \varepsilon\psi_{in}^2$. When ψ_{in} is a sum of waves with two frequencies, such as $\psi_{in} = e^{i\omega 1t} + e^{i\omega 2t}$, the second term gives cross-products that include second harmonics, $2\omega_1$ and $2\omega_2$, and sums and differences of the frequencies, $(\omega_1+\omega_2)$ and $(\omega_1-\omega_2)$. This semiclassical model treats the intensities of both harmonics and sidebands in the same way, but this may be incorrect.

A question we are addressing is if it is appropriate to treat sidebands or second harmonics as quasiparticles, where we can give them thermal weights expected for their energies and count them for doing statistical mechanics. Our theoretical treatment of the sidebands was yes, we can use their energies with boson statistics to predict their experimental intensities [3]. Our first data [3] were not

good enough to see the temperature dependence of the intensities, but our INS dataset from 2022 (partly shown in Fig. 1) indicate that we can treat the sidebands as independent quasiparticles. The second harmonics, however, seem to have thermal weights that are the square of the weights of phonons at the fundamental frequency. This analysis is underway now, however, and we may change our interpretation.

Camille Bernal-Choban just completed a Ph.D. thesis on the vibrational contributions to the latent heat of melting (fusion). Calorimetric measurements of the latent heat, L, give the entropy of fusion, ΔS_{fusion}, because $L = T_m \Delta S_{fusion}$ (T_m is the melting temperature). A common assumption is $\Delta S_{fusion} = 1.1\ k_B$/atom, an approximation known as "Richards's Rule." It is a very weak rule because ΔS_{fusion} varies from 0.5 to 3.7 k_B/atom for elements in the Periodic Table. We developed analyses of INS data to obtain the changes in vibrational entropy upon melting. This was nearly zero for Pb, and small for Sn, which follow Richard's Rule. Large deviations were found for Ge and Bi, however. Their deviations from Richard's Rule were proportional to the change in vibrational entropy upon melting. There is also an extra change in configurational entropy, which, surprisingly, is consistently about 80% of the change in vibrational entropy. This leads to the trend of Fig. 2. This surprisingly linear trend should be checked for more elements (such as Se, Ga, Al), and compounds, too.

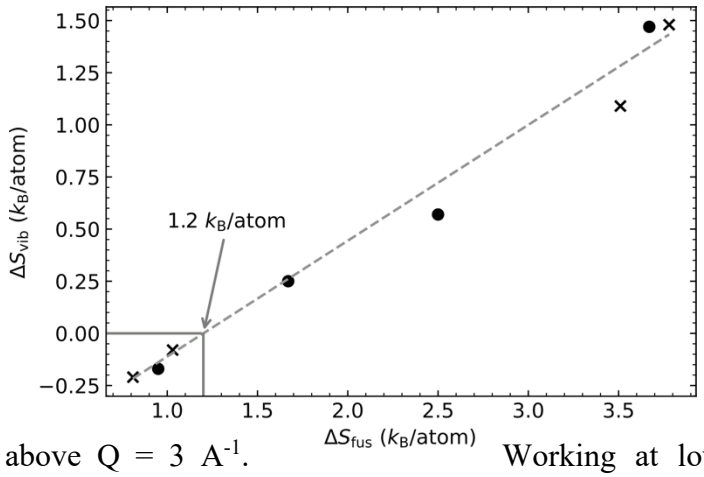

Fig. 2. Change in vibrational entropy upon melting versus total change in entropy of melting from calorimetry measurements.

Using INS to study vibrational modes in liquids is much more difficult than studying vibrations in crystals. A major issue is that all atoms in the liquid are moving, and give quasielastic scattering that broadens rapidly with Q, overwhelming the vibrational spectra above Q = 3 A^{-1}. Working at low Q brings a challenge of weak phonon intensity, causing an issue with multiple scattering. From Monte Carlo simulations of multiple scattering, we found that initial scatterings to higher Q can be scattered a second time into a broad range of angles, and some of them are interpreted as extra intensity at low Q. This gives a background that needs removal before obtaining a phonon DOS. Other issues are multiphonon corrections, and backgrounds from the sample holders, which must be robust when working with liquid metals in a neutron spectrometer. Finally, there is an issue of how the vibrational modes are sampled at low Q. Because INS depends on the polarization of the atom vibrations, **e**, as $\mathbf{e}\cdot\mathbf{Q}$, at low Q there is a low sensitivity to transverse vibrational modes. To mitigate this, we have sampled energy spectra at Q around the structure factor maximum, and have also used the same values of Q for the crystalline phase for comparison, since our goal is to obtain a change in vibrational entropy across melting. This comparative approach seems best.

Fig. 3. Approximate phonon DOS from selected energy cuts at low Q. A large softening is seen for Bi upon melting, but a much smaller change for Sn. (Sn follows Richard's Rule more closely than Bi.)

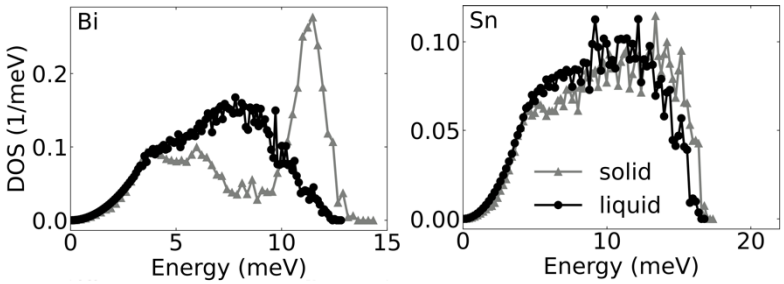

There are two indicators that the approach works. First, the Lorentzian function about the zero energy transfer scales appropriately with Q, indicating that the multiple scattering is less of a problem than some of our more pessimistic MCViNE simulations. Second, our molecular dynamics calculations with LAMMPS have shown surprisingly good agreement with the atom vibrational spectra in the liquid from INS. Nevertheless, the methods and trends should be checked with a few more elements and compounds.

Future Plans

We will continue to be guided by ab initio simulations, even though there are often differences from the INS measurements on materials with large anharmonicities. We are completing our work on phonon second harmonics in NaBr. We have made progress on anharmonic effects in an INS dataset from a large single crystal of Zn, which are now reduced to phonon dispersions at temperatures of 15, 300, 500, 690 K. We find prominent intermodulation phonon sidebands, and have identified the phonons that are mixing. The sideband features for Zn are not flat as for NaBr in Fig. 1, but have the same origin. Another nonlinear phenomenon was observed as a diffuse inelastic intensity in INS measurements on cuprite, Cu_2O, and this work has been submitted for publication.

The computational physics group developing the EPW package (electron-phonon Wannier) has found a large effect of electron-phonon interactions in the phonon dispersions of heavily-doped diamond (observed experimentally by high-resolution inelastic x-ray scattering). Samuel Poncé of UCLouvain, Belgium (a leader of the EPW code development) and I have started to look at these effects in heavily doped silicon. His preliminary calculations show that the phonon dispersions at the point W are nearly unchanged with doping, but the dispersions at Γ and especially L change by nearly 10% with p-doping of 5%. INS measurements can resolve phonon shifts of 1% or even less at 40-60 meV, although we expect broadening in the doped materials. We have begun a Raman study on silicon crystals at elevated temperatures to better plan the neutron work. Boron is an unfortunate absorber of neutrons, but its low concentrations should allow measurements with commercially-available wafers of 0.3 mm. Similar calculations have been performed for n-doped silicon (with P). They are interesting, too, and should be easier to measure, but their electron-phonon interactions are not so strong. The temperature dependences of these electron phonon interactions are essentially unknown, but we are working to do calculations for comparison for the Raman measuremens. The technological importance of doped silicon hardly needs mention, and highly-doped silicon is used in devices for power electronics.

The clean trend in Fig. 2 for ΔS_{fusion} should be checked for more elements (such as Se, Ga, Al), but it would be more interesting to study the melting of compounds, which may show bigger effects. One candidate is the compound AlSb, which has a much higher melting temperature (1063 C) than its constituents Al and Sb (660 C and 631 C), has a relatively large entropy of melting (2.8 k_B/atom), and is convenient for neutron scattering experiments. Computational work has proved useful for assessing vibrational, configurational, and electronic contributions to ΔS_{fusion}. We should perform these calculations before requesting beamtime. In short, the origin of ΔS_{fusion} at the level of atoms is a new topic for neutron scattering research.

References

1. D.S. Kim, O. Hellman, J. Herriman, H.L. Smith, J.Y.Y. Lin, N. Shulumba, J.L. Niedziela, C.W. Li, D.L. Abernathy, and B. Fultz, *Nuclear quantum effect with pure anharmonicity and the anomalous thermal expansion of silicon*, Proc. Nat'l Acad. Sciences **115**, 1992 (2018). [See also: C. Ash and J. Smith, *In Other Journals*, Science, **360**, 167 (2018).]

2. A.A. Maradudin and A.E. Fein, *Scattering of Neutrons by an Anharmonic Crystal*, Phys. Rev. **128**, 2589 (1962).

3. Y. Shen, C.N. Saunders, C.M. Bernal, D.L. Abernathy, M.E. Manley, and B. Fultz, *Quantum anharmonicity and intermodulation phonon sidebands in NaBr*, Phys. Rev. B **103**, 134302 (2021). doi: 10.1103/PhysRevB.103.134302.

4. C. M. Bernal-Choban, *Atomic dynamics in solids and liquids from inelastic neutron scattering*, Ph.D. thesis in materials science, California Institute of Technology, Sept. 18, 2023. doi:10.7907/3nv3-g144

5. C. M. Bernal-Choban, V. Ladygin, G. E. Granroth, C. N. Saunders, S. H. Lohaus, D. L. Abernathy, and B. Fultz, *The components of entropy in the latent heat of melting*, Proc. Nat'l Acad. Sci., submitted.

Publications

C. N. Saunders, D. S. Kim, O. Hellman, H. L. Smith, N. J. Weadock, S. T. Omelchenko, G. E. Granroth, C. M. Bernal-Choban, S. H. Lohaus, D. L. Abernathy, and B. Fultz, *Thermal expansion and phonon anharmonicity of cuprite studied by inelastic neutron scattering and ab initio calculations*, Phys. Rev. B **105**, 174308 (2022). doi: 10.1103/PhysRevB.105.174308

H. L. Smith, C. N. Saunders, C. Bernal-Choban, S. H. Lohaus, C. J. Stoddard, L. K. Decker, J. Y. Y. Lin, J. L. Niedziela, D. L. Abernathy, M. D. Demetriou, B. Fultz, *Vibrational Contributions to the Excess Entropy in Ultra-fragile Metallic Glasses*, Materialia **27**, 101710 (2023). doi: 10.1016/j.mtla.2023.101710

C. M. Bernal-Choban, H. L. Smith, C. N. Saunders, D. S. Kim, L. Mauger, D. L. Abernathy, B. Fultz, *Nonharmonic contributions to the high-temperature phonon thermodynamics of Cr*, Phys. Rev. B **107**, 054312 (2023). doi: 10.1103/PhysRevB.107.054312

Claire Nicole Saunders, *Thermal Behavior of Cuprous Oxide: A Comprehensive Study of Three- Body Phonon Effects and Beyond*, Ph.D. in Materials Science, May 19, 2022. doi: 10.7907/mate-2v65 presently: Visiting Researcher, Caltech.

Camille Bernal-Choban, *Atomic dynamics in solids and liquids from inelastic neutron scattering*, Ph.D. in Materials Science, California Institute of Technology, Sept. 18, 2023. doi: 10.7907/3nv3-g144 presently: postdoctoral fellow, Univ. Illinois, Urbana-Champaign

C. N. Saunders, V. V. Ladygin, D. S. Kim, C. M. Bernal-Choban, S. H. Lohaus, G. E. Granroth, D. L. Abernathy, and B. Fultz, *Diffuse Inelastic Neutron Scattering from Anharmonic Vibrations in Cuprite*, Phys. Rev. Lett., submitted.

C. M. Bernal-Choban, V. Ladygin, G. E. Granroth, C. N. Saunders, S. H. Lohaus, D. L. Abernathy, and B. Fultz, *The components of entropy in the latent heat of melting*, Proc. Natl Acad. Sci., submitted.

Exotic Uses of Neutrons an X-rays as Probes for Chiral Magnets

Dustin A. Gilbert, Materials Science and Engineering, University of Tennessee, Knoxville, TN 37919

Keywords: Skyrmions; Neutron scattering; Magnetic dynamics; Spin waves

Research Scope

This research focuses on using neutron and X-ray scattering as unique tools to investigate non-colinear magnetic systems, with a focus on magnetic skyrmions. These techniques, neutron scattering in-particular, have been used extensively to investigate skyrmions, and this work aims to expand their use through the development of novel sample environments and scattering geometries to elucidate further insights into these systems. These projects so-far have included grazing-incidence small angle neutron scattering (GISANS) and polarized neutron reflectometry (PNR), time involved SANS (TISANS),[1] and in-situ ferromagnetic resonance SANS (FMR-SANS); photoemission electron microscopy (PEEM) measurements have also been performed in these studies. We have also developed a software tool that calculates neutron scattering from micromagnetic simulations, coupling the physics of magnetism to experimental scattering. The key to many of these investigations has been our system of choice, namely hybrid skyrmions in Gd/Fe multilayers. This system is unique in-that it provides an extraordinarily strong neutron signal, so much so that reasonable statistics can be achieved with a single 1 cm^2 × 100 nm thick film. Furthermore, these skyrmions can achieve a well-ordered hexagonal structure which is stable at 300 K and H=0, making them both technologically relevant and easy to prepare for sample environments. Our recent work has focused on skyrmion dynamics and the spin waves which are generated during those dynamics.

Recent Progress

This last year focused on the publication of two works and the preparation of a third as two students who were sponsored by this project graduated and a new student started work in our lab. The two projects that were published are *In-situ GHz Dynamics of Skyrmions Probed with SANS*[2] and *Depth Profiles of Hybrid Magnetic Skyrmions Determined by Neutron Scattering*,[3] while the work which will soon be submitted is *Skyrmion lattice formation and destruction mechanisms probed with TISANS*. The first paper received significant attention, including several invited talks at domestic and international conferences (Nano2023, Intermag, MMM, TMRC), was featured in press releases by the University of Tennessee and on the cover page of Department of Energy BES webpage.

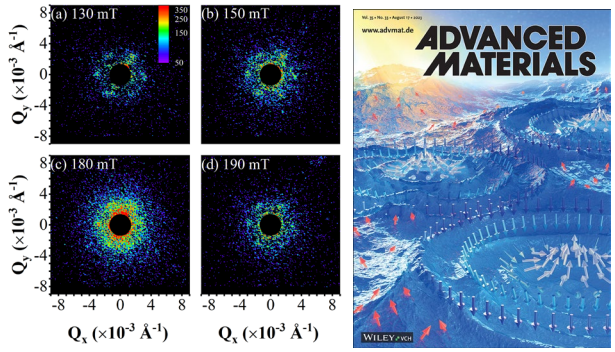

Figure 1 SANS measurement taken of dynamically excited skyrmions below, at and above the resonance condition. Cover from the published issue.

The work *In-situ GHz Dynamics of Skyrmions Probed with SANS* performed in-situ ferromagnetic resonance (FMR) on a skyrmion lattice while performing SANS. The skyrmion dynamics occurs at gigahertz frequencies, while dynamic SANS is limited to kilohertz based on the wavelength distribution. These measurements captured a time-averaged diffraction pattern from the skyrmions and was proposing to investigate the distortion of the lattice during dynamics. However, at resonance,

a large 'background' appeared at low-q, while the hexagonal pattern from the skyrmion lattice changed very little. This new feature had a magnitude ≈5× larger than the coherent diffraction from the skyrmion lattice, which was and still is a mystery to us. After trying the expected feature structures (Porod, quasielastic exp(-q^2), form factor, Lorentzian and Lorentzian squared) the model for a mass-fractal structure was found to fit well. This model is often used for nanoparticle gels or plastics, where the structure is constructed from identical building blocks and has a statistically determined self-similarity. We attribute this structure to the interference pattern from the spin waves which are generated during the dynamic excitation; distortions to the skyrmion lattice would have been observed in the hexagonal diffraction pattern. This implies that the spin waves have a near-uniform periodicity, consistent with other recently published modeling works. The fractal structure also suggests that small variations in the lattice structure can propagate to cause large changes in the spin wave structure, making it attractive for an alternative computing architecture. After further consideration, it was presented that each skyrmion possesses one of twelve dynamic modes, each of which generate a unique spin wave spectrum, resulting in the complex structure observed with SANS. This work confirmed the recently published simulation papers and provided new insights into dynamics in skyrmion systems. Mayber more importantly, the opportunity to investigate magnetic dynamics in other systems is really exciting, this is a much larger field which may now be able to use SANS to investigate spin wave systems beyond standing wave modes.

In the work *Depth Profiles of Hybrid Magnetic Skyrmions Determined by Neutron Scattering* we determined the 3D structure of hybrid magnetic skyrmions using GISANS. The 3D structure is important for all skyrmion systems because it determines their topology, but for the hybrid system in-particular, also contributes to their exceptional stability. At the time that this work was published there had been at-least two other works that had used electron holography to determine the 3D structure of skyrmions in B20 materials prepared as fine needles. However, as most researchers work in bulk or thin-film materials, it is important to determine the 3D structure in these systems. The added dependance on the structure for stability further motivates this work.

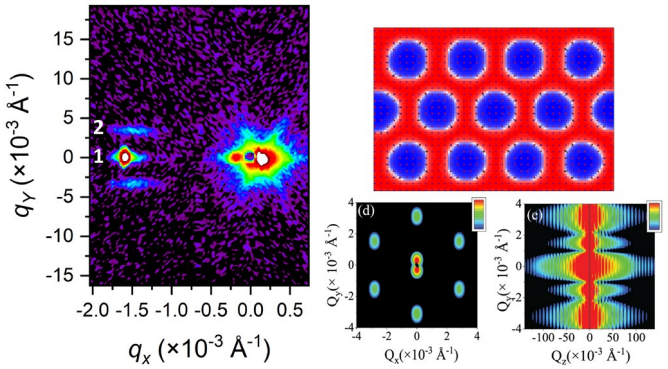

Figure 2 GISANS measurement taken of the stripe state in Gd/Fe multilayers, micromagnetic simulations and the calculated diffraction patterns in transmission and grazing geometries

For most skyrmion systems the signal is insufficient for SANS, let-alone GISANS, making it a challenging, if not impossible measurements. For skyrmions in Gd/Fe multilayers, we were able to capture sufficient signal to measure GISANS in the stripe, skyrmion and saturated states using GISANS and specular PNR. The PNR results were processed using Refl1D, but the GISANS was more obscure. Using a program co-developed with NIST,[4] we were able to take micromagnetic simulations performed with OOMMF and calculate the 3D neutron scattering pattern, including the nuclear, magnetic and imaginary scattering length densities. This analysis is very elegant because most scattering analysis is performed in vacuum, without any outside knowledge about the physicality of the converged structure, however the patterns calculated here are the magnetic configurations evolved following the well-established physics of magnetism. The results revealed a decoupling

between the skyrmion structure (namely the width of the in-plane winding) and the Bloch/Néel character of the winding, but generally supported the hybrid structure.

The work which we are putting the finishing touches on is *Skyrmion lattice formation and destruction mechanisms probed with TISANS*. This work is following up on a series of reports that skyrmions may have very slow dynamic modes. Specifically, magnetic dynamics often happen on the nanosecond timeframe, however some works have shown that skyrmions have very slow dynamics, on the order of seconds to hundreds of seconds.[5] Presumably, this is a consequence of the lattice shifting to align with the magnetocrystalline anisotropy or domains expanding and improving alignment. Many of these same mechanics exist when the skyrmions lattice is formed or destroyed. We used SANS to investigate the formation and destruction kinetics of three prototypical skyrmions materials (MnSi, (Fe,Co)Si, and Cu_2OSeO_3). Each material was cooled to below the Curie temperature, then the field is increased to find the boundaries of the skyrmions stability envelope. Then, using a second set of coils that we designed and machined, a step-like dynamic field is applied to the sample, pushing it into and out-of the stability envelope. The SANS pattern was captured and binned into 10 ms frames during post-processing. The structure of the diffraction pattern and its general intensity were tabulated versus time and trends elucidated. These measurements confirmed the long timeframes for formation and destruction (on the order of 100 ms), and provided new insight into the mechanics. This new capability is now available to other researchers, allowing some time resolution of magnetic dynamics and kinetics (up-to kilohertz).

Future Plans

Future plans for this research are two-fold. The first research topic proposes to expand the investigation of skyrmion and spin wave dynamics using SANS. Our recent work demonstrated that spin waves emitted from skyrmions can be probed with SANS, we now plan to investigate other skyrmion systems and perform similar measurements with small angle X-ray scattering. Specifically, skyrmions in Gd/Fe are soliton-like no symmetry-breaking DMI, resulting in a relatively weak coupling between them, and for the gyration modes, allowing 12 nearly degenerate dynamic states. In the follow-up work, we will measure the dynamics in Gd/Fe skyrmions excited in the breathing mode, which has only two degenerate states. Also, the dynamics modes in Cu_2OSeO_3 will be measured. This system has DMI and so has symmetry breaking; each skyrmion should have a nearly identical structure and gyrate coherently, leaving only stochastic contributions to contribute to the diffraction pattern. Time for both of these experiments has been awarded at GP SANS and will take place this coming year.

An interesting ambiguity within the Gd/Fe skyrmion SANS measurements which we published is the slow speed that the neutron moves through the sample. This is not commonly considered for neutron measurements, but for the 15 Å neutrons used in the study, the velocity is 263 m/s, thus passing through the ≈100 nm film in only 0.38 ns. The dynamics (at 2.23 GHz) occur in 0.45 ns, a comparable timeframe. Functionally, this means that each neutron is diffracting from a continuously changing structure; the question about whether time-independent scattering theory is the correct approach or not are not unreasonable. To consider this, we have submitted and been awarded time at the Advanced Light Source, BL 7.0.1.1, to perform FMR-SAXS as a complement to our FMR-SANS. Using X-rays, the diffraction pattern is captured effectively instantaneously, with the photon passing through the sample in only 0.3 fs. The new, high-speed detector may allow us to capture the diffraction pattern at specific instances in time, which would be really insightful, but even a time-integrated comparison to the SANS data would be very meaningful.

Finally, we hope to submit time to use USANS and further understand the spin wave dynamic structure. Notably, the data taken on Gd/Fe is already at very low-q, requiring long wavelengths, at the longest SANS instrument in the US. USANS will allow us to capture the ultra-low-q structure to even lower angles and higher accuracy. These measurements will also allow us to elucidate the nature of the scattering, that is, whether it is elastic or inelastic. The nature of the USANS measurement requires elastic scattering, thus if the sample is measured and nothing is observed, it provides new insights that the scattering is elastic.

The second focus on the coming year is to realize a skyrmion heterostructure comprised of MnSi/(FeCo)Si or $(Fe_{1-z}Co_z)Si$. These materials have a similar skyrmion stability window (temperature and magnetic field), but very different lattice structure. As a result of these differences, the skyrmions must terminate mid-film, or branch. For the case of termination, this generates chiral bobbers, a topologically trivial, but interesting none-the-less spin texture. For the branching, the branch-point has the qualities of a monopole quasiparticle. Unlike the monopoles in spin ice, these monopoles have no pairs. Furthermore, they potentially will form in very high densities, reflecting their originating skyrmion lattice. The structure will be confirmed with polarized neutron reflectometry and their electronic scattering properties by conventional transport measurements.

References

1. A. B. Author, C. D. Author, and E. F. Co-Author, *Title of the Publication*, Journal **Volume**, page (year).

1. Glinka C., Bleuel M., Tsai P., Zákutná D., Honecker D., Dresen D., Mees F., Disch S. *Sub-millisecond time-resolved small-angle neutron scattering measurements at NIST*. J Appl Crystallogr **53**, 598-604 (2020).
2. Tang N., Liyanage W. L. N. C., Montoya S. A., Patel S., Quigley L. J., Grutter A. J., Fitzsimmons M. R., Sinha S., Borchers J. A., Fullerton E. E., DeBeer-Schmitt L., Gilbert D. A. *Skyrmion-Excited Spin-Wave Fractal Networks*. Advanced Materials **35**, 2300416 (2023).
3. Liyanage W. L. N. C., Tang N., Quigley L., Borchers J. A., Grutter A. J., Maranville B. B., Sinha S. K., Reyren N., Montoya S. A., Fullerton E. E., DeBeer-Schmitt L., Gilbert D. A. *Three-dimensional structure of hybrid magnetic skyrmions determined by neutron scattering*. Physical Review B **107**, 184412 (2023).
4. Gilbert D. A., Maranville B. B., Balk A. L., Kirby B. J., Fischer P., Pierce D. T., Unguris J., Borchers J. A., Liu K. *Realization of ground-state artificial skyrmion lattices at room temperature*. Nature Communications **6**, 8462 (2015).
5. Bannenberg L. J., Qian F., Dalgliesh R. M., Martin N., Chaboussant G., Schmidt M., Schlagel D. L., Lograsso T. A., Wilhelm H., Pappas C. *Reorientations, relaxations, metastabilities, and multidomains of skyrmion lattices*. Physical Review B **96**, 184416 (2017).

Publications

1. Nan Tang, Sergio Montoya, W.L.N.C. Liyanage, Sheena Patel, Lizabeth J. Quigley, Alexander J. Grutter, Michael R. Fitzsimmons, Sunil Sinha, Julie A. Borchers, Eric Fullerton, Lisa Debeer-Schmitt, and Dustin A. Gilbert *In-situ GHz Dynamics of Skyrmions Probed with SANS* Advanced Materials 2300416 (2023).

   *Cover: Advanced Materials **35**, 2370231 (2023)* *Press Release: Phys.org, UTK News*

2. WLNC Liyanage, Nan Tang, Sergio Montoya, Lizabeth Quigley, Julie A. Borchers, Alexander J. Grutter, Sunil K. Sinha, Brian B. Maranville, Eric E. Fullerton, Lisa Debeer-Schmitt, and Dustin A. Gilbert *Depth Profiles of Hybrid Magnetic Skyrmions Determined by Neutron Scattering* Phys. Rev. B **107**, 184412 (2023).

3. Sergey V. Ushakov, Qi-Jun Hong, Dustin A. Gilbert, Kurt Leinenweber, Alexandra Navrotsky and Axel van de Walle *Thorium and Rare Earth Monoxides* Materials **16**, 1350 (2023).

4. Alessandro R Mazza, Elizabeth Skoropata, Jason Michael Lapano, Michael Chilcote, Cameron Jorgensen, Nan Tang, Zheng Gai, John Singleton, Matthew Brahlek, Dustin A. Gilbert, and Thomas Zac Ward *Hole doping in compositionally complex correlated oxide enables tunable exchange biasing* APL Mater. **11**, 031118 (2023).

5. Nan Tang, Jung-Wei Liao, Siu-Tat Chui, Timothy Ziman, Kai Liu, Chih-Huang Lai, Brian J. Kirby, Dustin A. Gilbert *Controlling magnetic configurations in soft-hard bilayers probed by polarized neutron reflectometry* APL Mater. **10**, 011107 (2022) ***Editor's Pick**

6. David A. Garfinkel, Nan Tang, Grace Pakeltis, Reece Emory, Ilia N. Ivanov, Dustin A. Gilbert, and Philip D. Rack *Magneto-Optical Properties of Au-Co Solid Solution and Phase Separated Thin Films and Nanoparticles* ACS Appl. Mater. Interfaces **14**, 15047 (2022).

7. Andy T. Clark, David Marchfield, Zheng Cao, Tong Dang, Nan Tang, Dustin Gilbert, Elise A. Corbin, Kristen S. Buchanan, and Xuemei M. Cheng *The role of magnetic particle motion in magnetization reversal of ultrasoft magnetorheological elastomers* APL Mater. **10**, 041106 (2022).

8. P. Quarterman, Yabin Fan, Zhijie Chen, Christopher J. Jensen, Rajesh V. Chopdekar, Dustin A. Gilbert, Mark D. Stiles, Julie A. Borchers, Kai Liu, Luqiao Liu, and Alexander J. Grutter *Understanding Antiferromagnetic Coupling in Magnetic Insulator/Metal Heterostructures* Phys. Rev. Mater. **6**, 094418 (2022).

9. Dustin A. Gilbert, Mi-Young Im, Kai Liu, and Peter Fischer *Element-Specific First Order Reversal Curves Measured by Magnetic Transmission X-ray Microscopy* APL Materials **10**, 111105 (2022).

10. Xin Wang, Brianna Musicó, Corisa Kons, Peter Metz, Veerle Keppens, Dustin A Gilbert, Yuanpeng Zhang, and Katharine Page *Local Cation Order and Ferrimagnetism in Compositionally Complex Spinel Ferrites* APL Materials **10**, 121102 (2022)

University of Minnesota Center for Quantum Materials (CQM): Structural and Electronic Properties of Titanates

Martin Greven (PI)[1], Turan Birol[2], Rafael Fernandes[1], Chris Leighton[2]

[1]School of Physics and Astronomy, University of Minnesota

[2]Department of Chemical Engineering and Materials Science, University of Minnesota

Keywords: Strontium titanate, rare-earth titanates, neutron scattering, x-ray scattering, plastic deformation

Research Scope

The University of Minnesota Center for Quantum Materials (CQM), founded in 2016, investigates the structural, electronic, and magnetic properties of select quantum materials, particularly complex oxides, which embody many of the most fundamental questions regarding quantum behavior of interacting electrons and are relevant to important technologies, including data storage, spintronics, catalysis, and fuel cells. *This abstract complements the main CQM abstract, focusing on the center's work on strontium titanate ($SrTiO_3$) and rare-earth (RE) titanates ($RETiO_3$).* This effort involves all four CQM faculty (*Birol*, *Fernandes*, *Greven, and Leighton*), and both neutron and x-ray scattering.

The properties of quantum materials are commonly tuned with variables such as magnetic field, doping, and pressure. A major CQM theme is the exploration of strain engineering, including entirely new approaches. One such approach is the irreversible, plastic deformation of single crystals, with has required the development of novel high-force pneumatic strain cells and led to ground-breaking results. Initial CQM efforts in this direction have focused on the classic incipient quantum paraelectric and superconductor $SrTiO_3$ as an experimental and theoretical model system. The RE titanates $RETiO_3$ exhibit fascinating Mott-insulating states, non-trivial magnetic transitions/crossovers, and lattice/charge/spin/orbital coupling. As such, they are model systems for the experimental and theoretical study of fundamental questions pertaining to the physics of doped Mott insulators, magnetism, *etc.*

Recent Progress

The high level of synergy within the CQM is exemplified by recent advances with strain tuning and engineering, such as pioneering work on enhanced superconductivity and ferroelectricity in *plastically* deformed $SrTiO_3$ [1]. This breakthrough result involved three senior CQM investigators (*Fernandes, Greven, Leighton*), state-of-the-art diffuse neutron and x-ray scattering at ORNL and ANL (Fig. 1(a)), novel uniaxial strain techniques, and theoretical modeling. Bulk superconductivity in this system is enhanced by about a factor of two with plastic deformation (Fig. 1(b)), with tantalizing initial transport evidence for a minority volume fraction with a *hundredfold* increase in T_c (30-40 K *vs.* 300-400 mK). Moreover, deformation-induced signatures of quantum-critical ferroelectric fluctuations and inhomogeneous ferroelectric order were also observed. Crucially,

diffuse neutron and x-ray data revealed that the enhanced superconductivity and ferroelectricity are correlated with the appearance of self-organized dislocation structures. Specifically, the results indicate that strain surrounding the self-organized dislocation structures induces local ferroelectricity and quantum-critical dynamics that strongly influence T_c, consistent with a theory of superconductivity enhanced by soft polar fluctuations. These pioneering results demonstrate the potential of plastic deformation and dislocation engineering for the manipulation of electronic properties of quantum materials. This work, which is further supported by more recent measurements [2], appeared as a *2023 DOE BES Highlight*. Moreover, it prompted additional collaborative experiments on plastically deformed $SrTiO_3$. For example, micro-SQUID data (by B. Kalisky, Bar Ilan, Israel) led to the surprising discovery of magnetism and, hence, multiferroicity in this novel system [3].

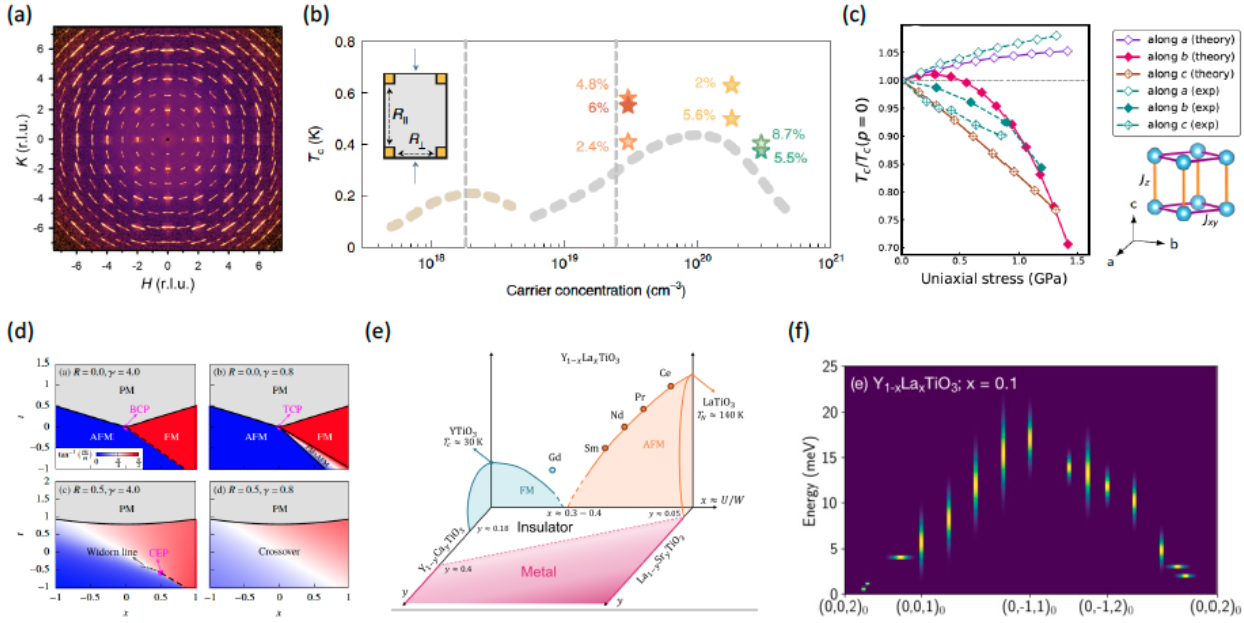

Fig. 1. (a) Diffuse neutron scattering (CORELLI, SNS) for lightly doped $SrTiO_3$, *plastically* deformed by 4.5% along [010]. The scattering is arc-like, with a fine pattern consistent with the formation of periodic dislocation walls, near which superconductivity and ferroelectricity are substantially enhanced [1]. (b) Superconducting phase diagram of undeformed $SrTiO_3$, showing the midpoints of resistive transitions for oxygen-vacancy-doped (brown dashed line) and niobium-doped (grey dashed line) samples. Vertical lines show doping levels at which additional bands cross the Fermi level. Stars indicate midpoints of the resistive transitions of plastically deformed samples in the channel perpendicular to the stress direction ($R_\perp$, see sketch). The deformation levels are indicated. From [1]. (c) Comparison of *elastic* stress dependence of the Curie temperature of $YTiO_3$ from ac susceptibility with mean-field results from DFT [4]. (d) Possible theoretical phase diagrams with strain-tunable metamagnetic critical endpoint in Mott-insulating $RETiO_3$ [5]. (e) Experimental phase diagram of $RETiO_3$ compounds. (f) Detailed spin-wave measurements (HB-3, HFIR) and theoretical modeling give fresh insight into the spin-dynamics of $Y_{1-x}La_xTiO_3$ [7].

A related example of CQM synergy is the demonstration of strain-tuned Curie temperature (T_C) in ferromagnetic $RETiO_3$, understood theoretically using a combination of first-principles and phenomenological calculations (*Birol*, *Fernandes, Greven*) (Fig. 1(c)) [4]. Complementary theoretical work (*Birol*, *Fernandes*) led to new insights into the strain-tunable metamagnetic critical endpoint in Mott insulating rare-earth titanates (Fig. 1(d) [5] and to the development of a theory of criticality for quantum ferroelectric metals (*Fernandes*) [6].

Figure 1(e) shows the rich phase diagram of the RE titanates. Synergistic experimental and theoretical CQM work also explored the effects of random antiferromagnetic exchange on the spin waves in the case of iso-valent substitution of La for Y (*Birol*, *Fernandes, Greven*) (Fig. 1(f)) [7]. This effort established $Y_{1-x}La_xTiO_3$ as a model system for the study of antiferromagnetic spin-exchange disorder in a three-dimensional Heisenberg ferromagnet. Furthermore, a collaborative electron spin resonance and nuclear magnetic resonance study between *Greven* and former CQM postdoc D. Pelc (U. Zagreb, Croatia) provided key insight into the interplay between orbital and spin degrees of freedom and indicated that full orbital degeneracy lifting is associated with FM order [8].

For her outstanding Ph.D. work on RE titanates and plastically deformed strontium titanate, former CQM graduate student Sajna Hameed received the 2022 Neutron Scattering Society of America (NSSA) Prize for Outstanding Student Research.

Future Plans

Studies of the effects of plastic deformation on electronic and magnetic properties will be extended to other perovskites. Initial results for the incipient ferroelectric $KTaO_3$ are very promising, again revealing deformation-induced self-organization of dislocations, as seen via diffuse scattering. An intriguing question is whether charge-carrier doped, plastically deformed $KTaO_3$ exhibits a bulk superconducting phase. *Greven* and *Leighton* plan in-situ elastic and plastic deformation experiments, including SANS, at ORNL and, potentially also at NCNR. In the case of rare-earth titanates, a combined neutron diffraction and μSR study on the ferromagnetic-paramagnetic transition in doped $Y_{1-x}Ca_xTiO_3$ will be completed. The incipient ferroelectric $EuTiO_3$ is of considerable interest both experimentally and theoretically. *Birol* will utilize DFT to map out the phase diagram of $EuTiO_3$ under uniaxial strain, extending earlier work on the multiferroicity of this compound under biaxial strain, and guiding experimental efforts. On the experimental side, initial efforts by *Greven* to grow and dope single crystals have been highly successful. As for $SrTiO_3$ and $KTaO_3$, *Greven* and *Leighton* plan in-situ elastic and plastic deformation experiments, including SANS, and to complement these with transport and thermodynamic measurements.

Publications (this abstract only; see main CQM abstract for a full listing)

44. S. Hameed, D. Pelc, Z. W. Anderson, A. Klein, R. J. Spieker, L. Yue, B. Das, J. Ramberger, M. Lukas, Y. Liu, M. J. Krogstad, R. Osborn, Y. Li, **C. Leighton**, **R. M. Fernandes**, and **M. Greven**, *Enhanced superconductivity and ferroelectric quantum criticality in plastically deformed strontium titanate*, Nat. Mater. **21**, 54 (2022).
45. I. Khayr, X. He, A. Najev, J. Budic, Z. Zhao, L. Yue, Y. Li, D. Pelc, and **M. Greven**, *Structural properties of plastically deformed $SrTiO_3$ and $KTaO_3$*, in preparation.
46. X. Wang, A. Kundu, B. Xu, S. Hameed, I. Sochnikov, D. Pelc, **M. Greven**, A. Klein, B. Kalisky, *Multiferroicity in plastically deformed $SrTiO_3$*, (arXiv:2308.14801).
47. A. Najev, S. Hameed, D. Gautreau, Z. Wang, J. Joe, M. Požek, **T. Birol**, **R. M. Fernandes**, **M. Greven**, and D. Pelc, *Uniaxial Strain Control of Bulk Ferromagnetism in Rare-Earth Titanates*, Phys. Rev. Lett. **128**, 167201 (2022).
48. Z. Wang, D. Gautreau, **T. Birol**, and **R. M. Fernandes**, Strain-tunable metamagnetic critical endpoint in Mott insulating rare-earth titanates, Phys. Rev. B **105**, 144404 (2022).
49. A. Klein, V. Kozii, J. Ruhman, and **R. M. Fernandes**, *Theory of criticality for quantum ferroelectric metals*, Phys. Rev. B **107**, 165110 (2023).

50. S. Hameed, Z. Wang, D. M. Gautreau, J. Joe, K. P. Olson, S. Chi, P. M. Gehring, T. Hong, D. M. Pajerowski, T. J. Williams, Z. Xu, M. Matsuda, **T. Birol**, **R. M. Fernandes**, and **M. Greven**, *Effect of random antiferromagnetic exchange on the spin waves in a three-dimensional Heisenberg ferromagnet*, Phys. Rev. B **108**, 134406 (2023).
51. A. Najev, S. Hameed, A. Alfonsov, J. Joe, V. Kataev, **M. Greven**, M. Požek, D. Pelc, *Magnetic resonance study of rare-earth titanates*, (arXiv:2211.12387).

University of Minnesota Center for Quantum Materials (CQM): Structural and Electronic Properties of Bismuthate and Cuprate Superconductors

Martin Greven (PI)[1], Chris Leighton[2]

[1]School of Physics and Astronomy, University of Minnesota

[2]Department of Chemical Engineering and Materials Science, University of Minnesota

Keywords: Cuprates, bismuthate superconductors, neutron scattering, x-ray scattering, strain

Research Scope

The University of Minnesota Center for Quantum Materials (CQM), founded in 2016, investigates the structural, electronic, and magnetic properties of select quantum materials, particularly complex oxides, which embody many of the most fundamental questions regarding quantum behavior of interacting electrons and are relevant to important technologies, including data storage, spintronics, catalysis, and fuel cells. *This abstract complements the main CQM abstract, focusing on the center's work on the bismuth perovskite and cuprate superconductors*. This involves two CQM faculty (*Greven* and *Leighton*) and both neutron and x-ray scattering.

The doped perovskite $BaBiO_3$ exhibits a maximum superconducting transition temperature (T_c) of 34 K and was the first high-T_c oxide discovered more than four decades ago, yet pivotal questions regarding the nature of both its metallic and superconducting states remain unresolved. CQM efforts involving this system are relatively recent and highly complementary to work on cuprates and titanates. The high-T_c cuprates are the most studied class of quantum materials and remain at the forefront of contemporary research. Since the inception of the CQM, *Greven* has made considerable advances in developing a comprehensive understanding of these materials, in large part due to the unique capability to grow high-quality crystals of the simple-tetragonal model system $HgBa_2CuO_{4+\delta}$. Samples with ever lower carrier concentration are becoming available, including for SANS and specific heat measurements with *Leighton*. *Greven* has also spearheaded the use of structural diffuse neutron and x-ray scattering, as well as plastic deformation, to better understand and modify cuprates.

Recent Progress

Although it is believed that superconductivity in the bismuthates is of conventional *s*-wave type, the nature of the pairing mechanism is still unresolved, with strong electron-phonon coupling and bismuth Bi^{3+}/Bi^{5+} valence disproportionation possibly playing a role. CQM synthesis efforts have yielded high-quality crystals covering the $BaBi_{1-x}Pb_xO_3$ (*via* melt-cooling) and $Ba_{1-x}K_xBiO_3$ (*via* electrolytic growth) phase diagrams. Using diffuse x-ray scattering (with M. Krogstad and R. Osborn, ANL), 3D-ΔPDF analysis, and Monte Carlo modeling, *Greven* obtained unprecedented insight into the local structure of $Ba_{1-x}K_xBiO_3$ across the insulator-metal boundary [1]. In particular, no evidence

of long- or short-range valence disproportionation was observed. Instead, strong local structural correlations that break inversion symmetry were found (Fig. 1). This resolves a central conundrum in bismuthates, indicating that disproportionation and polaronic effects are not relevant for the metallic and superconducting states. The unexpected finding of locally broken inversion symmetry has far-reaching implications for the physics of this system, including superconducting pairing, and it places the bismuthates in the wider context of materials with a tendency toward polar displacements. Additional structural data have been gathered that further solidify this understanding [2].

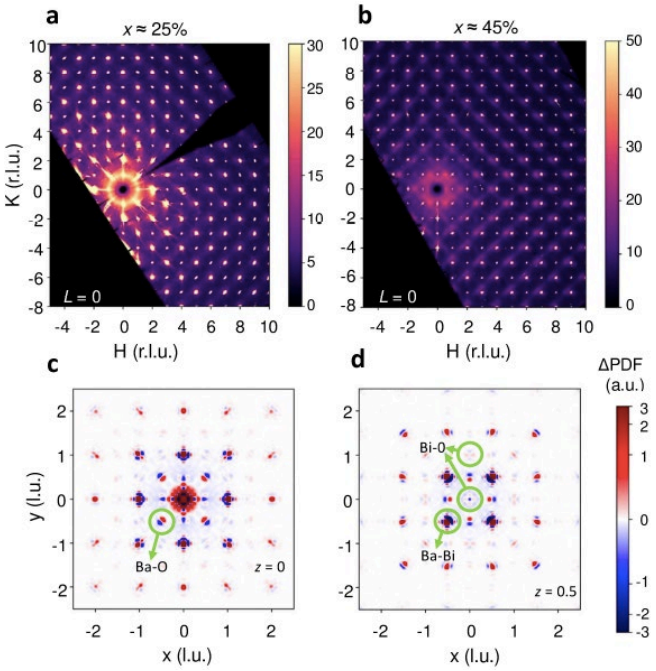

Fig. 1. Local structure of $Ba_{1-x}K_xBiO_3$. Diffuse x-ray scattering intensity ($T = 30$ K, $L = 0$) in the (a) insulating ($x \sim 0.23$) and (b) metallic ($x \sim 0.43$) state. Structured diffuse scattering that is asymmetric around the Bragg peaks is clearly seen in the metallic sample. (c) and (d) show vector pair distribution functions (3D-ΔPDF) obtained from the data in (b), for two representative planes, with Ba-O, Ba-Bi and Bi-O correlation peaks annotated.

Regarding the cuprates, structural work led by *Greven* culminated in a paper that documents and analyzes the nature and extent of pre-transitional short-range order using both neutron and x-ray diffuse scattering [3]. The work uncovered universal structural fluctuations in $La_{2-x}Sr_xCuO_4$ and $Tl_2Ba_2CuO_{6+\delta}$, two cuprates with distinct point disorder effects and with optimal superconducting transition temperatures that differ by more than a factor of two. The fluctuations were found to be present over wide doping and temperature ranges, including compositions that maintain high average structural symmetry, and to exhibit unusual, yet simple scaling behavior. The scaling regime is robust and universal, similar to the well-known critical fluctuations close to second-order phase transitions, but of a distinctly different origin. The observed behavior resembles pre-transitional phenomena in a broad class of systems with structural and magnetic transitions, leading to a proposed novel explanation based on rare structural fluctuations caused by intrinsic nanoscale inhomogeneity. There exist clear parallels with the behavior of superconducting fluctuations, as documented in prior CQM work by *Greven, Leighton* and *Fernandes*, which indicates that the underlying inhomogeneity plays an important role in cuprate physics. Crucially, the CORELLI instrument at SNS enabled the separation of quasi-static and dynamic diffuse scattering (Fig. 2(a)), which is impossible with x-rays, and triple-axis measurements at HFIR provided unique insight into the dynamic properties of the local structure. This collaborative effort involves both ORNL and ANL. More recent data confirm and deepen the initial findings [4].

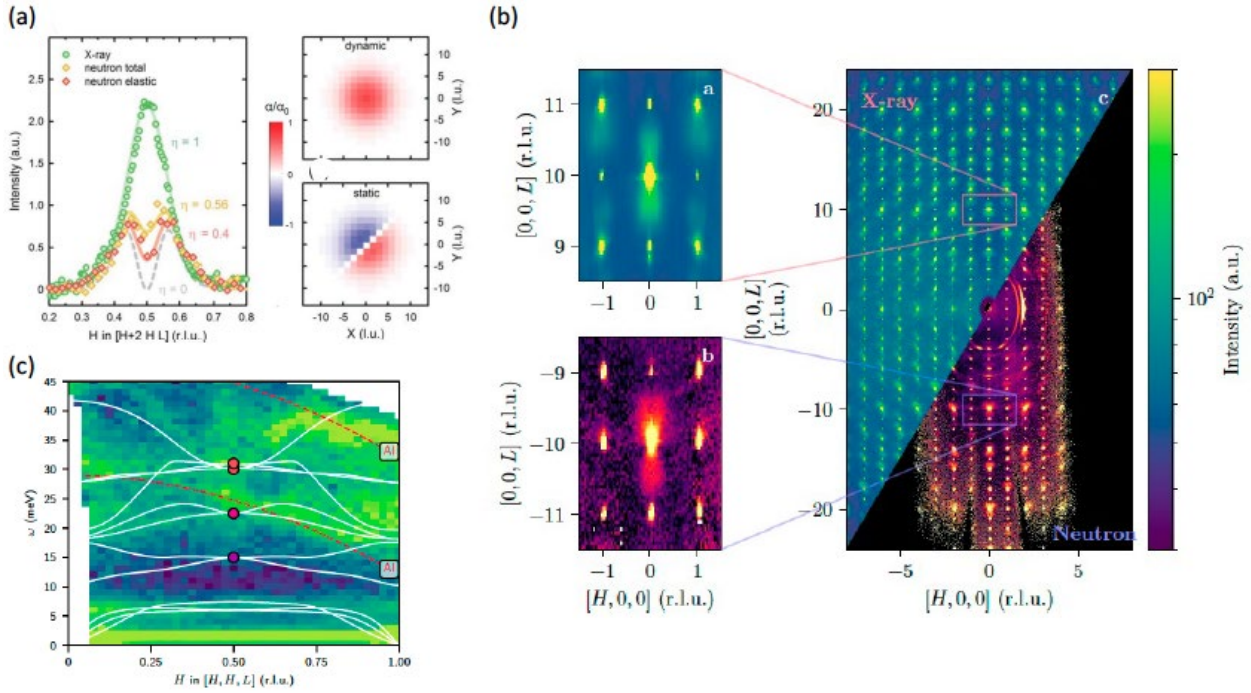

Fig. 2. (a) Integrated intensity for underdoped $La_{2-x}Sr_xCuO_4$ through the superstructure peak along [H 2+H 4] for total and quasielastic neutron diffuse scattering (diamonds; CORELLI, SNS), as well as X-ray scattering (APS) at a similar doping level and temperature (circles) above the structural phase transition. Lines are calculated diffuse scattering from a single nanoscale orthorhombic domain with a superposition of a dynamic Gaussian real-space contribution (top right) and a static real-space contribution with an antiphase boundary (bottom right). (b) Right: Scattering intensity (log scale) for underdoped $HgBa_2CuO_{4+\delta}$ in the [H 0 0]/[0 0 L] plane from x-ray scattering (upper left) and neutron scattering (lower right). Left: Zoom of data, as indicated. (c) Scattering intensity for $HgBa_2CuO_{4+\delta}$ ($T_c \approx 55$ K) as a function of q along [1 1 0] and energy transfer ω. Data collected on ARCS/SNS with $E_i = 50$ meV. Selected phonon modes calculated using density functional theory are overlayed. Red dashed lines indicate background scattering from aluminum in the sample holder.

In a closely related effort, again in collaboration with ORNL and ANL, diffuse neutron and x-ray scattering data were obtained for simple tetragonal $HgBa_2CuO_{4+\delta}$ that reveal significant correlated deviations from the average structure; similar to the work on the bismuthates [1], the scattering data were complemented by basic modeling of atomic displacements [5]. It is a distinct possibility that such underlying structural inhomogeneity is universal to the cuprates and that it constitutes the landscape on which emergent electronic correlations form and superconductivity develops.

Spin fluctuations have been proposed to be the pairing interactions in a wide range of unconventional superconductors. In the case of the cuprates, in which superconductivity emerges upon doping an antiferromagnetic Mott-insulating state, spin correlations might furthermore drive unusual pseudogap phenomena. *Greven* and collaborators at SNS/HFIR, U. Colorado (D. Reznik), and in France used unpolarized and polarized magnetic neutron scattering along with phonon calculations to study the simple tetragonal cuprate $HgBa_2CuO_{4+\delta}$ at very low doping ($T_c \approx 55$ K, hole concentration $p \approx 0.064$) [6]. In stark contrast to prior results for other underdoped cuprates, no evidence of incommensurate spin-density-wave or stripe correlations was found. Instead, the magnetic response of Hg1201 in both the superconducting and pseudogap states is gapped below $\Delta_{AF} \approx 6$ meV, commensurate over a wide energy range above the gap, and incommensurate above about 55 meV. Given the documented model nature of $HgBa_2CuO_{4+\delta}$, which exhibits high structural symmetry and minimal point disorder effects, the observed behavior appears to signify the unmasked response of the quintessential CuO_2 planes near the Mott-insulating state. These results for $HgBa_2CuO_{4+\delta}$ can therefore be expected to serve as a benchmark for a refined theoretical understanding of the cuprates.

Last, but not least, *Greven's* collaborations with experts in the use of complementary experimental techniques have continued to result in valuable insights into electronic and structural properties of the cuprates [7-10].

Future Plans

Led by *Greven,* a comprehensive study of electronic properties (cha ⌣ transport, specific heat, nonlinear magnetic response, *etc.*) of $Ba_{1-x}K_xBiO_3$ is underway, as are efforts to obtain larger single crystals for neutron scattering work, including SANS (by *Leighton*). *Greven* has obtained initial neutron and x-ray diffuse scattering data on non-superconducting $La_{2-x}Sr_xNiO_4$, a system that is isostructural to $La_{2-x}Sr_xCuO_4$ and is known to exhibit charge-spin "stripe" order, further demonstrate the universality of the scaling behavior observed for the cuprates. Further triple-axis experiments to elucidate the structural dynamics in $La_{2-x}Sr_xNiO_4$ are planned at HFIR, while SANS (*Leighton*) should prove helpful in better understanding structural and emergent magnetic inhomogeneity. With $HgBa_2CuO_{4+\delta}$, considerable efforts will be made by *Greven* to obtain samples with ever lower hole concentrations, approaching the superconductor to non-superconductor transition at 4-5% doping. Given the documented model-system nature of this cuprate, the prospect of investigating the transition to the non-superconducting state and, ultimately, to the Mott-insulating state at zero doping is significant. Transport data indicate that, among all cuprates, $HgBa_2CuO_{4+\delta}$ is least affected by unwanted point disorder in this part of the phase diagram, which should ultimately allow decisive experiments to determine the fundamental physics of the emergence of superconductivity with doping in the cuprates. The CQM is in a unique position in this regard. Specific heat measurements (*Leighton*) will serve to complement transport and thermodynamic data. Elastic and plastic deformation of $Ba_{1-x}K_xBiO_3$ and cuprates will be pursued *via in situ* scattering experiments, including SANS (*Leighton*), involving the new CQM strain cells; one of these cells is being tested and refined through a collaborative beam time proposal at ORNL. This will be complemented by in-house strain studies of electronic properties.

Publications (this abstract only; see main CQM abstract for a full listing)

52. S. Griffitt, M. Spaić, J. Joe, Z. Anderson, D. Zhai, M. J. Krogstad, R. Osborn, D. Pelc, **M. Greven**, *Local inversion-symmetry breaking in a bismuthate high-T_c superconductor*, Nat. Commun. **14**, 845 (2023).
53. D. Zhai, X. He, S. Gorregattu, S. Griffitt, M. Spaić, Z. Anderson, D. K. Shukla, J. Joe, M. J. Krogstad, R. Osborn, S. Sarker, J. Ruff, Y. Cai, D. Pelc, and **M. Greven**, *Superconductivity and local structural correlations in $Ba_{1-x}K_xBiO_3$*, in preparation.
54. D. Pelc, R. J. Spieker, Z. W. Anderson, M. J. Krogstad, N. Biniskos, N. G. Bielinski, B. Yu, T. Sasagawa, L. Chauviere, P. Dosanjh, R. Liang, D. A. Bonn, A. Damascelli, S. Chi, Y. Liu, R. Osborn, and **M. Greven**, *Unconventional short-range structural fluctuations in cuprate superconductors*, Sci. Rep. **12**, 20483 (2022).
55. R. J. Spieker, D. Zhai, M. Spaić, X. He, I. Khayr, N. Bielinski, M. J. Krogstad, F. Ye, R. Osborn, D. Pelc, and **M. Greven**, *Unusual short-range structural fluctuations in $La_{2-x}Sr_xCuO_4$*, in preparation.
56. Z. W. Anderson, Marin Spaić, N. Biniskos, L. Thompson, B. Yu, J. Zwettler, Y. Liu, F. Ye, M. Krogstad, R. Osborn, D. Pelc, and **M. Greven**, *Local structural correlations in $HgBa_2CuO_{4+\delta}$*, in preparation.
57. Z. W. Anderson, Y. Tang, V. Nagarajan, M. K. Chan, C. J. Dorow, G. Yu, T. Sterling, D. Reznik, D. L. Abernathy, A. D. Christianson, L. Mangin-Thro, P. Steffens, Y. Sidis, P. Bourges, and **M. Greven**, *Gapped commensurate antiferromagnetic response in the strongly underdoped model cuprate $HgBa_2CuO_{4+\delta}$*, in preparation.
58. K. Currier, C.Y. Lin, K. Gotlieb, R. Mori, H. Eisaki, **M. Greven**, A. Fedorov, Z. Hussain, A. Lanzara, *Driving Spin Texture in High-Temperature Cuprate Superconductors via Local Structural Fluctuations*, (preprint).
59. W. Tabiś, P. Popčević, B. Klebel-Knobloch, I. Biało, C. M. N. Kumar, B. Vignolle, **M. Greven**, N. Barišić, *Arc-to-pocket transition and quantitative understanding of transport properties in cuprate superconductors*, (arXiv:2106.07457).

60. T. E. Glier, M. Rerrer, L. Westphal, G. Lüllau, L. Feng, S. Tian, R. Haenel, M. Zonno, H. Eisaki, **M. Greven**, A. Damascelli, S. Kaiser, D. Manske, M. Rübhausen, *Direct observation of the Higgs mode in a superconductor by non-equilibrium Raman scattering*, (arXiv:2310.08162).
61. A. Montanaro, E. Maria Rigoni, F. Giusti, L. Barba, G. Chita, F. Glerean, G. Jarc, S. Y. Mathengattil, F. Boschini, H. Eisaki, **M. Greven**, A. Damascelli, C. Giannetti, D. Mihailovic, V. Kabanov, D. Fausti, *Dynamics of non-thermal states in optimally-doped* $Bi_2Sr_2Ca_{0.92}Y_{0.08}Cu_2O_{8+\delta}$ *revealed by mid-infrared three-pulse spectroscopy*, (arXiv:2310.10279).

Precise Chain Conformation and Dynamics Control For Conjugated Polymers In Organic Electronic Thin Film Devices

Xiaodan Gu, School of Polymer Science and Engineering, The University of Southern Mississippi

Program Scope

The aim of this early-career project is to provide fundamental knowledge to bridge the gap between solution state polymer conformations and deposited solid-state morphology, thus enabling robust structure and property relationship correlation for organic electronic devices. Filling this gap will help guide the rational design of proper processing parameters for controlling microstructures for solution process electronic devices and promoting device performance. To achieve the above goal, this proposal utilizes various DOE neutron and X-ray sources to probe the chain conformation and dynamics in both the solution and solid-state. This project will also utilize high-throughput instrumentation and machine learning to mine out key processing parameters that influence final device morphology and performance. We propose the following aims: 1) harness non-covalent interactions to pre-set CPs into preferred chain conformations; 2) utilize high throughput robotic processing and machine learning methodology to mine out key determining factors for obtaining highly ideal chain morphology; 3) develop grazing incidence scattering techniques and use ex situ neutron scattering and deuterium labeling to study chain conformation in solid-state bulk and thin films; 4) study heterogeneity of chain dynamics in bulk and thin film, and investigate the impact of chain dynamics on CPs' optoelectronic property.

Recent Progress

1. Synthesis of Deuterated Conjugated Polymers and Their Solution Scattering (Work Under Review)

The conjugated polymer's backbone conformation dictates the delocalization of electrons, and ultimately affects its optoelectronic properties. Conjugated polymers (CPs) can be viewed as semirigid rods, where their backbone is embedded among long alkyl sidechains. Thus, it is challenging to directly quantify the conformation of optoelectronically functional conjugated backbone experimentally. We made a progress to measure the chain conformation of donor-acceptor polymer. We used contrast variation neutron scattering to measure the conjugated backbone conformation for diketopyrrolopyrrole (DPP) polymers with selectively deuterated sidechains. We first synthesized sidechain deuterated polymer and confirmed the successful synthesis with NMR and FTIR techniques. Detailed synthesis will be discussed in the PI meeting. Using contrast variation neutron scattering, we found DPP-based conjugated polymers are much more rigid than poly(3-alkylthiophenes), with a persistence

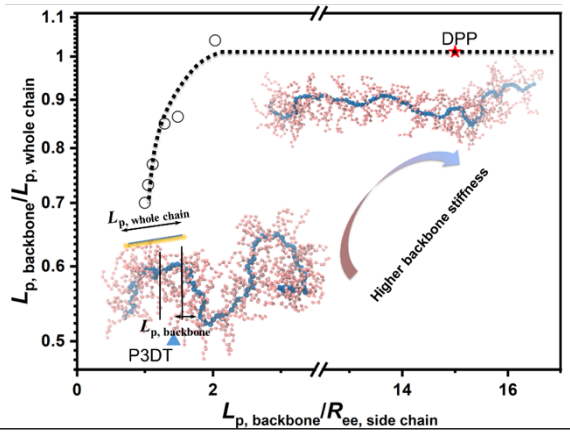

Figure 1. Normalized backbone *persistence length* to whole chain *persistence length* with increasing backbone rigidity to side chain end-to-end distance ($R_{ee,\ side\ chain}$) ratio.

length of approximately 18 nm for both its backbone section and the whole polymer chain. This indicates that the side chain interference on backbone conformation is not present for semi-rigid polymer which is further revealed by coarse-grained molecular dynamics (CG-MD) simulations. Combined with the first work we published concerning polythiophene, the **Figure 1** summarized finding for both semi-flexible chain (Lp of 3nm) to semi-rigid chains (Lp of 18nm). This suggest that backbone for polymer with long sidechain need be carefully measurement for lp lower than 10nm. A deviation from the bulk measurement is likely expected.

1. Effect Of Sidechain Hindrance on Molecular Chain Conformation (Work Published in Journal of Materials Chemistry A, 10-Year Anniversary Special Issue[1])

We further explored the influence of the side-chain length and branch point on the persistence length and optical absorption. SANS measurements were performed. Based on the contrast variation experiment, we performed those experiment directly on the non-deuterated samples. The chemical structure of those polymers is shown in **Figure 2a**. The chain rigidity of diketopyrrolopyrrole DPP-based and isoindigo IID based polymers increases with the bulkiness of side chains either by increasing the side-chain length or branch spacer length, owing to a decrease in the population of *cis* conformation between thiophene-thiophene building blocks (**Figure 2 d, g**). Interestingly, we observed that the optical shift due to steric hinderance of the sidechain for the polymers were not only correlated to the changes in polymer chain rigidity but also coplanarity of the polymer backbone. This is further confirm using molecular dynamics simulations. This work demonstrated the important of the sidechains on optoelectronic property of the conjugated polymers.

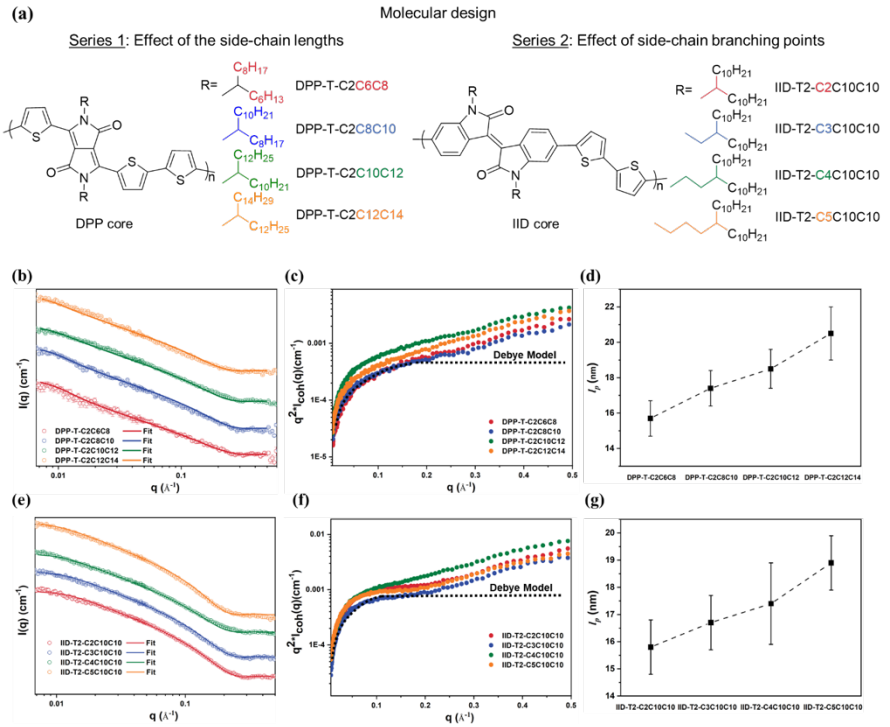

Figure 2. Studying different building block's structure on their conformation and related property (a) Structure of DPP-based polymers with different side-chain lengths and IID-based polymers with different side-chain branching positions. (b) SANS curves for DPP-based polymers in o-DCB-d4 at 130 °C. Lines are the best fitting via a flexible cylinder model. (c) Kratky plots for DPP-based polymers. (d) l_p of DPP-based polymers with varied side-chain lengths. (e) SANS curves for IID-based polymers in o-DCB-d4 at 130 °C. (f) Kratky plots for IID-based polymers. (g) l_p of IID-based polymers with various side-chain branch positions.

2. Effect Of Backbone Building Blocks on Molecular Chain Conformation (Work Published in Advanced Materials & Featured In Front Cover, Reported In The DOE Science Highlight [2])

Furthermore, we explored the influence of oligothiophene length on chain rigidity of conjugated polymers. We found that chain rigidity of DPP-based and naphthalene diimide (NDI) based polymers decreases with the introduction of a longer oligothiophene unit. All-atomistic molecular dynamic (AA-MD) simulations indicate that the decreased chain rigidity is due to an increased population in *cis* conformation and a less linear backbone. However, a controversial role of oligothiophene length in band gap for DPP-based and NDI-based polymers has been observed. We found the orbital energy alignment between donor and acceptor units plays a vital role in the trend of optical bandgap. Orbital energy alignment changed from sandwich-type (DPP-based polymers) to staggered-type (NDI-based polymers) since relative energy alignment varies. Under sandwich-type orbital energy alignment, the increased band gap with increasing oligothiophene length originates from the bandwidth reduction due to more localized charge density distribution and more flexible chains with intrachain twisting. For D-A CPs presenting staggered-type orbital energy alignment, the new hybridized higher HOMO with increasing oligothiophene length leads to a narrowing of the optical bandgap despite decreased chain rigidity. Our work highlighted the importance of both energy alignment and chain conformation on optoelectronic property.

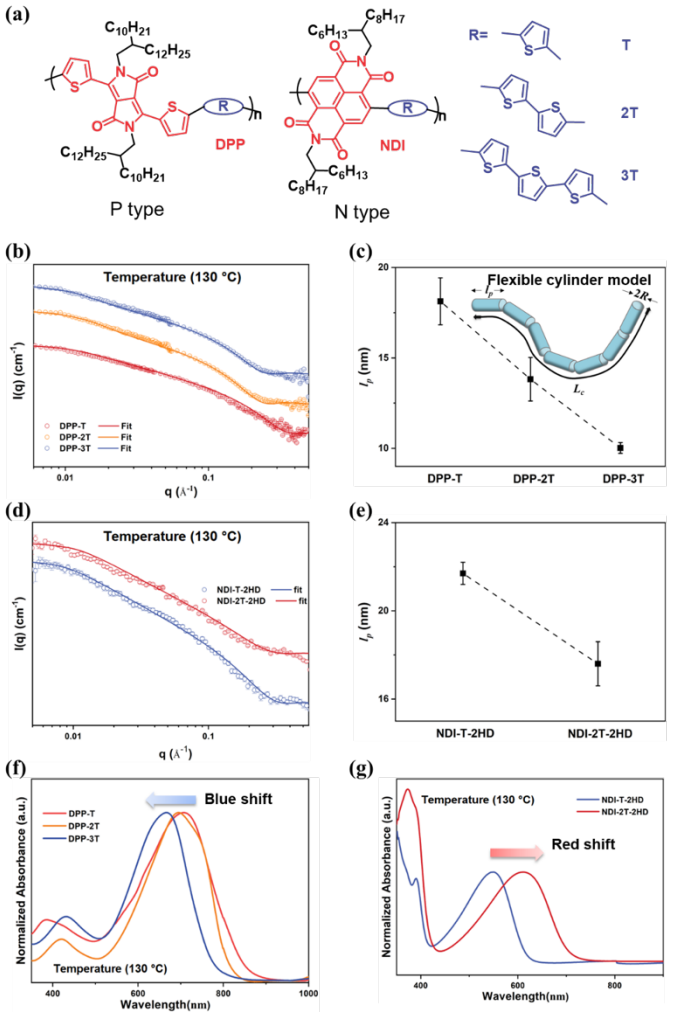

Figure 3. (a) Structure of DPP-based and NDI-based polymers with varied numbers of thiophenes. (b) SANS curves for DPP-nT polymers in o-DCB-d_4 at 130 °C. Lines are the best fitting via a flexible cylinder model. (c) Persistence length of DPP-nT polymers. (d) SANS curves for NDI-nT polymers in o-DCB-d_4 at 130 °C. (e) Persistence length of NDI-nT polymers. UV-vis spectra of DPP-nT (f) and NDI-nT (g) in o-DCB at 130 °C.

Future Plans

1. Our group has published two works and one more work under review on the solution assembly of conjugated polymers, elucidating few design rules to control chain rigidity. The next stage of the work involves performing chain conformation studies in confined states. We have investigated the chain conformation of the polymer in the melt state to obtain a single-chain conformation. The preliminary results showed that they have a similar conformation to when it is fully dissolved in a solution. However, before the polymer melts, we discovered that the aggregation of the polymer has a significant impact on the material's properties. The next step is to conduct a chain conformation study in the thin film state. We will start with samples coated on the silicon substrate. Subsequently, samples coated on a silicon wafer will be studied using grazing incidence geometry. Our graduate student, Kundu Thapa, will be visiting SNS for one year as part of the neutron scattering student program. We anticipate those work to be finished in the next period of PI meeting.

2. We plan to continue studying the dynamics of conjugated polymers using a suite of quasi-elastic neutron scattering and neutron spin-echo methods. Initial testing was conducted on both deuterated and non-deuterated conjugated polymers, and we observed two distinct dynamics in chain motion. Further all atomistic molecular dynamic simulation confirmed this observation. We are now testing the effect of chain motion on charge transport properties. Initial results suggest that the backbone motion of the polymer greatly impacts the overall transport property, as measured by thin film transistor devices, as well as a dielectric spectroscopy meter. We aim to publish this work next year.

References

(1) Cao, Z.; Li, Z.; Tolba, S. A.; Mason, G. T.; Xiong, M.; Ocheje, M. U.; Alesadi, A.; Do, C.; Hong, K.; Lei, T.; Rondeau-Gagné, S.; Xia, W.; Gu, X. Probing Single-Chain Conformation and Its Impact on the Optoelectronic Properties of Donor–Accepter Conjugated Polymers. *J. Mater. Chem. A* **2023**, *11* (24), 12928–12940. https://doi.org/10.1039/D2TA09389H.

(2) Cao, Z.; Tolba, S. A.; Li, Z.; Mason, G. T.; Wang, Y.; Do, C.; Rondeau-Gagné, S.; Xia, W.; Gu, X. Molecular Structure and Conformational Design of Donor-Acceptor Conjugated Polymers to Enable Predictable Optoelectronic Property. *Adv. Mater.* **2023**, *n/a* (n/a), 2302178. https://doi.org/10.1002/adma.202302178. (***Front Cover and DOE highlight***)

Publications
from Oct 2021 to Nov 2023

(1) Cao, Z.; Li, Z.; Tolba, S. A.; Mason, G. T.; Xiong, M.; Ocheje, M. U.; Alesadi, A.; Do, C.; Hong, K.; Lei, T.; Rondeau-Gagné, S.; Xia, W.; Gu, X. Probing Single-Chain Conformation and Its Impact on the Optoelectronic Properties of Donor–Accepter Conjugated Polymers. *J. Mater. Chem. A* **2023**, *11* (24), 12928–12940. https://doi.org/10.1039/D2TA09389H.

(2) Cao, Z.; Tolba, S. A.; Li, Z.; Mason, G. T.; Wang, Y.; Do, C.; Rondeau-Gagné, S.; Xia, W.; Gu, X. Molecular Structure and Conformational Design of Donor-Acceptor Conjugated Polymers to Enable Predictable Optoelectronic Property. *Adv. Mater.* **2023**, *n/a* (n/a), 2302178. https://doi.org/10.1002/adma.202302178. (***Front Cover and DOE highlight***)

(3) Alesadi, A.; Cao, Z.; Li, Z.; Zhang, S.; Zhao, H.; Gu, X.; Xia, W. Machine Learning Prediction of Glass Transition Temperature of Conjugated Polymers from Chemical Structure. *Cell Reports Phys. Sci.* **2022**, *3* (6), 100911. https://doi.org/10.1016/j.xcrp.2022.100911.

(4) Zhao, H.; Shanahan, J. J.; Samson, S.; Li, Z.; Ma, G.; Prine, N.; Galuska, L.; Wang, Y.; Xia, W.; You, W.; Gu, X. Manipulating Conjugated Polymer Backbone Dynamics through Controlled Thermal Cleavage of Alkyl Side Chains. *Macromol. Rapid Commun.* **2022**, *43* (24), 2200533. https://doi.org/10.1002/marc.202200533.

(6) Rosas Villalva, D.; Singh, S.; Galuska, L. A.; Sharma, A.; Han, J.; Liu, J.; Haque, M. A.; Jang, S.; Emwas, A. H.; Koster, L. J. A.; Gu, X.; Schroeder, B. C.; Baran, D. Backbone-Driven Host–Dopant Miscibility Modulates Molecular Doping in NDI Conjugated Polymers. *Mater. Horizons* **2022**, *9* (1), 500–508. https://doi.org/10.1039/D1MH01357B.

(7) Steelman, M. E.; Adams, D. J.; Mayer, K. S.; Mahalingavelar, P.; Liu, C.-T.; Eedugurala, N.; Lockart, M.; Wang, Y.; Gu, X.; Bowman, M. K.; Azoulay, J. D. Magnetic Ordering in a High-Spin Donor–Acceptor Conjugated Polymer. *Adv. Mater.* **2022**, *34* (45), 2206161. https://doi.org/10.1002/adma.202206161.

(8) Wang, Y.; Zhang, S.; Freychet, G.; Li, Z.; Chen, K.-L.; Liu, C.-T.; Cao, Z.; Chiu, Y.-C.; Xia, W.; Gu, X. Highly Deformable Rigid Glassy Conjugated Polymeric Thin Films. *Adv. Funct. Mater.* **2023**, *n/a* (n/a), 2306576. https://doi.org/10.1002/adfm.202306576.

(5) Luo, S.; Li, Y.; Li, N.; Cao, Z.; Zhang, S.; Ocheje, M. U.; Gu, X.; Rondeau-Gagné, S.; Xue, G.; Wang, S.; Zhou, D.; Xu, J. Real-Time Correlation of Crystallization and Segmental Order in Conjugated Polymers. *Mater. Horizons* **2023**. https://doi.org/10.1039/D3MH00956D.

(9) Allen, M. J.; Lien, H.-M.; Prine, N.; Burns, C.; Rylski, A. K.; Gu, X.; Cox, L. M.; Mangolini, F.; Freeman, B. D.; Page, Z. A. Multimorphic Materials: Spatially Tailoring Mechanical Properties via Selective Initiation of Interpenetrating Polymer Networks. *Adv. Mater.* **2023**, *35* (9), 2210208. https://doi.org/https://doi.org/10.1002/adma.202210208.

Investigating Possible Emergence of Quantum Spin Liquid State in Triangular Lattice Compounds

Sara Haravifard, Department of Physics, Duke University

Keywords: Triangular Lattice, Geometrically Frustrated, Magnetism, Quantum Spin Liquid, Neutron Scattering

Research Scope

The emergence of a quantum spin liquid (QSL), a state of matter that can result when electron spins are highly correlated but do not become ordered, has been the subject of considerable research in condensed matter physics [1]. Spin liquid states have been proposed as potential hosts for high-temperature superconductivity [2] and can exhibit topological properties [3] with applications in quantum information science. However, the unambiguous experimental realization of QSL behavior in real materials remains challenging. In this study, we investigate the novel compound $YbZn_2GaO_5$, which hosts triangular lattice of effective spin-1/2 moments.

Recent Progress

Our thermodynamic and inelastic neutron scattering (INS) measurements, conducted on high-quality single crystal samples of $YbZn_2GaO_5$, exclude the possibility of long-range magnetic ordering down to 60 mK. These measurements reveal a quadratic power law for the heat capacity and demonstrate a continuum of magnetic excitations in parts of the Brillouin zone. Additionally, our recent ac-susceptibility measurements rule out the possibility of spin freezing in this compound at temperatures as low as 20 mK, providing additional evidence of the dynamic nature of the ground state. Our experimental results provide compelling evidence that $YbZn_2GaO_5$ is a U(1) Dirac QSL with gapless spinon excitations concentrated at specific points in the Brillouin zone. These experimental findings align with our theoretical calculations for a Dirac QSL on the triangular lattice.

Future Plans

We plan to advance these studies by investigating the static and dynamics properties of the sister compound $TmZn_2GaO_5$.

References

1. Broholm, C., R. J. Cava, S. A. Kivelson, D. G. Nocera, M. R. Norman, and T. Senthil. "Quantum spin liquids." Science **367**, no. 6475 (2020): eaay0668.

2. Christos, Maine, Zhu-Xi Luo, Henry Shackleton, Ya-Hui Zhang, Mathias S. Scheurer, and Subir Sachdev. "A model of d-wave superconductivity, antiferromagnetism, and charge order on the square lattice." Proceedings of the National Academy of Sciences **120**, no. 21 (2023): e2302701120.

3. Sherman, Nicholas E., Maxime Dupont, and Joel E. Moore. "Spectral function of the J 1− J 2 Heisenberg model on the triangular lattice." Physical Review B **107**, no. 16 (2023): 165146.

Publications

1. Xu, Sijie, Rabindranath Bag, Nicholas E. Sherman, Lalit Yadav, Alexander I. Kolesnikov, Andrey A. Podlesnyak, Joel E. Moore, and Sara Haravifard. "Realization of U (1) Dirac Quantum Spin Liquid in YbZn2GaO5." arXiv preprint arXiv:2305.20040 (2023).

Understanding the role of polymer topology on molecular deformation and scission under extreme shear using *in situ* neutron scattering

Matthew E. Helgeson, Dept. of Chem. Eng., UC Santa Barbara
Patrick T. Underhill, Dept. of Chem. and Biol. Eng., Rensselaer Polytechnic Institute

Keywords: Polymers; rheology; neutron scattering; rheo-SANS; Brownian dynamics

Program Scope

Engineered polymers for energy production, efficiency, and recycling/upcycling can experience extreme deformations that break chemical bonds along the polymer backbone, leading to mechanical degradation and compromised performance. Modern macromolecular designs to engineer this behavior involve complex topologies including branched and star-like architectures. Previously established relationships between topology and mechanochemistry of polymers have remained largely empirical due to a lack of methods to characterize fluid and molecular microstructure in extreme flows. The proposed research aims to fill this gap by developing mechanistic, molecular-scale understanding for how topology affects polymer deformation at extreme shear rates, and how this deformation drives polymer scission. This will be achieved through combined *in situ* small angle neutron scattering (SANS) measurement, molecular scattering models and parameter-matched molecular simulations that can resolve single-molecule deformations, which will be applied to families of topologically complex polymers where synthetic control will be used to understand how the type and degree of branching on a polymer influence the distribution of molecular deformation and tension at extreme shear rates. Results will be combined with experiments to assess topology-dependent mechanical degradation of polymers observed. Ultimately, these studies will provide guidelines for engineering polymers to enhance mechanical stability, or conversely to engineer flows that direct the mechanical degradation of polymers for targeted materials properties and applications. This project critically leverages a recently developed *in situ* neutron scattering technique for SANS in high shear rate flows, called capillary rheo-SANS, which will be disseminated to the neutron scattering community through collaboration with beam scientists at neutron sources.

Recent Progress

In the previous reporting period, we established the use of capillary rheo-SANS measurements to characterize topology-dependent molecular anisotropy at extreme shear rates (exceeding 10^6 s^{-1}). We also adapted and optimized Brownian dynamics simulations of polymers in high shear rate flows to make direct comparisons with scattering measurements, and develop new scattering models to infer polymer conformation in flow. In the current period, we have made considerable progress in developing new scattering analyses to extract previously inaccessible information regarding polymer deformation and conformation under nonlinear deformations. We were also able to commission the capillary rheo-SANS device on the GP-SANS beamline at HFIR. Key results of these efforts and their impact are described in the sections below.

A thermodynamically-consistent connected rod (TCCR) model for scattering from polymer chains in deformation and flow. Previous scattering analyses to extract information regarding polymer configurations in flow have been limited to primitive reduced-dimensional quantification of scattering anisotropy (*e.g.* anisotropy parameters) or eigenfunction expansion methods (e.g. spherical harmonics), which require a number of physical assumptions to map the resulting scattering coefficients to real-space structure. Since these methods are not derived from physical models, they lack consistency with the known physics of single-molecule polymer rheology. To address this gap, we developed a first principles scattering model for polymer chains that directly incorporates features

of non-equilibrium thermodynamics to describe the chain configuration across multiple scales [1]. Specifically, we model a chain as a series of connected rods, whose chain propagation is fully defined by a series of rod-segment orientation distribution functions (OPDFs) (**Figure 1a**). By enforcing thermodynamic self-consistency of the segment-level OPDFs with the overall chain stretch, the model rigorously describes anisotropic chain configurations spanning individual chain segments to the end-to-end stretch and orientation of the chain. The TCCR model accurately describes equilibrium scattering from industrially-relevant linear poly(stearyl methacrylate-co-methyl methacrylate), revealing that these polymers possess a previously unreported bottlebrush-like configuration in solution with model parameters that are consistent with molecular simulations (**Figure 1b**). More importantly, the model correctly predicts the shape of scattering anisotropy of such wormlike chains in shear flow over a range of shear rates (**Figure 1c**), allowing the model to be used to extract the molecular stretch on the chains (**Figure 1d**). The resulting information can be used to test single-molecule rheology theories for polymers in nonlinear deformations, and more generally is the first (to our knowledge) complete molecularly-informed scattering model for polymers in flow. Near-term plans for future development with the model include translating the existing code [2] to the popular SasView scattering modeling software, and its extension to nonlinear chain topologies.

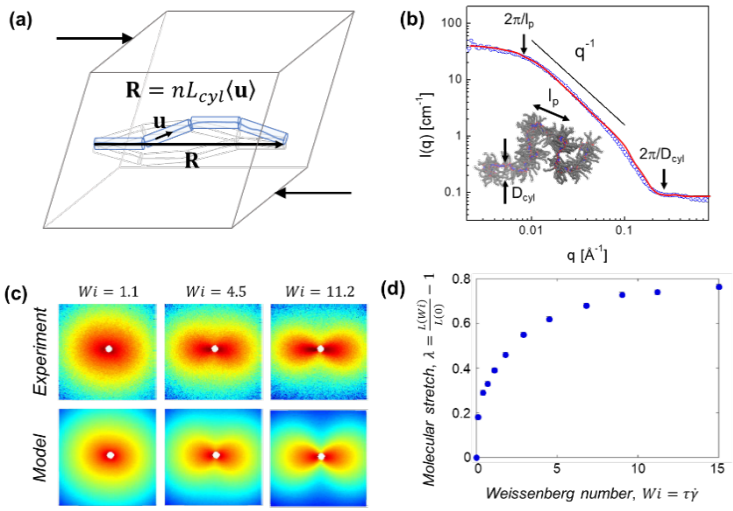

Figure 1. (a) Schematic of the TCCR model. (b) Equilibrium SANS data on a high-MW linear p(SMA-co-MMA) polymer and corresponding fit to the TCCR model. (c) Representative anisotropic SANS patterns obtained by experiments and simulations of the TCCR model, and (d) extracted best-fit molecular stretch for linear polymers in shear flow. [1]

A general framework for describing non-Gaussian configurations of deformed polymers, heteropolymers, and topologically-defined polymers. Molecular theories for interpreting polymer rheology and scattering typically rely on the assumption that polymer chains possess a Gaussian configuration, *i.e.*, their segment density distribution corresponds to a Gaussian distribution. This assumption fails to account for several features of real polymer molecules, including their finite extensibility when subjected to nonlinear deformations as well as the potential for heterogeneous chemistry and nonlinear topology used in many contemporary polymer designs. To address this challenge, we developed a general mathematical framework to describe the non-Gaussian features of polymer configurations that can be equivalently applied to both molecular simulation and scattering measurements [3]. The analysis uses the well-established Gram-Charlier expansion scheme, which describes a general non-Gaussian distribution as an expansion in terms of its moments with respect to a reference Gaussian distribution. The analysis produces a set of cumulants, $\{\kappa_i\}$, which serve as low-dimensional descriptors of the unknown segment density distribution distribution. The analysis produces equivalent fits to simulated data regardless of whether the cumulants are fit in real or Fourier-space, providing a route by which scattering measurements can be used to extract the moments without prior knowledge of the underlying distribution. When applied to deformed polymers in shear flow (**Figure 2a**), the analysis is capable of qualitatively differentiating between infinitely extensible (Rouse) and finitely extensible (FENE) chains, whereas Gaussian approximations would be incapable of doing so. The analysis can also be used to infer deviations from Gaussian behavior of heteropolymers such as sequence defined polypeptoids at equilibrium (**Figure 2b**). Taken together, these results demonstrate that our Gram-Charlier analysis provides a natural mathematical language to "fingerprint" non-ideal conformations

of polymers at equilibrium and in flow, and holds significant promise for advancing molecular theories of the physics and rheology of topology-defined polymers.

Characterizing flow-induced deformation of topology-defined polymers in extreme shear rate flows. During the current reporting period, reopening of ORNL to user-supplied sample environments allowed us to carry out two sets of capillary rheo-SANS experiments. The first was primarily spent in commissioning the capillary device on the GP-SANS instrument at HFIR. The second involved comparative characterization of linear and star polymers aimed at understanding the influence of model branched topology on the evolution of molecular deformation with increasing shear rate, ultimately to compare with results of molecular simulations. These experiments required significant developments in polymer synthesis to simultaneously access high molecular weights (MW) while

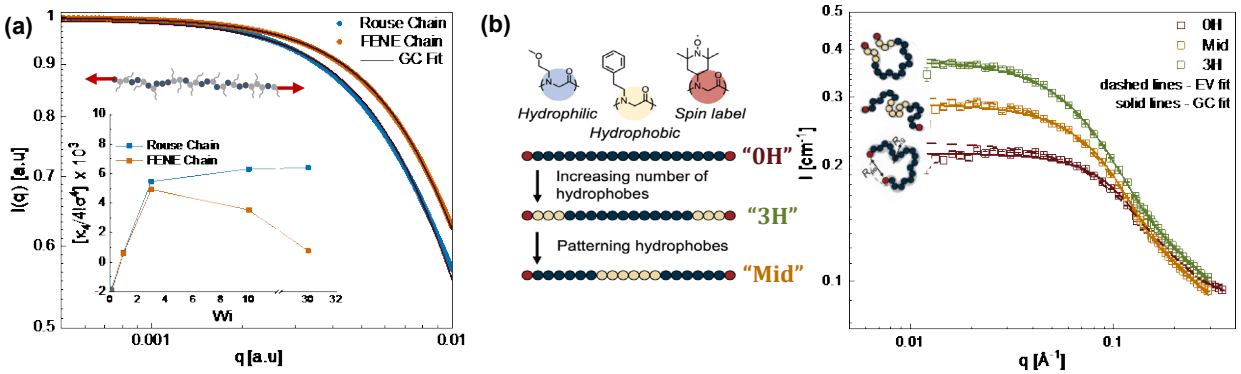

Figure 2. (a) Gram-Charlier expansion fit (solid lines) to the simulated scattering from Rouse and FENE chains at Wi=3. Inset plot shows trends in the higher order cumulant, κ_4, with increasing Wi indicating clear differences between the different models. (b) Sequence-defined polypeptoids show deviations from Gaussian conformation in solution due to sequenced hydrophobic associations. The Gram-Charlier analysis (GC fit) captures this better than conventional Gaussian excluded volume models (EV fit).

controlling topology and minimizing dispersity. Ruthenium-catalyzed atom transfer radical polymerization was adapted using initiators of varying functionality, resulting in high MW statistical copolymers of poly(SMA-co-MMA) with low polydispersity and controlled topology including four-armed star and linear topologies (**Figure 3**). Preliminary results of capillary rheo-SANS experiments on these polymers at shear rates above 10^5 s^{-1} reveal that the linear polymer undergoes significantly greater stretching and alignment relative to an equivalent 4-arm star polymer (**Figure 3**). We aim to use Brownian dynamics simulations to elucidate the molecular dynamics underlying these findings. For example, we have shown how the longest relaxation time shortens as the number of arms increases, leading to a smaller Weissenberg number and less alignment at a fixed shear rate. But the changes to the spectrum of relaxation modes are expected to show a bigger influence of finite extensibility for stars when compared at equal Weissenberg number.

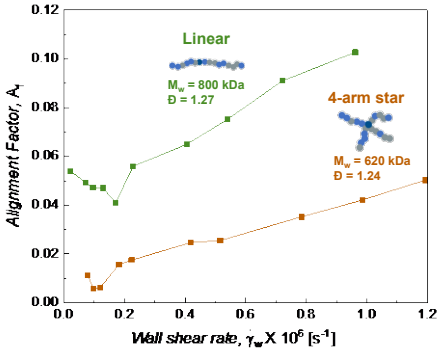

Figure 3. Measured alignment factor, A_f, extracted from capillary rheo-SANS indicating comparative anisotropy of a linear and 4-arm star polymer.

Future Plans

This project has produced new tools to model and mathematically describe the conformation of polymers under deformation and flow that is general to a wide cross-section of polymers under investigation for next-generation materials technologies, including topology-defined polymers and

heteropolymers that hold significant promise for expanded and optimized design for rheological performance and mechanical stability. Our experimental and computational results to date suggest that branched topologies (including star polymers and randomly branched polymers) exhibit complex dilute solution dynamics in extreme shear flows that are not accounted for in conventional theories of polymer dynamics. Remaining effort on the project (which is currently under no-cost extension) will be aimed at extending the existing experimental data set to include a more systematic study of topology and concentration effects, as well as bringing these remaining aspects of the work to publication.

In the longer term, our investigations to date have revealed the significant impact of chemistry on the conformation and properties of topology-defined polymers at equilibrium and in flow. For example, although the poly(SMA-co-MMA) polymers used in our studies were previously thought to achieve thermorheological modification through a coil-like conformation that expands with increasing temperature [4], our studies instead revealed that high-MW linear p(SMA-co-MMA) adopts a bottle-brush conformation in solution (**Figure 2b**). This surprising preliminary finding reveals a previously untapped potential – the ability to combine topology with polymer-polymer and polymer-solvent interactions to tailor and dramatically alter single-molecule polymer structure and rheology, especially in high-shear flows where we have established that non-Gaussian molecular configurations can play a dominant role. Thus, we are currently preparing a renewal proposal to explore this exciting new possibility. Overall, our collective work to date holds exceptional potential for elucidating the mechanisms by which polymers deform in high shear rate flows, and how combinations of molecular chemistry, topology, and intermolecular interaction can be used to alter and manipulate these mechanisms.

References

[1] J. Zhang, G.S. Smith, P.T. Corona, P.T. Underhill, L.G. Leal and M.E. Helgeson (2024). A self-consistent connected-rod model for small angle scattering from deformed semiflexible chains in flow. Macromolecules, *In Press*.

[2] J. Zhang, G.S. Smith (2023). ConnectedRodModel; https://github.com/Helgeson-Lab-UCSB/ConnectedRodModel

[3] A. Datta, X. Wang, S. Mengel, A. DeStefano, R.A. Segalman, P.T. Underhill and M.E. Helgeson. Fingerprinting non-Gaussian conformations of polymers from small angle scattering via Gram-Charlier analysis. Macromolecules, *Submitted*.

[4] B.G.P. van Ravensteijn, R.B. Zerdan, C.J. Hawker and M.E. Helgeson (2021). Role of architecture on thermorheological properties of poly (alkyl methacrylate)-based polymers. Macromolecules 54(12): 5473-5483.

Publications

C.J. Dahlman, N.R. Venkatesan, P.T. Corona, R.M. Kennard, L. Mao, N. Smith, J. Zhang, R. Seshadri, M.E. Helgeson and M.L. Chabinyc, "Structural Evolution of Layered Hybrid Lead Iodide Perovskites – Colloidal Nanocrystals or Ruddlesden-Popper Phases?", *ACS Nano*, 2020, 14(9): 11294-11308. [DOI: 10.1021/acsnano.0c03219]

L.T. Andriano, N. Ruocco, J.D. Peterson, D.P. Olds, S. Costanzo, D. Vlassopoulos, M.E. Helgeson, K. Ntetsikas, N. Hadjichristidis, L.G. Leal, "Microstructural characterization of a star-linear polymer blend under shear flow by using rheo-SANS", *Journal of Rheology*, 2020, 64:663. [DOI: 10.1122/1.5121317]

B.G.P. van Ravenstein, R.B. Zerdan, C.J. Hawker and M.E. Helgeson, "Role of Architecture on Thermorheological Properties of Poly(alkyl methacrylate) based Polymers", *Macromolecules,* 2021, 54(12): 5473-5483. [DOI: 10.1021/acs.macromol.1c00149]

P.T. Corona and M.E. Helgeson, "Stretching the limits: New flow-SANS experiments provide unprecedented characterization of polymer deformations in extreme flows", Neutron News, 2021, 32(1): 17-18. [DOI: 10.1080/10448632.2021.1875770]

J. Zhang, A. Jurzyk, M.E. Helgeson and L.G. Leal, "Modeling Orthogonal Superposition Rheometry to Probe Nonequilibrium Dynamics of Entangled Polymers", *Journal of Rheology*, 2021, 65(5): 983-998. [DOI: 10.1122/8.0000272]

P.T. Corona, K. Dai, M.E. Helgeson and L.G. Leal, "Testing orientational closure approximations in dilute and non-dilute suspensions with Rheo-SANS", *Journal of Non-Newtonian Fluid Mechanics*, 2023, 315: 105014. [DOI: 10.1016/j.jnnfm.2023.105014]

P.T. Corona, B. Berke, M. Guizar-Sicairos, L.G. Leal, M. Liebi and M.E. Helgeson**, "Fingerprinting soft material nanostructure response to complex flow histories", *Physical Review Materials*, 2022, 6(4): 045603. [DOI: 10.1103/PhysRevMaterials.6.045603]

J. Zhang, G.S. Smith, P.T. Corona, P.T. Underhill, L.G. Leal and M.E. Helgeson, "A self-consistent connected-rod model for small angle scattering from deformed semiflexible chains in flow", Macromolecules, 2024, *In press*.

B.G.P. van Ravensteijn, P.T. Corona, K. Dai, R.B. Zerdan, K.M. Weigandt, R.P. Murphy, C.J. Hawker and M.E. Helgeson, "Architecture-dependent polymer stretching and scission in extreme shear flows," Macromolecules, *Submitted*.

A. Datta, X. Wang, S. Mengel, A. DeStefano, R.A. Segalman, P.T. Underhill and M.E. Helgeson, "Fingerprinting non-Gaussian conformations of polymers from small angle scattering via Gram-Charlier analysis", Macromolecules, *Submitted*.

Neutron Scattering Studies of Hybrid Excitations

R. P. Hermann, M. E. Manley
Materials Science & Technology Division, Oak Ridge National Laboratory, Oak Ridge, TN

Keywords: phonon, magnon, phason, tunneling, disorder

Research Scope

This project studies how hybridization between atomic vibrations and spin excitations control transport and functionalities in energy materials. We use and develop neutron scattering methods and complement them by resonant ultrasound and Mössbauer spectroscopy. First, we aim to unveil how lattice non-linearity, incommensurability, and hybridization with molecular modes control heat and charge propagation. We have focused on phason mediated thermal transport and on lattice anharmonicity and thermodynamics in antimony oxides featuring lone electron pairs and molecular modes. Second, we aim to understand how spin structure and transport are controlled by disorder and lattice coupling. We have characterized the spin structure and dynamics in MnTe and the structure and dynamics in a novel iron-bearing high-entropy oxide. Our third aim is to determine constraints from lattice topology and quantum fluctuations on thermal transport. We have shown that synthesis conditions can tune the atomic tunneling in $BaTiS_3$ through variability in the lattice constant. The better understanding of atomic-scale dynamics generated by our work will provide input for transport and phase-stability modeling in functional energy materials.

Recent Progress

Phasons dominate thermal transport in fresnoite. Phasons originate in materials that host two or more incompatible translational symmetries, *aka* incommensurate structures. Incommensuration leads to novel quasiparticles: phasons and amplitudons. In fresnoite, $Ba_2TiSi_2O_8$, phasons propagate supersonically. We combined inelastic neutron scattering (INS) and anisotropic thermal diffusivity measurements to assess the phason contribution to thermal transport. Using the best possible momentum resolution at HYSPEC, SNS, we determined the *momentum* width of the phason modes –*i.e.* their reciprocal mean-

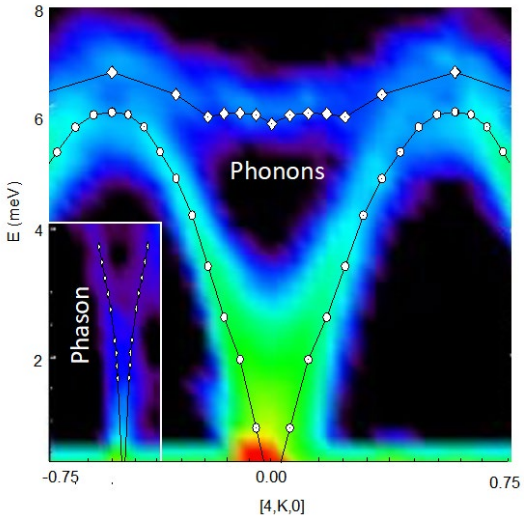

Fig. 3: Phonon and phason (lower left inset) dispersions in fresnoite determined by INS using HYSPEC at the SNS. White symbols denote the fitted mode centers used to generate the dispersions, overlaid on the scattering intensities.

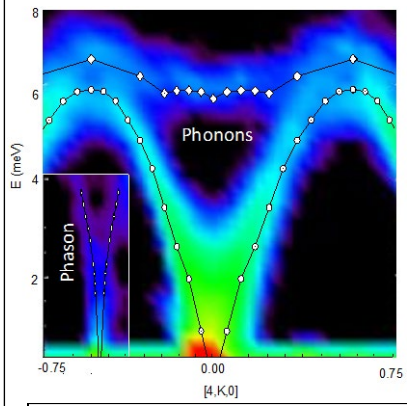

Fig. 1: Phonon and phason (lower left inset) dispersions in fresnoite determined by using HYSPEC, SNS. White symbols: fitted mode centers, overlaid on the scattering intensities.

free-path (mfp). The phason mfp is an order of magnitude larger than that of phonons, see Fig. 1, due to their weak interactions. Using calorimetry data and crystallographic considerations, we also determined the phason specific heat. Combined with phason velocities and mfp, we then modeled the thermal diffusivity and showed that phasons contribute most of the thermal transport at room temperature. We have demonstrated, for the first time, that phasons can be the dominant heat carrier in incommensurate systems and can't be neglected in thermal transport models.[O1]

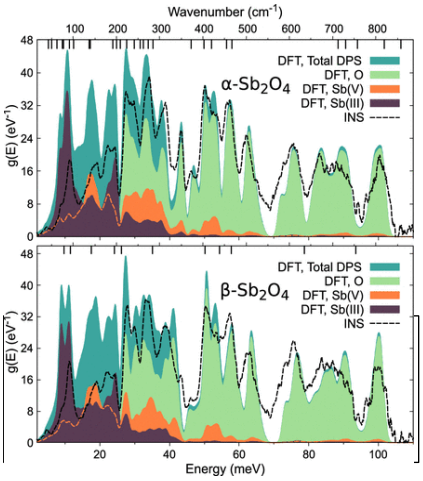

Competing phases in lone pair compounds. Electronic lone-pairs are important features in the electronic structure that can challenge structure, dynamics, and phase stability calculations. We have shown which contributions to the free energy of the mixed-valence antimony oxide α-Sb_2O_4 help stabilize it relative to β-Sb_2O_4 by combined INS at VISION, SNS, ^{121}Sb nuclear inelastic scattering, and DFT calculations, see, Fig. 2.[O2] We find that vibrational entropy does not play an essential role in determining the phase transition. However, calculations of oxygen vacancy energies, ^{121}Sb Mössbauer spectroscopy, and thermogravimetric analysis suggest that both materials can host significant oxygen vacancies and that β-Sb_2O_4 has a higher oxygen affinity. This highlights the importance of oxygen partial pressure to predict formation conditions and phase stability. Overall, our antimony oxide studies[O2,O3] reveal that DFT calculations of the lattice dynamics with appropriate dispersion corrections capture the lattice dynamics, up to a scaling factor in the vibrational energies, which neutron spectroscopy can provide. These studies also illustrate the efficiency of VISION for characterizing high-energy molecular vibrational modes, even in hydrogen-free materials.

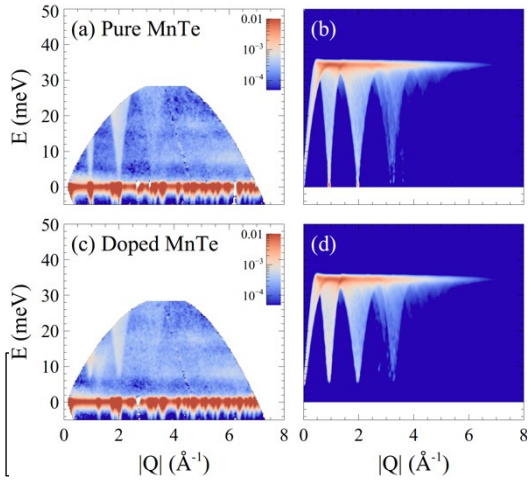

Tuning magnetic structure and dynamics in MnTe. We have shown that small amounts of Li (~0.5%) doping can tune the magnetic anisotropy and drive MnTe from a planar to an axial spin structure.[O4] Neutron diffraction data and DFT modelling show that the spin reorientation is not localized near the dopant, but is rather a full-volume effect driven by a modification of the Fermi-level. We have collaborated with the Frandsen group (Brigham-Young University) to show that anisotropic magnetic correlations in MnTe persist above the Néel temperature by means of the magnetic 3D-PDF method[1] (3-D Pair Distribution Function).[O5] Using INS, we also provided input for transport modelling (with Vashaee, NCSU)[O6] and showed that doping drives a topological transition in the magnon dispersion, where a gap opens, whereas undoped MnTe supports one gapped and one ungapped magnon branch, see Fig. 4. The magnon gap is tunable from ~2 to 6 meV with Li-content between 0.3 and 5%. The observed inelastic scattering response can be reproduced using SpinW[2] by refining exchange and anisotropy constants. This could have implications for future antiferromagnetic spintronics and for manipulating spin waves in related materials featuring Mn-Te layers, such as $MnBi_2Te_4$.

Disorder in magnetic systems. Earlier we had revealed the magnetic order in the (Mg,Co,Ni,Cu,Zn)O rocksalt high-entropy oxide and its nearly continuous magnetic phase transition near at ~120 K. Now we have advanced our understanding of structure stabilization in rocksalt oxide family. Initially, phase diagram calculations had a range of stable cation compositions[3] and in which iron was entirely absent. In collaboration with P. Cao (Auckland University), we have combined neutron diffraction, Mössbauer spectroscopy, magnetometry, and DFT-based calculations (with V. Cooper, ORNL) to reassess the initial claims. Neutron diffraction and x-ray spectroscopies show that a novel synthesis route can stabilize a phase-pure rocksalt oxide with divalent iron and manganese, (Mg,Mn,Fe,Co,Ni)O, that orders magnetically at ~205 K.[O7] This route involves fine-tuning of the oxygen content using metal oxalate precursors and MnO_2 as an oxygen generator. A revised model, that includes oxygen partial pressure, redefines a wider phase space with fifteen new target compositions, that could provide a pathway towards novel crystalline materials synthesis with targeted cation disorder.

Atomic tunneling dynamics in crystalline solids. Following our initial observation of atomic tunneling in the $BaTiS_3$ 'hexagonal perovskite'[4] and to advance our understanding of atomic vibrations in the quantum limit, we have studied the temperature dependence of the tunneling states in $BaTiS_3$ using the CNCS, SNS, spectrometer. The tunneling line takes the form of a sharp localized excitation with $E \sim 0.5$ meV. The temperature-dependence of the intensities show that the excitation does not have phononic nature. In contrast, the excitation intensity on the Stokes side (neutron energy loss) *decreases* with increasing temperature, see Fig. 4, as expected for a *two-* or *finite n*-level system. The data also indicates a complex manifold for the excitations nearest the ground state. The temperature dependence of the intensities can constrain multiplicities in a model Hamiltonian. We have also shown that the titanium tunneling dynamics in $BaTiS_3$ is elusive and sample dependent. Detailed crystallography with powder diffraction and single crystal diffraction (with C. Hoffman, SNS) shows that the $BaTiS_3$ system exhibits 0.7% variability in the *c*-lattice constants, which depends on the synthesis condition. Because the lattice constant controls the distance between tunneling pockets for Ti, this behavior can be selectively suppressed or expressed. A final ingredient to this study is forthcoming through millikelvin calorimetry.

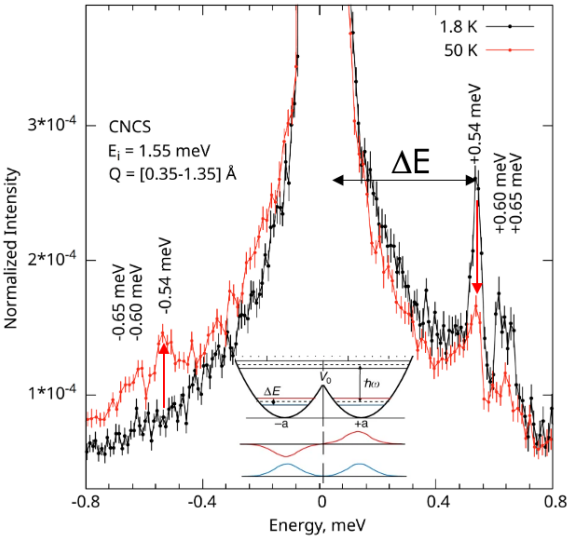

Fig. 4: Inelastic neutron scattering (CNCS, SNS, 30 μeV resolution) of the atomic tunneling states in $BaTiS_3$. The Stokes-side intensity (E>0) decreases with increasing temperature. Inset: the tunneling transition correspond to scattering between a symmetric (blue, ground state) and anti-symmetric wavefunction (red, excited state).

We have also organized a satellite workshop to the SNS/HFIR User Meeting titled "Single crystal data processing for direct geometry chopper spectrometers", which identified research directions for advancing spin- and lattice dynamics studies, notably the need for improved analysis workflows and sample environment, and the possibilities for this field that will arise from the STS.

Future Plans

Neutron methods development – we will pursue our work on using Larmor precession at HB-1A to determine Grüneisen parameters with INS at moderate pressure, up to 0.1 GPa. First inelastic scattering measurements showed that the pathway to improve the large volume pressure cells we developed. The use of liquid pressure transmitting medium is problematic. Hence, we will work to improve on cell design and prepare for similar measurements on the HYSPEC instrument at the SNS, after the shutdown. The development of a gas-driven pressure cell is challenging mostly due to safety constraints in the experimental hall of HFIR.

Switchable thermal transport – (Pb,Sb)Se is a material with structural hysteresis (thermal bistability) with a factor 3 contrast in thermal transport at 300 K, depending on the hysteretic path. We will study the reversible hysteretic 2D to 3D phase transition to clarify the role of vibrational thermodynamics and entropy in the thermal conductivity switching. We will also finish our study of the defect-induced sharpening in phonon modes in vacancy-doped PbSe (Pb $\rightarrow$ 2/3Sb+1/3 vacancy). Using triple-axis (HB3, HFIR) data complemented with data at ARCS, SNS, a comprehensive picture of phonon dispersion relations in both undoped PbSe and vacancy doped PbSe is emerging. Our microscopic observation of phonon sharpening correlates with an increase in lattice thermal conductivity upon doping. Ongoing modeling efforts will provide final elements to this.

Spin-wave in disordered materials – We will finalize our work on disorder in magnetic materials by analyzing and modeling inelastic scattering data on (Tb,Y)Sb single crystals, acquired at HYSPEC, SNS, with advanced modeling using the SU(N)NY software.[5] Likewise we will analyze and model the inelastic neutron scattering data, and muon spin rotation and magnetic pair-distribution function (with B. Frandsen) data in the Fe(II)/Mn(II)-based high-entropy oxide, to clarify the nature of lattice and spin waves in these disordered materials and to assess whether the divalent iron carries orbital angular momentum.

References

1. T. Weber and A. Simonov, *The three-dimensional pair distribution function analysis of disordered single crystals: basic concepts.* Zeitschrift für Kristallographie 227, 238-247 (2012).
2. S. Toth and B. Lake, *Linear spin wave theory for single-Q incommensurate magnetic structures*, Journal of Physics: Condensed Matter **27**, 166002 (2015).
3. K. C. Pitike, S. Kc, M. Eisenbach, C. A. Bridges and V. R. Cooper, *Predicting the Phase Stability of Multicomponent High-Entropy Compounds*, Chemistry of Materials **32**, 7507 (2020).
4. B. Sun, S. Niu, R. P. Hermann, *et al. High frequency atomic tunneling yields ultralow and glass-like thermal conductivity in chalcogenide single crystals*, Nat. Commun. **11**, 6039 (2020).
5. H. Zhang and C. D. Batista, *Classical spin dynamics based on SU(N) coherent states*, Phys. Rev. B **104**, 104409 (2021).

Publications

(10 selected out of 20)

O1. M. E. Manley, A. F. May, B. L. Winn, D. L. Abernathy, R. Sahul, and R. P. Hermann, *Phason dominated thermal transport in incommensurate fresnoite*, Phys. Rev. Lett. **129**, 255901 (2022).

O2. D. H. Moseley, R. Juneja, L. L. Daemen, I. Sergueev, R. Steinbrügge, O. Leupold, Y. Cheng, V. R. Cooper, L. Lindsay, M. K. Kidder, M. E. Manley, and R. P. Hermann, *Vibrations and Phase Stability in Mixed Valence Antimony Oxide*, Inorg. Chem. **62**, 16464 (2023).

O3. D.H. Moseley, C. A. Bridges, L.L. Daemen, Q. Zhang, M.A. McGuire, E. Cakmak, and R.P. Hermann, *Structure and Anharmonicity of α- and β-Sb_2O_3 at Low Temperature*, Crystals **13**, 752 (2023).

O4. D. H. Moseley, K. M. Taddei, J. Yan, M. A. McGuire, S. Calder, M. M. H. Polash, D. Vashaee, X. Zhang, H. Zhao, D. S. Parker, R. S. Fishman, and R. P. Hermann, *Giant doping response of magnetic anisotropy in MnTe*, Phys. Rev. Materials **6**, 014404 (2022).

O5. M.M.H. Polash, D. Moseley, J. Zhang, R. P. Hermann, and D. Vashaee, *Understanding and design of spin-driven thermoelectrics*, Cell Reports Physical Science **2**, 100614 (2021).

O6. R. Baral, J. A. Christensen, P. K. Hamilton, F. Ye, K. Chesnel, T. D. Sparks, R. Ward, J. Yan, M. A. McGuire, M. E. Manley, J. B. Staunton, R. P. Hermann, and B. A. Frandsen, *Real-space visualization of short-range antiferromagnetic correlations in a magnetically enhanced thermoelectric*, Matter **5**, 1853–1864 (2022).

O7. Y. Pu, D. H. Moseley, Z. He, K. C. Pitike, M. E. Manley, J. Yan, V. R. Cooper, V. Mitchell, V. K. Patterson, B. Johannessen, R. P. Hermann, and P. Cao, *(Mg,Mn,Fe,Co,Ni)O: A rocksalt high-entropy oxide containing divalent Mn and Fe*, Science Advances adi8809 (2023).

O8. R. Juneja, X. Li, S. Thébaud, D. H. Moseley, Y. Q. Cheng, M. E. Manley, R. P. Hermann, and L. Lindsay, *Phonons in complex twisted crystals: Angular momenta, interactions, and topology*, Phys. Rev. B **106**, 094310 (2022).

O9. H. W. Suriya Arachchige, W. R. Meier, M. Marshall, T. Matsuoka, R. Xue, M. A. McGuire, R. P. Hermann, H. Cao, and D. Mandrus, *Charge density wave in kagome lattice intermetallic ScV_6Sn_6*, Phys. Rev. Lett. **129**, 216402 (2022).

O10. E. Xiao, H. Ma, M. S. Bryan, L. Fu, J. M. Mann, B. Winn, D. L. Abernathy, R. P. Hermann, M. E. Manley, and C. A. Marianetti, *Validating first-principles phonon lifetimes via inelastic neutron scattering*, Phys. Rev. B **106**, 144310 (2022).

Topological magnons and topological electronic properties in metallic Kagome magnets

Xianglin Ke, Department of Physics and Astronomy, Michigan State University, MI 48824

Program Scope

The experimental discovery of topological insulators following their theoretical prediction has opened an emerging research arena in searching for new topological states of quantum matter. On the one hand, the integration of non-trivial electronic band topology and magnetism is anticipated to give rise to a rich variety of novel topological quantum phenomena. On the other hand, it has been shown recently that topology provides new perspectives which go beyond fermionic systems and can be elegantly generalized to non-electronic bosonic systems, such as magnons which are the quanta of low-energy magnetic excitation of ordered magnets. The primary objective of this program is to study magnetic materials hosing nontrivial topology of both magnons and electronic states.

Recent Progress

We have been investigating topological electronic and magnetic properties of various systems, some of which are highlighted as follows.

A. Kagome magnets RMn_6Sn_6. Metallic Kagome systems have emerged as an interesting platform to investigate effects of lattice geometry and electronic correlation on novel physical properties of materials, including magnetism, topology, charge density wave, superconductivity. For RMn_6Sn_6, the Mn ions form a Kagome lattice, which play an essential role in both magnetism and electronic properties of this system, while rare-earth ions R serve as a tuning parameter to later the magnetic couplings between neighboring Kagome planes. One of such materials is $TbMn_6Sn_6$, in which we have found large anomalous Nernst effect and anomalous thermal Hall effect (THE) (Figure 1). The anomalous transverse transport is consistent with the Berry curvature contribution from the massive Dirac gaps in the 3D momentum space as demonstrated by our first-principles calculations. Furthermore, the transverse thermoelectric transport exhibits asymmetry with respect to the applied magnetic field, i.e., an exchange-bias behavior. Together, these features place $TbMn_6Sn_6$ as a promising system for the outstanding thermoelectric performance based on anomalous Nernst effect [1].

By partially replacing Tb with, we have also investigated the complex magnetic phase diagram and its correlation with the transport properties in $Tb_{1-x}Y_xMn_6Sn_6$ Kagome magnets. In contrast to $TbMn_6Sn_6$ which is a ferrimagnet and hosts Chern gapped Dirac fermions near the Fermi level, YMn_6Sn_6 is an antiferromagnet with incommensurate spins ordering due to the competition of interlayer couplings and shows topological Hall effect. By mixing Tb and Y in $Tb_{1-x}Y_xMn_6Sn_6$ to tune the inter-Kagome plane exchange couplings, we have revealed a complex magnetic phase diagram via neutron diffraction, electronic and thermal transport measurements. This study sheds light on the correlation between magnetism and topological properties of this Kagome system [2].

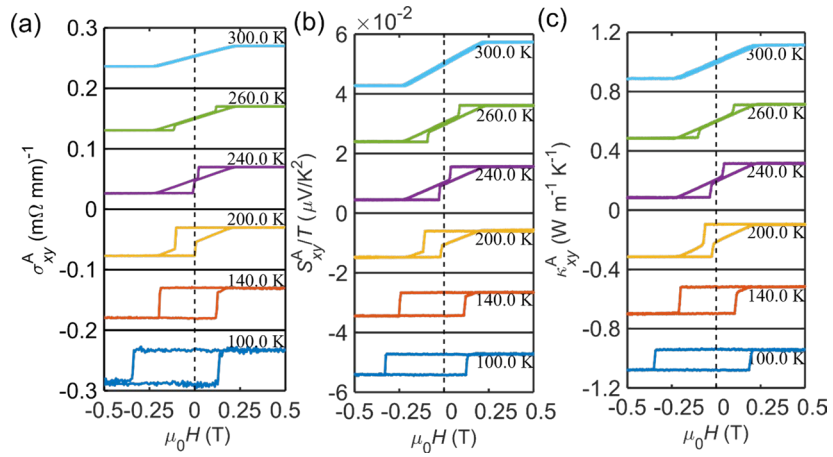

Figure 1. Hysteresis and temperature dependence of transverse transport properties of Dirac Kagome magnet $TbMn_6Sn_6$. Magnetic field dependence of anomalous Hall conductivity σ_{xy}^A (a), anomalous Nernst coefficients scaled by temperature S_{xy}^A/T (b), and anomalous thermal Hall conductivity κ_{xy}^A (c) measured at selected temperatures.

B. van der Waals (vdW) magnets. Two-dimensional (2D) vdW magnets have been a fertile playground for the discovery and exploration of physical phenomena and new physics. We have performed thermal transport measurements, which serve as a complimentary tool to inelastic neutron scattering to probe low energy excitations, on a 2D vdW insulating magnet VI_3 in which V magnetic ions form a hexagonal lattice. We have observed a large THE with the thermal Hall signal persists in the absence of an external magnetic field and flips sign upon the switching of the magnetization (Fig. 2). In combination with theoretical calculations, we show that VI_3 exhibits a dual nature of the THE, i.e., dominated by topological magnons hosted by the ferromagnetic honeycomb lattice at higher temperatures and by phonons induced by the magnon-phonon coupling at lower temperatures. Our results not only position VI_3 as the first ferromagnetic system to investigate both anomalous magnon and phonon THEs, but also render it as a potential platform for spintronics/magnonics applications [3].

We have also studied the thermal transport properties of an insulating vdW triangular magnet $FeCl_2$ where the Fe ions occupy a triangular lattice. We have observed large magneto-thermal conductivity and THE in this material. The magneto-thermal conductivity reaches over ~700%, indicating strong magnon-phonon coupling. Furthermore, we find an appreciable thermal Hall signal which changes sign concurrently with the spin-flip transition from the antiferromagnetic state to the polarized ferromagnetic state. Our theoretical calculations suggest that the large Berry curvature induced at the anticrossing points of the hybridized magnon and acoustic phonon modes of $FeCl_2$ can be associated with the observed THE [4].

We have also investigated the strong coupling between charge, lattice, and spin degrees of freedom in antiferromagnetic topological insulator $MnBi_2Te_4$. The discovery of an intrinsic antiferromagnetic topological insulator in $MnBi_2Te_4$ has attracted intense attention, most of which lies on its electrical properties. In this work, we report electronic, thermal, and thermoelectric transport studies of this newly found AFM-TI. The temperature and magnetic field dependence of its resistivity, thermal conductivity, and Seebeck coefficient indicate strong coupling between charge, lattice, and spin degrees of freedom in this system. Furthermore, $MnBi_2Te_4$ exhibits a large anomalous

Nernst signal, which is associated with non-zero Berry curvature of the field-induced canted antiferromagnetic state [5].

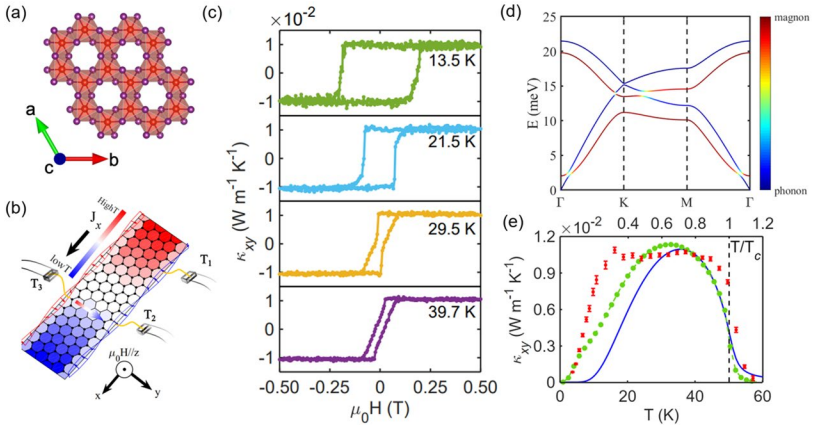

Figure 2. Anomalous thermal Hall effect of 2D van der Waals magnet VI_3. (a) The schematic crystal structure of VI_3 viewed in the *ab* plane. Vanadium atoms are in red and Iodine atoms are in purple. (b) A schematic of the experiment set-up. The color indicates temperature profile. (c) Thermal Hall conductivity $\kappa_{xy}(H)$ measured at various temperatures. (d) The calculated magnon and phonon bands with the magnon-phonon coupling. (e) Comparision of experimental data (red) of anomalous $\kappa_{xy}(T)$ with the calculated values without (blue) and with (green) the magnon-phonon coupling being considered.

C. Antiferromagnetic Skyrmion candidate. We have extended our research to antiferromagnetic Skyrmion materials which exhibit topological Hall effect. One of such candidates is the $ThCr_2Si_2$-type $NdMn_2Ge_2$. Through neutron diffraction, electronic, and thermoelectric transport measurements, we show that, in both the canted antiferromagnetic phase and conical magnetic phase with an out-of-plane ferromagnetic component, the system exhibits both anomalous Nernst effect and topological Nernst effect (TNE). Both the anomalous thermoelectric linear response tensor and TNE are quite comparable to the magnitudes reported in other topological semimetals (Fig. 3). These features demonstrate that $NdMn_2Ge_2$ is a unique magnetic material with its topological character arising from the Berry phase of both real space and momentum space [6].

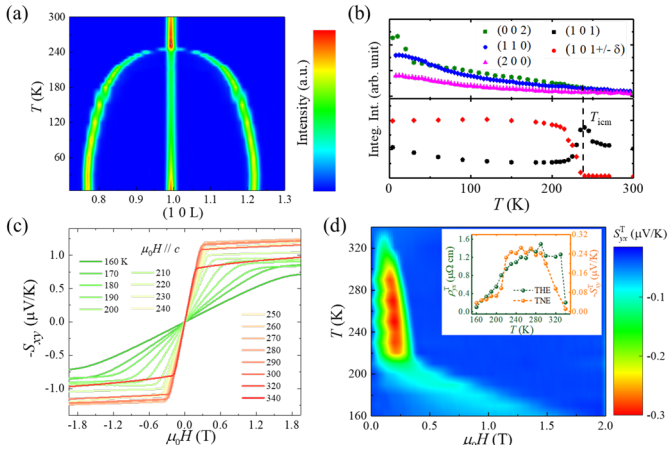

Figure 3. Magnetic, electronic, and thermoelectric properties of a Skyrmion antiferromagnet $NdMn_2Ge_2$. (a) $T - (1\ 0\ L)$ contour map of neutron diffraction intensity showing an incommensurate phase transition near 245 K. (b) Temperature dependence of integrated neutron scattering intensity of various Bragg reflections. (c) Magnetic field dependence of Nernst effect coefficient $-S_{xy}$.(d) $T - H$ contour map of topological Nernst effect.

Future Plans

In the future we will study the effect of lattice geometry on magnetism, thermal, and topological electronic properties and the application of topological concept to magnetism.

References

Publications

1. Heda Zhang, Jahyun Koo, Chunqiang Xu, Milos Sretenovic, Binghai Yan, and **Xianglin Ke**, "*Exchange-biased topological transverse thermoelectric effects in a Kagome ferrimagnet*", Nature Communications **13**, 1091(2022).
2. M. Sretenovic, T. Heitmann, T. Hong, H. Cao, and **X. Ke**, "*Magnetic phase transitions, electronic and thermal transport properties of $Tb_{1-x}Y_xMn_6Sn_6$ Kagome magnets*", in preparation (2023).
3. H. Zhang, C.Q. Xu, C. Carnahan, M. Sretenovic, N. Suri, D. Xiao, and **X. Ke**, "*Anomalous thermal Hall effect in an insulating van der Waals magnet*", Phys. Rev. Lett. **127**, 247202 (2021).
4. Chunqiang Xu, Caitlin Carnahan, Heda Zhang, Milos Sretenovic, Pengpeng Zhang, Di Xiao, and **Xianglin Ke**, "*Thermal Hall effect in a van der Waals triangular magnet $FeCl_2$*", Phys. Rev. B 107, L060404 (2023).
5. H. Zhang, C.Q. Xu, S.H. Lee, Z.Q. Mao, and **X. Ke**, "*Thermal and thermoelectric properties of an antiferromagnetic topological insulator $MnBi_2Te_4$*", Phys. Rev. B **105**, 184411 (2022).
6. Chunqiang Xu, Wei Tian, Pengpeng Zhang, and Xianglin Ke, "*Large anomalous Nernst Effect and topological Nernst effect in the noncollinear antiferromagnet $NdMn_2Ge_2$*", Phys. Rev. B **108**, 064430 (2023).
7. V. Petkov, T Durga Rao, A. Zafar, AM Milinda Abeykoon, E. Fletcher, J. Peng, Z.Q. Mao, and **X. Ke**, "*Lattice distortions and the metal-insulator transition in pure and Ti-substituted $Ca_3Ru_2O_7$*", J. Phys. Conden. Matter. **51**, 015402 (2023).
8. V. Petkov, R. Amin, M. Jakhar, V. Barone, AM. Milinda Abeykoon, M. Sretenovic, and **X. Ke**, "*Charge density wave, local lattice distortions, and topological electronic states in $NbTe_4$*", Phys. Rev. B **108**, 174112 (2023).
9. Tao Hong, Imam Makhfudz, **Xianglin Ke**, Andrey A. Podlesnyak, Daniel Pajerowski, Barry Winn, Merce Deumal, and Mark M. Turnbull, "*Interplay between magnetic frustration and quantum criticality in the unconventional Ladder antiferromagnet $C_9H_{18}N_2CuBr_4$*", under review (2023).
10. Matt Boswell, Qiang Zhang, **Xianglin Ke**, and Weiwei Xie, "*Antiferromagnetic $KHoSe_2$ with Ho^{3+} triangular lattice*", under review (2023).

Hybrid Organic-Inorganic Nanosheets with Emergent Properties

Seung-Hun Lee (PI) and Joshua J. Choi (Co-PI)
University of Virginia

Program Scope

Hybrid organic-inorganic perovskites (HOIPs) have achieved striking success in various applications such as solar cells, light emitting diodes and photodetectors. Two-dimensional (2D) nanosheets of HOIPs can be considered as quantum confined nanosheets with controllable structures and dimensions. Forming interfaces between two-dimensional nanomaterials gives rise to novel emergent phenomena that do not exist in individual components. 2D HOIPs provide the possibility of placing different organic molecules in between the 2D nanosheets, providing a transformative research opportunity to study how organic molecule dynamics interact with inorganic lattices in nanostructures and how their couplings give rise to new emergent properties.

In this program, the structure and properties of HOIPs are investigated at multiple length scales to achieve a full understanding of the microscopic mechanism of the photovoltaic effect. Specifically, this research program is testing the hypothesis that the structure and dynamics of organic molecules between the nanosheets will influence electronic and optical coupling across neighboring nanosheets and thus play a central role in determining the optoelectronic properties of 2D HOIP stacks. The experimental approach is to employ several complimentary techniques that can probe from atomic to macroscopic properties: molecular structure and dynamics at the microscopic level, charge recombination at the mesoscopic level, and the solar cell efficiency at the macroscopic level. Neutron diffraction and time-of-flight neutron scattering spectroscopy are used to characterize the structure and rotational and vibrational dynamics. Optical spectroscopy, electrical transport measurements and solar cell fabrication and testing are employed to determine the impact of organic cations on the bulk properties and photovoltaic performance of the HOIPs.

Recent Progress

Using time-of-flight neutron spectroscopy and Raman scattering, we identified and quantitatively separated the lattice vibrational and molecular rotational dynamics of two perovskites, butylammonium lead iodide $(BA)_2PbI_4$ and phenethyl-ammonium lead iodide $(PEA)_2PbI_4$. By examining the corresponding temperature dependence, we found that lattice vibrations extracted from neutron spectra are qualitatively consistent with the lattice dynamics from Raman scattering. We also showed that the temperature dependence of the rotational dynamics of organic molecules in these materials is inversely proportional to their photoluminescence quantum yields while the vibrational dynamics do not show predominant correlations with their optoelectronic properties. We postulated that the rotational motions of the polarized molecules could significantly interrupt the binding energy potential of excitons, cause the exciton decompositions, enhance the non-radiative recombination rates, and hence reduce the photoluminescence yield.[1]

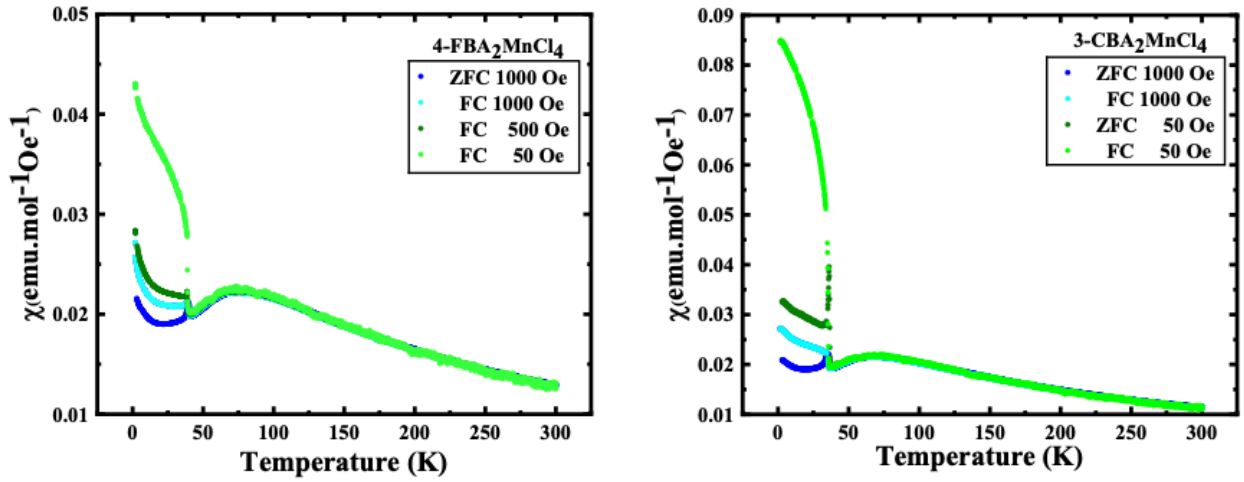

Figure 1. Bulk susceptibility data obtained from 4-FBA_2MnCl_4 (left panel) and 3-CBA_2MnCl_4 (right panel).

We have also synthesized and investigated $MnCl_4$-based 2D HOIPs. We conducted zero field cooling (ZFC) and field cooling (FC) bulk susceptibility measurements on powder samples of $(C_6H_5CH_2NH_3)_2MnCl_4$, 3-$(C_7H_9ClN)_2MnCl_4$ (3-CBA_2MnCl_4) and *x*-$(C_7H_9FN)_2MnCl_4$ (*x*-FBA_2MnCl_4) where $x = 2$ and 4 represent different relative attachments of NH_3 molecules and F/Cl atoms to the benzene ring. The figure above shows the data of 4-FBA_2MnCl_4 and 3-CBA_2MnCl_4. Understanding the data will require neutron scattering measurements including neutron powder diffraction measurements.

In addition to the HOIPs, we have launched a quantum magnetism collaboration with Hiroaki Ueda's group at Kyoto University on Ti^{3+} (s = ½) based kagome systems to investigate the low temperature physics of quantum kagome antiferromagnets. We are performing the time-of-flight neutron scattering measurements on single crystals of $Cs_8K_3RbTi_{12}F_{48}$ in December of the year 2023 at J-Parc and will be able to present the results at the DOE PI meeting in January of the year 2024.

Future Plans

To understand the zero-field cooling (ZFC) and field cooling (FC) bulk susceptibility measurements obtained from the powder samples of $(C_6H_5CH_2NH_3)_2MnCl_4$, 3-$(C_7H_9ClN)_2MnCl_4$ (3-CBA_2MnCl_4) and *x*-$(C_7H_9FN)_2MnCl_4$ (*x*-FBA_2MnCl_4), we will perform neutron diffraction and inelastic measurements on the samples.

After the TOF measurements using the 4Seasons spectrometer on the single crystals of $Cs_8K_3RbTi_{12}F_{48}$ in December of the year 2023, we will perform any further neutron scattering experiments that are necessary on the system. In addition, we will also perform neutron scattering experiments on single crystals of another isostructural system $Cs_8Na_3LiTi_{12}F_{48}$. The single crystals of $Cs_8Na_3LiTi_{12}F_{48}$ are already available for our neutron scattering experiments.

Publications

1. *Structural dynamics and optoelectronic properties of two-dimensional hybrid organic-inorganic perovskites,* H. S. Rajeev, X. Hu, W-L. Chen, D. Zhang, T. Chen, M. Kofu, R. Kajimoto, A. Z. Chen, M. Yoon, Y-M. Chang, J. J. Choi, S.-H. Lee, to be submitted (2023).

2. *Zero-point entropies of spin-jam and spin-glass states in a frustrated magnet*, C. Piyakulworawat, A. Thennakoon, J. Yang, H. Yoshizawa, D. Ueta, T.-J. Sato, K. Shen, W-T. Chen, K. Matan, S.-H. Lee, submitted (2023).
3. *Photo-excited charge carrier lifetime enhanced by slow cation molecular dynamics in lead iodide perovskite $FAPbI_3$*, M. Hiraishi, A. Koda, H. Okabe, R. Kadono, K. A. Dagnall, J. J. Choi, S.-H. Lee, Journal of Applied Physics **134**, 055106 (2023).
4. *Quantum-dot-doped lead halide perovskites for ionizing radiation detection*, A. M. Conley, E. S. Sarabamoun, K. A. Dagnall, L. U. Yoon, H. S. Rajeev, S.-H. Lee, J. J. Choi, ACS Applied Optical Materials **1**, 715-723 (2023).
5. *Ytterbium-doped cesium lead chloride perovskite as an x-ray scintillator with high light yield,* K. A. Dagnall, A. M. Conley, L. U. Yoon, H. S. Rajeev, S.-H. Lee, J. J. Choi, ACS Omega **7(24)**, 20968-20974 (2022).
6. *Organic molecular dynamics and charge-carrier lifetime in lead iodide perovskites* A. Koda, H. Okabe, M. Hiraishi, R. Kadono, K. A. Dagnall, J. J. Choi, S.-H. Lee, PNAS **119**, e2115812119 (2022).

Scattering and Spectroscopic Studies of Quantum Materials

Young Lee (Stanford University and SLAC National Accelerator Laboratory), Jiajia Wen (SLAC National Accelerator Laboratory), and Hong-Chen Jiang (SLAC National Accelerator Laboratory)

Keywords: Quantum magnets, spin liquids, correlated electrons

Research Scope

Our project focuses on studying quantum materials with a comprehensive effort involving crystal growth, sample characterization, neutron and x-ray scattering, and numerical simulations. This past year we have primarily focused on studying a new quantum spin liquid material based on the spin-1/2 kagome lattice using inelastic neutron scattering techniques. Such materials may be relevant to our understanding of high-temperature superconductivity and have possible applications in quantum information. We developed new models for the measured spin correlations, including new numerical simulations which detail the further neighbor spin correlations in the spin liquid state. These efforts further our goal to expand the base of spin liquid compounds and associated experimental signatures and compare with theoretical predictions based on realistic Hamiltonians. In addition, we study the effects of disorder on the quantum ground states, including intertwined spin and charge order in unconventional superconductors and quantum spin liquids. These activities further integrate neutron scattering and quantum magnetism efforts within SLAC and also involve outside collaborations with other groups focused on the synthesis, characterization, and theory of quantum materials.

Recent Progress

We have recently completed a comprehensive set of inelastic neutron scattering measurements of the spin excitations of the kagome quantum spin liquid (QSL) material Zn-barlowite. We measured the spin excitations in a co-aligned sample composed of ~200 deuterated single crystals which we grew hydrothermally. The measurements involved experiments using the Cold Neutron Chopper Spectrometer (CNCS) at the Spallation Neutron Source (SNS). We developed new analysis tools for extracting the extremely weak intrinsic signal of the kagome moments from the strong background scattering. The resulting data quality allows us to make several important conclusions. First, we could determine how the small population of interlayer impurities interact with the intrinsic spinon excitations at low energies. Second, we found that the intrinsic spin excitation spectrum is universal across different spin-1/2 kagome materials. Third, we have strong experimental evidence that the ground state has a spin-gap, consistent with theoretical predictions. This provides the best evidence for the existence of a spin liquid in any known quantum material. Our new results are consistent with our previous conclusions regarding the intrinsic physics of the kagome layers [1-3], as well as the role played by disorder. [4-5]

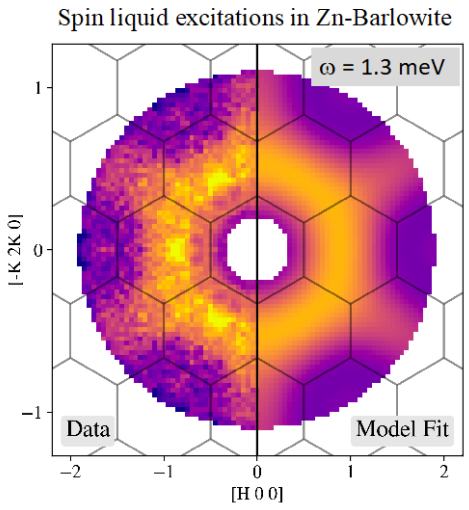

Figure 1) Inelastic neutron scattering on a single crystal sample of Zn-barlowite at T=1.7K taken at the CNCS instrument at the SNS.

Due to the high-quality of the dynamic structure factor data in Zn-barlowite, we could analyze the contributions of various spin correlations to the total scattering. For the first time, we determined that the second and third neighbor correlations within the kagome plane were significant, in addition to the nearest neighbor correlations. We performed density matrix

renormalization group (DMRG) calculations based on the kagome antiferromagnetic Hamiltonian. Comparison with the data showed that the measured spin correlations place the Zn-barlowite material firmly within the spin liquid phase of the extended phase diagram (including DM interactions and second neighbor coupling).

To further understand the low energy spin excitations near the impurities in Zn-barlowite, we used local resonance techniques to successfully correlate the distribution of the low energy spin excitations with that of the local spin susceptibility. We found evidence for the gradual growth of domains with a local spin polarization induced by the 5% Cu^{2+} defect spins occupying the interlayer non-magnetic Zn^{2+} sites. These spin-polarized domains grow upon cooling down to , where gapless excitations induced by interlayer defects dominate the low-energy sector of spin excitations within the kagome planes. These results complement our previous findings that impurities can couple locally to the neighboring kagome spins and affect the spatial homogeneity of the spin-gap.

In another interesting quantum material, we studied the electronic nematic structural phase transition in $Tm_{1-x}Y_xVO_4$, tuned by magnetic field and substitutional disorder, with neutron scattering. We found that nematic fluctuations onset prior to the proper structural phase transition everywhere along the temperature-field phase boundary. We also demonstrated that substitutional disorder introduces local perturbations of both xy and x^2-y^2 symmetries, which may be modelled by the two-component random field Ising model. This is strong evidence that nematic quantum criticality is random-field in nature. Thus, we determined that $Tm_{1-x}Y_xVO_4$ emerges as a viable non-magnetic analogue to the random-field Ising model, and is the first experimental system described by random-fields of two-components.

Future Plans

We have upcoming beamtime to investigate the spin excitations in the kagome quantum spin liquid Zn-barlowite with neutron scattering in high magnetic fields at the High Flux Isotope Reactor (HFIR). We will focus on changes to the low-energy kagome spin fluctuations as the spin-gap is closed with high fields, which may be indicative of a quantum phase transition. We will perform DMRG calculations of the spin Hamiltonian in high fields to support the analysis of the data. In addition, we will analyze our recent high-resolution inelastic x-ray scattering data of the lattice dynamics in kagome materials characterized by different ground states. The phonon dispersions in Barlowite 2 (a likely valence bond crystal (VBC) state) and Zn-Barlowite (a likely quantum spin liquid state) have subtle differences. We will investigate the role of spin-phonon coupling in determining the ground states. We also plan to investigate the effects of high-pressure and strain on the thermodynamics and transport in single crystals of Zn-barlowite. Finally, we will explore using numerical simulation to compute the dynamic spin structure factors for the QSL and VBC states for realistic Hamiltonians to compare with Zn-barlowite and Barlowite 2, respectively. The spin dynamics require much longer computation times compared to static correlations.

References

1. R. W. Smaha, W. He, J. M. Jiang, J.-J. Wen, Y.-F. Jiang, J. P. Sheckelton, C. J. Titus, S. G. Wang, Y.-S. Chen, S. J. Teat, A. A. Aczel, Y. Zhao, G. Xu, J. W. Lynn, H.-C. Jiang, Y.S. Lee, *Materializing rival ground states in the barlowite family of kagome magnets: quantum spin liquid, spin ordered, and valence bond crystal states,* npj Quantum Mater.**5**, 23 (2020).
2. Rebecca W. Smaha, Jonathan Pelliciari, Ignace Jarrige, Valentina Bisogni, Aaron T. Breidenbach, Jack Mingde Jiang, Jiajia Wen, Hong-Chen Jiang, and Young S. Lee, "*High energy spin excitations in the quantum spin liquid candidate Zn-barlowite probed by resonant inelastic x-ray scattering*," Phys. Rev. B **107**, L060402 (2023).
3. Jiaming Wang, Weishi Yuan, Philip M. Singer, Rebecca W. Smaha, Wei He, Jiajia Wen, Young S. Lee, and Takashi Imai, *Emergence of spin singlets with inhomogeneous gaps in the kagome lattice Heisenberg antiferromagnets Zn-barlowite and herbertsmithite,* Nature Physics **17**, 1109 (2021).

4. R.W. Smaha, I. Boukahil, C. J. Titus, J. M. Jiang, J. P. Sheckelton, W. He, J.-J. Wen, J. Vinson, S. G. Wang, Y.-S. Chen, S. J. Teat, T. P. Devereaux, C. D. Pemmaraju, and Y. S. Lee, *Site-specific structure at multiple length scales in kagome quantum spin liquid candidates*, Phys. Rev. Materials, **4**, 124406 (2020).
5. Weishi Yuan, Jiaming Wang, Philip M.Singer, Rebecca W. Smaha, Jiajia Wen, Young S. Lee, Takashi Imai, "*Emergence of the spin polarized domains in the kagome lattice Heisenberg antiferromagnet Zn-barlowite (Zn0.95Cu0.05)Cu3(OD)6FBr,*" npj Quantum Materials **7**, 120 (2022).

Publications

1. Rebecca W. Smaha, Jonathan Pelliciari, Ignace Jarrige, Valentina Bisogni, Aaron T. Breidenbach, Jack Mingde Jiang, Jiajia Wen, Hong-Chen Jiang, and Young S. Lee, "*High energy spin excitations in the quantum spin liquid candidate Zn-barlowite probed by resonant inelastic x-ray scattering*," Phys. Rev. B **107**, L060402 (2023).
2. J.-J. Wen, W. He, H. Jang, H. Nojiri, S. Matsuzawa, S. Song, M. Chollet, D. Zhu, Y.-J. Liu, M. Fujita, K.M. Suzuki, S. Asano, J. M. Jiang, C. R. Rotundu, C.-C. Kao, H.-C. Jiang, J.-S. Lee, and Y. S. Lee, "*Enhanced charge density wave with mobile superconducting vortices in La1:885Sr0:115CuO4*," Nature Communications **14**, 733 (2023).
3. Hong-Chen Jiang, Steven A Kivelson, Dung-Hai Lee, "*Superconducting valence bond fluid in lightly doped 8-leg cylinders*," Phys. Rev. B **108**, 054505 (2023).
4. Yi-Fan Jiang, Hong-Chen Jiang, "*Nature of quantum spin liquids of the Heisenberg antiferromagnet on the triangular lattice: A parallel DMRG study*," Phys. Rev. B, **107**, L140411 (2023).
5. Cheng Peng, Yao Wang, Jiajia Wen, Young S. Lee, Thomas P. Devereaux, Hong-Chen Jiang, "*Enhanced superconductivity by near-neighbor attraction in the doped Hubbard model*," Phys. Rev. B **107** (20), L201102 (2023).
6. Weishi Yuan, Jiaming Wang, Philip M.Singer, Rebecca W. Smaha, Jiajia Wen, Young S. Lee, Takashi Imai, "*Emergence of the spin polarized domains in the kagome lattice Heisenberg antiferromagnet Zn-barlowite (Zn0.95Cu0.05)Cu3(OD)6FBr*," npj Quantum Materials **7**, 120 (2022).
7. 1. J. Wang, W. Yuan, P. M. Singer, R. W. Smaha, W. He, J.-J. Wen, Y. S. Lee, and T. Imai, "*Freezing of the Lattice in the Kagome Lattice Heisenberg Antiferromagnet Zn-Barlowite ZnCu3(OD)6FBr*," Phys. Rev. Lett.,**128**, 157202 (2022).
8. 1. Pierre Massat, Jiajia Wen, Jack M. Jiang, Alexander T. Hristov, Yaohua Liu, Rebecca W. Smaha, Robert S. Feigelson, Young S. Lee, Rafael M Fernandes , Ian R. Fisher, "*Field-tuned ferroquadrupolar quantum phase transition in the insulator TmVO4*", PNAS, Vol. **119** No. 28 e2119942119 (2022).
9. Feng Ke, Jiejuan Yan, Roc Matheu, Shanyuan Niu, Nathan R. Wolf, Hong Yang, Ketao Yin, Jiajia Wen, Young S. Lee, Hemamala I. Karunadasa, Wendy L. Mao, and Yu Lin, "*Quasi-One-Dimensional Metallicity in Compressed CsSnI3*," Journal of the American Chemical Society **144**, 23595-23602 (2022).
10. Feng Ke; Jiejuan Yan; Shanyuan Niu; Jiajia Wen; Ketao Yin; Hong Yang; Nathan R. Wolf; Yan-Kai Tzeng; Hemamala I. Karunadasa; Young S. Lee, Wendy L. Mao, Lin, Yu, "*Cesium-mediated electron redistribution and electron-electron interaction in high-pressure metallic CsPbI3*," Nature Communications **13**, 7067 (2022).

Neutron Scattering Study of Spin-Lattice Interactions

Chen Li, University of California, Riverside

Keywords: Spin-lattice interactions, dissipation, antiferromagnetic materials, spintronics materials, magnon and phonon dynamics

Research Scope

We aim to explore the dissipation of spin dynamics in antiferromagnetic materials due to lattice dynamics using neutron scattering. The project characterizes the temperature, pressure, and magnetic field modulation of Néel vectors, magnetic anisotropy, spin wave, and magnon-phonon hybridization to understand the rules that govern spin-lattice interactions and their roles in damping of spin dynamics and transport properties. This knowledge may be used to engineer desired material properties by mutual control between spin and lattice dynamics.

The project provides insights on key physics questions: (1) What are the mechanisms of interactions between spin and lattice degrees of freedom? (2) What is the role of the phonon in damping coherent spin excitation? (3) How to reduce such interactions to improve coherence in quantum devices? (4) What are the selection rules for angular momentum transfer between spin and lattice degrees of freedom? (5) How to control the spin order and dynamics by phonon or vice versa? Moreover, by pushing quantum materials near their instability by these interactions, we also explore novel emergent physics and unconventional material properties.

Antiferromagnetic materials have many advantages that make them attractive for quantum devices with better energy efficiency. [1–4] The lattice degree of freedom represents an approach to altering the energy landscape of the exchange interactions and the anisotropy of these materials for control. The proposed work also provides information on materials under their operational conditions to exploit the functionality and optimize the performance of antiferromagnetic materials. One of the central challenges in spintronics is to reduce dissipation to improve coherence. Suppression dissipation leads to longer lifetimes of quantum states and mean free paths, and higher operating temperatures, thus better energy efficiency. By exploiting the selection rules of interactions between lattice and spin degrees of freedom, it may be possible to create protected states to minimize dissipation. Moreover, it might be possible to leverage the interactions to efficiently couple spintronics and electronic devices via acoustic intermediates.

Recent Progress

At long wavelengths, the spin-phonon interaction manifests itself as magnetostrictive and magnetoelastic effects [5]. At shorter wavelengths, magnon-phonon interactions originate from the dynamical local strains created by phonons and show up as resonance and hybridization. [6] We recently observed this hybridization through transport measurements. [7] **(Fig. 1)** In the hybridization regions, a large number of scattering channels satisfy the kinetic conditions and reduce the phonon and magnon lifetimes. Such effects have rarely been investigated, and accurate

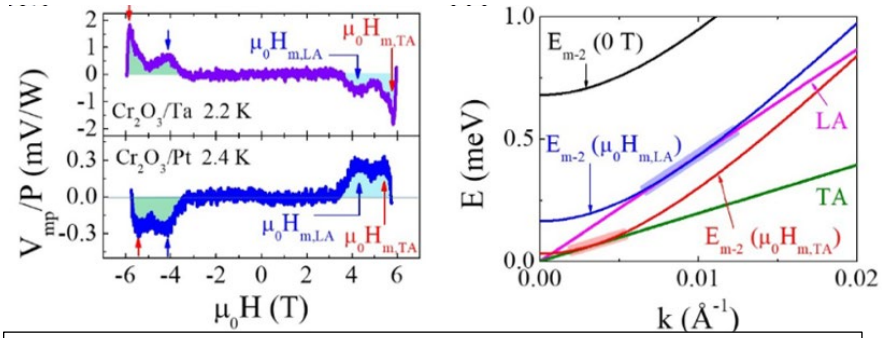

Figure 1 Lattice-phonon interactions shown for Cr2O3/heavy metal heterostructure by spin Seebeck effect. (left) Extracted magnon-polaron signal; (right) Our atomistic calculation of the dispersions showing hybridization. [7]

modeling requires taking kinetic conditions into account. More importantly, there are symmetry constraints related to the polarization of phonon and magnon, [8] and the selection rules are still unknown. [9]

The spin dynamics in many antiferromagnetic materials is still poorly understood, and their control requires quantitative information on magnetic anisotropy and damping. Pressure represents a direct approach to altering the energy landscape of exchange interactions and anisotropy in these materials, as shown by our work on Fe_3GeTe_2. (**Fig. 2**) This was also shown for low-dimensional materials, where considerable strain can alter spin-orbit coupling and Rashba effects.

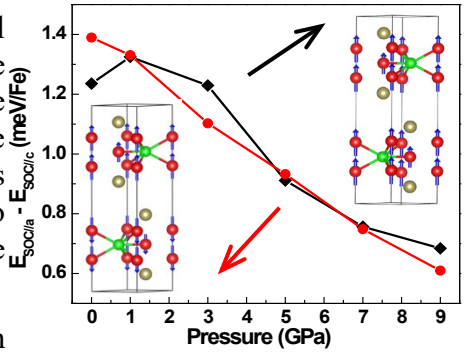

Figure 2 The magnetic anisotropy of Fe_3GeTe_2 is strongly pressure dependent and differs between spin states. The calculation is performed by non-colinear DFT with spin-orbit coupling. *[17]*

Beyond the dispersion measurements, inelastic neutron scattering intensity, particularly its $\boldsymbol{Q}$ dependence, contains valuable information. Magnons and phonons have distinct scattering structural factors. This is no longer the case when spin and phonon interact strongly, as demonstrated by our recent discovery in NiO. [10] Our temperature and field-dependent inelastic neutron scattering measurements on this material showed an unexpected manifest of spin-phonon interactions in the INS intensity (**Fig. 3**). A surprisingly strong transverse acoustic phonon mode is observed, although this branch is forbidden in for one-phonon neutron scattering. Even more surprising is the fact that such intensity does not follow the expected $\boldsymbol{Q}$ dependence for phonons between different zones. This behavior does not follow the predicted intensity by magnetovibrational scattering either. [11,12] Instead, the $\boldsymbol{Q}$ dependence partially follows the magnetic form factor through the lower order zones. Such anomalous scattering intensity originates from the perturbation to the phonon polarization by spin-phonon interaction induced renormalization.

Anomalous temperature dependence of the scattering intensity also provides information on the spin-lattice interactions. We have shown in NiO that temperature anomalies could be the result of strong spin-phonon interactions. One striking property of NiO is the suppression of thermal transport near the Néel temperature. Our INS work found that the temperature dependence of phonons in the antiferromagnetic phase NiO mostly follows the quasiharmonic model, in which changes in lattice dynamics are driven by lattice dilation. During the antiferromagnetic transition, the phonons suddenly soften. This is a clear indication that the spin-phonon coupling is significant.

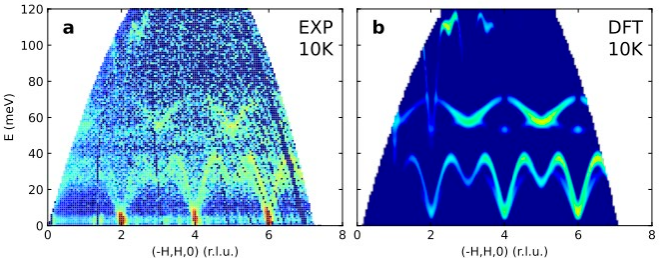

Figure 3 Dynamical structure factor of antiferromagnetic NiO from INS on ARCS (left) and simulated phonon and magnon S(**Q**, E) by first-principles calculation (right). [10,18]

Future Plans

Our future work focuses on insulating and semiconducting AFM materials with high Néel temperatures and long mean free paths for spintronics applications. Top candidates include NiO, Cr_2O_3, MnF_2, $FeCl_2$, and $CuCl_2$. Some semiconducting AFM materials will also be considered, such as II-VI, I-VI-III-VI chalcogenides. The spin-lattice couplings in these materials are expected to be large because of their high magnetoelastic coefficients, confirmed by our preliminary inelastic neutron scattering and Raman work. The main tools of the work are neutron diffractometers and spectrometers at SNS and HFIR. The combination of different types of sample environment including

temperature, pressure, and magnetic field with neutron scattering presents a unique opportunity to overcome some long-standing challenges in characterizing antiferromagnetic quantum materials.

To identify materials with strong spin-phonon interactions and quantify such interactions, we will study magnetoelastic effects and magnetic anisotropy and focus on the Néel vector orientation under pressure by neutron diffraction and first-principles calculation. It should be noted that even though the static magnetoelastic effects are different from the phonon-induced spin-lattice interactions, it quantifies the interactions between the lattice and magnetic anisotropy. We expect that the pressure effects on the magnetic an isotropy are significant in antiferromagnetic materials with large magnetoelastic coefficients and hypothesize that such a large anisotropy leads to strong spin-lattice coupling. As an example, Cr_2O_3 is particularly interesting due to the strong spin-lattice interactions shown by its magnetostriction of 28 ppm. [13,14] The easy-axis magnetic anisotropic energy of pure Cr_2O_3 is small [15] and indicates that the magnetic anisotropy in this material is sensitive to pressure and so is the Néel vector.

Several mechanisms could be responsible for the decoherence and dissipation of spin excitation. By mapping the phonon and magnon dispersions, the magnon lifetime and mean free path will be obtained to infer the strength of interactions with other magnons, phonons, impurities, and boundaries. Neutron measurements will be performed to identify the linewidth and intensity anomalies that arise from interactions between magnons and phonons to quantify spin-phonon interactions. We will carry out INS scattering experiments with an emphasis on low energy regions to exploit the high energy resolution and obtain the magnon dispersion and, for heavily damped modes, also linewidth. The spin wave gap from the magnon dispersion is a direct measurement of magnetic anisotropy. Closing the anisotropic gap is predicted to create exceptional points in the magnon dispersion. [16] Near the exceptional points, the spectrum becomes gapless, extremely sensitive to small perturbations, and discontinuous in group velocity. The effective magnetic anisotropy can be tuned by pressure and magnetic field. We will use first-principles models to evaluate the magnon-magnon and magnon-phonon interaction strengths and their contributions to the dissipation process; an example of such calculation is shown in **Fig. 4**. INS under temperatures, fields, and pressures will be used to provide information on the energy, linewidth, and scattering intensity of magnon and phonon excitations.

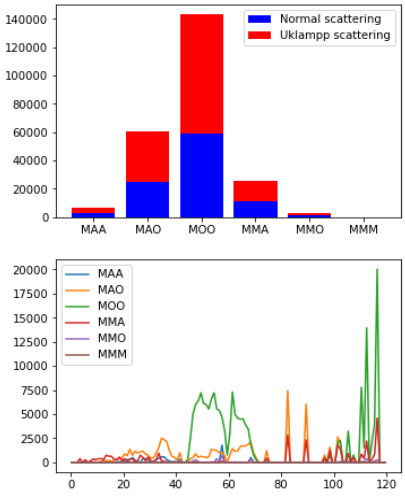

Figure 4 Magnon-phonon interaction scattering space calculation for NiO. Integrated (upper) Energy-dependent in units of meV (lower). M: magnon; A: acoustic phonon; O: optical phonon. (Preliminary calculation)

Materials simulations and scattering modeling will be compared with diffraction and INS results to investigate the selection rules of spin-phonon and magnon-phonon interactions and their strength. It is expected that the symmetry of the structures, anisotropy, and excitations dictate the selection rules of these interactions and their strength. We will first focus on the hybridization conditions for magnon and phonon dispersion by analyzing the symmetry representations of the modes involved. Symmetry analysis for materials of interest will be performed using group theory (an example of NiO is shown in **Fig. 5**). The magnon and phonon representations will be evaluated through their compatibility for allowed and forbidden hybridizations and compared with the INS results. It should be noted that the lattice and magnetic structures often belong to different space groups. Such a comparison needs to consider the proper conversion between the two. The selection rules for general spin-phonon interactions are related but different. We expect that the symmetry of magnetic anisotropy determines the phonon modes that are strongly coupled in such interactions. To

verify this, we will separate the spin contribution to the phonon anharmonicity from phonon-phonon contributions.

In summary, combining scattering and computational tools to quantify magnetic anisotropy, exchange interactions, phonon and magnon dispersion, linewidth, and scattering intensity under external stimuli, we will provide information on the mechanism of interactions between spin and lattice degrees of freedom, in particular their selection rules and coupling strength. The knowledge will help to understand how spin excitation dissipates to the lattice and how to control this dissipation in magnetic materials.

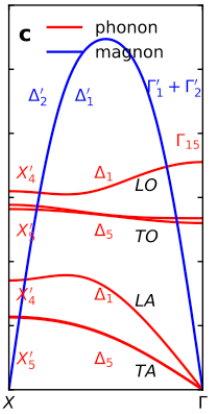

Figure 5 Symmetry analysis of magnon and phonon modes in NiO labelled in representations in Betha notations. [18]

References

[1] A. H. MacDonald and M. Tsoi, *Antiferromagnetic Metal Spintronics*, Philosophical Transactions Royal Soc Math Phys Eng Sci **369**, 3098 (2011).
[2] T. Jungwirth, X. Marti, P. Wadley, and J. Wunderlich, *Antiferromagnetic Spintronics*, Nature Nanotechnology **11**, 231 (2016).
[3] V. Baltz, A. Manchon, M. Tsoi, T. Moriyama, T. Ono, and Y. Tserkovnyak, *Antiferromagnetic Spintronics*, Rev Mod Phys **90**, 015005 (2018).
[4] L. Šmejkal, Y. Mokrousov, B. Yan, and A. H. MacDonald, *Topological Antiferromagnetic Spintronics*, Nat Phys **14**, 242 (2018).
[5] R. White, *Quantum Theory of Magnetism: Magnetic Properties of Materials*, 3., comple (Springer, 2007).
[6] H. B. M. ller, J. C. G. Houmann, and A. R. Mackintosh, *Magnetic Interactions in Tb and Tb-10% Ho from Inelastic Neutron Scattering*, Journal of Applied Physics **39**, 807 (1968).
[7] J. Li, H. T. Simensen, D. Reitz, Q. Sun, W. Yuan, C. Li, Y. Tserkovnyak, A. Brataas, and J. Shi, *Observation of Magnon Polarons in a Uniaxial Antiferromagnetic Insulator*, Phys Rev Lett **125**, 217201 (2020).
[8] A. P. Cracknell, *A Group Theoretical Study of Selection Rules for Magnon-Phonon Interactions in Ferromagnetic HCP Metals*, Journal of Physics F: Metal Physics **4**, 466 (1974).
[9] S. H. Liu, *New Magnetoelastic Interaction*, Physical Review Letters **29**, 793 (1972).
[10] Q. Sun, B. Wei, Y. Su, H. Smith, J. Y. Y. Lin, D. L. Abernathy, and C. Li, *Mutual Spin-Phonon Driving Effects and Phonon Eigenvector Renormalization in Nickel (II) Oxide*, Proc National Acad Sci **119**, (2022).
[11] A. W. Sáenz, *Magnetic Scattering of Neutrons by Exchange-Coupled Lattices*, Phys Rev **119**, 1542 (1960).
[12] S. Raymond, N. Biniskos, K. Schmalzl, J. Persson, and T. Brückel, *Total Interference between Nuclear and Magnetovibrational One-Phonon Scattering Cross Sections*, Arxiv (2018).
[13] K. L. Dudko, V. V. Eremenko, and L. M. Semenenko, *Magnetostriction of Antiferromagnetic Cr2O3 in Strong Magnetic Fields*, physica status solidi (b) **43**, 471 (1971).
[14] M. R. J. Gibbs, *Modern Trends in Magnetostriction Study and Application* (Springer Science & Business Media, 2012).
[15] S. Foner, *High-Field Antiferromagnetic Resonance in Cr 2 O 3*, Phys Rev **130**, 183 (1963).
[16] W. D. Heiss, *The Physics of Exceptional Points*, J Phys Math Theor **45**, 444016 (2012).
[17] Q. Cai, Y. Zhang, D. Luong, C. A. Tulk, B. P. T. Fokwa, and C. Li, *Spin–Phonon Interactions and Anharmonic Lattice Dynamics in Fe3GeTe2*, Adv. Phys. Res. **2**, (2023).
[18] Q. Sun et al., *Spin-Phonon Interactions Induced Anomalous Thermal Conductivity in Nickel (II) Oxide*, Mater Today Phys 101094 (2023).

Publications

As a recently funded project, there is no publication (June 1, 2023 – present).

The following manuscripts under review or in preparation are supported by the program:

Qiyang Sun, Bin Wei, Yaokun Su, Douglas L. Abernathy and Chen Li, Magnetoelectric coupling induced anomalous stiffening of longitudinal optical phonon modes in Cr_2O_3, (Under review)

Yaokun Su and Chen Li, Uncovering Obscured Phonon Dynamics from Two-dimensional Inelastic Neutron Scattering Measurements using Machine Learning, (Under review)

Qiyang Sun, Douglas L. Abernathy and Chen Li, Temperature-dependent magnon dynamics in magnetoelectric Cr_2O_3, (In preparation)

Yaokun Su, António M. dos Santos, and Chen Li, Pressure dependence of magnetocrystalline anisotropy and exchange

interactions in Cr_2O_3, (In preparation)

Machine learning on neutron scattering (DE-SC0021940)

Mingda Li, MIT

Keywords: Machine learning, topological materials, neutron scattering

Research Scope

The primary aim of this project is to design and validate novel physics-informed machine-learning architectures that can lead to direct connection of the structure-property relations for neutron scattering. To achieve this, we integrate the machine learning with into various scattering spectroscopies. This objective is driven by the recognition of high dimensional neutron scattering data, and the frequent challenge to acquire reliable microscopic information in materials. Over the past two years, this project has provided answers to several different scattering techniques:

1. **Time-resolved diffraction:** The framework that aims to extract the mode-resolved thermal transport from time-resolved diffraction patterns (Publication No. 1, open-source codes available)[1].

2. **Polarized neutron reflectometry:** The framework that aims to fit neutron reflectometry data (Publication No. 2, open-source codes available)[2].

3. **X-ray absorption:** The possible connections between local structure, and class of band topology (Publication No. 3, open-source codes available)[3].

4. **Magnetic scattering:** A general-purpose magnetism classifier that inputs crystal structure and outputs the type of magnetism (Publication No. 4, open-source codes available)[4].

5. **Inelastic scattering:** A general-purpose predictor that inputs crystal structure and outputs full phonon dispersion relation (Publication No. 5, open-source codes available)[5].

Additionally, we have developed a method to improve the detection of the detector signal for X-ray and neutrons (Publication No. 6). Our contributions also include the review on machine learning on magnetism and scattering (Publications No. 7, No. 9), classifier for Majorana zero mode for topological quantum computing (Publication No. 8), and involvement in supporting the effort on neutron vibrational spectra prediction (Publication No. 10).

Recent Progress

Recent Progress A: Machine learning predicting phonon dispersion relation from atomic coordinates. Recently, we have proposed a graph neural network termed virtual nodes graph neural network. Unlike common graph neural network where the nodes represent the atoms, here the virtual nodes represent the collective excitations. By using the virtual node approach, it is possible to construct the entire 3N phonon bands in the correct Brillouin zone (**Figure 1**, left). This enables a direction, end-to-end prediction of phonon bandstructures (**Figure 1**, right). The proposed approach is expected to be applicable to a variety of problems where the dimension of the output is variable, particularly capable of solving a number of challenging problems that cannot be solved using machine-learning interatomic potential approach.

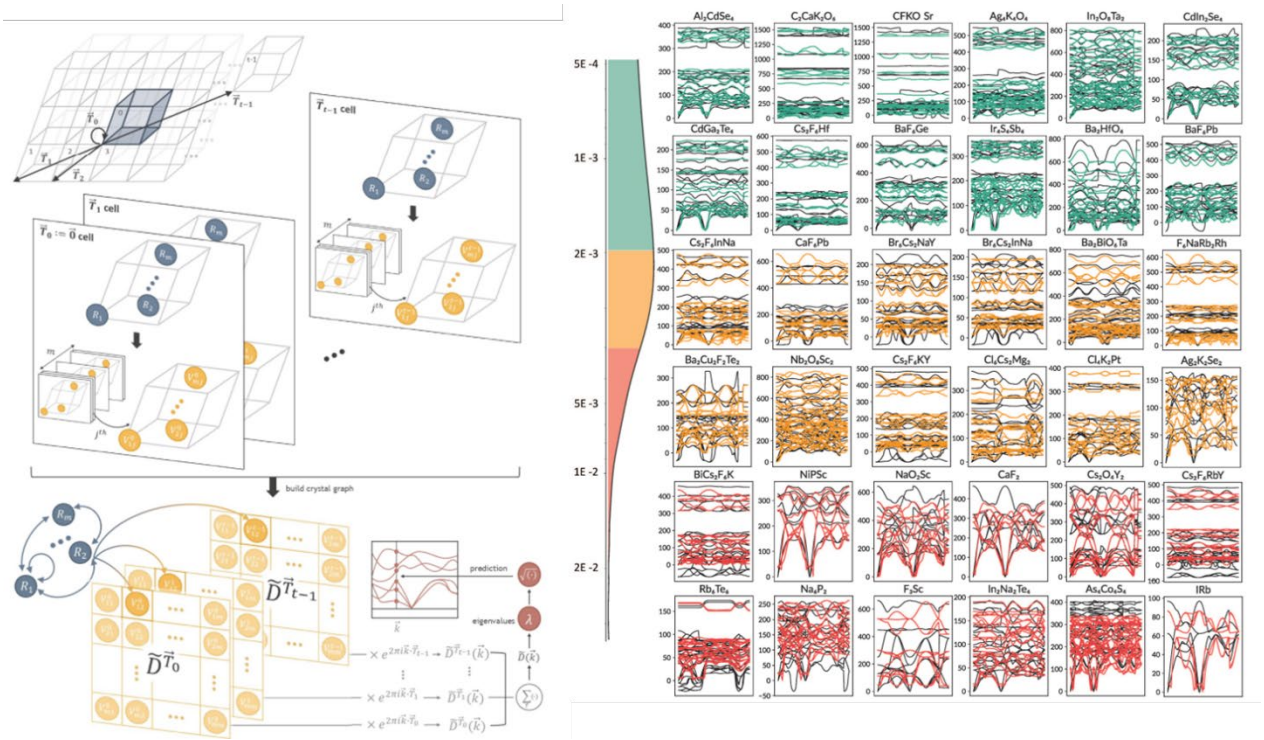

Figure 4. (Left) Momentum-dependent virtual node structure in a graph neural network. For each unit cell and its first-nearest neighboring unit cells, each builds a virtual dynamical matrix. After the phase factor summation, a virtual dynamical matrix is built. Unlike the ab initio calculation or machine-learning interatomic potential approach which obtains the interatomic forces, here, the value of the virtual dynamical matrix is inferred as a graph neural network problem through message passing and graph convolution. (Right) typical results of the phonon bandstructures in crystalline solids.

Recent Progress B: Machine-learning prediction on Majorana zero modes. In this study, we develop a machine-learning framework to differentiate Majorana zero modes (MZMs) from other signals using zero-bias peak (ZBP) data. MZMs, which are unique quasiparticles with non-Abelian statistics, are crucial for fault-tolerant topological quantum computation. The main indicator of MZMs is ZBPs observed in tunneling differential conductance. However, distinguishing MZMs from ZBPs is challenging due to the interference of topologically trivial states that also produce ZBP signals. Our method uses quantum transport simulations based on tight-binding models to create training data. The effectiveness of machine learning in this classification is further validated by persistent cohomology analysis, which proves fundamentally that the MZM classification is a machine separable problem, regardless of detailed machine learning algorithms (**Figure 2**). Notably, even with added noise in the data, the XGBoost classifier achieves 85% accuracy for 1D conductance data and 94% for 2D data, which includes Zeeman splitting effects. When applied to previous ZBP experiments, our model indicates that certain data are more likely associated with MZMs. This approach provides a quantitative method for evaluating MZMs using ZBP data and highlights the potential of machine learning in analyzing exotic quantum systems, integrating experimental and computational data.

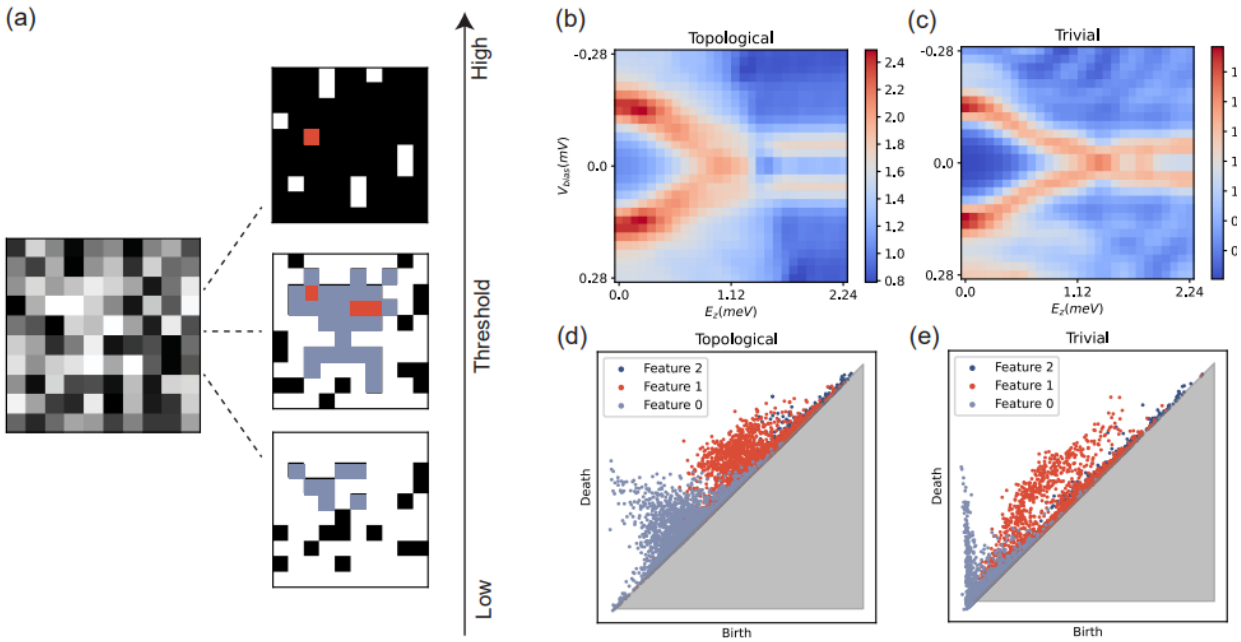

Figure 5. Persistent cohomology analysis with the scanning tunneling conductance data. (a) Schematic of the principles on persistent cohomology, using simplified 2D data as an example. As the masking threshold is tuned from minimum to maximum magnitudes, features that mark isolated clusters (light blue) and surrounded loops (red) emerge and die out. Only features near a centered area are colored for better visualization. (b, c) Typical computationally generated tunneling conductance data used for machine learning training, for topological and trivial classes, respectively. The 2D heatmap plots are tunneling conductance dI/dV as a function of bias voltage Vbias and Zeeman energy; (d, e) Topological data analysis on topological MZM and trivial classes, respectively, using persistent cohomology analysis. Although the individual raw data in (b, c) are barely distinguishable with bare eyes, an obvious difference is shown between the topological MZM class and the other topological trivial classes through topological data analysis.

Future Plans

Future Plan A: Neural network for full magnetic structure prediction. In this work, we unveil a novel neural network platform characterized by its unified representation that exhibits local equivariance to rotation, parity, and time-reversal symmetry. This unique feature of the platform significantly reduces the requirement for extensive data augmentation, which is typically necessary to account for the symmetries inherent in the representations constructed. The platform's design is particularly notable for its inclusion of time-reversal equivariance, a critical aspect that is expected to greatly enhance the development of efficient machine learning models tailored for spin systems.

Each symmetry incorporated into the platform is formulated using the concept of projective representation over the complex field. This means that the representations are not only compatible with, but also specifically designed for quantum systems. These systems are understood as equivalent up to global phases, aligning with the principles of quantum mechanics.

Furthermore, the platform's sophisticated approach to symmetry incorporation allows for the potential to address more complex quantum phenomena, such as the full magnetic structure of materials. By understanding and accurately modeling the intricate interactions and orientations of spins in a material, this platform could provide unprecedented insights into the magnetic properties at a fundamental level. This capability would be incredibly valuable in fields like condensed matter physics and materials science, where understanding magnetic structures is essential for the development of new materials and technologies.

The combination of local equivariance and projective representation over the complex field not only ensures compatibility with quantum principles but also opens up new avenues for exploring and

solving complex problems in quantum physics. The possibility of solving the full magnetic structure with this platform is a testament to its versatility and potential impact on the field of quantum computing and beyond. This advancement represents a significant step forward in the application of machine learning to quantum systems, providing a more nuanced and effective approach to understanding and manipulating the quantum world.

References

1. Chen ZT, Shen XZ, Andrejevic N, Liu TT, Luo D, Nguyen T, Drucker NC, Kozina ME, Song QC, Hua CY, Chen G, Wang XJ, Kong J, Li MD. Panoramic Mapping of Phonon Transport from Ultrafast Electron Diffraction and Scientific Machine Learning. *Advanced Materials* 2023, **35:** 2206997.
2. Andrejevic N, Chen Z, Nguyen T, Fan L, Heiberger H, Zhou L-J, Zhao Y-F, Chang C-Z, Grutter A, Li M. Elucidating proximity magnetism through polarized neutron reflectometry and machine learning. *Applied Physics Reviews* 2022, **9**(1).
3. Andrejevic N, Andrejevic J, Bernevig BA, Regnault N, Han F, Fabbris G, Nguyen T, Drucker NC, Rycroft CH, Li M. Machine-Learning Spectral Indicators of Topology. *Advanced Materials* 2022, **34**(49)**:** 2204113.
4. Merker HA, Heiberger H, Nguyen L, Liu T, Chen Z, Andrejevic N, Drucker NC, Okabe R, Kim SE, Wang Y, Smidt T, Li M. Machine learning magnetism classifiers from atomic coordinates. *iScience* 2022, **25**(10).
5. Okabe R, Chotrattanapituk A, Boonkird A, Andrejevic N, Fu X, Jaakkola TS, Song Q, Nguyen T, Drucker N, Mu S, Liao B, Cheng Y, Li M. Virtual Node Graph Neural Network for Full Phonon Prediction. *arXiv e-prints* 2023**:** arXiv:2301.02197.

Publications

1. Z Chen, X Shen, N Andrejevic, T Liu, D Luo, T Nguyen, NC Drucker, M Kozina, Q Song, C Hua, G Chen, X Wang, J Kong, and M Li, "Panoramic mapping of phonon transport from ultrafast electron diffraction and machine learning", *Advanced Materials* **35**, 2206997 (2023).
2. N Andrejevic, Z Chen, T Nguyen, L Fan, H Heiberger, V Lauter, LJ Zhou, YF Zhao, CZ Chang, A Grutter, and M Li, "Elucidating proximity magnetism through polarized neutron reflectometry and machine learning", *App. Phys. Rev.* **9**, 011421 (2022).
3. N Andjejevic, J Andrejevic, BA Bernevig, N Regnault, F Han, G Fabbris, T Nguyen, NC Drucker, CH Rycroft and M Li, "Machine learning spectral indicators of topology", *Advanced Materials* **34**, 2204113 (2022).
4. HA Merker, H Heiberger, LK Nguyen, T Liu, Z Chen, N. Andrejevic, NC Drucker, R. Okabe, Y. Wang, T. Smidt and M Li, "Machine Learning Magnetism Classifiers from Atomic Coordinates". iScience: Cell Press **25**, 105192 (2022).
5. R Okabe, A Chotrattanapituk, A Boonkird, N Andrejevic, X Fu, TS Jaakkola, Q Song, T Nguyen, NC Drucker, S Mu, B Liao, Y Cheng, and M Li, "Virtual Node Graph Neural Network for Full Phonon Prediction," arXiv:2301.02197 (2023).
6. R Okabe, S Xue, J Yu, T Liu, B Forget, S Jegelka, G Kohse, L-W Hu and M Li, "Tetris-inspired detector with neural network for radiation mapping," arXiv:2302.07099 (2023).
7. R Okabe, M Li, Y Iwasaki, N Regnault, C Felser, M Shirai, A Kovacs, T Schrefl, and A Hirohata*, "Materials Informatics for the Development and Discovery of Future Magnetic Materials", IEEE Magentic Letters, DOI:10.1109/LMAG.2023.3320888 (2023).
8. M Cheng*, R Okabe, A Chotrattanapituk and M Li, "Machine Learning Detection of Majorana Zero Modes from Zero Bias Peak Measurements," arXiv:2310.18439 (2023).
9. NC Drucker, T Liu, Z Chen, R Okabe, A Chotrattanapituk, T Nguyen, Y Wang and M Li, "Challenges and Opportunities of Machine Learning on Neutron and X-ray Scattering". *Synchrotron Radiation News* **35**, 16 (2022).

10. YQ Cheng, G Wu, MB Stone, A Savici, M Li and A Ramirez-Cuesta, “Direct prediction of inelastic neutron scattering spectra from crystal structure”, Machine Learning: Science & Technology 4, 015010 (2023).

Neutron Scattering on Topological Quantum Materials (DE-SC0020148)

Mingda Li, MIT

Keywords: Topological materials, neutron scattering, flat band, X-ray scattering, quantum geometry.

Research Scope

The primary aim of this project is to deepen our understanding of the intricate microscopic interactions within topological quantum materials. To achieve this, we employ a combination of neutron scattering, various experimental techniques, and computational methods, with an eye towards advancing microelectronic and quantum information technologies. This objective is driven by the recognition that, despite their promising electronic and functional characteristics – a fact underscored by the 2016 Nobel Prize in Physics – the intrinsic 'topology' of these materials remains immeasurable. Consequently, researchers have had to rely on different indirect indicators to discern this topology. Over the past two years, this project has provided answers to several critical questions:

1. The potential influence of band topology on magnetism, especially magnetic fluctuations (Publication No. 1).

2. The possible connections between crystal structure, specifically local structure, and band topology (Publication No. 2).

3. The indications of band topology in the neutron dynamical structure factor (Publication No. 3).

4. The impact of topology on magnetism in heterostructures (Publication No. 4).

5. The relationship between scattering phenomena and quantum entanglement (Publication No. 5).

Additionally, we have developed a method to precisely control the disorder in topological materials for enhanced scattering studies (Publication No. 6). Our contributions include the discovery of three-dimensional flat band systems (Publication No. 7), a comprehensive review of advancements in topological superconductors and kagome superconductors (Publications No. 8 and No. 9), and involvement in thermal transport studies within topological materials (Publication No. 10). More recently, we have observed a novel form of symmetry breaking in a kagome flat band systems (Recent Progress B).

Recent Progress

Recent Progress A: The interplay of topology and magnetic excitations. Recently, we have demonstrated the role that the topological singularity of Weyl points can do to stabilize the magnetic fluctuation, in magnetic Weyl semimetal CeAlGe (**Figure 1**, top row). This results in a meta-stable magnetic phase with finite correlation well above the magnetic transition temperature (Publication 1) [1]. More recently, through inelastic neutron scattering at a finite magnetic field, we aim to further elucidate the microscopic magnetic correlations mechanism in the region with enhanced spin-spin correlation, beyond the previous macroscopic thermodynamic measurements (**Figure 1**,a-h). This could support the understanding on the interplay between band topology and magnetism.

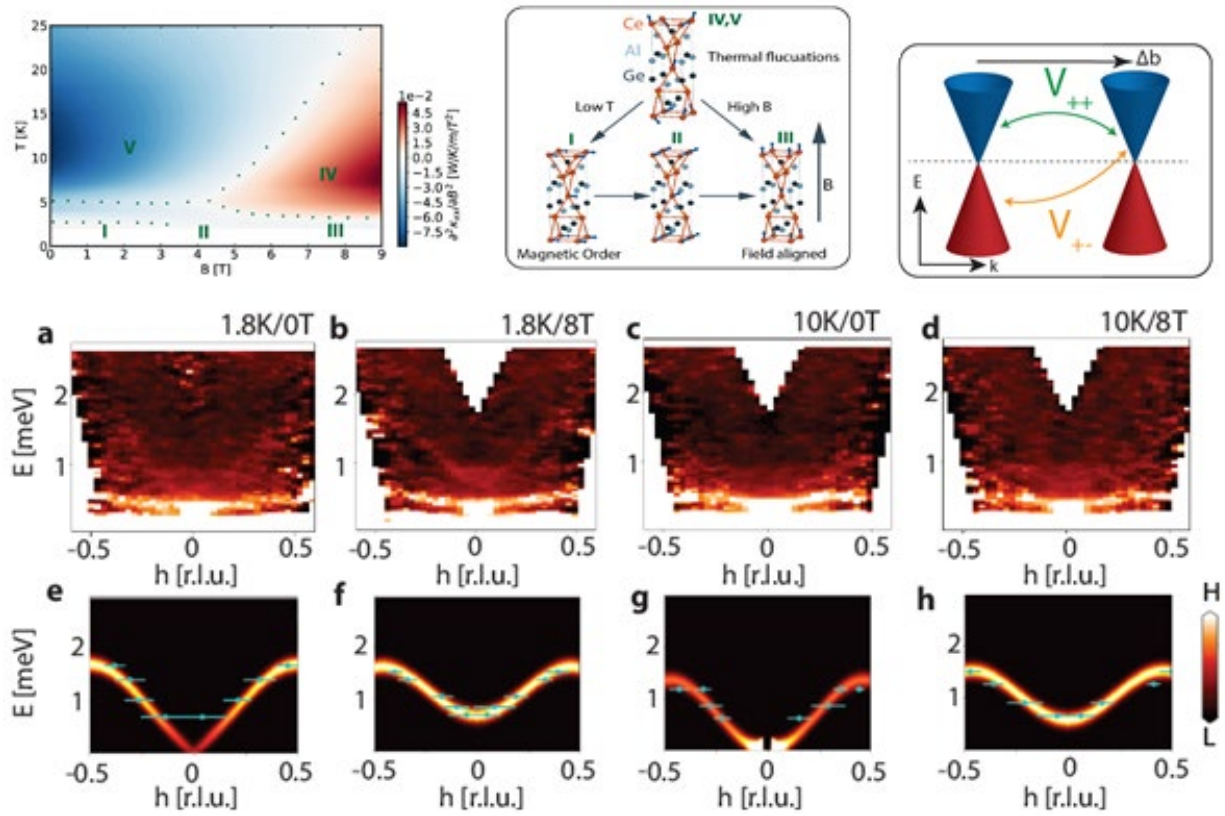

Figure 6. (Top row) Published results in the Weyl stabilized magnetism. (Left) The second derivative of the thermal transport as a function of magnetic field and temperature, which is an indicator of the phase diagram shown in the Middle. The dark-blue region ~12.8 Kelvin shows a number of anomalies from transport and scattering, which is explained as the coupling between the Weyl nodes with the magnetization (Right). (a-h) More recent results in the spin-wave excitations of CeAlGe above and below the magnetic transition temperature ~4K, at zero and finite magnetic field. The fitting of the spin-wave excitations indicates an anomalous enhancement of the spin correlator above the magnetic transition.

Recent Progress B: The nematicity from incipient flat band in a kagome metal. The Kagome lattice, a unique geometric arrangement, has become a focal point in the study of various complex and fascinating phenomena in physics. This structure is crucial for understanding a range of topological and electron-related phases, including unusual Hall states, density wave formations, and superconductivity. While much of the interest has centered around two key aspects of the lattice's electronic band structure—the Dirac crossing and the van Hove singularity—the most striking feature, the flat band, has largely remained a mystery. In this research, we provide new insights into the effects of these flat electron bands, which are located away from the Fermi level, in the Kagome metal (**Figure 2**, top left). Heat capacity (**Figure 2**), transport, neutron and X-ray scattering measurements demonstrate clear signs of nematicity around a small temperature region without symmetry breaking of long-range magnetic ordering, a property that indicates a breakdown in rotational symmetry within the Kagome plane. These results pave the way for a deeper understanding of the complex behaviors in Kagome lattices and related materials.

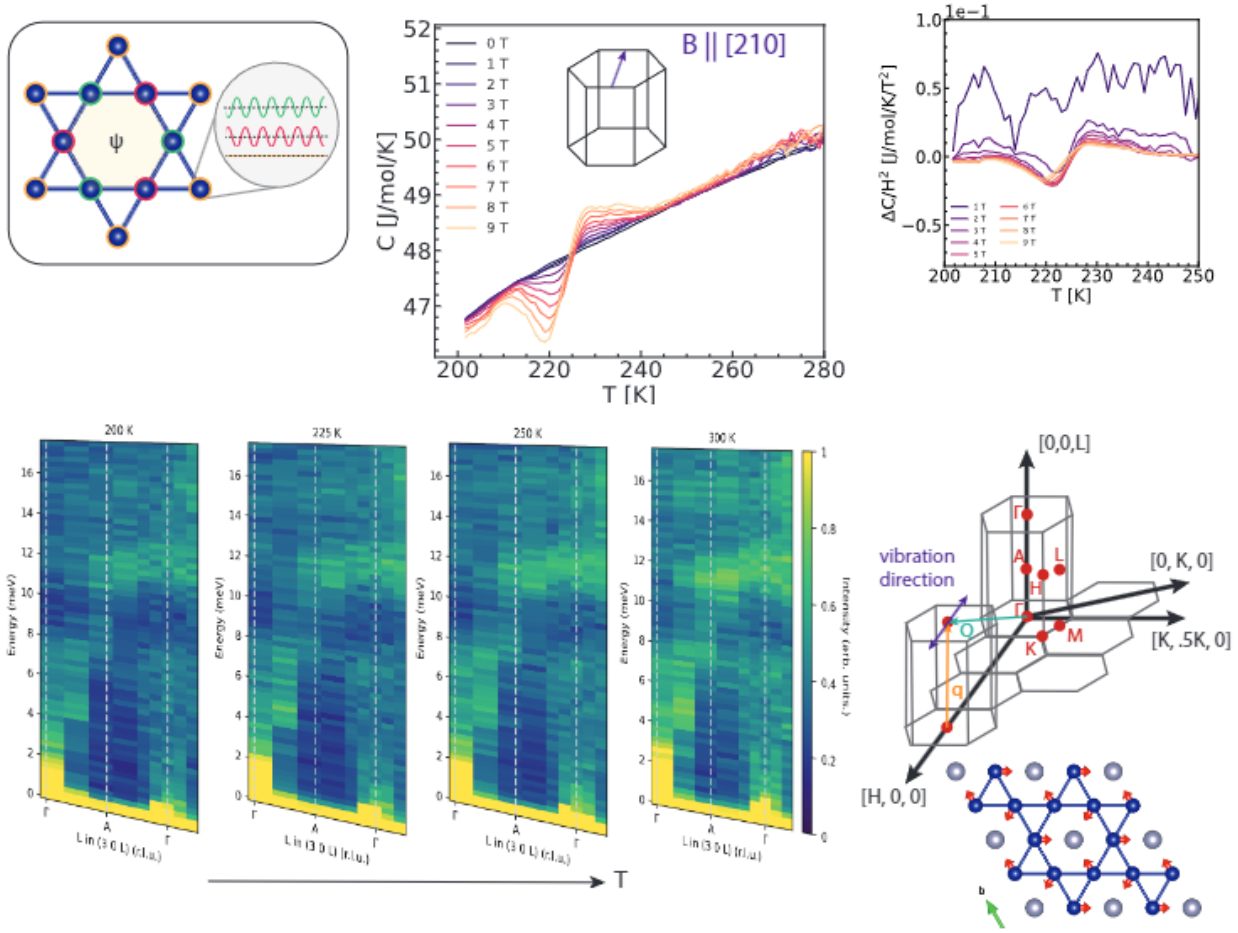

Figure 7. (Top-left) The kagome metal and the formation of the flatband as a destructive interference effect. (Top-middle) The heat capacity measurement as a function of magnetic field, showing an anomalous modulation around T~220K. (Top-right) The heat capacity shows a clear scaling ~H^2, which sparkled further neutron and X-ray measurements. (Bottom-left) The phonon softening near ~220K from inelastic neutron scattering, which agrees with *ab initio* calculations with the presence of the nematicity at finite temperature. (Bottom right) The schematic of the symmetry breaking in the kagome plane.

Future Plans

Future Plan A: In our forthcoming research agenda, we are committed to significantly enhancing the scope and precision of measurements obtainable through neutron scattering. Traditionally, neutron scattering has been instrumental in assessing the symmetric component of the susceptibility tensor, a method renowned for its efficacy yet not without its constraints. Our primary objective is to advance the theoretical framework of scattering experiments, particularly by innovating the conditions under which the probe operates. Specifically, we propose a novel experimental setup where both the incoming and outgoing neutron beams are subject to distinct potential fields. This innovative approach, predicated on manipulating the probe's potential, is designed to unlock new measurement possibilities.

Preliminary findings suggest that this modification – the introduction of differential potential fields to the neutron probe – could be pivotal in allowing access to the heretofore elusive off-diagonal elements of the susceptibility tensor. This breakthrough has profound implications, particularly in the realm of quantum materials research. For instance, it can significantly augment our ability to investigate and understand complex phenomena such as topological superconductivity.

Moreover, this extension of scattering theory and experimental methodology is not just a mere enhancement of existing techniques; it represents a paradigm shift in how neutron scattering can be

employed to probe the intricate properties of materials. By enabling the measurement of both symmetric and off-diagonal components of the susceptibility tensor, we anticipate a more comprehensive understanding of the electronic and magnetic properties of materials.

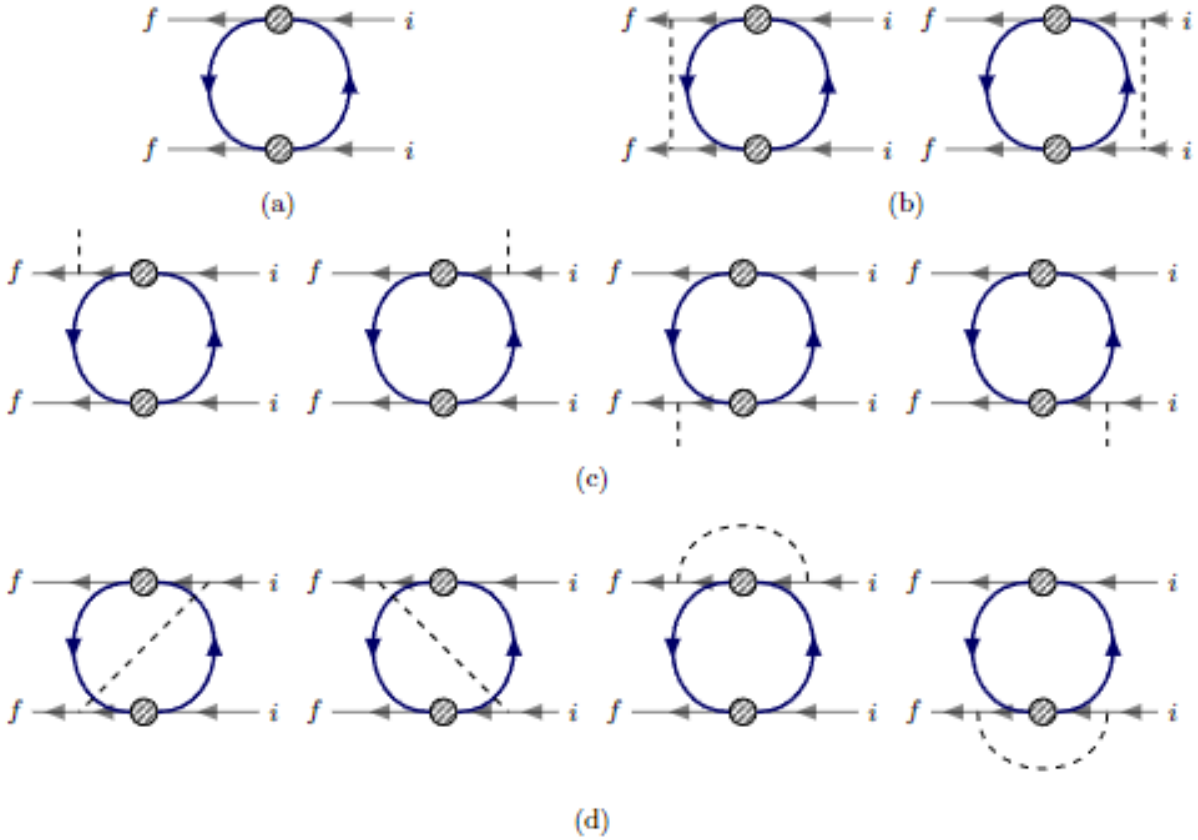

Figure 8. The Feynman diagrams represent the scattering rate with (a) zeroth-ordered probe potential (b) classical second-order probe potential (c) first-ordered probe potential (d) quantum second-order probe potential. The grey line represents probe, while the dark blue line represents system excitation.

References

Publications

1. Drucker NC*, T Nguyen, F Han, P Siriviboon, X Luo, N Andrejevic, Z Zhu, G Bednik, QT Nguyen, Z Chen, LK Nguyen, T Liu, TJ Williams, MB Stone, AI Kolesnikov, S Chi, J Fernandez-Baca, C Nelson, A Alatas, T Hogan, AA Puretzky, S Huang, Y Yue and M Li, "Topology stabilized fluctuations in a magnetic nodal semimetal", *Nature Communications* **14**, 5182 (2023).
2. N Andjejevic, J Andrejevic, BA Bernevig, N Regnault, F Han, G Fabbris, T Nguyen, NC Drucker, CH Rycroft and M Li, "Machine learning spectral indicators of topology", *Advanced Materials* **34**, 2204113 (2022).
3. T Nguyen, Y Tsurimaki, R Pablo-Pedro, G Bednik, T Liu, A Apte, N Andrejevic, and M Li, "Topological Signatures in Nodal Semimetals through Neutron Scattering", *New J. Phys.* **24**, 013016 (2022).
4. N Andrejevic, Z Chen, T Nguyen, L Fan, H Heiberger, V Lauter, LJ Zhou, YF Zhao, CZ Chang, A Grutter, and M Li, "Elucidating proximity magnetism through polarized neutron reflectometry and machine learning", *App. Phys. Rev.* **9**, 011421 (2022).
5. J Hales, U Bajpai, T Liu, DR Baykusheva, M Li, M Mitrano and Y Wang, "Witnessing Light-Driven Entanglement using Time-Resolved Resonant Inelastic X-Ray Scattering", *Nature Communications* **14**, 3512 (2023).

6. M Mandal, A Chotrattanapituk, K Woller, H Xu, N Mao, R Okabe, A Boonkird, T Nguyen, NC Drucker, T Momiki, J Li, J Kong, and M Li, “Precise Fermi-level engineering in a topological Weyl semimetal via fast ion implantation,” arXiv:2310.07828 (2023). (Under revision)
7. JP Wakefield, M Kang, PM Neves, D Oh, S Fang, R McTigue, SYF Zhao, TN Lamichhane, A Chen, S Lee, S Park, JH Park, C Jozwiak, A Bostwick, E Rotenberg, A Rajapitamahuni, E Vescovo, JL McChesney, D Graf, JC Palmstrom, T Suzuki, M Li, R Comin, and JG Checkelsky, "Three Dimensional Flat Bands in Pyrochlore Metal CaNi2", *Nature* **623**, 301 (2023).
8. M Mandal, NC Drucker, P Siriviboon, T Nguyen, A Boonkird, TN Lamichhane, R Okabe, A Chotrattanapituk and M Li, “Topological superconductors from a materials perspective*”, Chem. Mater.* **35**, 6184 (2023).
9. T Nguyen and M L, "Electronic properties of correlated kagomé metals AV3Sb5 (A = K, Rb, Cs): A perspective", *J. Appl. Phys.* **131**, 060901 (2022).
10. MS Akhanda, S Krylyuk, DA Dickie, AV Davydov, F Han, M Li and M Zebarjadi, “Phase-transition-induced Thermal Hysteresis in Type-II Weyl Semimetals MoTe2 and Mo1-xWxTe2”, DOI:10.1016/j.mtphys.2022.100918, Materials Today Physics (2022).

Chain Exchange in Block Copolymer Nanoparticles

Timothy P. Lodge and Frank S. Bates, University of Minnesota

Keywords: Block copolymer, chain exchange, SANS, dynamics, self-assembly

Research Scope

Block copolymer (BCP) self-assembly is a versatile route to nanostructured materials, both in solution and in the bulk state. BCPs are macromolecules that comprise at least two distinct polymeric blocks that are covalently connected. This linkage suppresses the natural tendency of the two polymers to separate on a macroscopic scale leading to spontaneous formation of a nanostructured material; of particular interest are particle phases, which includes micelles in solution and various symmetries in the bulk (*e.g.*, body-centered cubic, face-centered cubic, and Frank-Kasper (FK) phases). Both the structural length scale and the packing symmetry can be tuned via BCP molecular weight and composition. Much is known about the equilibrium structure of BCPs, but in many cases equilibrium is not attained on a reasonable timescale. Conversely, very little is known about the mechanisms by which a BCP can attain equilibrium, and how the molecules manage to overcome barriers to motion; these barriers largely arise from difficulties of one block traversing a nanodomain rich in the other [1]. As BCP nanoparticles are of great interest across a broad swath of applications (including drug delivery, theranostics, biomedical imaging, food and agricultural formulations, and viscosity modifiers for engine oil) understanding the associated equilibration dynamics will inform the design and implementation of practical processing strategies. The most fundamental mechanism is chain exchange, whereby individual molecules escape from one nanoparticle and relocate to another. Chain exchange is necessary for equilibration, but may not be sufficient. Quantitative measurements of chain exchange, using the powerful tool of time-resolved small-angle neutron scattering (TR-SANS) illustrated in Figure 1 [3], form the core of this proposal. The system of polystyrene-*b*-poly(ethylene-*alt*-propylene) (PS-PEP) in the PEP-selective solvent squalane, has been thoroughly demonstrated to be nearly ideal for these studies [1,2,3]. TR-SANS, to be conducted at NIST or ORNL (HFIR), requires controlled synthesis of selectively isotope labeled (*i.e.*, deuterium substituted) BCPs. Supporting SAXS measurements (for particle size, shape, and packing symmetry), rheology (for kinetics of structural evolution), and transmission electron microscopy (direct

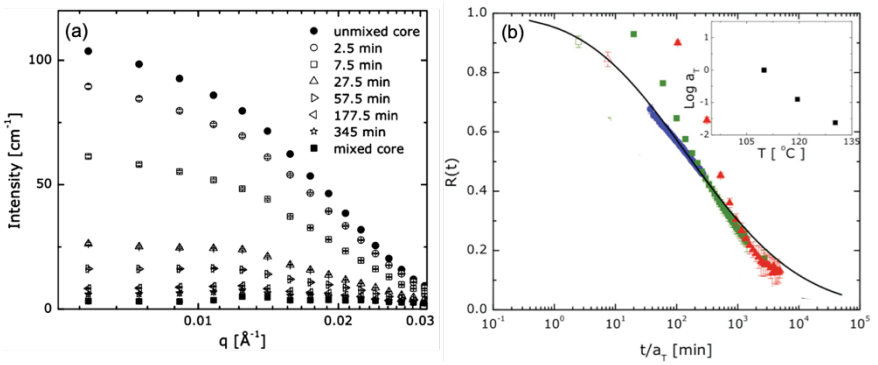

Fig 1. (a) TR-SANS measurements of 15 vol% PS-PEP in squalane at 120 °C. (b) Relaxation profile for the same sample at a reference temperature of 110 °C. Measurements were conducted at three different temperatures and shifted by a shift factor (a_T) to yield a master curve.

imaging of nanostructure) will also be important.

One thrust will employ TR-SANS measurements in concentrated solutions and melts aimed at unraveling the complex set of factors that determine the kinetics of formation of sphere packings, especially the newly-discovered FK phases. For example, in FK phases there are typically multiple particle sizes (*e.g.*, 5 in the sigma phase), whereas the default BCC packing has just one. Consequently, chain exchange is necessary to obtain an FK phase from an initial BCC state; TR-SANS can monitor this process, while supporting SAXS measurements will provides access to the time evolution of lattice symmetry. The first priority will be to establish protocols for preparing initially randomized mixtures of protonated and deuterated micelles over the complete concentration range (Figure 2). In previous work, we were able to do this up to c = 15% diblock polymer by intensive mixing of separate BCC solutions [2]. It is not clear whether this can be done up to the undiluted melt. However, a selective, volatile co-solvent should allow for concentration of pre-formed and pre-mixed micelles. Previously, we made the first TR-SANS measurements in these modestly concentrated solutions (c =15 vol%). Unexpectedly, the rate of chain exchange was at least an order of magnitude lower than in dilute solutions. As highly concentrated and bulk polymers are of particular interest for many applications, further research in this area is desirable; we will target 15% ≤ c ≤ 100%. Using deuterated and protonated monomers, we will synthesize several pairs of PS-PEP diblock polymers with varying core block fractions to ensure that spherical micelles are formed across the entire range. We will characterize morphologies and domain sizes of these block copolymers in squalane using SAXS. Then we will target particular compositions and molecular weights where FK phases are found in solution; this may involve blending copolymers or even adding PS homopolymer dopants. In our experience FK phases typically form slowly after initial BCC ordering, so these kinetics will first be mapped out by rheology and SAXS.

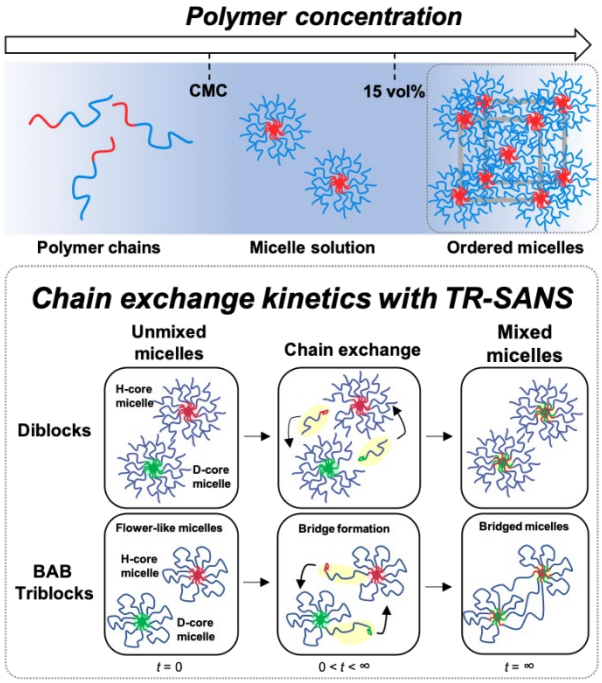

Fig. 2. Overview scheme of polymer concentration-dependent chain exchange kinetics with TR-SANS.

A second thrust will address unanswered questions in solution dynamics, utilizing various chain and micellar architectures. Priorities include connecting chain escape to stress relaxation process in triblock networks. We will explore the dynamics of gels formed from concentrated PS-PEP-PS triblock polymers. As these BCPs have two PS endblocks, the PEP blocks can form either loops, or bridges where the PS blocks reside in different neighboring micelles (Figure 2). We have previously used rheology to measure the stress relaxation time, presumably related to the end block pull-out time of a bridged chain ($\tau_{pullout}$). Surprisingly, we found that $\tau_{pullout}$ was significantly *shorter* than the chain exchange time measured via TR-SANS for equivalent diblock polymers [4]. We are developing the method based on a volatile corona-selective co-solvent, to prepare dilute solutions of flower-like micelles, where a lack of larger bridged aggregates has been confirmed using dynamic light scattering (DLS). The samples are then concentrated by co-solvent removal at low T. Annealing

at elevated *T* leads to bridge formation, via endblock exchange, which results in measurable changes in the rheological properties.

Recent Progress

The current project got underway in the late spring of 2023. The previous award had a different focus, namely whether a particularly appealing state of soft matter, the bicontinuous microemulsion (BuE), could be fabricated from ion-containing polymers. The standard recipe for a polymeric BuE involves two homopolymers, A and B, plus a well-designed AB copolymer surfactant. We succeeded in achieving this goal, both for the case of polymers with added salt, and for polymers in which one component is a poly(ion). Surprisingly, the thermodynamic conditions under which the BuE was obtained closely matched the neutral case, despite the introduction of much more strongly-interacting materials. We further demonstrated a facile means to crosslinking one of the domains to prepare robust, nanostructured materials. This work has been documented in the nine recent publications listed below.

The first step in the new project was for the graduate student (Joanna White) and postdoctoral fellow (Taehyung Kim) to master sequential living anionic polymerization of PS and 1,4-polyisoprene, followed by hydrogenation of the PI to afford PEP. This they have both achieved and prepared a series of well-defined PS-PEP and PS-PEP-PS materials. An example is shown in Figure 3, for a PS-PEP-PS triblock and its PS-PI-PS precursor. SEC confirms a narrow molar mass distribution (Panel a), and ^{1}H NMR the composition, and successful hydrogenation (Panel b). SAXS, rheology, and dynamic light scattering have been employed to characterize self-assembly in dilute and concentrated squalane solution.

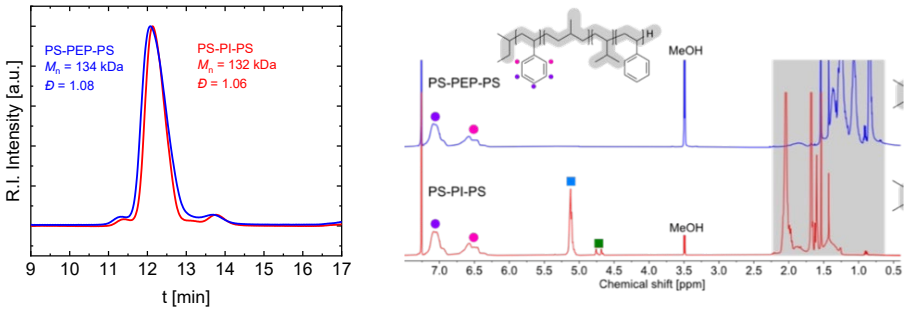

Fig 3. (a) SEC traces of PS-PI-PS and PS-PEP-PS; (b) corresponding NMR spectra.

We have also made initial SAXS and rheological measurements on PS-PEP-PS triblocks, after first making dilute "flower-like micelles" in squalane (Figure 2), then concentrating to 20% with a volatile PEP-selective solvent. The high glass transition of the PS cores prevents any chain rearrangement during this process. Annealing in a rheometer at 120 °C shows a steady increase in dynamic elastic modulus *G*' (Figure 4a), which we attribute to the slow establishment of PEP bridges between PS micelles. This is very promising for the future TR-SANS measurements, as it strongly suggests that concentrated micelle packings can be achieved without premature chain exchange. Note that it is not clear what fraction of PS endblocks have exchanged to form bridges, a question that only TR-SANS can answer. SAXS analysis (Figure 4b) also indicates a slow refinement of the structure with annealing. The prominent intensity minimum, indicative of the spherical micellar cores, remains

largely fixed in wavevector q, as expected, while the low q maximum moves to lower q, indicating a more refined, disordered micelle structure.

Future Plans

The next phase of the research will involve synthesis of matched BCPs with perdeuterated and normal polystyrene blocks, by living anionic polymerization. The initial targets in terms of block molecular weights are provided by the recently synthesized diblock and triblock materials. However, the

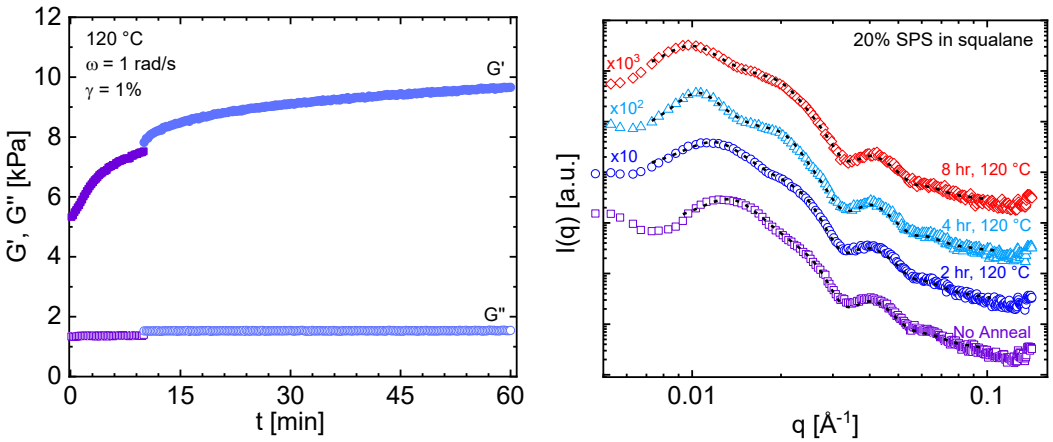

Fig. 4. (a) Dynamic moduli as a function of annealing at 120 °C for a 20% PS-PEP-PS solution; the growth of *G'* suggests creation of bridging PEP blocks;(b) SAXS reveals concurrent refinement of a disordered micelle packing.

isotopically labeled materials are made on a smaller scale (1– 5 g) due to the cost of deuterated monomer, which can affect the precise product obtained. Therefore, if necessary, normal materials will be prepared subsequently to match the deuterated materials. In our experience matching molar mass to within 5% is readily achievable, and perfectly adequate for this research. We have been awarded beamtime at HFIR for spring 2024, where we anticipate accomplishing a significant set of TR-SANS measurements. At present accessibility of beamtime at NIST remains uncertain; we are exploring options for measurements overseas.

References

1. T.P. Lodge, C.L. Seitzinger, S.C. Seeger, S. Yang, S. Gupta, K.D. Dorfman, *Dynamics and Equilibration Mechanisms in Block Copolymer Particles*", ACS Polymer Au, **2**, 397 (2022).
2. S.-H. Choi, F.S. Bates, and T.P. Lodge, *Molecular Exchange in Ordered Diblock Copolymer Micelles*, Macromolecules, **44**, 3594 (2011).
3. J. Lu, F.S. Bates, T.P. Lodge, T. P. *Remarkable Effect of Molecular Architecture on Chain Exchange in Triblock Copolymer Micelles*, Macromolecules, **48**, 2667 (2015).
4. A.J. Peters, T.P. Lodge, *Comparison of Gel Relaxation Times and End-Block Pullout Times in ABA Triblock Copolymer Networks*, Macromolecules **49**, 7340 (2016).

Publications

1. C. Zheng, B. Zhang, F. S. Bates, T. P. Lodge, *Effect of poly[oligo(ethylene glycol) methyl ether methacrylate] side chain length on the swelling behavior in A/B/A-B ternary blends with polystyrene*, Soft Matter, **19**, 4519-4525 (2023). 10.1021/acsapm.2c02220
2. B. Zhang, C. Zheng, F. S. Bates, T. P. Lodge, *Self-Assembly of Charged Diblock Copolymers with Reduced Backbone Polarity,* ACS Applied Polymer Materials, **15**, 10044-10052 (2023). 10.1021/acsapm.2c02220
3. M. B. Sims, J. W. Goetze, G. Diaz Gorbea, Z. M. Gdowski, T. P. Lodge, F. S. Bates, *Photocrosslinkable polymeric bicontinuous microemulsions*, ACS Applied Materials & Interfaces, **15**, 10044 (2023). 10.1021/acsami.2c22927
4. B. Zhang, S. Cui, T. P. Lodge, F. S. Bates, *Structure and Phase Behavior of Bottlebrush Diblock Copolymer-Linear Homopolymer Ternary Blends*, Macromolecules, **56**, 1663-1673 (2023). 10.1021/acs.macromol.2c02434
5. C. Zheng, B. Zhang, F. S. Bates, T. P. Lodge, *Self-assembly of partially charged ternary blends with different charge fractions*, Macromolecules, **55**, 4766-4755 (2022). 10.1021/acs.macromol.2c00518
6. M. B. Sims, B. Zhang, Z. M. Gdowski, T. P. Lodge, F. S. Bates, *Noninvasive photocrosslinking of microphase-separated diblock polymers through coumarin dimerization*, Macromolecules, **55**, 3317-3324 (2022). 10.1021/acs.macromol.2c00356
7. B. Zhang, C. Zheng, M. B. Sims, F. S. Bates, T. P. Lodge, *Influence of Charge Fraction on the Phase Behavior of Symmetric Single-Ion Conducting Diblock Copolymers*, ACS Macro Lett., **10**, 1035-1040 (2021). 10.1021/acsmacrolett.1c00393
8. S. Xie, B. Zhang, F. S. Bates, T. P. Lodge, *Phase Behavior of Salt-Doped A/B/AB Ternary Polymer Blends: The Role of Homopolymer Distribution*, Macromolecules, **54**, 6990-7002 (2021). 10.1021/acs.macromol.1c00928
9. B. Zhang, S. Xie, T. P. Lodge, F. S. Bates, *Phase behavior of diblock copolymer-homopolymer ternary blends with a compositionally asymmetric diblock copolymer*, Macromolecules, **54**, 460-472 (2021). 10.1021/acs.macromol.0c01745

Topological Quantum States Probed by Neutron Scattering
Despina Louca, University of Virginia
Keywords: Dirac magnons, halides, ilmenits

Research Scope

The search for novel topological quantum states and the pursue to understand their origin, the quasiparticles involved, and their interactions, have been a central theme in condensed matter physics[1]. Pioneering theoretical studies have advanced the field of topological quantum science and motivated experimental studies of exotic phenomena in topological materials[2]. The field has rapidly expanded to extend topological concepts to bosonic systems that are charge neutral, with no valence and conduction bands, and with linear band crossing points occurring at finite energies[3]. Emergent quantum effects have been observed in magnetic topological insulators, axion insulators, and quantum Hall systems[4]. In magnon systems, the Dzyaloshinskii-Moriya interaction (DMI) plays a similar role as spin-orbit coupling (SOC) resulting in anisotropic exchange interactions. It is present in systems with no inversion symmetry and yields topological bands. Topological magnetic insulators are stabilized by interactions through opening of a Chern insulating gap in the magnon spectrum. Magnetic systems are a platform from which we can explore interactions of electron correlations, symmetry breaking and Berry curvature with magnetism. Magnetic topological insulators combine non-trivial band topologies and magnetic order. It is postulated that this may lead to the observation of chiral Majorana fermions[1]. Stoichiometric magnetic topological systems are hard to find but a few proposed systems can be tested for quantized magnetoelectric coupling, axion electrodynamics and dissipationless spin currents.

The central theme of the project includes exploring quantum materials that could deploy new quantum technologies, by rendering new routes towards the realization of quantum circuits and networks. Topological materials afford a rich materials platform because of their distinct crystal structures, tunability and responses to electric, magnetic and strain fields. Their emerging quantum effects, i.e. QHE, fractional QHE, quantum spin hall and spintronics, we hypothesize stem from the unique electronic and magnon behaviors, entangled with their specific structural characteristics due to strong electron-lattice, magnon-phonon, and electron-magnon couplings. Neutron scattering (NS) is the most valuable experimental tool in the investigation of topological magnons. It can be used to establish the existence of non-trivial gap structures, identify signatures of magnetic coupling, determine the strength of exchange interactions, and provide insights into entanglement. Although gapped magnon topologies can be predicted theoretically, in practice gap structures, nodal lines and Dirac points can be observed directly from NS.

Recent Progress

In this abstract, we will focus on the chromium halides and ilmenites. CrX_3, a bosonic Dirac material, consists of weakly bound van der Waals honeycomb layers, with a hexagonal arrangement of magnetic Cr^{3+} ions with spin S = 3/2. The ground state is either ferromagnetic (FM), as in $CrBr_3$ and CrI_3 with an out-of-plane spin orientation, or antiferromagnetic (AFM) with an in-plane FM alignment that alternates in the perpendicular direction, as in the insulating $CrCl_3$. Dirac magnons have been predicted at the crossing of acoustic and optical spin waves, analogous to Dirac fermions in graphene. This is shown in Fig. 1 (left). From elastic and inelastic neutron scattering measurements

of the temperature dependence of the magnon and phonon excitations in $CrCl_3$, we observed gapless Dirac magnons at the lowest temperature where the dispersion intensity drops to zero at 4.5 meV. Fortunately, the VISION trajectories pass through the Dirac magnon, affording great resolution of the spectrum at that energy (Fig. 1 (right)). We showed that, distinct from $CrBr_3$ and CrI_3, gapless Dirac magnons are present in bulk $CrCl_3$, with inelastic neutron scattering intensity at low temperatures approaching zero at the K point. Upon warming, magnon-magnon interactions induce strong renormalization and decreased lifetimes, with a ~25% softening of the upper magnon branch intensity from 5 to 50 K, though magnon features persist well above TN. Moreover, an unusual negative thermal expansion (NTE) of the a-axis lattice constant and anomalous phonon behavior were observed below 50 K, indicating magnetoelastic and spin-phonon coupling arising from an increase in the in-plane spin correlations that begins tens of Kelvin above T_N.

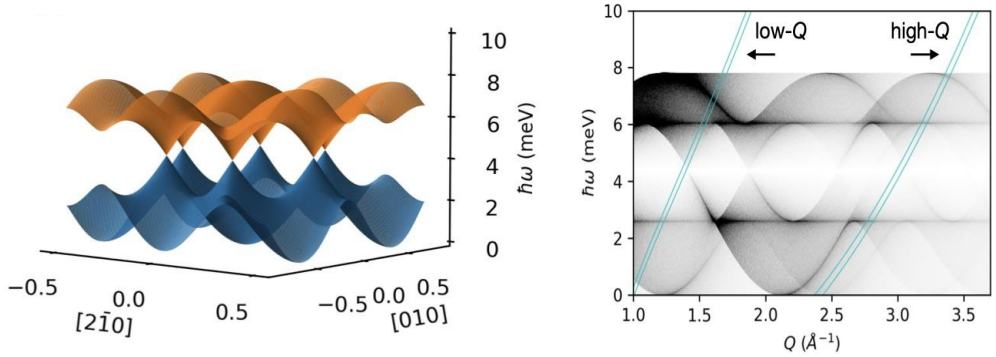

Fig. 1: (left) Spin-wave dispersion in the (HK0) R-plane. The crossing points between optical and acoustic branches are Dirac nodes. (right) Powder average structure function simulation with low and high Q trajectories accessible at Vision at the SNS.

A second system to study is the ilmenite lattice of $CoTiO_3$. This system has garnered attention recently because of the emergence of Dirac magnons at the intersection of optical and acoustic magnon branches and possible Kitaev physics arising from the quasi-2-D magnetic structure of the honeycomb lattice. Ilmenite $CoTiO_3$ has a layered structure with alternating layers of CoO_6 and TiO_6 octahedra. Co^{2+} is in the $3d^7$ electronic configuration with nominally S = 3/2 in an octahedral environment. Below the Néel transition, the magnetic order is ferro in-plane and antiferromag- netic across planes. The layers are stacked similarly to the ABC layer order of rhombohedral graphene, with each layer displaced in-plane by a third of a unit cell. A magnetic anisotropy introduces interesting magnetic properties in the system such as strong easy-plane anisotropy and bond dependent anisotropy as well as *spin-orbit excitons* and *Dirac nodal line magnons*. Recent studies suggested this system is a Dirac magnon in a 3D quantum XY type magnet. Each magnetic ion has a trigonally distorted oxygen environment, and the local electronic states are determined by the trigonal distortions and SOC. Recent inelastic neutron scattering measurements provided evidence for crystal-field excitations as well as a single-ion anisotropy that gives rise to a pseudospin with a S = 1/2 doublet ground state. Based on the crystal structure, the Co ions reside in a trigonally distorted oxygen environment where the local electronic configuration of Co^{2+} is determined by the crystal field (trigonal distortion, Δ, estimated to be around 45 meV) and SOC constant λ. Thus, the magnetic properties are determined by the ground state doublet which in turn depends on Δ and λ. We recently carried out inelastic neutron measurements on VISION and the results are shown in Fig. 2. Shown in Fig. 2(a) are the spin-wave calculations and the two Q-trajectories that are accessible on VISION. Specifically, the

low Q trajectory approaches the Dirac point very closely, but based on these calculations, it is not exactly at the Dirac node. Shown in Fig. 2 (b) is the dynamic susceptibility as a function of temperature, Bose corrected. We can deduce that the magnon contribution ends around 12 meV. The magnon contribution is depicted in 2(c) where the low-Q and high-Q data are compared with the magnon density of states of the XY model. The results show a broad agreement with the data. In the vicinity of the Dirac node, the data appear to indicate that it is gapless even though the spin-wave models show a small gap. However, both the low-Q and high-Q trajectories show no gap in the data at ~8meV. Shown in Fig. 2(d) is a schematic of the crystal-field splitting and spin excitations that give rise to the spin-orbit exciton proposed in this system. These correspond to the intensity in the dynamic susceptibility from 12 to ~35 meV. Further analysis is needed to evaluate the temperature

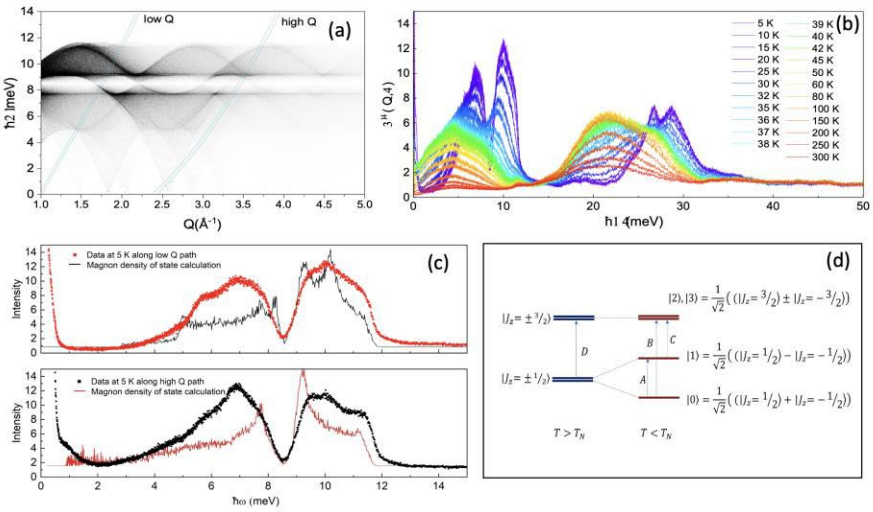

dependence. We will further compare the J-exchange constants and determine the absence of the gap at the Dirac nodes.

Fig. 2. (a) Powder-averaged S(Q,ω) simulated via SpinW, with low- and high-Q trajectories depicted in light blue. These calculations show that the magnon spectrum ends by around 12 meV and the Dirac node is between 8-9 meV. The low-Q trajectory traverses the magnon dispersion close to the Dirac node. (b) The dynamic susceptibility as a function of temperature. Intensity above 12 meV is due to phonons, while below is due to magnons. (c) The Dirac node is clearly observed. The Dirac node appears to be gapless. (d) A schematic of the crystal field diagram indicating the different transitions linked to the spin-orbit exciton.

Future Plans

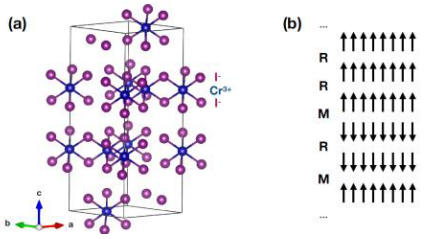

Fig. 3: (a) The crystal structure of CrI_3. (b) Proposed diagram of the M-AFM and R-FM stacking order.

Many van der Waals layered materials have the remarkable property of exhibiting multiple stacking sequences, leading to variations in their material properties and topological characteristics. A promising example to investigate is CrI_3, where antiferromagnetic (AFM) behavior has been reported in flakes of nanometer thickness, in contrast with the ferromagnetism (FM) reported in the bulk, allowing for very large tunneling magnetoresistance. Ideally, CrI_3 is monoclinic (M) at room temperature with space group C2/m and exhibits a layer-sliding transition below 180 K to a rhombohedral (R) structure. The C2/m and R-3 structures can be constructed, layer-by-layer, by repeating M- or R-type stacking operations. In reality though, even single crystals often have inhibited structural transitions, keeping some degree of M-type stacking down to low temperatures; such stacking disorder is presumably more prevalent in powder samples, especially after grinding. The link between AFM and M-type stacking has been explored in detail in nanometer thick flakes[5], but the presence of AFM in bulk samples has not been reported, though studies on magnetic susceptibility and muon spin rotation provide hints as to the presence of a second magnetic order below 50 K. Our neutron scattering and magnetization measurements on CrI_3 powder showed that our ground powder sample preserved a significant volume fraction of M-type stacking down to 5 K, and an analysis of the magnetic scattering showed that AFM spin alignment, arising below 50 to 55 K, is present across M-type stacking boundaries. Like the other chromium trihalides, CrI_3 consists of layers of honeycomb lattices of Cr^{3+} ions with S = 3/2 spins (Fig. 3(a).) Ideally, bulk crystals of CrI_3 become FM below T_C = 61 K, with the spins oriented out-of-plane. Our recent data indicate that magnetic diffuse scattering is present that is consistent with a model where the spin direction flips across M-type interlayer boundaries. The presence of the monoclinic phase is associated with AFM order that sets in at low temperatures, below the FM transition of the rhombohedral phase (Fig. 3(b)).

Future plans also involve investigating proposed axionic insulators to elucidate the nature of magnetoelectric coupling through applications of electric and magnetic fields. Axionic insulators are topological insulators with non-zero quantized Chern-Simons magnetoelectric coupling. Axion insulators exhibit a large quantized magnetoelectric response under symmetry protection. The correlated topological phase has been predicted to arise from the formation of a charge density wave (CDW) instability in Weyl semimetals. Axion fields, long known in quantum field theory, are a new state of quantum matter where the magnetoelectric response couples to the low-energy magnetic fluctuations.

References

1. M. Z. Hasan and C. L. Kane, *Colloquium: Topological Insulators*, Rev. Mod. Phys. **82**, 3045-3067 (2010).
2. F. D. M. Haldane, *Model for a Quantum Hall Effect without Landau Levels: Condensed- Matter Realization of the "Parity Anomaly,* Phys. Rev. Lett. **61**, 2015–2018 (1988).
3. R. Yu, W. Zhang, H. J. Zhang, S. C. Zhang, X. Dai, and Z. Fang*, Quantized Anomalous Hall Effect in Magnetic Topological Insulators,* Science **329**, 61–64 (2010).
4. S. Pershoguba, *Dirac Magnons in Honeycomb Ferromagnets,* Phys. Rev. X **8**, 011010 (2018).
5. B. Huang, G. Clark, E. Navarro-Moratalla, D. R. Klein, R. Cheng, K. L. Seyler, Di. Zhong, E. Schmidgall, M. A. McGuire, D. H. Cobden, W. Yao, D. Xiao, P. Jarillo-Herrero, X. Xu, *Layer-Dependent Ferromagnetism in a van Der Waals Crystal down to the Monolayer Limit.* Nature **546**, 270–273 (2017).

Publications

1. J. L. Hart, L. Bhatt, Y. Zhu, M.-G. Han, E. Bianco, S. Li, D. Hynek, J. A. Schneeloch, Y. Tao, D. Louca, P. Guo, Y. Zhu, F. Jornada, E. J. Reed, L. F. Kourkoutis, J. J. Cha, *"Emergence of layer stacking disorder in c-axis confined $MoTe_2$",* Nature Comm. **14**, Article number: 4803 (2023).
2. Y. Tao, L. Daemen, Y. Cheng, J. C. Neuefeind, D. Louca, "*Investigating the magnetoelastic properties in FeSn and Fe_3Sn_2 flat band metals*", Phys. Rev. B **107** (17), 174407 (2023).
3. S. S. Philip, S. Liu, J. C. Y. Teo, P. V. Balachandran, D. Louca, "*Exploring the Dirac nature of $RbBi_2$*", Physical Review B **107** (3), 035143 (2023).
4. S. Yano, Chin-wei Wang, Jason S. Gardner, Wei-Tin Chen, Kazuki Iida, R. A. Mole, and Despina Louca, "*Weak trimerization in the frustrated 2D triangular Heisenberg antiferromagnet $Lu_yY_{1-y}MnO_3$*", Phys. Rev. B **107** (21), 214407 (2023).
5. Z. Xu, F. Restrepo, J. Zhao, U. Chatterjee, D. Louca, "*Octahedral to tetrahedral bonding transitions in the local structure of phase change optical media $Ge_2Sb_2Se_{5x}Te_{5-5x}$ with Se doping*", AIP Advances **13** (4) (2023).
6. John A. Schneeloch, Luke Daemen, and Despina Louca, "*Antiferromagnetic-ferromagnetic homostructures with Dirac magnons in van der Waals magnet CrI_3*", accepted Phys. Rev. B. (2023).
7. J. A. Schneeloch, Y. Tao, Y. Cheng, L. Daemen, G. Xu, Q. Zhang, and D. Louca, "G*apless Dirac magnons in $CrCl_3$*", npj Quantum Materials **7**, 66 (2022).
8. Yu Tao, Douglas L. Abernathy, Tianran Chen, Taner Yildirim, Jiaqiang Yan, Jianshi Zhou, John B. Goodenough, and Despina Louca, "*Lattice and magnetic dynamics in YVO_3 Mott insulator studied by neutron scattering and first-principles calculations*", Phys. Rev. B **105**, 094412 (2022).
9. J. A. Schneeloch, Y. Tao, J. A. Fernandez-Baca, G. Xu and D. Louca, "*Large change of interlayer vibrational coupling with stacking in $Mo_{1-x}W_xTe_2$*", Phys. Rev. B **105**, 014102 (2022).
10. M. Shiomi, K. Kojima, N. Katayama, S. Maeda, J. A. Schneeloch, S. Yamamoto, K. Sugimoto, Y. Ohta, D. Louca, Y. Okamoto, and H. Sawa, "*Charge-ordered state satisfying the Anderson condition in $LiRh_2O_4$ arising from local dimer order*" Phys. Rev. B **105**, L041103 (2022).

Controlling magnetism via charge modifications in quantum material heterostructures

Steven May

Department of Materials Science and Engineering, Drexel University, Philadelphia, PA

Keywords: quantum materials, epitaxial heterostructures, correlated oxides, kagome metals, interfacial magnetism

Project Scope

A forefront challenge in materials physics is understanding and harnessing the sensitivity of correlated and topological states in quantum materials to external perturbations, such as changes in charge density. Magnetism is an ideal platform for probing these relationships as exchange interactions in 3*d* transition metal-based compounds, such as oxides and intermetallics, are directly linked to bond environments, charge densities, and orbital occupancy. Developments over the last few years have set the stage for unique opportunities to manipulate magnetism in epitaxial heterostructures based on two different families of 3*d* quantum materials: correlated oxides and topological kagome metals.

In this project, both *ex situ* and *in situ* neutron scattering techniques will be used to provide new approaches for measuring, understanding, and, ultimately, controlling magnetism within quantum matter heterostructures. In the first sub-effort, we aim to employ electrolytic gating to control over magnetism in A_2BO_4 Ruddlesden-Popper films, utilizing both cationic and anionic intercalation to alter spin structures in these systems. In the second sub-effort, we seek to understand how magnetism, in particular interfacial ferromagnetism, in *M*Sn and M_3Sn_2 (*M* = Fe, Co, Mn) kagome metals is impacted by perturbations such as interfacial formation with other metals (both kagome intermetallics and elemental 3*d* metals). The third sub-effort focuses on the development and implementation of sample environments that enable *in situ* measurement of antiferromagnetism during electrolytic gating, depth-dependent ferromagnetism as ions are inserted, and magnetic depth-profiles in topological heterostructures under applied pressure.

Recent Progress

This project started in September 2023. Initial work has focused on synthesizing the heterostructures. We use molecular beam epitaxy to grow films and superlattices of complex oxides and kagome intermetallic compounds. We have begun by growing epitaxial films of kagome metal Fe_3Sn_2,[1] which is ferromagnetic making it an ideal candidate for polarized neutron reflectometry (PNR) studies of interfacial magnetism. Our first aim is to understand how electron and hole doping, which will move the Fermi level relative to the flat bands of the kagome materials, alter magnetism. We have synthesized $Fe_{3-x}Mn_xSn_2$ (hole doped) and $Fe_{3-y}Co_ySn_2$ (electron doped) films with x and y concentrations up to 1. In order to achieve smooth and continuous films, a buffer layer of Co or Fe must first be grown on the Al_2O_3 (001) substrates. To date, we have utilized Co (or Fe) layers that are on the order of 7 nm, but aim to reduce this thickness as we better understand the growth process. The Fe_3Sn_2 films are 20-30 nm thick with smooth surfaces and interfaces as evidenced by thickness fringes measured with the specular x-ray diffraction. Only 000*l* peaks are observed [Fig 1(a)], confirming that the films are *c*-axis oriented. The surfaces are smooth, as confirmed by x-ray reflectivity [Fig. 1(b)], while in-plane diffraction measurements confirm that the films are epitaxial [Fig. 1(c)]. The *c*-axis parameters of the films expand with Mn incorporation and contract with Co incorporation [Fig. 1(d)]. All samples show ferromagnetic behavior in magnetometry measurements [Fig. 1(e)] but given the ferromagnetic buffer layer, further measurements are needed to isolate the magnetization of the Fe_3Sn_2-based films from the Co buffer layer. This also points to the need for polarized neutron reflectometry to determine the depth-profile of magnetization in heterostructures with magnetic buffer layers. Once we establish the magnetic phase diagram of the $Fe_{3-x}Mn_xSn_2$ and $Fe_{3-y}Co_ySn_2$ systems, we will be positioned to understand charge-transfer induced magnetic effects at Fe_3Sn_2-based interfaces, which will be studied in depth using PNR.

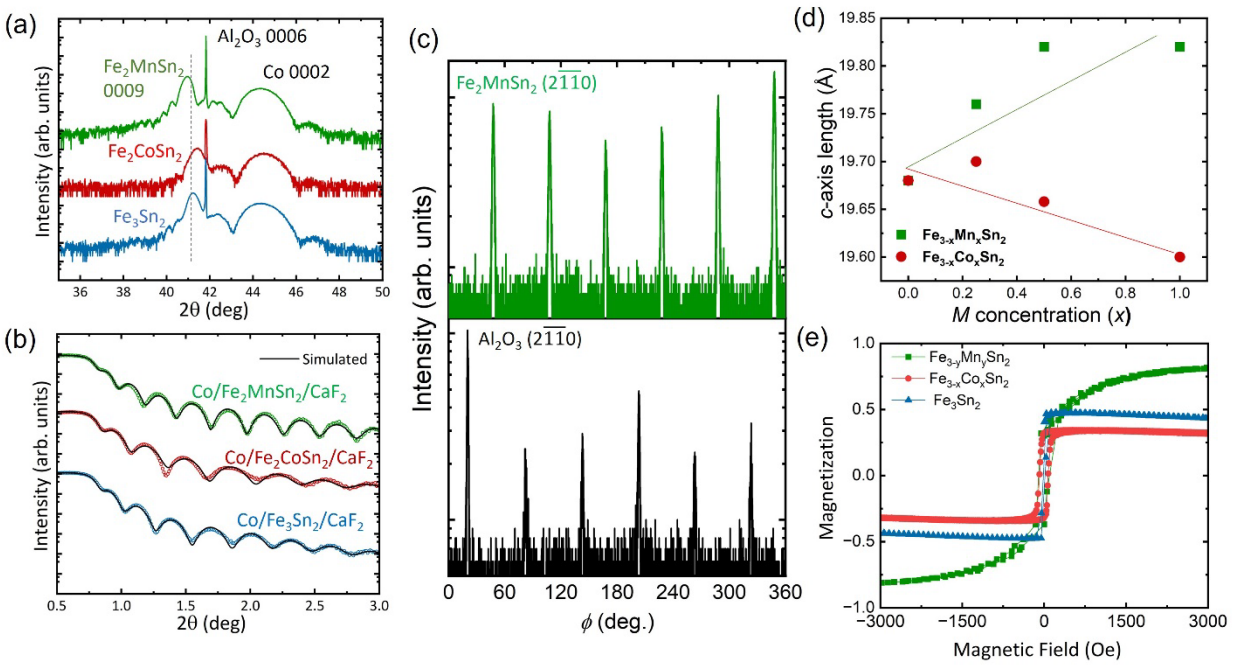

Fig. 1. (a) X-ray diffraction 00*L* scans, (b) x-ray reflectivity, and (c) phi scans from Fe_3Sn_2, Fe_2MnSn_2, and Fe_2CoSn_2 epitaxial films grown on Co buffer layers and capped with CaF_2. (d) The *c*-axis expands and contracts for Mn and Co alloying, respectively. (e) Room temperature magnetic hysteresis loops with magnetization contributions from both the kagome metal and the Co buffer layers.

We are also synthesizing thin films of Sr_2CoO_{4-x} and Sr_2FeO_{4-x}. These Ruddlesden-Popper materials are chosen as we hypothesize that the layered structure will allow a wider range of ions to be intercalated within these films as compared to ABO_3 perovskites. In particular, we aim to demonstrate intercalation of Li^+ and Cl^-, in addition to O^{2-} and H^+, for which voltage-driven insertion has already been demonstrated in perovskite films. We are focused on cobaltites and ferrites because these materials have a rich array of magnetic phases in bulk, including ferro-, anitferro- and even helimagnetic states, depending on the nominal oxidation state of Co and Fe within the A_2BO_4 structure.[2,3] We therefore anticipate that the magnetic state can be dynamically tuned with voltage-driven intercalation of ions into the oxide framework. Our previous work established that both O^{2-} and H^+ can be inserted and removed from $SrFeO_{3-x}$ films using electrolytic gating and we aim to build off of these results for this project.[4] Synthesis efforts of these materials are in their initial stages, but we have realized epitaxial Sr_2CoO_{4-x} (Fig. 2). Near-term studies are needed to determine the oxygen stoichiometry of the as-grown films, to determine material stability, and demonstrate synthesis of Sr_2FeO_{4-x} films.

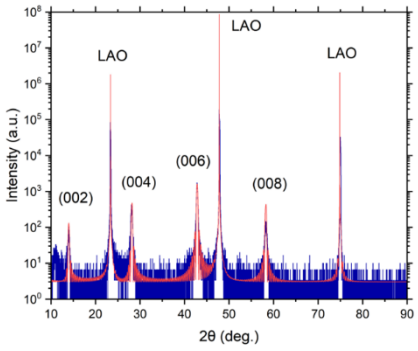

Fig. 2. X-ray diffraction of a Sr_2CoO_{4-x} epitaxial film on $LaAlO_3$. The red lines are simulations of an ideal $Sr_2CoO_4/LaAlO_3$ heterostructure.

Future Plans

Tuning magnetism in layered oxides with electrolytic gating. Our starting point in this area will be to use ionic liquids to insert and remove O^{2-} and H^+ into Sr_2CoO_{4-x} and Sr_2FeO_{4-x} films. Changes in magnetization and electronic behavior will be probed by magnetometry and variable temperature transport measurements. Neutron diffraction will be carried out to map out the changes in spin structure within materials of the same as-grown composition following systematic changes to Co and Fe oxidation states induced by voltage-driven insertion of O^{2-} and H^+.

Interfacial magnetism in kagome heterostructures. We will exploit the layer-by-layer control afforded by molecular beam epitaxy to enable model studies of how interfacial charge transfer and non-bulk-like stacking sequences alter magnetism in M_xSn-based heterostructures. We will design and characterize a series of superlattices and control samples (random alloy films) to investigate magnetism at kagome interfaces in which charge transfer would move the Fermi level up or down within Fe_3Sn_2 layers. Using PNR, we will obtain the saturation magnetization within the Fe_3Sn_2 blocks and $Fe_{1.5}M_{1.5}Sn_2$ blocks (M = Co, Mn), as well as the depth-dependence of magnetization across the interfaces. We will investigate the impact of finite thickness on the stability of the magnetically ordered state down to a single confined Fe_3Sn monolayer. This will be pursued by creating $(CoSn)_n/(FeSn)_1$ superlattices (where $n \geq 8$) in which a single Fe_3Sn monolayer is embedded within paramagnetic CoSn. The magnetization of these structures will be determined using PNR.

In situ measurements of Fe_3Sn_2 under applied pressure. In addition to charge transfer and confinement, strain or pressure is another means by which non-bulk-like magnetism may arise in quantum heterostructures. We aim to perform PNR measurements on Fe_3Sn_2 films under applied pressure using *in situ* pressure cells designed for the Magnetism Reflectometer beamline (MAGREF, BL-4A) at the SNS.[5] These measurements will reveal how the saturation magnetization changes with increasing pressure, up to ~1.5 GPa, providing the first experimental insights into how ferromagnetism in Fe_3Sn_2 is impacted by lattice contraction.

Development of a cell for *in situ* neutron diffraction during electrolytic gating. We aim to develop a biasing cell that can be utilized across multiple instruments, specifically targeting VERITAS (HB-1A) and CORELLI (BL-9) as instruments on which antiferromagnetic diffraction peaks can readily be measured from thin films. This cell will be used to track the intensity of reflections arising from antiferromagnetic spin structures as ions such as H^+, O^{2-}, and Li^+ are inserted and removed from $Sr_2CoO_{4-\delta}$ and $Sr_2FeO_{4-\delta}$ films using electrolytic gating.

References

[1] L. Ye, M. Kang, J. Liu, F. von Cube, C. R. Wicker, T. Suzuki, C. Jozwiak, A. Bostwick, E. Rotenberg, D. C. Bell, L. Fu, R. Comin, and J. G. Checkelsky, *Massive Dirac fermions in a ferromagnetic kagome metal*, Nature **555**, 638 (2018).

[2] N. Sakiyama, I. A. Zaliznyak, S. H. Lee, Y. Mitsui, and H. Yoshizawa, *Doping-dependent charge and spin superstructures in layered cobalt perovskites*, Physical Review B **78**, 180406 (2008)

[3] P. Adler, M. Reehuis, N. Stüßer, S. A. Medvedev, M. Nicklas, D. C. Peets, J. Bertinshaw, C. K. Christensen, M. Etter, A. Hoser, L. Schröder, P. Merz, W. Schnelle, A. Schulz, Q. Mu, D. Bessas, A. Chumakov, M. Jansen, and C. Felser, *Spiral magnetism, spin flop, and pressure-induced ferromagnetism in the negative charge-transfer-gap insulator Sr_2FeO_4*, Physical Review B **105**, 054417 (2022)

[4] B. M. Lefler, W. M. Postiglione, C. Leighton, and S. J. May, *Voltage Control of Patterned Metal/Insulator Properties in Oxide/Oxyfluoride Lateral Perovskite Heterostructures via Ion Gel Gating*, Advanced Functional Materials **32**, 2208434 (2022).

[5] E.-J. Guo, R. Desautels, D. Lee, M. A. Roldan, Z. Liao, T. Charlton, H. Ambaye, J. Molaison, R. Boehler, D. Keavney, A. Herklotz, T. Z. Ward, H. N. Lee, and M. R. Fitzsimmons, *Exploiting Symmetry Mismatch to Control Magnetism in a Ferroelastic Heterostructure*, Physical Review Letters **122**, 187202 (2019).

Publications

We do not have publications to report as the project just started three months ago.

Using phonon mode analysis to study optoelectronic organic materials

Adam Moulé
University of California, Davis

Keywords: Inelastic neutron scattering, organic electronics, optoelectronic materials, structure analysis, dynamic disorder

Research Scope

Our long-term goal is to link the phonon spectrum, measured using inelastic neutron scattering (INS), to organic electronic materials (OEMs) properties, such as electronic and excitonic transport, in both ordered and disordered materials to enable accurate optoelectronic property prediction. In our last award, our objective was to develop inexpensive computational tools to enable accurate interpretation of INS spectra in disordered OEMs. We succeeded in developing new simulation tools that enable the simulation of more complex samples over larger volumes and are currently applying these tools to simulation of small molecule crystals with internal disorder like amorphous side chains or a mixture of syn and anti conformers of the same molecule.

Our objectives for the current three years (starting summer 2022) are to design and build an optical excitation sample environment for the VISION instrument and to use our newly developed computational tools to predict charge and exciton mobility in increasingly complex OEM materials. Our central hypothesis is that electronic and excitonic materials properties of OEMs can be predicted if the model is simultaneously validated against quantitative structural and dynamic data. The ideal data for model validation and prediction of these properties is INS coupled with structural measurements from x-ray and/or neutron diffraction. The rationale underlying the proposed studies is that there are currently no accurate tools available that can predict materials properties in non-crystalline OEMs, so our research represents a clear and urgent need.

We will test our central hypothesis by pursuing the following three specific aims:

1. Quantify the effects of structural and dynamic disorder on charge transport: We will study defective/complex molecular crystals to determine the separate effects of structural and dynamic disorder on charge transport.
2. Refine modeling methods to interpret INS data from complex OEM samples: We will refine inexpensive modeling methods to accurately simulate INS spectra of amorphous materials. We will include MD/DFT and MD/DFTB methods into Davis Computational Spectroscopy (DCS) Flow, our GitHub workflow, for INS spectrum simulation.
3. Develop a new optical excitation sample environment at the VISION beamline: We will support Ph.D. student Daniel Vong to design and test a new optical excitation sample environment on VISION to enable measurement of excited state phonons.

Recent Progress

The Moule group had a complete turnover of researchers on this project over the first six months. Lukas Cavalcante (postdoc) completed his research and moved on to a data science job in the SF bay area in August 2022. His final paper was published early in 2023.[5] It represents a new direction for our INS research. We had measured INS on a metal organic framework (MOF) material called MOF-UiO66. In this paper we examined a single sample with Zr_6O_8 nodes surrounded by a 12-coordinate ligand matrix composed of terphalate linkers. However, it is well known that ALL MOF samples have considerable structural disorder. In addition, from NMR data, we knew that the ratio on average each node had only 11 terphalate linkers and a last "defect site" composed of acetate. We used DFT to predict the INS spectra of the four different possible perfect MOF structures that have been

identified from x-ray diffraction and showed that our sample was predominantly the most dense of these possible crystalline conformers. We then simulated the defect structures that could form including the acetate defect sites and showed that the defect sites in our sample include not just acetate, but formate also. Finally, we used the INS data and DFT to identify the defect site structure in the MOF. This was the first ever paper that showed this level of detail on a MOF defect site structure, which is why we got a Materials Horizons paper. Our goal was to expand the use of INS into MOFs and specifically to get a new assistant professor at UC Davis to start using INS as part of his regular research.

Makena Dettman completed his PhD and graduated in December 2022. His final paper was published in Advanced Functional Materials in 2023.[4] This work was a continuation of prior research using INS to characterize the dynamic disorder of organic crystals. Dynamic disorder (phonons) in organic materials localizes charges and excitons. To predict the charge mobility, we used the INS spectra to determine the dynamic disorder. The first paper of Daniel Vong, published in the Journal of Physical Letters, demonstrated that our method, validated by INS, was by far the most accurate charge mobility prediction compared to all other theory groups worldwide.[6] The goal of Makena's final paper was to translate our results, relating dynamic disorder, to molecular design. He developed a visualization tool to quantify the effect of dynamic disorder on charge mobility (the effective electron phonon coupling) on a per atom basis.

Figure 1: the molecular structure of the molecule BTBT (white -H, gray – C, yellow – S, next to a simulation depicting the electron/phonon coupling for each atom. The motion of carbon atoms between the two sulfurs cause the greatest reduction in charge mobility. This is one example of many simulations performed. This work enables synthesis researchers to systematically improve materials properties based on phonon data.

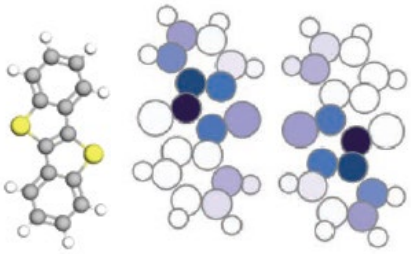

Daniel Vong graduated with a PhD in June 2023. He has a DOE SCGSR fellowship to work with Luke Daemen at SNS on the VISION instrument from January 2022 – January 2023. He designed, built and tested a sample changer for the vision beamline (that allows Luke to go home a sleep)[2] and a light excitation sample environment that enables simultaneous optical excitation and INS measurement.[3] The sample stick was patented. In the Review of Scientific Instruments paper, he demonstrated the use of this instrument to monitor cross-link reactions for a photo resist and light induced dimerization reactions for anthracene. Next, he used the sample environment to measure, for the first time, the excited state phonon spectra of the molecules tetracene and pentacene.[1] Through spring 2023, my new postdoc (Farah) and Daniel simulated the changes to the molecular environment for the triplet exciton using the phonons measured using the new sample environment. We were able to show an intermolecular rearrangement due to the triplet exciton that helps to explain singlet fission (SF) in tetracene. SF is a process in which one excited singlet state separates into two separate triplets. This process is very exciting because it offers a pathway to achieve two excitons using one photon. If this process was 100% efficient in a photovoltaic device (PV), then it would break the Schockley/Queiser limit for the most efficient PV device, increasing it from ~37% to ~46%. Tetracene has been highly studied because SF has been shown to occur even though 2 times the T_1 energy is larger than the S_1 energy, which should be energetically impossible. Our work shows that the intermolecular arrangement of ground state molecules around the triplet lowers the energy difference between S_1 and $2*T_1$ to within kT at room temperature. This paper has been reviewed in the Journal of Physical Chemistry letters and will be published in early 2024.

The main project of my new postdoc, Farahnaz Maleki, has been to use INS as a means to quantify, model, and validate partially ordered molecular crystals. Working with John Anthony (U. Kentucky) we measured two samples of benzodithiophene (BDT) trimers (with and without fluorine substitutions), each of which has two dihedral bonds. Using gas phase simulations, we showed that anti configurations of the BDT-trimers are more stable and planar than syn configurations. However, when we simulate a crystal of BDT-trimers (VASP) we anticipate seeing eight different nearest neighbor conformers. Figure 2a shows the eight conformers and Figure 2b shows the relative energetic differences between the conformers. Interestingly, the all-anti conformer is the least favorable conformer in the crystal. This very long and complex article explores how to simulate and validate INS data for multiple conformers inside of a single crystal. We develop a new method to fingerprint structures by simulating single atom spectra of each proton and then using the measured INS spectrum validate the ratio's of each conformer. This paper is very important because it both develops a new method to dissect INS data and also it will greatly change how synthetic chemists develop new structures. The predominant paradigm in the organic electronics community is that all anti-conformers are the most stable. This work shows and validates that in fact, anti-conformers are less stable in the crystal due to unfavorable intermolecular interactions and that syn conformers are stabilized in the crystal by H-bonds. We expect to submit this paper to Chemistry of Materials in spring 2024.

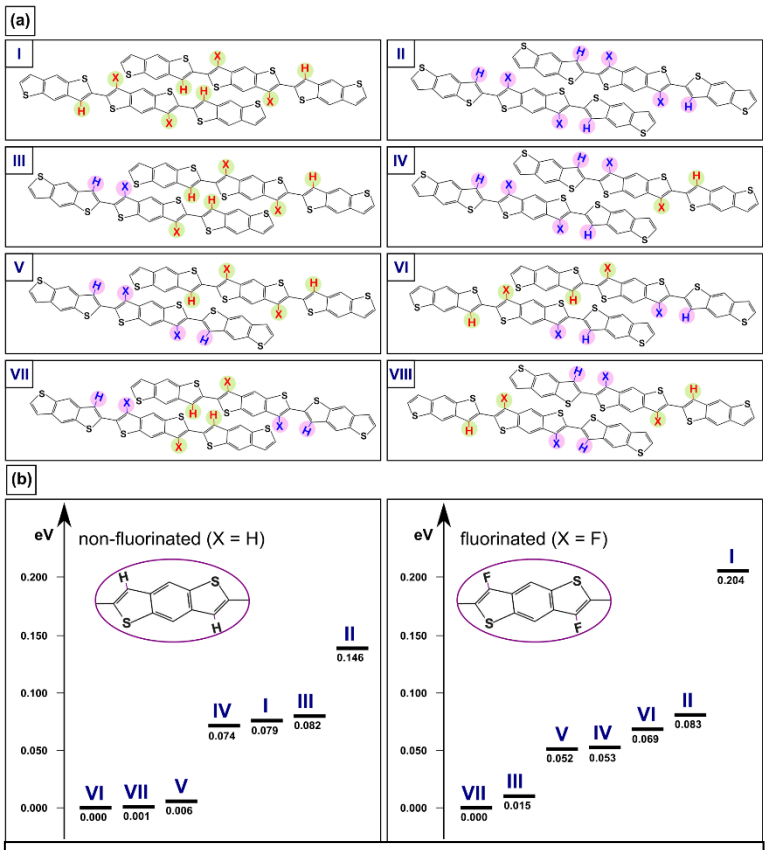

Figure 2: a) Eight different nearest neighbor conformers of BDT-trimers for both protonated and fluorinated samples. b) relative energies for the conformers.

Future Plans

New PhD students Toulik Maitra and Chen-Wei (Ray) Chiang were hired in January 2022.

Toulik is examining all 50+ INS spectra that we have measured since 2012. We noticed several systematic trends. First, we noticed that all data show a systematic peak with increase with increasing energy, but that the slope of the INS peak with increase is higher in samples with more disordered crystals, suggesting that this parameter can be used to quantify disorder in crystalline

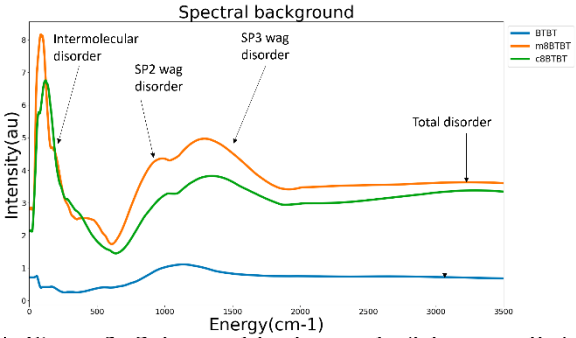

Figure 3: Subtracted background of three small molecule samples. Labels indicate the energy regions that show structural disorder in different parts of the molecular crystal.

domains. Second, we developed a method to subtract the background of the INS spectrum from the peaks. Here we found that the total background signal increases for more amorphous samples (polymers) and that the shape of the background (energy distribution) could be separated into contributions from proton-wags connected SP2 (conjugated) and SP3 (side chain) carbons. The low energy data shows intermolecular disorder. Figure 3 shows three similar molecules with no side chain (BTBT) and with one (m8BTBT) or two (C8BTBT) octyl side chains. Here we see that although C8BTBT has more side chain, it is overall more ordered and has more ordered side chains than m8BTBT. This project is very exciting because it enables INS interpretation of disordered sample regions and has implications for the design of BWAVES.

Ray is working on simulation of the INS spectra of polymer samples synthesized by Xiaodan Gu (U. Southern Mississippi). These polymers have protonated and deuterated side chains of different lengths. Our goal is to use the above methods to extract information about the conformations of the polymer backbone, that are relevant to the materials properties from the INS spectrum. This is complex because usually INS spectra can only be simulated using plane wave DFT (vasp), but there are far too non-crystalline conformers. The simulation using vasp or molecular dynamics is too expensive. We have already used simulations of polymer fragments to determine the likely local conformers. Next, we will use data analysis to identify the key backbone peaks that identify the backbone planarity. This is high risk / high reward research with no known solution.

Publications [1-6]

[1] D. Vong, F. Maleki, E.C. Novak, L.L. Daemen, A.J. Moulé, Measuring Intermolecular Excited State Geometry for Favorable Singlet Fission in Tetracene, Journal of Physical Chemistry Letters (in press) (2024).

[2] D. Vong, E.C. Novak, M.M. Ruiz-Rodriguez, S.R. Elorfi, B. Thomas, A.J. Morris, A.J. Moulé, L.L. Daemen, Compact, portable, automatic sample changer stick for cryostats and closed-cycle refrigerators, Review of Scientific Instruments 94(8) (2023).

[3] D. Vong, E.C. Novak, A.J. Moulé, L.L. Daemen, Photochemistry sample sticks for inelastic neutron scattering, Review of Scientific Instruments 94(8) (2023).

[4] M.A. Dettmann, L.S.R. Cavalcante, C.A. Magdaleno, A.J. Moule, Catching the killer: Dynamic disorder design rules for small-molecule organic semiconductors, Advanced Functional Materials (2023) 2213370.

[5] L.S.R. Cavalcante, M.A. Dettmann, S. T., D. Yang, L.L. Daemen, B.C. Gates, A.R. Kulkarni, A.J. Moule, Elucidating Correlated Defects in Metal Organic Frameworks Using Theory-Guided Inelastic Neutron Scattering Spectroscopy, Material Horizons 10 (2023) 187-196.

[6] D. Vong, M.A. Dettmann, T.L. Murrey, S.M. Gurses, T. Nematiaram, D. Radhakrishnan, L.L. Daemen, J.E. Anthony, K.J. Koski, A. Troisi, C.X. Kronawitter, A.J. Moule, Quantitative Hole Mobility Simulation and Validation in Substituted Acenes, Journal of Physical Chemistry Letters 13(24) (2022) 5530-5537.

Quantum multipolar fluctuations in spin-orbit magnets
Martin Mourigal, Georgia Institute of Technology, Atlanta, GA
Cristian Batista, University of Tennessee, Knoxville, TN

Keywords: Spin dynamics, quasiparticle decay and fractionalization, semi-classical approaches, inelastic neutron scattering under pressure, novel triple-axis spectrometers concepts

Research Scope

Magnetic insulators consist of networks of quantum spins at the vertices of virtually perfect and infinitely periodic lattices. These systems are often clean enough to realize fragile many-body states deep in the quantum regime, making them ideal for probing fundamental quantum physics questions. In cases where single crystals can be grown, or when large volumes of polycrystalline samples are available, inelastic neutron scattering is the ultimate quantitative tool for probing the correlation functions that characterize these many-body states in thermodynamic equilibrium. Understanding these bulk systems is crucial for advancing energy and quantum technologies. For example, thin films or two-dimensional systems derived from these bulk materials can be integrated into devices or interfaced with other strongly correlated electronic materials to generate new functionalities.

A particularly intriguing and exotic quantum effect in magnetic insulators is the destruction of conventional broken symmetry states at low temperatures, such as long-range magnetic structures, and their replacement with quantum entanglement structures. This phenomenon is well understood in one-dimensional Heisenberg magnets, where gapless fractionalized excitations and topological order emerge in half-integer and integer spin systems. In higher-dimensional networks (two and three dimensions), these phenomena are unified under the concept of quantum spin-liquid and emergent gauge fields, which describe the interplay of fractional excitations and topological order; a notable example is the Kitaev model. However, these systems have been challenging to obtain and study experimentally because their small gap makes them sensitive to material imperfections such as site disorder, and their dynamical responses at finite temperatures often resemble those of correlated, yet conventional, paramagnets. Despite the advanced capabilities of direct-geometry time-of-flight spectrometers at the Spallation Neutron Source, quantitative studies of these systems are still rare.

Instead of directly targeting quantum spin-liquid candidates, this program studies magnetic systems that are approximatively product states. The systems of interest here typically have low ground-state quantum entanglement and might display magnetic ordering at sufficiently low temperatures yet exhibit unusual dynamical properties. These properties serve as a stringent benchmark for quantum-many body theory. The program combines materials synthesis, neutron scattering experiments, and modeling at Georgia Tech with theoretical developments led by the University of Tennessee. The aim is to maximize the use of the neutron scattering cross-section (quantitative, momentum-, energy- and spin-resolved) to expand the physics knowledge derived from inelastic neutron scattering experiments, ranging from model magnetic Hamiltonians to new effects in quantum many-body theory. The program aims to close the knowledge gap in interpreting neutron scattering data by developing and testing new semi-classical descriptions. It seeks to understand why these descriptions are effective, identify their limitations, and unveil genuine quantum effects. Under this umbrella, this program focuses on three families of systems: (1) magnetic systems near a quantum melting point, (2) frustrated magnets exhibiting a classical spin-liquid regime at low temperatures, facilitating complex collective spin dynamics, and (3) anisotropic spin-orbital compounds, where the dimensionality of the local Hilbert space influences the nature of low-energy fluctuations. Two model magnetic systems, the pyrochlore Heisenberg antiferromagnet $MgCr_2O_4$ [1] and the triangular spin-orbital system FeI_2 [2], have been pivotal in this program, leading to significant conceptual advances

in semi-classical descriptions of spin dynamics using Landau-Lifshitz simulations and generalized spin-wave theory for coherent states of SU(N) [3].

Internally, the program emphasizes training postdoctoral, graduate, and several undergraduate students in neutron scattering research (and condensed matter physics in general), as well as fostering new research directions that advance neutron scattering. Recent focuses included understanding prismatic analysis for multiplexed triple-axis neutron spectrometers via Monte-Carlo simulations and exploring GPa-scale pressure control of magnetic systems using magnetometry and neutron scattering. Externally, this program leverages several essential resources through collaborations: the IQM and PARADIM crystal growth facilities at Johns Hopkins, the neutron sources at ORNL, and the SU(N)NY.jl simulation code base from Los Alamos.

Recent Progress

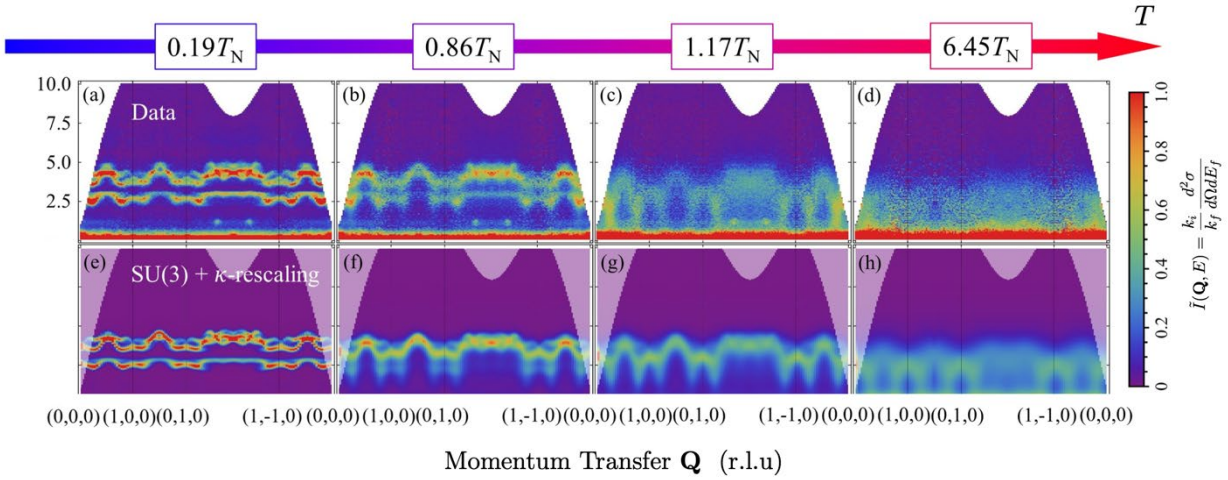

Fig. 1 Evolution of magnetic excitations in FeI_2 as a function of temperature and successful modeling using Landau-Lifshitz dynamics simulations for SU(3) coherent states. Measurements on SEQUOIA at SNS.

A novel form of magnon decay in spin-orbital magnet FeI_2 (Experiment+Theory): In the uniaxial spin-one system FeI2, a unique scenario unfolds where dipolar and quadrupolar spin fluctuations coexist at low energy, becoming observable in neutron scattering due to spin-orbit coupling. Utilizing high-field magnets on the HYSPEC beamline, we controlled the relative energies between these different excitations, which can be interpreted as distinct quasiparticle flavors with varying masses. This control enabled us to initiate their mutual quantum mechanical decay, which yields a finite lifetime for the quasiparticles. This decay mechanism, involving different flavors of magnons, is observed for the first time in this compound (Product: #6 below). The study underscores the role of flat excitation bands and Kitaev-like anisotropic magnetic exchange interactions in generating new quantum phenomena within magnetically ordered systems that may appear usual at first glance. This study developed a one-loop correction approach generalized to spin-wave theory based on coherent states of SU(3) to explain the data.

Quantum to classical crossover in FeI_2 (Experiment+Theory): As a follow-up to the above work, we tackled the challenge of simulating quantum spin systems at finite temperatures by examining the zero-field spin dynamics of FeI2 over two decades of temperature and crossing the ordering temperature. The harmonic spin-wave theory that relies on a fixed magnetic structure and quantum harmonic oscillators needs to be abandoned in favor of the Laudau-Lifshitz equation of motion of classical moments to account for the disordered component of the underlying magnetic structure. Both approaches must be generalized to treat dipolar and quadrupolar fluctuations on equal footing (Ref. 3 and Product #4 below). Even then, we discovered that a temperature-dependent renormalization of classical moments, self-consistently chosen to enforce the quantum sum rule for the dynamical structure factor, is essential to match calculated and measured spectra across temperatures (Product #9). Once implemented, this simple procedure allowed us to quantitatively explain the FeI_2 data from the SEQUOIA spectrometer across all measured temperatures, including when the dynamics change rapidly for a temperature around the Neel transition. These studies have significantly expanded the arsenal of modeling approaches to model the neutron scattering response of complex spin-orbital magnets at finite temperatures while retaining a moderate computational cost. See Fig. 1.

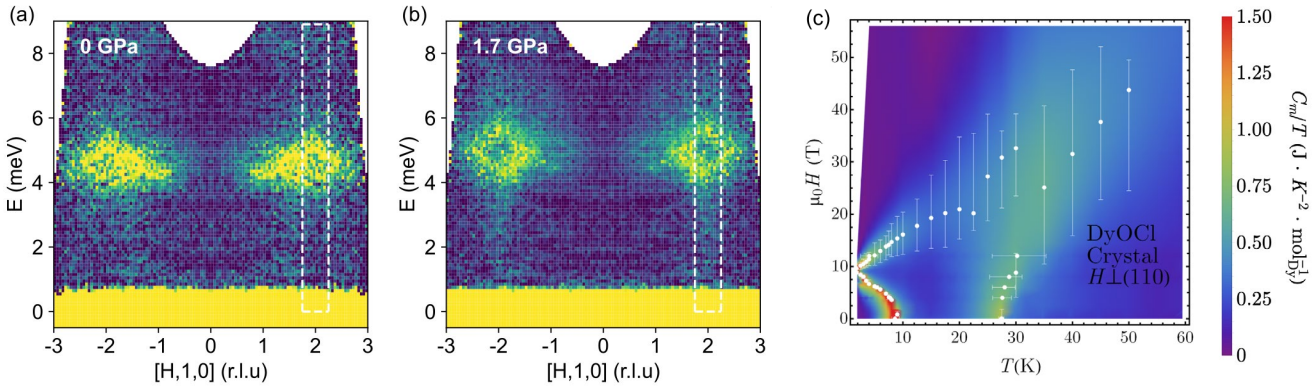

Fig. 2 (a,b) Control of magnetic excitations in the ordered phased of MgCr2O4 using hydrostatic pressure (HYSPEC, SNS) (c) Phase diagram of DyOCl showing the interplay between quadrupolar and dipolar ordering.

Magnon deconfinement proximate to a quantum melting point (Theory): The previous two studies focused on FeI_2, a magnetic system exhibiting conventional dipolar magnetic order and exotic transverse quantum fluctuations. However, when a magnetic system nears a quantum melting point, longitudinal quantum fluctuations reduce the expectation value of the magnetic order. This significantly complicates the spin-dynamics calculations, as semiclassical approaches fail, leading to different instability in the underlying quasiparticles: magnon fractionalization (or unbinding) into pairs of spinons. The triangular-lattice spin-1/2 Heisenberg antiferromagnet serves as a prototypical example where both magnon decay and magnon fractionalization can occur. A Parton Schwinger boson theory was developed to understand the latter phenomenon better (Product #3). This theory suggests that an interacting spinon gas effectively models magnetic states near quantum melting points. It demonstrates the presence of two-spinon bound states and a low-energy two-spinon continuum within this Hamiltonian model, laying the foundation for future research.

Pressure control of magnetic excitations in $MgCr_2O_4$ (Experiment): Applying pressure is a commonly used method to manipulate the magnetic Hamiltonian of magnetic materials, aiming to either approach a quantum melting point or control competing interactions. In the case of $MgCr_2O_4$, its classical spin-liquid regime and intricate magnetic ordering are expected to be highly sensitive to changes in magnetic excitation interactions. We recognized that direct exchange influences this

system and embarked on a new research direction. This involves examining the effects of GPa-scale hydrostatic pressure on crystal and powder samples, utilizing a combination of SQUID-based magnetometry and inelastic neutron scattering studies, see Fig. 2(a,b). Our research, led by an undergraduate student (Product #8), applied pressure up to approximately 2 GPa. It revealed that at low temperatures, $MgCr_2O_4$ accommodates multiple magnetic ground states. The pressure raises the ordering temperature and broadens the excitation bandwidth, resulting in the predominance of certain magnetic domains that were previously insignificant at ambient pressure. This highlights the emergence of a new short-range ordered phase. Conducted jointly at Georgia Tech and the Spallation Neutron Source (SNS), this study sets the stage for future investigations into the impact of GPa-scale pressure on magnetic excitations in magnetic systems.

Dipolar and quadrupolar magnetism in DyOCl (New Direction): In exploring new directions in material systems, we have delved into the study of rare-earth oxy-halides. These materials offer a promising avenue for realizing anisotropic exchange models in two-dimensional contexts. A graduate student trained in sample preparation successfully grew both powder and single-crystal samples of this material family. This led to the discovery of a unique interplay between quadrupolar and dipolar orders, see Fig. 2(c). Moreover, by altering the halide component, we effectively controlled the magnetism from long-range to short-range order. DyOCl demonstrates typical long-range order, while DyOBr and DyOI show partial ordering. We propose a model where magnetic disorder is influenced by increasing Van der Waals gaps, affecting magnetic correlations within bilayers.

Monte-Carlo Ray-tracing simulations for prismatic analysis for TAS (New direction): A new line of research, led by an undergraduate student, focuses on developing design principles for a novel cold triple-axis spectrometer (MANTA) intended for the High Flux Isotope Reactor. Drawing inspiration from the CAMEA spectrometer at the Paul Scherrer Institute, we explored various prismatic analyzer systems using Monte-Carlo ray-tracing simulations to optimize performance (Product #10). This work introduces a novel statistical approach aimed at enhancing energy measurement capabilities. The insights gained from these simulations are expected to contribute significantly to developing the new spectrometer at HFIR.

Future Plans

Our plans for the remaining of the current funding period will focus on the analysis of neutron scattering data from $FeBr_2$, a compound related to FeI_2. Utilizing the high-magnetic field capabilities at ORNL, we've measured the saturated magnon dispersion and the excitations in various phases. We plan to refine and test our approach to extract magnetic Hamiltonians from the data including at finite temperature. On the conceptual side, we plan to develop spin-wave theory approaches to understand the magnetically ordered phases of $MgCr_2O_4$ which requires to efficiently optimize exchange interactions in a very-large unit-cell. On the synthesis side, analogues to DyOCl with more isotropic moments, such as CeOCl are being pursued.

References [1]. X. Bai, J. A. M. Paddison, E. Kapit, S. M. Koohpayeh, J.-J. Wen, S. E. Dutton, A. T. Savici, A. I. Kolesnikov, G. E. Granroth, C. L. Broholm, J. T. Chalker, and M. Mourigal, "*Magnetic excitations of the classical spin liquid $MgCr_2O_4$*", Physical Review Letters **122**, 097201 (2019). [**2].** X. Bai, S.-S. Zhang, Z. L. Dun, H. Zhang, Q. Huang, H. D. Zhou, M. B. Stone, A. I. Kolesnikov, F. Ye, C. D. Batista, M. Mourigal, "*Hybridized quadrupolar excitations in the frustrated and spin-anisotropic magnet FeI_2*", Nature Physics **17**, 467-472 (2021). [**3].** H. Zhang, C. D. Batista, "*Classical spin dynamics based on SU(N) coherent states"*, Phys. Rev. B **104**, 104409 (2021).

Representative publications (December 2021 to December 2023)

#10. A. Desai, T. Williams, M. Daum, G. Sala, A. Aczel, B. Winn, G. Granroth, and M. Mourigal, "*Monte-Carlo ray-tracing studies of multiplexed prismatic graphite analyzers for the cold-neutron triple-axis spectrometer at the High Flux Isotope Reactor*", Submitted (December 2023), https://doi.org/10.48550/arXiv.2312.03233.

#9. D. Dahlbom, D. Brooks, S. Chi, A. I. Kolesnikov, M. B. Stone, H. Cao, K. Barros, M. Mourigal, C. D. Batista, and X. Bai, "*Quantum to classical crossover in generalized spin systems: example of the temperature-dependent spin dynamics of FeI_2*", Submitted (October 2023), https://doi.org/10.48550/arXiv.2310.19905.

#8. L. S. Nassar, H. Lane, B. Haberl, B. Winn, M. Graves-Brook, S.M. Koohpayeh, and M. Mourigal, "*Pressure control of magnetic order and excitations in the pyrochlore antiferromagnet $MgCr_2O_4$*", Physical Review B (Accepted, December 2023); https://doi.org/10.48550/arXiv.2309.02496.

#7. C. Kim, S. Kim, P. Park, T. Kim, J. Jeong, S. Ohira-Kawamura, N. Murai, K. Nakajima, A. L. Chernyshev, M. Mourigal, S.-J. Kim and J.-G. Park, "*Bond-dependent anisotropy and magnon breakdown in cobalt Kitaev triangular antiferromagnet*", Nature Physics **19**, 1624–1629 (2023); https://doi.org/10.1038/s41567-023-02180-7.

#6. X. Bai, S.-S. Zhang, H. Zhang, Z. L. Dun, W. A. Phelan, V. O. Garlea, M. Mourigal, C. D. Batista, "*Instabilities of heavy magnons in an anisotropic magnet*", Nature Communications **14**, 4199 (2023); https://www.nature.com/articles/s41467-023-39940-1.

#5. Field-induced spin level crossings within a quasi-XY antiferromagnetic state in Ba2FeSi2O7, Minseong Lee, Rico Schönemann, Hao Zhang, David Dahlbom, Tae-Hwan Jang, Seung-Hwan Do, Andrew D. Christianson, Sang-Wook Cheong, Jae-Hoon Park, Eric Brosha, Marcelo Jaime, Kipton Barros, Cristian D. Batista, and Vivien S. Zapf, Physical Review B **107,** 144427 (2023); https://doi.org/10.1103/PhysRevB.107.144427.

#4. David Dahlbom, Cole Miles, Hao Zhang, Cristian D. Batista, and Kipton Barros, Langevin dynamics of generalized spins as SU(N) coherent states, Physical Review B **106**, 235154 (2022); https://doi.org/10.1103/PhysRevB.106.235154.

#3. E. A. Ghioldi, Shang-Shun Zhang, Yoshitomo Kamiya, L. O. Manuel, A. E. Trumper, and C. D. Batistam, "*Evidence of two-spinon bound states in the magnetic spectrum of $Ba_3CoSb_2O_9$*"; Physical Review B **106**, 064418 (2022); https://doi.org/10.1103/PhysRevB.106.064418.

#2. Jing Zhou, Guy Quirion, Jeffrey A. Quilliam, Huibo Cao, Feng Ye, Matthew B. Stone, Qing Huang, Haidong Zhou, Jinguang Cheng, X. Bai, M. Mourigal, Yuan Wan, and Z. L. Dun, "*Anticollinear order and degeneracy lifting in square lattice antiferromagnet $LaSrCrO_4$*", Physical Review B **105**, L180411 (2022); https://doi.org/10.1103/PhysRevB.105.L180411.

#1. A. Legros, S.-S. Zhang, X. Bai, H. Zhang, Z. L. Dun, W. A. Phelan, C. D. Batista, M. Mourigal, and N. P. Armitage, "*Observation of 4- and 6-magnon bound-states in the spin-anisotropic frustrated antiferromagnet FeI_2*", Physical Review Letters **127**, 267201 (2021); https://doi.org/10.1103/PhysRevLett.127.267201.

Designing Novel Nanostructures Using Sequence-Defined Biopolymers

Bradley D. Olsen, MIT

Keywords: sequence-defined, protein polymer, SANS, simulation, interaction parameter

Research Scope

One of the largest research challenges in soft materials is using chemistry to design molecules where the arrangement of atoms encodes for the formation of exquisite, hierarchically structured materials that can approach the complex and highly functional systems made in biology. The problem of encoding material structure using primary sequence for linear chains requires the ability to design a polymer with a given property function, f(s), where s is the contour variable along the backbone of the polymer chain and f is a vector of relevant properties along the length of the chain that encodes for self-assembly behavior. Recent work by our group has achieved success on this second front by incorporating the f(s) function into self-consistent field theory (SCFT), enabling sequence-defined polymers to be simulated. Combining these simulations with biological expression of sequence-defined polymers gives us a platform for the systematic exploration of this challenge in sequence-controlled design. In this project, we will use elastin-like proteins (ELPs) as model sequence-controlled polymers, encoding self-assembled nanostructures to be characterized with neutron scattering. The interplay of experiment and theory will be used to systematically explore three key aims: (1) reducing the degrees of freedom in sequence design space through spectral representations and symmetry operations, (2) developing efficient parameterizations of sequence interaction functions based on monomer sequences, and (3) implementing theory and experiment in an inverse design cycle capable of targeting sequences likely to form nanostructures not yet observed in soft matter systems. Taken together, these aims will provide a large advance in our fundamental understanding of the scope of sequence-controlled polymer design.

Recent Progress

Simulation Methods for Sequence-Defined Polymers. Sequence-defined polymers open up a high-dimensional space for molecular self-assembly and material design, requiring more advanced tools for exploration of this space. Here, classical self-consistent field theory (SCFT) is extended to sequence-defined polymers; this new formalism uses a set of four-dimensional fields and a set of descriptor functions representing the polymer sequence. The self-consistent equations resulting from this formalism are invariant to sequence complexity. Its computational cost is shown to be a factor N_s (number of points used to discretize the polymer contour length) more expensive than the current SCFT formalism, but this added computational cost can be significantly reduced through choice of sequence representation. A variety of copolymers of varying complexity are simulated with the new sequence SCFT formalism and are shown to match literature results. Additionally, sequence SCFT is shown to enable a method of investigating the configurational distribution of polymer chains which make up a phase-separated structure. Moving beyond simpler block copolymers to sequence-defined polymers where each monomer in the chain sequence can be individually specified comes with the

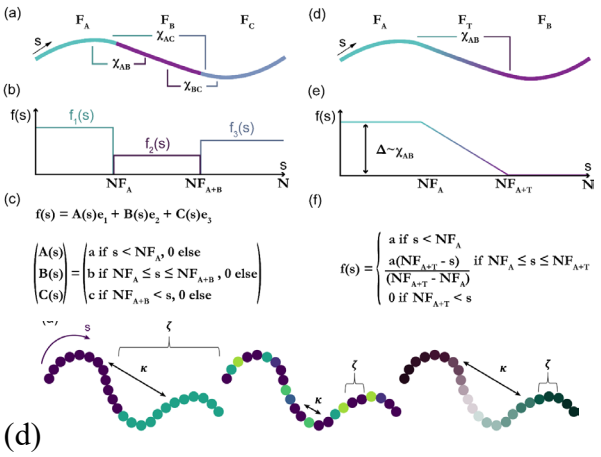

Figure 1. Illustration of models for sequence-defined polymers. Rather than modeling polymers as having a discrete chemical identity for each monomer, the chemistry is captured via a vector sequence function f(s) where s is the contour variable. These functions are conceptually illustrated in a-c for examples of block and taper copolymers. D shows that these sequences have both a length scale of definition ranging from blocks to monomers, and a length scale of sequence correlation, which can be independent.

challenge of a vast design space, where every monomer-level change in sequence produces another permutation that could result in different self-assembled structures. This is the limit represented by the protein polymers considered in this work where there are 20 possible amino acids, so a sequence of length N has 20^N possible chemical identities. To explore how many degrees of freedom in a sequence are relevant, sequence functions encoding physiochemical properties as a function of the polymer contour are transformed into Fourier mode coefficients representing different scales of sequence correlation along a polymer chain. Nanostructure formation is shown to be most sensitive to perturbations that occur in a few critical Fourier modes. These modes—often encoding long wavelength sequence features—correspond to the important spatial length scales of morphologies.

Another key question is the dimensionality required for the sequence function f(s). To understand the underlying dimensionality required to capture pairwise interactions, we are using a data-driven approach based on a large database of polymer solution activity coefficient data collected by the DECHEMA and DIPPR (AIChE) projects. By applying algorithms developed in network science to fit the data, we can determine the minimum dimensionality of n-dimensional space that satisfies the constraints of the experimental data, where the χ parameters represent distances between nodes in the networks. Evaluating various quality of fit metrics then gives us insight into the underlying number of degrees of freedom that must be captured in order to effectively model these interactions. In the future, high-throughput SANS (*vide infra*) can be used to selectively reinforce areas of the network with low connectivity which provides for a much more robust fit to the data.

Increasing the Throughput of SANS. SANS is an invaluable measurement technique for the characterization of many soft matter and biological systems; however, acquisition time is costly and severely limited in supply. Therefore, accurately estimating the minimum experimental time required to achieve a given state of knowledge is of high value. An algorithm, predicted by simulation of SANS data using Monte Carlo (MC) bootstrapping, has been proposed to accelerate small angle neutron scattering (SANS) experiments by reducing the measurement time while achieving comparable accuracy in parameter estimation within 5% error tolerance and model differentiation. We measured SANS data for model block copolymer micelles, contrast matched chains, and protein hydrogels was acquired in narrow time slices, allowing the generation of experimental data across a wide range of data acquisition timesThe scattering data with reduced numbers of counts and full number of counts were fitted to SANS model functions to perform parameter estimation and model differentiation. For parameter estimation, we found that we were able to reduce the number of counts

down to 0.01, 0.1, and 0.5to 1%, 10%, and 50% of fraction of the original total counts for the polymer in solution, the spherical micelle, and the protein hydrogel, respectively, while still achieving parameter estimation to within 5% of the parameter estimated from full total counts. For model differentiation, Akaike Information Criterion (AIC) and Bayesian Information Criterion (BIC) as the criteria for model differentiation and are used to predict the best fit, found that reduced numbers of counts could identify the best model for our samples from a group of related candidate models for each material. We also compared the uncertainty of parameter estimation from MC bootstrapping with experimental replicates at 0.01 fraction of counts. We found that the variance of the parameter distribution in experimental replicates is smaller than bootstrapping replicates. This algorithm can help SANS users optimize valuable beamtime and accelerate the structural characterization using SANS for libraries of materials while reliably obtaining reliable parameter estimation and model differentiation.

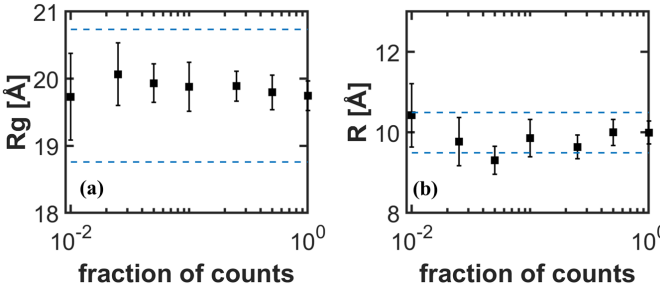

Figure 3. (a) Radius of gyration (R_g) as a function of the fraction of total counts. The error bars are 95% confidence intervals from the curve fitting. The dashed blueline represents 5% of the R_g value extracted from the total counts' dataset. (b) Micelle radius as a function of the fraction of total counts. The error bars are 95% confidence intervals from the curve fitting. The dashed blueline represents 5% of the value extracted from the total counts' dataset.

Protein Polymer Materials. A final key aim of our work was to measure the interactions of ELPs as a function of sequence based on measurements of solubility in cosolvents and buffers. To quantify interactions, we systematically designed, synthesized and studied a library of different ELPs with monomer substitutions to measure the effect of those substitutions on solubility as a function of ethanol and sodium chloride concentration. We synthesized a library of seven different ELPs, and measured their transition temperature at protein concentration of 1mg/mL for ethanol concentration from 0 to 40 vol% and sodium chloride concentration from 0 to 200mM. Measurements were performed with and without the 6xHis purification tag because of the key role that it can have on solubility. This data provides a comprehensive study of the effect of sequence design on cononsolvency in ELP protein polymers, a major discovery originally made by our group that is now more fully understood in its scope and importance as a result of this work. A manuscript is in preparation on this cononsolvency effect.

Future Plans

With the development of sequence self-consistent field theory (SCFT), it is now possible to solve for the equilibrium morphology of a fully sequence-defined polymers. However, the dimensionality of the sequence design space is still prohibitively large for a full combinatorial screening of all possible morphologies. Inverse design promises to speed up discovery of novel morphologies by back-calculating the sequence design necessary to generate a desired target. Building from SCFT, we are investigating the inversion of the SCFT equations, combined with alternate ways of representing sequence functions as a combination of spectral basis functions. A limited implementation of the adjoint method has shown promising results. By treating the chemical potential field as a Chebyshev series, a profile that returns the lamellar phase was constructed by treating the problem as a PDE constrained optimization. However, more work is required to extend this result through all the remaining self-consistent equations, as well as make the algorithm robust enough to solve highly complex morphologies.

Predictions are then synthesized using protein expression to test the ability to discover new nanostructures. Initially, we tried to target the formation of cylinders on a square lattice (p4mm); normally they form only on a hexagonal lattice (p6mm). Using our algorithm, we were able to produce a small number of predictions for sequence functions where the square lattice was lower free energy than the hexagonal lattice. These then had to be translated into protein sequences. In order to estimate the relative interaction parameters, we used a simple group contribution methods[119] to estimate ELP interactions and provide the effective Flory-Huggins functional needed to predict self-assembly. We then designed six different sequences that were the exact target design and the target design shifted slightly to both sides in composition as shown in Table 1.

Table 1. ELP sequences targeting p4mm phase.

Name	**ELP sequence**
SN65	$(VPGSG)_{26}(VPGNG)_{35}(VPGSG)_{39}$
SN75	$(VPGSG)_{30}(VPGNG)_{25}(VPGSG)_{45}$
SN85	$(VPGSG)_{34}(VPGNG)_{15}(VPGSG)_{51}$
SI65	$(VPGSG)_{26}(VPGIG)_{35}(VPGSG)_{39}$
SI75	$(VPGSG)_{30}(VPGIG)_{25}(VPGSG)_{45}$
SI85	$(VPGSG)_{34}(VPGIG)_{15}(VPGSG)_{51}$

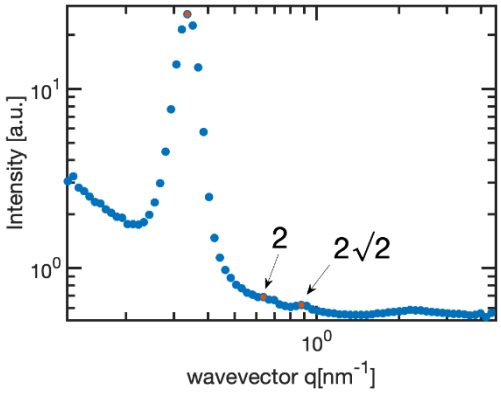

Figure 7. SANS scattering pattern for SI65 at 60°C. The peaks are shown in orange. The structure corresponds to p6mm. The $\sqrt{3}$ peak was suppressed.

Genes encoding for all these sequence-designed protein polymers were purchased, cloned, and expressed and purified to yield the protein materials. Using recently developed methods for optimizing protein expression, combinatorial strain/plasmid screens were performed to determine high yield conditions, of which all proteins were found to exhibit selectively high growth in the pETSUMO plasmid and C41(DE3) cell strain.[120] The purified proteins were dissolved at 50% w/v and SANS was used to characterize their phase formation at 20°C and 60°C. For SN65, SN75, SN85, the samples were liquid like and disordered according to the scattering patterns. We did not have enough protein samples for SI75 and SI85 at the beamtime due to difficulties in protein purification, but we were able to obtain SANS scattering pattern for SI65 at both 20°C and 60°C, which corresponds to hexagonally packed cylinders or *p6mm*. We will be performing SAXS on concentration series of all six of the triblocks to analyze their phase formation and phase diagram as a function of water content. Random phase approximation will be used to calculate the interaction parameters and the value will be compared against the target values in the gene design. Our future work is building on these initial efforts to produce a more cohesive and accurate design pipeline.

Publications

1. “Hindered Segmental Dynamics in Associative Protein Hydrogels Studied by Neutron Spin Echo.” A. Rao, H. Yao, and B.D. Olsen. *Physical Review Materials* **2023***, 7,* 075602.

2. “Predicting Transport of Intra-Articularly Injected Growth Factor Fusion Proteins Into Human Knee Joint Cartilage.” Y. Krishnan, Y.J. Yang, S.K. Branes, H.-H.K. Hung, B.D. Olsen, P.T. Hammond, and A.J. Grodzinsky. *Acta Biomaterialia* **2022**, *153*, 243-259.

3. “EXPANSE: A Time-of-Flight Expanded Angle Neutron Spin Echo Spectrometer at the Second Target Station of the Spallation Neutron Source.” C. Do, R. Ashkar, C. Boone, W.R. Chen, G. Ehlers, P. Falus, A. Faraone, J.S. Gardner, V. Graves, T. Huegle, R. Katsumata, D. Kent, J.Y.Y. Lin, B. McHargue, B.D. Olsen, Y. Wang, and D. Wilson. *Review of Scientific Instruments* **2022**, *93*, 075107.

4. Xie, O.; Olsen, B. D. “A Self-Consistent Field Theory Formalism for Sequence-Defined Polymers.” *Macromolecules* **2022,** *55* (15), 6516-6524.

5. Xie, O. and Olsen, B.D. “Fourier Spectra of Polymer Sequences Guide the Reduction of Sequence-Controlled Polymer Design Space.” *Submitted* **2023**.

Designing an *in situ* tribometer for neutron reflectivity measurements of soft gels

Angela Pitenis (UC Santa Barbara)

Keywords: friction, hydrogels, gradients

Research Scope

Hydrogels are three-dimensional polymer networks held together by crosslinks and swollen in water. This class of materials is commonly used to retain moisture and reduce friction across many industrial applications (e.g., biomedical devices, oil recovery, and consumer products). However, the fundamental mechanisms of hydrogel lubrication are not completely understood, which can frustrate efforts to design low friction hydrogel-based materials and coatings. Furthermore, hydrogel structures within the bulk and near the surface are heterogeneous and dynamic. Depending on hydrogel polymerization conditions, polymer density is thought to increase gradually (steep depth-wise gradient) or rapidly (shallow gradient) from the surface to the bulk [1-4]. Characterizing the polymer density and thickness of the surface gel layer is needed to establish structure-property relationships in hydrogel mechanics and lubrication. The primary goal of this work is to develop a new sample environment ("Tribo-NR") for neutron reflectivity that will enable the application of compressive (normal) loads and shear (lateral) forces to hydrogels against rigid and flat surfaces *in situ* during neutron reflectivity experiments.

Recent Progress

Since the start of these research efforts in the Fall 2023, our group has refined the design of the custom Tribo-NR sample environment using CAD software and incorporated 3D models of actual components (e.g., motorized stages, load cell, adapter plates, enclosure) into the prototype. Our group is currently using an existing tribometer in our laboratory to investigate mounting and clamping options for large gel samples (50 mm diameter) that will be used for the Tribo-NR. We have been in frequent communication with Dr. Erik Watkins at Oak Ridge National Laboratory who has assisted in the informed design of the instrument and its operation in the neutron beamline.

Future Plans

Once the working prototype of the Tribo-NR is constructed, we will conduct validation measurements at UC Santa Barbara prior to installing it on the beamline at Oak Ridge National Laboratory. Our first experiments with the Tribo-NR will involve polyacrylamide hydrogel samples in compression, similar to those conducted by the Spencer group [3]. Our group has extensive experience working with this type of material system [2,4]. We will compare the polymer density profiles of polyacrylamide hydrogels in pure compression with those in sliding experiments to test the competing hypotheses that polymer density at the hydrogel surface either 1) remains as high in sliding as it is in pure compression due to poroelasticity and polymer relaxation, or 2) is reduced during sliding by the entrainment of fluid within the mesh and rehydration.

References

1. Kii, Akishige; Xu, Jian; Gong, Jian Ping; Osada, Yoshihito; Zhang, Xianmin, *Heterogeneous Polymerization of Hydrogels on Hydrophobic Substrate*, Journal of Physical Chemistry B **105**, 4565-4571 (2001)
2. A.A. Pitenis, J.M. Urueña, A.C. Cooper, T.E. Angelini, W.G. Sawyer, *Superlubricity in Gemini Hydrogels*, Journal of Tribology **138**, 21– 23 (2016)
3. Y. Gombert, R. Simic, F. Roncoroni, M. Duebner, T. Geue, N.D. Spencer, *Structuring Hydrogel Surfaces for Tribology*, Advanced Materials Interfaces **6** 1901320 (2019)
4. A.L. Chau, C.E.R. Edwards, M.E. Helgeson, A.A. Pitenis, *Designing Superlubricious Hydrogels from Spontaneous Peroxidation Gradients*, ACS Applied Materials & Interfaces, **15**, 43075–43086 (2023)

Publications

N/A

Deciphering Low Energy Spin and Orbital Dynamics in Frustrated Quantum Magnets

Kemp Plumb, Brown University, Department of Physics, Providence, RI 02912

Keywords: Frustrated magnetism, quantum spin liquids, orbital physics, Kitaev interaction, inelastic neutron scattering

Research Scope

Quantum spin liquids are novel states of matter that exist in magnetic materials near absolute zero and are defined by the presence of long-range entanglement. They are of fundamental interest because they defy the conventional paradigm of symmetry breaking and local order parameters, while at the same time have great practical significance for future quantum information applications. These quantum states are predicted to appear in frustrated magnetic materials where magnetic interactions compete to destabilize classical magnetic ordering. Typically, these phases emerge in materials with many closely competing electronic energy scales, but they are notoriously difficult to predict. Tantamount to this theoretical challenge is the experimental task of identifying such quantum states of matter.

The overarching goal is to obtain a detailed quantitative understanding of the interplay between spin, orbital, and lattice energy scales in materials where strong spin-orbit coupling and strong electronic correlations compete to determine the ground state. We employ a suite of inelastic and elastic neutron scattering techniques to uncover the order and collective excitations that characterize quantum ground states in model materials. Emphasis is placed on materials with strong-spin orbit coupling and orbital degeneracy. In this case, spin orbit coupling can overcome the tendency towards degeneracy breaking Jahn-Teller distortions and quantum fluctuations between the spin+orbital configurations can dominate the ground state giving rise to multipolar orderings and quantum spin-orbital liquids.

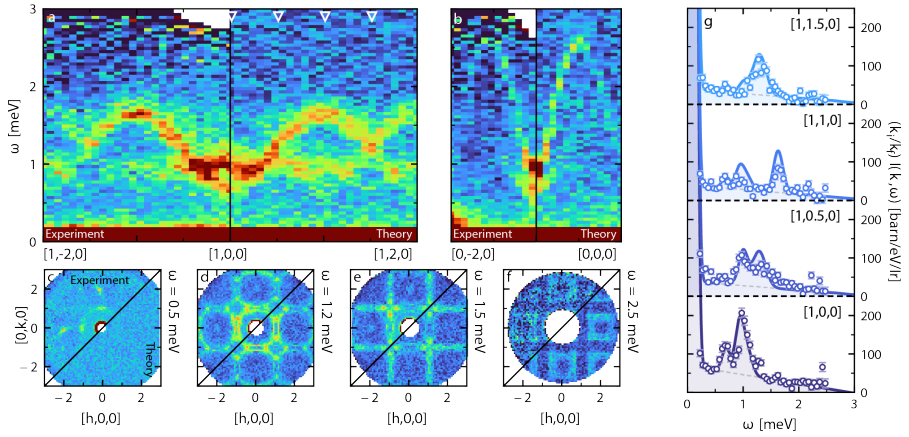

Figure 9: (a) Inelastic neutron scattering and non-linear spin wave model for K_2Ir2Cl_6. The observed excitation gap is generated by significant quantum zero-point fluctuations on the FCC lattice. Semi-classical linear spin wave theory fails at even a qualitative level, but non-linear theory quantitatively captures all features of the spectra [S1].

Recent Progress

Spin+orbital magnets: In $GaTa_4Se_8$ a single unpaired electron occupies the highest molecular orbital of tetrahedral clusters. The molecular orbital wavefunctions maintain the character of the d-orbitals and strong spin-orbit coupling results in the formation of highly quantum j_{eff}=3/2 molecular orbitals [1, 2]. Exchange interactions between the spin-orbital entangled j_{eff}=3/2 states can potentially stabilize

multipolar ordering and/or a spin orbital liquid phase on the FCC lattice of $GaTa_4Se_8$. On the other hand, depending on the balance of energy scales, Jahn-Teller instabilities can also act to locally remove the orbital degeneracy and stabilize a classical Neel state. We have completed a detailed investigation of the lattice dynamics around a spin-orbital singlet transition in the lacunar spinel $GaTa_4Se_8$ [P1]. Neutron pair distribution measurements reveal local distortions on Ta_4 clusters exist even in a nominally high symmetry cubic phase and neutron phonon density of states measurements reveal that these are dynamic. We have identified the phonon modes contributing to the dynamic local distortions and show they modulate intercluster bonds. Thus, we believe that these phonons mediate intercluster spin-obrital exchange and affect an orientational symmetry breaking spin-orbital singlet ground state in GaTa4Se8 [P1]. These measurements reveal how strong spin orbit coupling is strong can enable inter-site orbital exchange and act to generate magnetic phases with fluctuating spin and orbital degrees of freedom.

Highly frustrated magnets with anisotropic exchange: We have been investigating magnetic excitations in the frustrated FCC iridate K_2IrCl_6 [s2]. K_2IrCl_6 represents a near ideal realization of a canonical model of frustrated magnetism: the face centered cubic lattice antiferromagnet, but with the addition of Kitaev exchange interactions. The magnetic structure of this material was first measured in the 1960's [3]; however, the magnetic excitations have surprisingly not been investigated.

Our inelastic neutron scattering measurements on K_2IrCl_6 reveal a striking dichotomy of the static and dynamic correlations. Static correlations apparently indicate a classically ordered state, but the dynamic correlations are dominated by quantum fluctuations. Even though K_2IrCl_6 exhibits a well-formed Neel state and exhibits long-lived spin wave excitations, we find that non-linear corrections from quantum zero-point fluctuations are essential to describe the spectra at even a qualitative level [Fig. 1]. Using non-linear spin wave theory, we constrained the spin Hamiltonian and determine that K_2IrCl_6 is a near ideal realization of the nearest neighbor Heisenberg Kitaev antiferromagnet on the FCC lattice. The dominant magnetic interactions in K_2IrCl_6 have a sub-extensive degeneracy and favor ground state selection via quantum order-by-disorder, as revealed by the large excitation gap that is entirely due to quantum fluctuations [Fig. 1]. Inelastic neutron scattering measurements at intermediate temperatures reveal the appearance of correlated dynamic spin correlations and a novel nodal line spin-liquid state. Because the nodal line spin-liquid fluctuates in a *sub-extensively* degenerate manifiold, it is susceptible to perturbations, and in K_2IrCl_6 a weak but relevant next nearest neighbor exchange interaction usurps the spin liquid, selectig the observed Neel state at low temperature. Thus, magnetic order in K_2IrCl_6 reflects the sub-dominant interactions and is not a good basis for understanding the excitations.

Future Plans

We are aiming to develop a systematic understanding of the relative influence of spin-orbit coupling and Jahn-Teller instabilities in orbitaly degenerate systems, since the balance of these energy scales is tuned by chemical composition. Towards this goal, we have carried out an investigation of the lattice dynamics across the family of lacunar spines GaM_4X_8, M = (V, Nb, Ta), X = (S, Se), where atomic spin orbit coupling can be systematically varied by changing the transition metal site from V to Ta, and ligand hybridization varied by changing from S to Se.

We have synthesized single crystals of new rare earth based Kitaev materials and will continue exploring their phase diagram and excitations.

We have also begun an exploration of the influence of quenched disorder, or non-magnetic impurity substitution on the FCC lattice. In contrast to thermal and quantum fluctuations that both stabilize collinear magnetic ordering, magnetic dilution, or quenched disorder, favors anti-collinear states. In the limit of weak dilution, the competition between quenched disorder and fluctuations (thermal and quantum) should stabilize an intermediate spiral state. Thus, it may be possible to tune between collinear and spiral like magnetic orders with weak magnetic dilution in K2IrCl6. We aim to map the phase diagram for weak magnetic dilution, well below the percolation threshold, and explore the evolution of the finite temperature nodal line spin liquid state into a possible spiral spin liquid.

References

1. H. S. Kim et al, Spin-orbital entangled molecular j_{eff} states in lacunar spinel compounds. *Nat. Commun*. 5, 3988 (2014).
2. M. Y. Jeong et al., Direct experimental observation of the molecular J eff = 2 ground state in the lacunar spinel $GaTa_4Se_8$, *Nat. Commun.* 8, 782 (2017).
3. Hutchings and Windsor, The magnetic structure of K_2IrCl_6, *Proc. Phys. Soc.* 91, 928 (1967)
4. C. L. Henley, Ordering by disorder: Ground-state selection in FCC vector antiferromagnets, *J. Appl. Phys.* 61 3962 (1987)

Publications

[P1] Tsung-Han Yang, S. Kawamoto, T. Higo, SuYin Grass Wang, M. B. Stone, Jeorg Neuefeind, Jacob P. C. Ruff, Milinda Abeykoon, Yu-Sheng Chen, S. Nakatsuji, K. W. Plumb, Bond Ordering and Molecular Spin-Orbital Fluctuations in the Cluster Mott Insulator $GaTa_4Se_8$. Phys. Rev. Research 4, 033123 (2022).

Submitted

[S1] Tsung-Han Yang, Tieyan Chang, Yu-Sheng Chen, K. W. Plumb, Spin-orbital ordering and continuous phase transition in the cluster Mott insulator $GaNb_4Se_8$, (2023).

[S2] Q. Wang, J. A. Rodriguez-Rivera, Andrey Podlesnyak, Wei Tian, Masaaki Matsuda, Philip J. Ryan, Jong-Woo Kim, Jeffrey G. Rau, Kemp W. Plumb, Pulling Order Back from the Brink of Disorder in the FCC iridate K_2IrCl_6 (2023).

Neutron and X-ray Scattering Analysis of Organic Mixed Ionic Conducting (OMIEC) Composite Formulations from Blends of Conjugated Polymers and Block-Copolymers

Lilo D. Pozzo, Boeing-Roundhill Professor of Chemical Engineering, University of Washington, Seattle WA

Keywords: Conjugated polymers, block copolymers, small angle neutron scattering, automation, artificial intelligence.

Research Scope

Polymer blends, harnessing desirable properties from two or more complementary materials, have important applications in medical implants, electronics, and clean energy amongst others. In this project we investigate how polymer-polymer and polymer-solvent interactions affect the phase morphology and performance in composite polymer formulations comprised of a non-conjugated block-polymer component and a conjugated (conductive or semi-conductive) polymer additive in solution and in the solid state. These complex blends are of interest for organic electronic device applications as the matrix component complements conductive polymers with important properties such as mechanical durability, environmental stability, long-range organization, and/or ionic conductivity. Meanwhile the conjugated component retains good optoelectronic performance at loading fractions as low as 1 wt%.[1] The use of formulations to tune structure and properties of composite conjugated soft materials can simplify the molecular design process since it is possible to 'swap' components and to modify formulation compositions without invoking complex synthesis of new macromolecules. However, this also opens a large design space that is poorly understood and where there are few established design rules to optimize materials. Thus, new methods are essential to the effective navigation of the design space.

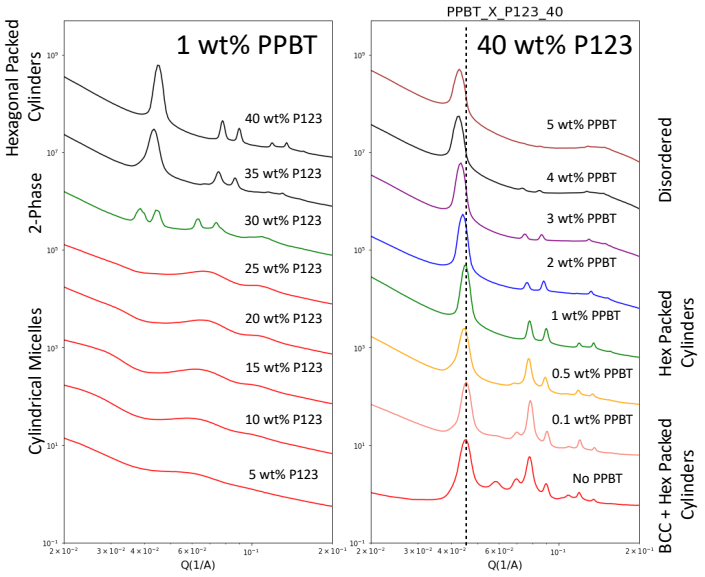

Figure 1. SAXS profiles from Pluronic P123 block-copolymer mesophases with integrated conjugated polymer Poly[3-(Potassium-4-butanoate)thiophene-2,5-diyl] (PPBT) as a function of relative concentrations.

Small angle and ultra-small angle neutron and X-ray scattering (SANS/SAXS) are particularly useful tools to characterize complex composite blends and the resulting self-assembled conjugated polymer components over length scales spanning from micrometers to fractions of a nanometer. Moreover, these tools are amenable for integration in high-throughput (HT) analysis workflows where robotics/automation and artificial intelligence (AI) are leveraged to accelerate the exploration of large multidimensional design spaces. We use SANS and SAXS, as well as electrochemical testing to develop a deeper understanding of how molecular architecture, processing and composition affects structure and morphology, and how this ultimately modifies performance of these composite

materials. Moreover, we develop and integrate HT tools to facilitate the formulation, structural analysis, and ultimately to help develop phase diagrams of the resulting morphology of these materials.

We are specifically interested in formulation of structured composites where the non-conjugated component is a block copolymer capable of self-assembly into mesoscale structures with long range structural order (micelles and cubic, cylindrical, and lamellar mesophases). Structured blends can include functional ionic conducting block copolymers to produce composite organic mixed ionic electronic conductors (OMIECs) (**Figure 1**). SANS and SAXS experiments demonstrate that the block-copolymer templates can induce the organization of the conjugated polymer component over long length scales at significant loadings (up to 5wt%) without negatively affecting long-range order. We also develop and integrate laboratory automation and AI tools to accelerate developments in our understanding of phase behavior in complex multi-component systems such as these, where multiple dimensions or variables (e.g. chemistry, composition, architecture, solvents, and processing) are expected to control the resulting morphology and material properties.[2,3] These tools have broad applicability to further the use of neutron and X-ray scattering in accelerated materials discovery.

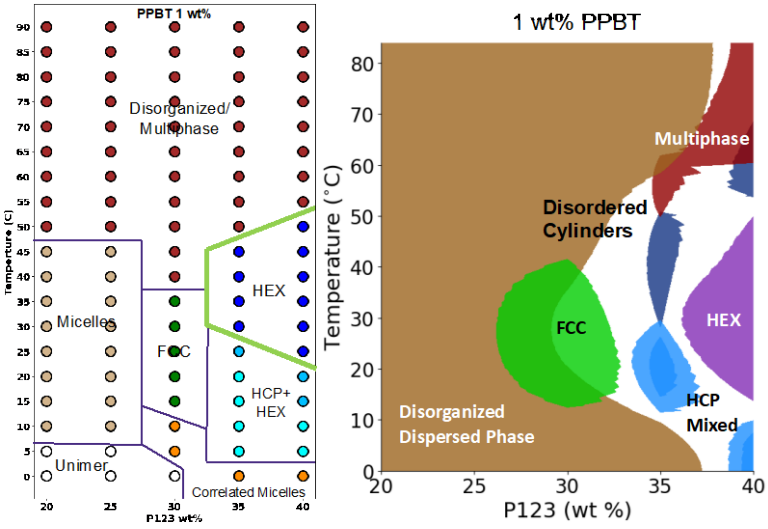

Figure 2. Phase diagram for PEO-PPO-PEO and PPBT blends at variable concentrations and temperatures. (Left) phase diagram developed by human categorization process. (Right) Automated phase map generated using un-supervised classification process.

Recent Progress

A HT workflow was developed to rapidly formulate large arrays of samples from amphiphilic block copolymers based on triblock polyethylene oxide (PEO) and polypropylene oxide (PPO) with the general architecture PEO_x-PPO_y-PEO_x in the presence of the water-soluble conjugated polymer poly-potassium-butanoate thiophene (PPBT). A liquid handling robotic platform was used to formulate several 100's of samples that were then screened with HT-SAXS at the Advanced Photon Source (APS) using a specially designed cartridge system in the 12_IDC SAXS beamline.[3] Phase diagrams were outlined both as a function of composition and as a function of temperature. **Figure 2** shows how a shape-similarity algorithm was developed and successfully used to automatically generate phase-diagrams from several hundreds of measurements without human intervention.[3] The algorithm captures the general trends that a laborious human-classified process can identify. **Figure 1** also outlines how the addition of a stiff conjugated polymer (PPBT) is able to bias the formation of

cylindrical morphologies. The conjugated polymer also causes the swelling of the lattice, indicating incorporation of the polymer. Recent Rheo-SANS experiments at the Australian Center for Neutron Scattering (ACNS) were also performed to demonstrate that mesophases incorporating conjugated polymers could be shear-aligned into single crystals as had been hypothesized in the project objectives (**Figure 3**).

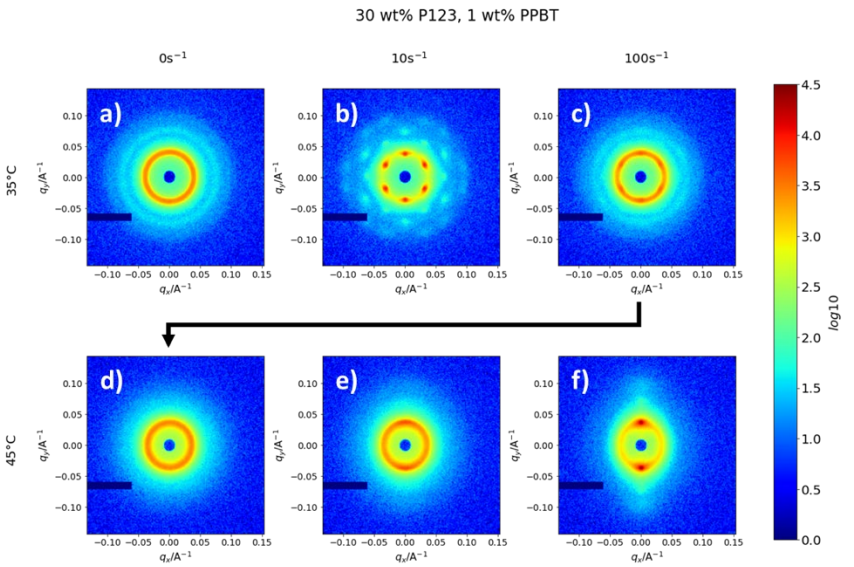

Figure 3. Rheo-SANS of OMIEC blends in steady shear. (a-c) Shows the effects of shear alignment on a composite sample in a cubic crystal morphology at 35C. (d-f) Shows the effect of shear alignment on the same sample after transition to a hexagonally packed cylinder morphology at 45C.

Recent advances also explored mechanochemical synthesis of high-χ block copolymers incorporating a fluoropolymer block (heptafluorobutyl acrylate or HFBA) and a hydrophilic ionic conducting polyether block (polyethylene glycol ethyl ether acrylate or PEGEEA).[4] The design principle here is that the fluoropolymer block facilitates interactions with hydrophobic conjugated polymers in organic solvents while the PEG-block facilitates ion conduction in formulated OMIECs after coating. These new block-copolymers were explored as structured ionic-conducting components in blends with poly-3-hexyl-thiophene (P3HT) to generate a new class of OMIEC materials. A family of PEGEEA-HFBA block-copolymers with variable block sizes and PEG side-chain lengths were synthesized and analyzed in solvents of varied quality to characterize their complexation in solution (SANS) and in the solid-state (SAXS). SANS experiments demonstrate successful formation of cylindrical micelle-like structures with P3HT at the core and the PEGEEA-HFBA copolymer decorating the surface.

Future Plans

In addition to completing the structural characterization of newly designed OMIEC materials, we will follow the initial analysis of PEGEEA-HFBA + P3HT blends with HT electrochemical screening using robotic facilities developed at Argonne National Laboratory (ANL). We have been allocated time in the PolyBot robotic platform and students working in this project will be spending 3 months at ANL (through a DOE SCGSR Fellowship) learning to use this platform and executing experiments in collaboration with ANL researchers (Dr. Jie Xu).[5] This tool will help to rapidly measure OMIEC performance metrics, such as transconductance, on formulated blends with PPBT and P3HT with variable block-copolymers and dopants. We will also continue expanding on the structural analysis of different versions of PEGEEA-HFBA blends with conjugated polymers, such as P3HT and PEDOT, to facilitate the formulation of new OMIEC materials. Initial experiments demonstrate the organic electrochemical transistors can be formulated with these materials, but their electrochemical switching speed is slow. We hypothesize that this is due to a sub-optimal selection of formulation parameters for structured blends that can be further optimized. SAXS will be used to analyze coated

materials and to correlate structural metrics with performance metrics obtained from HT electrochemical analyses. We aim to extract guiding principles from these experiments to help optimize other OMIEC blend materials. Furthermore, we continue to work on improving the toolkit that is available for the HT analysis of SANS/SAXS data to facilitate extraction of new knowledge. For example, we aim to integrate our autophase-map tool with an active sampling campaign to bias the selection of datapoints that facilitate identification of phase boundaries.

References

1. CM Wolf, L Guio, SC Scheiwiller, RP O'Hara, CK Luscombe, LD Pozzo, *Blend Morphology in Polythiophene–Polystyrene Composites from Neutron and X-ray Scattering*, Macromolecules, **54(6)**, 2960-2978 (2021)

2. K. Vaddi, H. Thart Chiang, L. Pozzo, *Autonomous retrosynthesis of gold nanoparticles via spectral shape matching*, Digital Discovery, **1**, 502-510, (2022)

3. K. Vaddi, K. Li, L. Pozzo, *Metric geometry tools for automatic structure phase map generation*, Digital Discovery, **2**, 1471-1483, (2023)

4. P. Chakma, S.M. Zeitler, F. Baum, J. Yu, W. Shindy, L.D. Pozzo, M.R. Golder, *Mechanoredox Catalysis Enables a Sustainable and Versatile Reversible Addition-Fragmentation Chain Transfer Polymerization Process*, Angewandte Chemie International Edition, **62(2)**, e202215733, (2023)

5. A. Vriza, H. Chan, J. Xu, *Self-driving laboratory for polymer electronics*, Chemistry of Materials, 35(8), 3046-3056, (2023)

Publications

1. K. Vaddi, K. Li, L. Pozzo, *Metric geometry tools for automatic structure phase map generation*, Digital Discovery, **2**, 1471-1483, (2023)

2. L.B. Zasada, L. Guio, A.A. Kamin, D. Dhakal, M. Monahan, G.T. Seidler, C.K. Luscombe, and D. J. Xiao, *Conjugated Metal–Organic Macrocycles: Synthesis, Characterization, and Electrical Conductivity*, Journal of the American Chemical Society, **144(10)**, 4515–4521, (2022)

3. C. Wolf, L. Guio, S. Scheiwiller, V. Pakhnyuk, C. Luscombe, L.D. Pozzo, *Strategies for the development of conjugated polymer molecular dynamics force fields validated with neutron and X-ray scattering*, ACS Polymers Au, **1(3)**, 134-152 (2021)

Neutron scattering investigation of novel phases created by application of electric field

Dmitry Reznik

Keywords: flash sintering, quantum materials, low-dimensional systems, copper oxide superconductors

Research Scope

Application of electric fields at high temperatures (few hundred C) to many inorganic materials has been shown to induce a nonlinear response, creating novel phases characterized by altered electronic and optical properties, structural modifications, and strong luminescence.[1] These phases can be made metastable at ambient conditions by a liquid nitrogen (LN_2) quench. For example normally transparent TiO_2 crystals become black and crystalline yttria-stabilized zirconia (YSZ) becomes shiny and turns into an electronic conductor. Our group found that this treatment enhances oxygen vacancy ordering in Pr_2CuO_4, which results in a strongly modified phonon spectrum and increased low temperature *c*-axis conductivity and magnetic susceptibility.[2] This enigmatic phenomenon is commonly referred to as Flash. This proposal aims to investigate it in the context of quantum materials.

The goal of our research is to uncover the atomistic mechanism of Flash, to use Flash combined with a quench to engineer new metastable quantum materials, and to learn if a new "control knob" could be developed based on tuning electric current and temperature during Flash. Other control knobs are chemical doping, pressure, magnetic field, etc. Developing and understanding these tuning parameters is one of the most important directions towards harnessing quantum materials.
The first thrust will focus on wide gap insulators YSZ, TiO_2, and $SrTiO_3$, with the goal of achieving atomistic understanding of Flash in single crystals. Second thrust will look into how to use Flash to alter structure and bulk properties of correlated copper and iridium oxides. The former belong to the copper oxide superconductor family, and the latter are well known for the unique interplay between electron-electron interactions and spin-orbit coupling. The third thrust will advance neutron-scattering-based techniques relevant for the first two thrusts and also for research on quantum and energy materials in general.

While many groups worldwide investigate the nonlinear response to electric fields, our focus on single crystal investigations and neutron scattering measurements sets our work apart and has already demonstrated feasibility.

At the core of the project are novel applications and development of the state-of-the-art neutron scattering techniques for fundamental research on electric field-modified materials that exhibit novel emergent phenomena and unique properties that could be impactful for clean energy technologies.
Our group has a strong track record in neutron scattering and computational techniques/modeling used to investigate materials similar to the ones discussed here. Preliminary results already demonstrated feasibility of the novel research approaches to understanding Flash and control of structure and properties of quantum materials.[2] The temporary shutdown of the SNS is the biggest obstacle to progress, but we have a research plan in place to address this, with the first year dedicated

to sample preparation, bulk measurements, x-ray diffraction, and the key neutron work planned for after the shutdown.

Project participants are developing a new sample environment allowing in-situ neutron scattering measurements at the SNS while electrical current flows through the sample at high temperature. This capability will be accessible to all SNS users. The project will also pioneer laptop-compatible software implementing new time-of-flight data analysis workflow, which will increase the analysis speed and reduce RAM requirements by an order of magnitude while eliminating the need for remote work on high performance computers. It builds on the Phonon Explorer software that is already in use by several neutron scattering groups.[3]

Recent Progress

We demonstrated a novel approach to the structural and electronic property modification of perovskites, focusing on Pr_2CuO_4, an undoped parent compound of a class of electron-doped copper-oxide superconductors. Currents were passed parallel or perpendicular to the copper-oxygen layers with the voltage ramped up until a rapid drop in the resistivity was achieved, a process referred to as ”Flash”.[1] The current was then further increased tenfold in current-control mode. This state was quenched by immersion into liquid nitrogen. Flash can drive many compounds into different atomic structures with new properties, whereas the quench freezes them into a long-lived state. Single-crystal neutron diffraction of as-grown and modified Pr_2CuO_4 revealed a $\sqrt{10}x\sqrt{10}$ superlattice due to oxygen-vacancy order. The diffraction peak intensities of the superlattice of the modified sample were significantly enhanced relative to the pristine sample. Raman-active phonons in the modified sample were considerably sharper. Measurements of electrical resistivity, magnetization and two-magnon Raman scattering indicate that the modification affected only the Pr-O layers, but not the Cu-O planes. These results point to enhanced oxygen-vacancy order in the modified samples well beyond what can be achieved without passing electrical current. Our work opens a new avenue toward electric field/quench control of structure and properties of layered perovskite oxides.[2]

In a different project, we used flash as a new method of creating a (132) Mangreli phase of TiO_2 that is very difficult to make by standard annealing techniques.[4] These phases occur in slightly oxygen-deficient TiO_2, where oxygen vacancies order into planes with the structure collapsing and sheets of Ti^{3+} appear as a result.

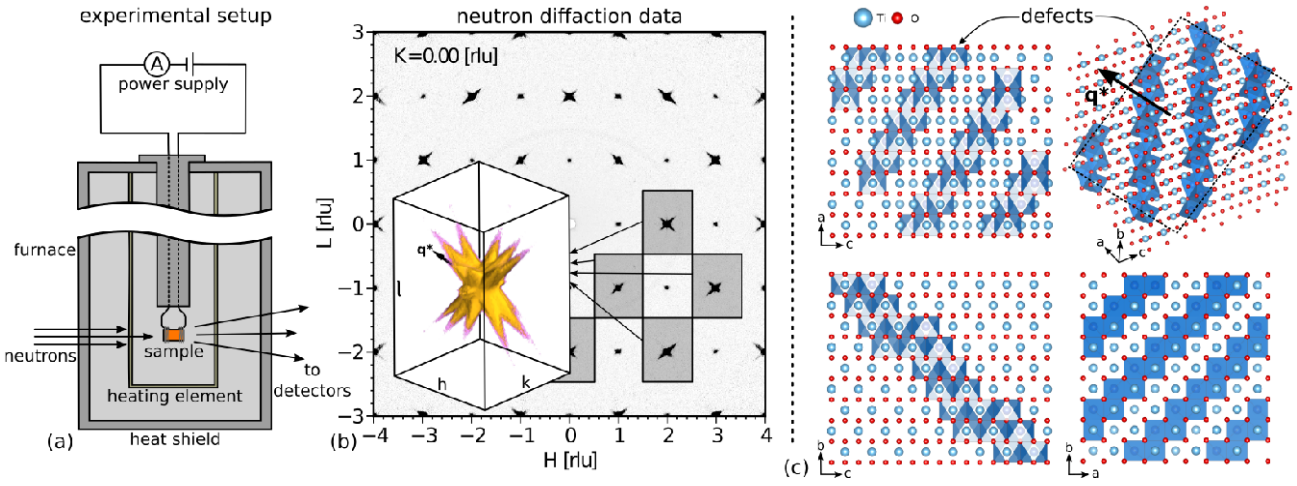

FIG. 1. (a) Schematic of the in-situ flash experiment. (b) Scattering pattern in the H-L plane with K=2. The inset in (b) shows the diffuse scattering features summed into the 1st Brillouin zone as discussed in the text. (c) A model of the Magnreli phase shear plane as described in ref. [2]. The vector q∗ in (c) and the inset in (b) point along (132). The displacement vector for the structure in (c) is 1/2[011].

We developed in-situ apparatus for performing measurements of diffuse scattering as well as of phonons on CORELLI and ARCS. The experiments on CORELLI were successfully completed whereas the first ARCS experiment failed due to problems with the instrument. We were able to identify the Mangreli phase thanks to characteristic rods in the diffuse scattering pattern that indicate the formation of parallel planes of defects perpendicular to the [132] reciprocal lattice vector. We also carried out ex-situ electrical resistivity and transport measurements on quenched samples and found very unusual properties that we are now trying to understand. (See for example, Fig. 2)

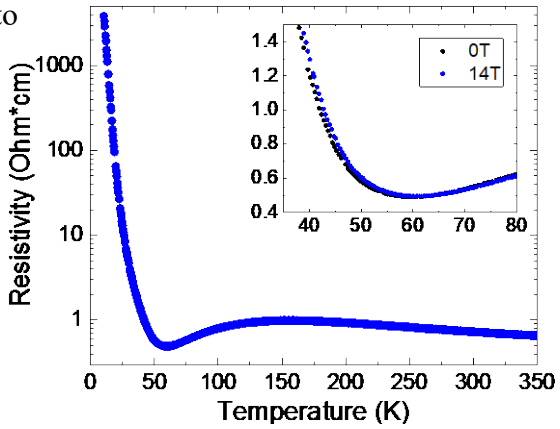

FIG. 2. Anomalous electrical resistivity of flashed TiO_2. The sharp rise towards low temperatures indicates a metal-insulator transition, possibly a Mott transition, which is a subject of the current investigation.

Future Plans

The research will involve a combination of materials synthesis, neutron scattering measurements, theory, and simulations. The focus will be on three topics:

1. Elucidating the physical mechanism underlying the nonlinear response during Flash.
2. Flash as a path to long-lived metastable quantum materials with new functionality.
3. Development of novel approaches that exploit the unique aspects of neutron scattering to investigate emergent behavior in materials on the atomic scale under strongly field driven steady-state conditions.

Measurements of local structure of single crystal samples of selected materials in-situ and in the quenched state by neutron diffraction on the CORELLI instrument at the SNS**.** Single crystal diffuse neutron scattering will be used to directly probe defect–defect correlations, i.e., the tendency for

defects to cluster into nanoscale ordered structures. The latter may be an important mechanism for the observed thresholding behavior. Accurate modeling of local structural distortions associated with the diffuse scattering will be performed, which will allow us to "forward-engineer" observed diffraction patterns as was done for TiO_2 (Fig. 6). Experimental results will be compared with the predictions of MD calculations and models of local structure. This work will establish which types of structural deformations and defects and at what concentrations appear in select materials during Flash. Furthermore, we will learn about nonlocal correlations.

Phonon measurements to establish phonon occupation numbers during Flash will be performed in-situ with the necessary sample environment already developed for both the SNS and HFIR. Away from thermal equilibrium, the occupation of each bosonic mode corresponds to an effective temperature, which can be measured separately for each excitation. This thrust will test the hypothesis that the Flash phenomenon is a result of nonthermal phonon occupation numbers induced by the electric current. Our group has extensive experience with investigating phonons away from thermal equilibrium.[5]

References

1. M. Yu, S. Grasso, R. Mckinnon, T. Saunders and M. J. Reece, Review of flash sintering: materials, mechanisms and modeling, Adv. Appl. Ceramics, **116**, 24 (2017)
2. S. Roy, Susmita Roy, Feng Ye, Zachary Morgan, Syed IA Jalali, Yu Zhang, Gang Cao, Nobu-Hisa Kaneko, Martin Greven, Rishi Raj, Dmitry Reznik*, Structural changes induced by electric currents in a single crystal of* Pr_2CuO_4, Phys Rev. Mat. **7**, 083803 (2023)
3. D. Reznik and I. Ahmadova, *Automating Analysis of Neutron Scattering Time-of-Flight Single Crystal Phonon Data,* Quantum Beam Science **4**, 41 (2020).
4. Eiichi Yagi and Ryukiti R Hasiguti *{312} Planar Faults in Slightly Vacuum-Reduced Rutile* (TiO_2). Journal of the Physical Society of Japan **43** 1998 (1977).
5. N. Pellatz, S. Roy, J.W. Lee, J.L. Schad, H. Kandel, N. Arndt, C.-B. Eom, A.F. Kemper, and D. Reznik, *Relaxation timescales and electron-phonon coupling in optically-pumped* $YBa_2Cu_3O_{6.9}$ *revealed by time-resolved Raman scattering,* Phys. Rev. B Letters **104**, L180505 (2021).

Publications

1. S. Roy, Susmita Roy, Feng Ye, Zachary Morgan, Syed IA Jalali, Yu Zhang, Gang Cao, Nobu-Hisa Kaneko, Martin Greven, Rishi Raj, Dmitry Reznik*, Structural changes induced by electric currents in a single crystal of* Pr_2CuO_4, Phys Rev. Mat. **7**, 083803 (2023)
2. N. J. Weadock, T. C. Sterling, J. A. Vigil, A. Gold-Parker, I. C. Smith, B. Ahammed, M. J Krogstad, F. Ye, D. Voneshen, P. M. Gehring, A. M. Rappe, H.-G. Steinrück, E. Ertekin, H. I. Karunadasa, D. Reznik, M. F. Toney, *The nature of dynamic local order in* $CH_3NH_3PbI_3$ *and* $CH_3NH_3PbBr_3$, Joule **7**, 1051 (2023)
3. S. Roy, T.C. Sterling, D. Parshall, E. Toberer, M. Christensen, D.T. Adroja, and D. Reznik, *Occupational disorder as the origin of flattening of the acoustic phonon branches in the clathrate* $Ba_8Ga_{16}Ge_{30}$, Phys. Rev. B Letters **107**, L020301 (2023)
4. P. Kurzhals, G. Kremer, T. Jaouen, C. W. Nicholson, R. Heid, P. Nagel, J.-P. Castellan, A. Ivanov, M. Muntwiler, M. Rumo, B. Salzmann, V. N. Strocov, D. Reznik, C. Monney, F. Weber, *Electron-momentum dependence of electron-phonon coupling underlies dramatic phonon renormalization in* YNi_2B_2C Nature Comms. **13** (1), 228 (2022)
5. A. Sokolik, S. Hakani, S. Roy, N. Pellatz, H. Zhao, G. Cao, I. Kimchi, D. Reznik, *Spinons and damped phonons in spin-1/2 quantum-liquid* $Ba_4Ir_3O_{10}$ *observed by Raman scattering,* Phys. Rev. B **106**, 075108 (2022)
6. Ph. Kurzhals, G. Kremer[2], Th. Jaouen, C. W. Nicholson, R. Heid, P. Nagel, J.-P. Castellan, A. Ivanov, M. Muntwiler, M. Rumo, B. Salzmann, V. N. Strocov, D. Reznik, C. Monney, and F. Weber, *Electron-momentum*

dependence of electron-phonon coupling underlies dramatic phonon renormalization in YNi_2B_2C, Nature Communications, **13,** 228 (2022).

Process-Structure Relationships of Lithium-Ion Battery Cathodes

Dr. Jeffrey J. Richards, Department of Chemical and Biological Engineering, Northwestern University

Keywords: Small-angle neutron scattering, lithium-ion batteries, rheology, in situ experiments

Research Scope

Understanding the link between how porous lithium-ion battery (LIB) electrodes are manufactured and the structure-function relationships that determine the performance is critical to accelerating the development of emergent battery technologies with higher rate cycling and capacity[1]. Porous electrodes are manufactured by suspending a mixture of micron-sized electrochemically active material, polymer binder, and carbon black (CB) in a solvent and depositing it onto a metallic current collector. The complex processing conditions encountered during formulation create many challenges for quantifying structure-property relationships. The overall goal of this DOE project is to leverage advanced neutron scattering techniques to understand what formulation and processing conditions are necessary for achieving electrode structures that are responsible for high-performance LIB.

To gain this fundamental understanding, the focus of the research effort includes three objectives: (1) Quantifying the microstructure of carbon black in LIB slurries, (2) Processing-structure relationships in slurries using slot-die coating, and (3) *In operando* studies of porous electrodes in relevant electrochemical contexts.

Recent Progress

The funded project started in September 2021 and for the past two years, the team has made significant progress towards the aims described in the research proposal. The team, together with the scientists at Oak Ridge National Laboratory, has also secured a 3-year collaborative beamtime proposal for SANS measurements at Spallation Neutron Source (BL-6 EQ-SANS).

Rheo-Electric Measurements of LIB slurries

Engineering slurry formulation and coating processes to form highly conductive and mechanically robust cathodes require quantitative prediction of the CB microstructure evolution in the slurry[2]. We first focused on developing a framework for quantifying the microstructural evolution of CB and revealing how it can be linked to the slurry rheological and electrical properties. By conducting simultaneous rheo-electric measurements on CB/polyvinylidene difluoride (PVDF) suspensions, we showed that the fluid Mason number (Mn_f), which describes the balance between the hydrodynamic force and the cohesive force, can predict the structure of CB regardless of the PVDF molecular weight and loading. In Fig 1A, for suspensions containing the same weight percent of CB, the relative viscosity is collapsed into a single master curve as a function of Mn_f, suggesting that the addition of polymers only indirectly modifies the CB structure by increasing the medium viscosity. By using this microstructural link, we then showed that the dielectric strength (Fig 1B), a scalar descriptor for electron polarization within a conductive cluster, can also be collapsed into master curves. Combining the rheo-USANS data[3] measured previously by the group, we further attributed the power-law scaling observed in the strong flow regime to the self-similar breakup of CB agglomerates. These results reveal a microstructural connection linking slurry rheology to its electrical response which can be used to guide the design of processes that control the mechanical and electrical properties of slurry coatings.

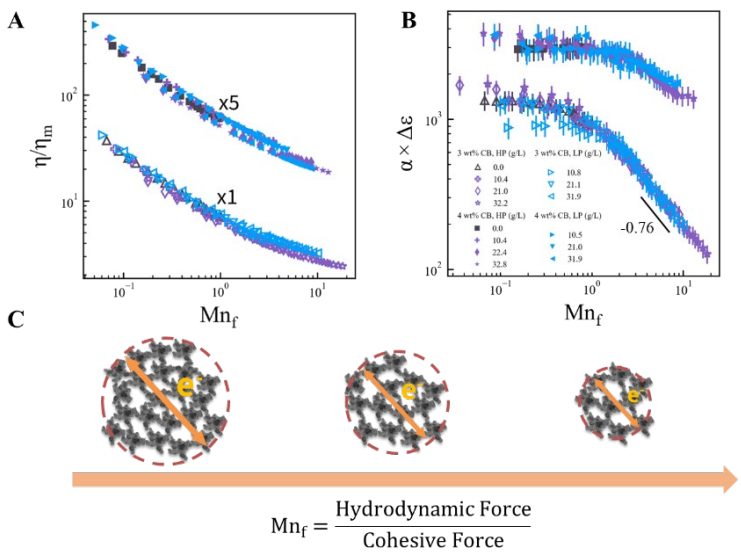

Figure 1. Shear-Dependent Rheology and Dielectric Properties of Carbon Black in Polymer Solutions. (A). *Viscosity normalized to the medium viscosity plotted against the Mason number. Samples are 3 wt% CB and 4 wt% CB added with polymers of different molecular weights and loadings.* ***(B).*** *Dielectric strength shifted by a factor of unity plotted against the Mason number. Power-law scaling, indicated with a solid line, is observed for the 3 wt. % sample group, and the power-law value is −0.76.* ***(C).*** *Illustration of CB agglomerate as a function of the Mason number. Increasing Mason number leads to smaller agglomerate size and dielectric strength.*

Slot-Die Coater Designed for SANS Measurements of LIB Slurries

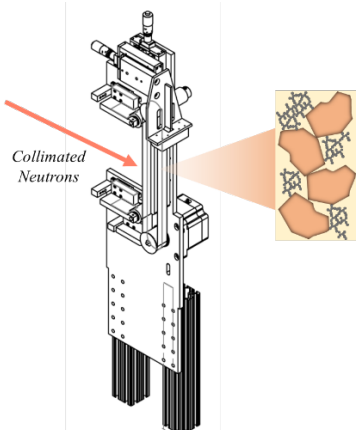

Figure 2. *Illustration of the custom-made slot-die coater operating under simultaneous neutron measurements.*

At the industrial scale, manufacturing of LIB cathodes is often performed in a roll-to-roll fashion using conditions that are very different than those that can be generated with existing sample environments available at neutron facilities in the US. The last two decades have seen the proliferation of *in situ* Rheo-SANS techniques that have sought to link processing with well-defined flow fields to microstructure and interrogate material behavior far from equilibrium. However, roll-to-roll processing involves complex flow fields that mix extensional flows, shear flows, and capillary interactions that cannot be easily mimicked in more idealized laboratory instruments. To investigate the structural evolution of LIB slurries under slot-die coating conditions, we have fabricated a custom-made slot-die coater (Fig 2) that is compatible with the SANS instrument at ORNL (BL-6, SNS). This versatile sample environment will enable not only the quantifications of the structure formed under different industrial-relevant processing conditions but also the temporal characterization of structural evolution under drying conditions. The initial feasibility has been evaluated by the beamline scientists.

Generalized Contrast-Variation Method for Nanoscale Characterization of LIB Cathodes

The electrochemical performance of LIBs heavily depends on the interfaces that form between the porous cathodes and the electrolytes in assembled battery cells. Despite numerous efforts to investigate these interfaces, most characterization techniques are limited to *ex situ* analysis and cannot simultaneously provide information on the structure and the chemical composition. SANS is a well-suited technique for characterizing these interfaces as it is the only *in situ* method as contrast variation can reveal both the structural and chemical information at the nanoscale. Our initial efforts focused on establishing a new framework for analyzing contrast-variation SANS (CV-SANS) data that can be leveraged to obtain quantitative information on the LIB cathode interface.

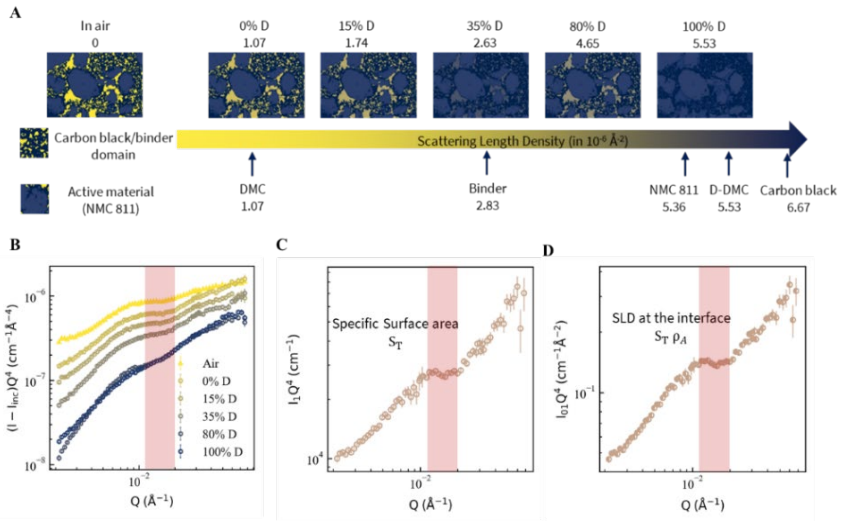

Figure 3. CV-SANS Measurements on a LIB Cathode and Generalized-CV Method Analysis. (A). *Cartoon illustration of the contrast variation series measurements using an X-ray tomography image from Xu et al.*[5] *.* ***(B).*** *Porod's plots of subtracted 1D scattering curves.* ***(C).*** *The basic function I_1 obtained from the Gen-CV method. The specific surface area accessible to solvent is highlighted in the shaded region.* ***(D).*** *The basic function I_{01} obtained from the Gen-CV method. The specific surface area accessible to solvent weighted by the SLD is highlighted in the shaded region.*

In Fig 3A, we illustrate a series of CV-SANS measurements conducted on one cathode by showing scattering length densities (SLD) with the colormap. The Porod's plot (IQ^4 vs. Q) of the 1D SANS curves at different solvent SLDs is shown in Fig 3B, and the region where the electrode/solvent

interface is probed is highlighted. The power-law scaling in the highlighted region changes as a function of solvent SLD, suggesting that unresolved structural features that are not interfacial scattering are present. To fully exploit the information contained within the CV-SANS data, we developed a generalized contrast-variation method (Gen-CV) that builds upon the contrast-variation method first proposed by Sturman for characterizing particles in suspensions[4]. We decomposed the whole series of CV-SANS curves into three basic functions: I_1, I_{01}, and I_0. As shown in Fig 3C, I_1 is the scattering of the solid phase without considering the SLD, and therefore can be regarded as the shape of the solid phase. A closer look at I_1 shows a Porod's region unambiguously in the previously hypothesized Q region. $I_1 Q^4$ obtained in the shaded region is quantitatively the same as the specific surface area, S_T, that is accessible to the solvent. To further extract the surface-averaged chemical information at the interface, we can simply calculate $\frac{\langle I_{01} Q^4 \rangle}{\langle I_1 Q^4 \rangle}$ in the same Q region of interest, as highlighted in Fig 3D. In addition to the structural and chemical properties at the interface, the decomposition of the basic functions allows us to directly compare the dry and wet electrode structures. As shown in Fig 4A, I_0 is the scattering of the wet electrode structure at 0 solvent SLD, and the wet and dry structures are distinctly different. Both quantitative differences observed can be explained by the polymer conformational changes induced by the addition of solvent. Therefore, by using the Gen-CV method and extracting three basic functions, we can obtain valuable nanoscale structural and chemical information of LIB cathodes at the electrode/solvent interface and compare directly the wet and dry structures. We further leveraged the interfacial information obtained from scattering measurements to differentiate the species at the interface. In collaboration with the Lopez lab at Northwestern University, we manufactured electrodes with varying processing conditions (coating speed, slurry solid content, and calendaring). As shown in Fig 4B, we observed a strong correlation between the capacity at cycle 100 and the amount of CB surface exposed to solvent. This trend is consistent with the literature which shows that CB surface facilitates parasitic reactions that accelerate performance deterioration. In addition, we observed that for electrodes manufactured from high coating speed, less CB surface is present at the electrode/solvent interface, which we attribute to better dispersion and coverage of PVDF.

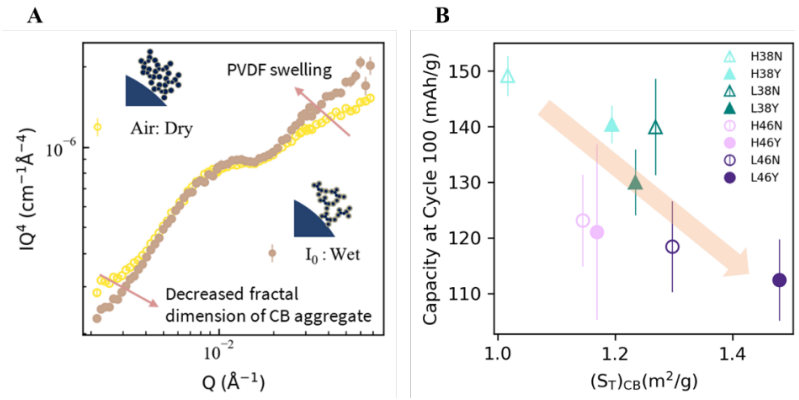

Figure 4. Microstructural Insight Obtained from Gen-CV method. (A). *Porod's plot of the dry structure (I_{air}) and wet structure (I_0) scattering data. structural differences at two length scales are observed and can be explained by the swelling of polymer chains.* ***(B).*** *The performance of cathodes manufactured at various conditions plotted against the solvent-accessible CB surface area obtained from Gen-CV method. More solvent-accessible CB surface area is correlated to lower performance at the 100th cycle, suggesting more cathode degradation.*

Future Plans

1. To validate the microstructural link identified in rheo-electric measurements of LIB slurries, we will conduct rheo-USANS measurements to probe the structure of CB. Furthermore, we will extend our studies to LIB slurries containing active materials.

2. The custom-made slot-die coater will be tested in late 2024 after the restart of SNS. We will conduct feasibility tests and a set of experiments to demonstrate the applications of the sample environment. We anticipate that this sample environment will be highly integrated as part of the BL-6 environment and other users can leverage this sample environment to investigate the processing of any solution-based systems that exist ubiquitously in the energy storage space.
3. The successful development of the Gen-CV method shows that there are quantitative links between the structure and properties of LIB cathodes. We will further use CV-SANS to quantify the structural evolution of LIB electrodes *operando***.**

References: (1) Hawley, W. B. & Li, J., *J Energy Storage* 25, 100862 (2019). (2) Saraka, R. M., Morelly, S. L., Tang, M. H. & Alvarez, N. J., *ACS Appl Energy Mater* 3, 11681–11689 (2020). (3) Hipp, J. B., Richards, J. J. & Wagner, N. *J., J Rheol (N Y N Y)* 65, 145–157 (2021). (4) Feigin, L. A. & Svergun, D. I. *(Springer US, 2013)*. (5). Lu, X. et al. *Nature Communications 2020 11:1* **11**, 1–13 (2020).

Publications (2022 - Present)

1. Q. Liu, and J.J. Richards, *Rheo-electric measurements of carbon black suspensions containing polyvinylidene difluoride in N-methyl-2-pyrrolidone*, Journal of Rheology, **67**, 647-659 (2023)
2. J.J. Richards, P. Ramos†, and Q. Liu†, *A review of the shear rheology of carbon black suspensions*, Frontiers in Physics, **11**, 01-11 (2023)
3. J. Griffith†, Y. Chen†, Q. Liu, Q. Wang, J.J. Richards, D. Tullman-Ercek, K. Shull, M. Wang, *Quantitative high-throughput measurement of bulk mechanical properties using commonly available equipment*, Materials Horizons, **10**, 97-107, (2023)
4. H. Lin, M. Majii, N. Cho, J. Zeeman, J. Swan, and J.J. Richards, *Quantifying the hydrodynamic contribution to electrical transport in non-Brownian suspensions*, Proceedings of the National Academy of Sciences, **119**, 0-7, (2022)
5. H. Lin, B. Blackwell, C. Call, S. Liu, C. Liu, M.M. Driscoll, and J.J. Richards, *FSVPy: A python-based package for fluorescent streak velocimetry (FSV)*, Journal of Rheology, **67**, 197-206 (2023)
6. Y. Gupta†, Q. Liu†, J.J. Richards, *Obtaining structural information of lithium-ion battery slurries with simultaneous rheo-electric measurements* (In preparation)
7. Q. Liu† W. Brenneis†, G. Nagy, M. Doucet, J. Lopez, J.J. Richards, *In situ nanoscale characterization of lithium-ion battery cathodes with contrast-variation small-angle neutron scattering measurements* (In preparation)
8. J. Hipp†, P. Ramos†, Q. Liu, N. Wagner, and J.J. Richards, *Shear-induced electrical properties of carbon black suspensions in the strong-shear regime* (In preparation)
9. K. Patel, S. Bowles, E. Matolyak, D. Vogus, C. Wang, G. Nagy, and J.J. Richards, *Mapping structure and rheology of pH-responsive resins for low-VOC coatings* (In preparation)

Magnetic Structure and In-Situ Synthesis of van der Waals Metal Chalcophosphates with Neutron and X-ray Diffraction

Efrain E. Rodriguez
Department of Chemistry and Biochemistry
University of Maryland, College Park, MD 20742

Research Scope: This program uses polarized neutron and other neutron diffraction techniques to study both structure and dynamics in van der Waals (vdW) magnetic materials. We pivot from studying transition metal phosphates where we looked for an exotic ferroic order known as ferrotorodicity to studying transition metal thiophosphates and selenophosphates, which are a rising class of vdW materials. These vdW transition metal chalcophosphates consist of a single layer of metal ions sandwiched between two layers of sulfide and selenide anions, and these layers in turn stack to form crystals (Figure 1a). They fill an important space in the world of 2D materials since they are primarily Mott insulators with antiferromagnetic order.[1,2] These metal chalcophosphates can exhibit interesting phenomena at the two-dimensional limit, such as potential multiferroic behavior such as in the case of $(Cu_{0.5}Cr_{0.5})PS_3$ [3] or strongly correlated electron behavior in $NiPS_3$ and $NiPSe_3$.[4] We are to pursue three thrusts in our neutron studies: 1) cobalt and iron-containing TMCs which have a honeycomb lattice that could support exotic phenomena such as a quantum spin liquid, 2) nickel-containing TMCs where strongly correlated electron behavior has been predicted, and 3) copper-containing TMCs where magnetoelectric coupling could lead to new multiferroic phenomena.

Research Progress: Here, we present the use of neutron diffraction methods to study both the magnetic structure and the synthesis of vdW materials with the formula MPQ_3 where M = transition metal and Q = S or Se. We present three diffraction studies of these systems: **1)** Neutron powder and single-crystal analysis of a series of solid solutions $NiP(S_{1-y}Se_y)_3$ and $FeP(S_{1-y}Se_y)_3$ where we perform a stacking fault analysis to understand how such disorder inherent to layered vdW systems affects the long-range antiferromagnetic behavior. We present data from HB-2A (Oak Ridge) and PANDA (PSI, Switzerland) along with X-ray diffraction to contrast how neutrons and X-rays can elucidate the nature of these stacking faults. **2)** Single crystal neutron diffraction of the potential multiferroic $(Cu_{0.5}Cr_{0.5})PS_3$. In the indium-containing analogue, the Cu^+ cations displace in one direction, breaking symmetry and ushering in a ferroelectric transition above room temperature. By replacing In^{3+} with Cr^{3+}, we want to induce long-range magnetic order with potential ferroelectricity. We find through magnetic-field dependent studies on WAND^2 (Oak Ridge) and single crystal studies on DEMAND (Oak Ridge), that takes on a A-type antiferromagnetic order occurs at zero field, a spin flop occurs at small field is applied normal to the 2D, and finally a forced ferromagnet above 6 T. **3)** In-situ diffraction studies of the synthesis of the $CoPS_3$ compound and some preliminary results on the selenide version $CoPSe_3$, which has never been synthesized before. We are particularly interested in this compound for its potential to exhibit frustrated magnetism based on the Co^{2+} cations (and therefore potential effective S = ½ centers) located in the honeycomb sublattice. Compared to the rest of the series, however, the Co-analogues are the least stable, and our *in-situ* studies of the metathesis reaction $CoCl_2 + MgPS_3 \rightarrow CoPS_3 + MgCl_2$ reveals clues as to the formation and stability of these vdW materials.

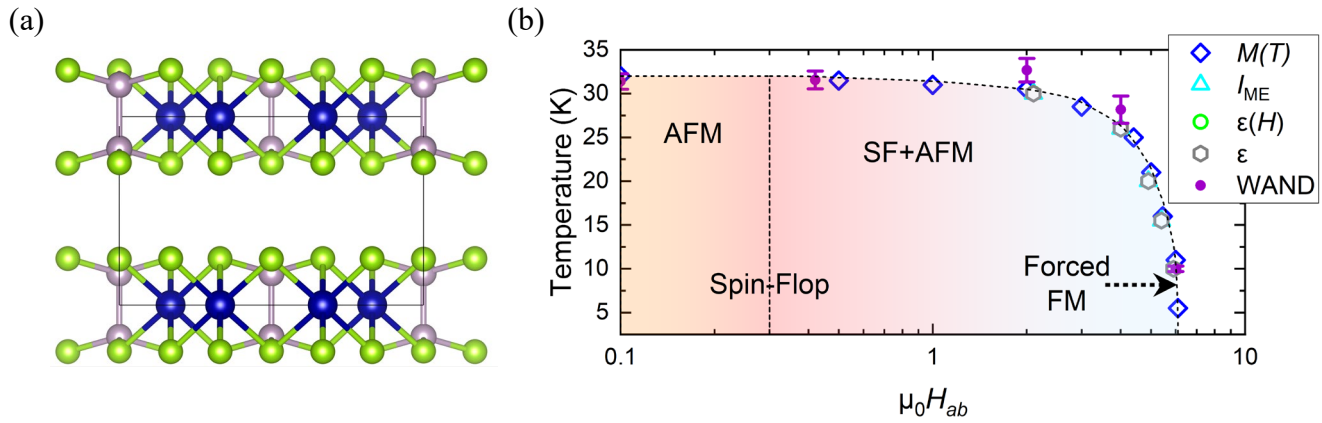

Figure 1. The structure and magnetic behavior of van der Waals materials MPQ_3 where M = transition metal and Q = S, Se. In (a) the typical crystal structure of an MPQ_3 material where the transition metal, in blue) fills in the octahedral positions made with the layers of $(P_2Q_6)^{4-}$ anionic units. In (b) the proposed phase diagram of the potential multiferroic $(Cu_{0.5}Cr_{0.5})PS_3$ from magnetoelectric measurements and WAND$_2$ single crystal neutron diffraction measurements.

Future Plans: In the context of the different projects enumerated above we would like to keep expanding on the three different areas. **1)** Polarized single-crystal neutron diffraction studies of the $NiP(S_{1-y}Se_y)_3$. The single crystal neutron diffraction experiments have reviewed a smaller than anticipated moment in the series as the amount of Se increases. With polarized neutrons we would like to solve the magnetic structures for the selenium rich side of the phase diagram. We would like to perform such studies with the new polarized capabilities at Oak Ridge. From a synthesis point of view, we now plan to carry out intercalation studies of both the $NiP(S_{1-y}Se_y)_3$ and $FeP(S_{1-y}Se_y)_3$ series. Preliminary results using alkali metals in liquid ammonia led to the easy intercalation of cations and ammonia molecules in the iron series. Since the Ni analogue is a Mott insulator with a high degree of 2D character, we will prioritize charge doping these compounds. Powder neutron diffraction will be key to understanding their nuclear and magnetic structures. **2)** Now that we have completed our single crystal neutron diffraction of the potential multiferroic $(Cu_{0.5}Cr_{0.5})PS_3$, we plan to go in two different directions. We plan to also grow crystals of the selenide analogue $(Cu_{0.5}Cr_{0.5})PSe_3$, and also study the V^{3+} containing sample $(Cu_{0.5}V_{0.5})PS_3$. In fact, we have some single crystals now of $(Cu_{0.5}V_{0.5})PS_3$ although we need larger crystals for neutron studies. We will continue to work with our collaborators to characterize the magnetoelectric properties of these materials and perform more neutron diffraction studies at Oak Ridge. **3)** Given our progress in the in-situ diffraction studies of the synthesis of the $CoPS_3$ compound, we have now extended it to the solid solutions $CoP(S_{1-y}Se_y)_3$. Preliminary magnetic susceptibility studies of powder samples do not exhibit long-range magnetic order down to 2 K. Therefore, we want to pursue single crystal growth of the thermodynamically accessible phases to study if indeed the honeycomb lattice supporting Co^{2+} effective S = ½ centers could lead to interesting magnetic frustration effects, including quantum spin liquid behavior.

References:

1. M. A. Susner, M. Chyasnavichyus, M. A. McGuire, P. Ganesh, and P. Maksymovych, "Metal Thio- and Selenophosphates as Multifunctional van der Waals Layered Materials," *Advanced Materials*, vol. 29, no. 38, p. 1602852, 2017.
2. M. Zhu, H. Kou, K. Wang, H. Wu, D. Ding, G. Zhou, and S. Ding, "Promising functional two-dimensional lamellar metal thiophosphates: Synthesis strategies, properties and applications," *Materials Horizons*, vol. 7, no. 12, pp. 3131–3160, 2020.

3. C. B. Park, A. Shahee, K. T. Kim, D. R. Patil, S. A. Guda, N. Ter-Oganessian, and K. H. Kim, “Observation of Spin-Induced Ferroelectricity in a Layered van der Waals Antiferromagnet $CuCrP_2S_6$,” *Advanced Electronic Materials*, p. 2101072, 2022.
4. H. S. Kim, K. Haule, and D. Vanderbilt, “Mott Metal-Insulator Transitions in Pressurized Layered Trichalcogenides,” *Physical Review Letters*, vol. 123, no. 23, p. 236401, 2019.

Publications:

1. Diethrich, T. J.; Gnewuch, S.; Dold, K. G.; Taddei, K.; Rodriguez, E. E.*, “Tuning Magnetic Symmetry and Properties in the Olivine Series Li1-xFexMn1-xPO4 through Selective Delithiation” Chemistry of Materials, 2022, 34, 5039–5053.
2. A. McDannald, M. Frontzek, A. T. Savici, M. Doucet, E. E. Rodriguez, K. Meuse, J. Opsahl-Ong, D. Samarov, I. Takeuchi, A. G. Kusne, and W. Ratcliff, “On-the-fly autonomous control of neutron diffraction via physics-informed bayesian active learning” Applied Physics Reviews, 2022, 9, 021408.
3. Diethrich, T. J.; Gnewuch, S.; Zavalij, P.Y.; Rodriguez, E. E.* “Orbital contribution to paramagnetism and non-innocent thiophosphate anions in layered Li2MP2S6 where M = Fe, Co,” Inorganic Chemistry, 2021, 60, 10280-10290.

National School on Neutron and X-ray Scattering

Stephan Rosenkranz, Jessica McChesney, Chengjun Sun
Argonne National Laboratory

Bianca Haberl, Adam Aczel, Michael Manley
Oak Ridge National Laboratory

Program Scope

The National School on Neutron and X-ray Scattering (NXS) educates graduate students at North American Institutions in the use of the wide array of neutron and x-ray techniques available at large-scale user facilities. In an annual, two-week school, organized jointly and hosted by Argonne National Laboratory and Oak Ridge National Laboratory, NXS provides a comprehensive introduction to the underlying theory of neutron and synchrotron x-ray scattering and imaging techniques through lectures and hands-on tutorials on how to prepare for and perform X-ray experiments at the Advanced Photon Source at Argonne National Laboratory (ANL) and neutron experiments at the Spallation Neutron Source and the High Flux Isotope Reactor at Oak Ridge National Laboratory (ORNL). The goal is to educate the next generation of users of large neutron and x-ray facilities on how to utilize such facilities to their fullest potential to provide detailed information regarding atomic structures, dynamics, and chemical makeup relevant to a wide range of scientific disciplines. NXS distinguishes itself from other more topical schools in the United States by providing a broad grounding in the fundamentals of both neutron and x-ray scattering techniques, emphasizing the complementary nature of these structural, spectroscopic, and imaging probes.

Recent Progress

2022 NXSchool: After two years of virtual formats, the NXS was held again in person from July 10-22, 2022 with students onsite at Oak Ridge National Laboratory July 10-16 and at Argonne National Laboratory July 17-22. Interest to participate in the NXS was again very high with 217 applicants received for the 60 available seats, an oversubscription of 3.6. Applications were received form 102 unique Institutions in 40 different U.S. States and from Canada and Puerto Rico. All applications were ranked by the scientific Co-directors based on the applicants' qualifications and merit to benefit from participation in the school. 60 students (32 female and 15 from Minority Serving Institutions), representing a diverse group from all across the United States and Canada and from a wide range of scientific fields, were then selected to participate in the school.

The participants received 40 lectures covering different topics across a wide range of neutron and x-ray scattering techniques, in addition to overviews of the National Laboratories, national and international neutron and synchrotron x-ray user Facilities, and tours of facilities at Oak Ridge and Argonne National Laboratory. The program was updated with new lectures covering the current status

Fig 1. The class of NXS 2022 at ORNL

and future impact of high-performance computing and artificial intelligence on neutron and x-ray scattering science with respect to self-driving experiments and analysis and modeling of large data sets. Another new lecture was added to illustrate differences and complementarity of experiments performed at steady-state versus pulsed neutron sources.

Students also participated in hands-on tutorials designed to provide the students and introduction on how to successfully perform experiments at neutron and synchrotron x-ray user facilities. Each student was assigned four x-ray and four neutron tutorials, based on preferences that students submitted and ensuring students will get an overview over a wide range of different techniques. Due to the emergence of COVID during the second week at ANL, x-ray tutorials could only be performed in-person for one day, with the remaining experiments switching to a virtual format.

Fig. 2: 2022 and 2023 NXSchool students during hands-on experiments and data science tutorials at ORNL

Fig 3: The Class of NXS 2023 at ANL.

2023 NXSchool: The 25th NXS was held in person from August 6-18, 2023 with students onsite at Oak Ridge National Laboratory August 6-12 and at Argonne National Laboratory August 13-18. The school was again widely advertised to Institutions across all of North America with efforts to reach out to underrepresented regions and communities. The oversubscription remained very high with 193 applications received from 89 unique institutions from 37 states and Canada. The Co-directors then again ranked all applications and selected a diverse group of 60 students (23 female, 14 from Minority Serving Institutions) from all across the United States and Canada, representing a wide range of scientific fields.

The program was again updated to include a lecture to illustrate the importance and value of multi-modal measurements to obtain insight into complex phenomena. This new lecture was given by an Alumni of the NXSchool who participated for the first time as lecturer.

At ORNL, students performed four different tutorials, most including hands-on, live experiments. Because of the APS-U shutdown of the synchrotron, live x-ray experiments were not possible and access to several beamlines for tours was not possible due to ongoing construction. However, the students got the unique opportunity to get tours to see insight the storage ring, which is otherwise never accessible, and got to see the old as well as the new setup of magnets and undulators. The students were then given virtual tutorials in order to enable detailed interactions with beamline and other staff scientist in small groups. New tutorials were also offered to give interactive introductions to Data Sciences. At ORNL a tutorial provided an overview of the vast landscape of useful tools available, an introduction to python scripting for neutron sciences, and how to use conda and create, manage, and use collaborative repositories such as git. At ANL, a tutorial provided a hands-on introduction to BlueSky, a python-based framework for communicating with instrumentation and data acquisition, visualization, and analysis that was developed at NSLS-II and is being adopted by several other light sources, including APS.

Fig. 4: Jonathan Lang, APS X-ray Science Division Director, provides a tour of the APS-U High-Energy X-ray Microscope feature beamline under construction in the new Long-Beamline building to NXS 2023 students

Fig. 5: View inside the storage ring tunnel with a new magnet module visible in the back.

The participants of both the 2022 and 2023 NXSchool were very positive about their experiences despite restrictions to virtual tutorials. The students also gave very high ratings of lecturers and experiments and remarked that the knowledge provided will be of high value to their future professional career.

Future Plans

Planning for the 26th National School on Neutron and X-ray Scattering is underway. With both the Advanced Photon Source and the Spallation Neutron Source scheduled to come on again after upgrades in spring and early summer of 2024, respectively, the NXS may be held later than usual, either in August or September, to ensure tutorials with live experiments can be offered at all facilities. We anticipate being able to hold the school in a traditional, onsite format with 60.

The NXSchool will be advertised widely and to underrepresented colleges with the application opening in early spring 2024. The program Co-Directors will review the program and working with the advisory committee update lectures and tutorials where deemed necessary to keep up with novel advances in techniques and methods.

Publications

1. M. Frontzek, B. Haberl, M.E. Manley, S. Rosenkranz, U. Ruett, *The 23rd National School on Neutron & X-ray Scattering 2021 – Virtual School with Remote Experiments,*
Neutron News **32**, 12-16 (2021). DOI: https://doi.org/10.1080/10448632.2021.1996855

Neutron and x-ray scattering investigations of the impact of short-range correlations on properties of energy and quantum materials

Stephan Rosenkranz, Omar Chmaissem*, Raymond Osborn, Daniel Phelan
Argonne National Laboratory; *and Northern Illinois University

Keywords: short-range order, local structure, single crystal diffuse scattering, 3D-ΔPDF

Research Scope

Many emergent phenomena and materials' properties required to enable future technologies derive from the presence of local disorder and short-range correlations embedded in a long-range ordered crystalline lattice. This program employs and further develops advanced instrumentation and methods to obtain detailed insight into the role of such complex disorder from single crystal diffuse and inelastic neutron scattering measurements. Expanding on our previous developments of efficient methods to measure full volumes of single crystal diffuse neutron scattering, which enables analysis of the data via Fourier transformations such as the 3D-ΔPDF method, a particular focus is now on developing methods to accurately characterize correlations that are neither local nor long-range and to obtain reliable and physically interpretable models of the local structure from these diffuse scattering data. We further started to develop tools to efficiently analyze quasi-elastic neutron scattering data from single crystals measured over full volumes of momentum-transfers in order to gain novel insight into the dynamics of short-range correlations. These methods are applied and further refined to study phenomena in bulk quantum and energy materials of interest, such as correlated motion in solid state ion conductors, complex short-range spin fluctuations in novel pentagonal frustrated spin glasses, and the relation of short-range, intertwined spin, charge, and lattice correlations on phenomena such as superconductivity and metal-insulator transitions in lower dimensional oxides.

Recent Progress

Ionic and Lattice Correlations: Halide perovskites are of great interest due to their advanced photoelectric properties of importance for solar energy, thermoelectric, and radiation detection applications. Previous single crystal inelastic neutron and diffuse x-ray scattering investigations performed in collaboration with Olivier Delaire, Duke University, revealed the presence of quasi-static, quasi two-dimensional (2D) lattice fluctuations that originate on a local scale from collective $PbBr_6$ octahedral rotations in the inorganic lead-halide compound $CsPbBr_3$ [1]. In order to obtain a detailed understanding of the short-range ordering and universality of these octahedral rotations, we performed single crystal diffuse neutron and x-ray scattering measurements as a function of temperature on a series of inorganic halide perovskites as well as a double perovskite compound. We find that quasi-2D diffuse scattering exists for all samples in their high temperature, cubic phases. By constructing effective Hamiltonians based on Glazer-tilts of the octahedra, we performed Monte Carlo simulations of the local structure and found that the octahedral tilts defining the lower symmetry structures at lower temperatures persist into the higher symmetry, higher temperature phases in short-range, quasi-2D form. The 2D-form arises from the strong correlation of the tilts in the plane perpendicular to the rotation axis, whereas the rotations from one such plane to the neighboring plane are only weakly correlated.

We have also started to develop tools to efficiently analyze 4D volumes of quasi-elastic scattering S($\boldsymbol{Q}$,ω) from single crystals. Determining detailed $\boldsymbol{Q}$-dependences of the quasielastic linewidths can provide novel insight into correlated motion of importance for the performance of solid-state ionic conductors. First studies performed on CNCS on $SrCl_2$ confirm this, with the incoherent scattering agreeing with a Chudley-Elliott jump diffusion model, the first time such an analysis has been performed on 4D-S(Q,ω) data throughout the Brillouin zone, whereas the coherent linewidths reveal, for the first time in a single crystal, de Gennes narrowing, indicative of correlated ion motion (see Fig.1).

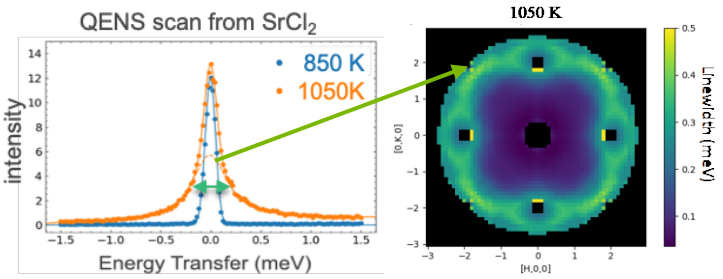

Fig. 1: Quasielastic linewidths of the coherent cross section in $SrCl_2$ determined from 4D-S($\boldsymbol{Q}$, ω) measured on CNCS showing minima corresponding to scattering intensity maxima, reminiscent of de Gennes narrowing due to short range defect correlations.

Complex spin correlations: Single crystal diffuse and inelastic neutron scattering was employed to investigate, in collaboration with Art Ramirez, U.C. Santa Cruz, spin freezing in Fe_2TiO_5 and the evolution of the spin correlations upon increasing spin vacancies through substitution of Ga^{3+} for Fe^{3+}. We find highly anisotropic, instantaneous spin correlations well above the freezing temperature T_g in the shape of surfboards with lifetimes that increase as T_g is approached, indicating the change from fluctuating to static intra-surfboard correlations below T_g. However, remnant spin fluctuations were observed down to well below T_g reflecting the behavior of the spin cloud background due to the combination of frustration and the randomness of Fe/Ti distribution. Upon further increasing the concentration of vacancies upon Ga substitution, we find that the surfboards remain the dominant magnetic unit up to high vacancy concentrations but with a decrease in the size of the surfboards.

Intertwined order: Utilizing in-situ neutron diffraction as a function of temperature in hydrogen/argon and oxygen gas atmospheres to remove and re-introduce oxygen, respectively, we investigated the complex procedure required to synthesize the tetragonal, multiferroic phase of $Sr_{1-x}Ba_xMn_{1-y}Ti_yO_{3-\delta}$. We observe a large miscibility that suppresses intermediate vacancy-ordered superstructures in the heavily Ba-substituted materials, instead enabling the formation of non-centrosymmetric distortions that stabilize ferroelectricity. We also investigated the possible emergence of novel multiferroic phases in $Y_{1-x}Tb_xMnO_{3+\delta}$, where the endmembers are type-I and type-II multiferroics, respectively, with different structural, magnetic, and ferro-electric order. We find the Mn sublattice transforms from antiferromagnetic (δ=0) to ferromagnetic order upon oxygenation ($\delta \approx 0.45$) and Tb substitution (x=0.3 and 0.5). At the same time, we observe relaxor-type ferroelectric behavior in the oxygenated samples with colossal dielectric permittivity at frequencies in the 1-100 kHz range. However, in contrast to their stoichiometric counterparts, their dielectric permittivity shows no anomaly at the magnetic transition temperatures.

In the novel quasi-one-dimensional compound KMn_6Bi_5, which becomes superconducting under pressure, utilizing single crystal and powder neutron diffraction on very small samples, we discovered the presence of coupled spin (SDW) and charge (CDW) density waves. This provides a new family of compounds to further investigate the evolution and impact of these intertwined order on superconductivity, a long-standing question in cuprates, and of interest also to nickelates.

The presence of multiple orders that intertwine spin and orbital degrees of freedom have also been implied in the emergence of superconductivity in iron-based superconductors. Our single crystal diffuse scattering measurements on hole doped '122' family of compounds show broad rods of diffuse scattering along *l*, that are near ½½0 for smaller values of momentum transfer *Q*, indicating short-range chemical order of Ba and Na atoms. The progressive shift of the rods closer to the zone center as *Q* increases is further indicative of size effect scattering. These observations are confirmed with a 3D-ΔPDF analysis and DISCUS [2] simulation showing that such effects are will important to include in scattering studies of nematic correlations.

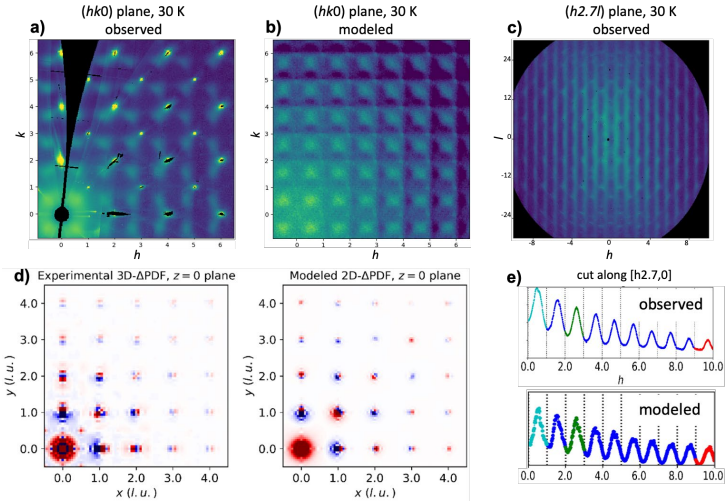

Fig. 2: a-c) Observed and modeled diffuse scattering from $Ba_{0.74}Na_{0.26}Fe_2As_2$. d) ΔPDF maps at z=0. e) The shift of the diffuse peak intensity away from half-integer h-values with increasing *Q* are due to the size effect, as reproduced with the model.

Future Plans

Ionic correlations and lattice strain: A broad range of energy technologies, including batteries, fuel cells, thermoelectricity, and relaxor behavior are intrinsically coupled to ionic disorder. We will investigate diffusion in solid state fast ion conductors, which is known to be strongly affected by correlated ion motion. We plan to utilize single crystal diffuse and quasi-elastic neutron scattering to study the static and dynamic correlations in different systems involving copper, lithium, and oxygen ions respectively. A starting material is $Cu_{2-x}Se$, in which fast ion conductivity is induced through the 'melting' of the Cu-sublattice which has been suggest as an important ingredient to reduce thermal conductivity and leading to much improved thermoelectric properties. Recent CORELLI experiment on a single crystal of Cu1.8Se show complex diffuse scattering in the superionic high temperature state. The 3D-dPDF map of the copper interatomic vectors generated from this data (Fig. 3) shows that there is a higher probability that neighboring copper sites alternate between the regular and distorted sites. This alternation is likely part of a correlated dynamic process that we will study with 4D-QENS measurements, from which we will also be able to determine diffusion pathways and average residence times from the Q-dependence of the quasielastic linewidths.

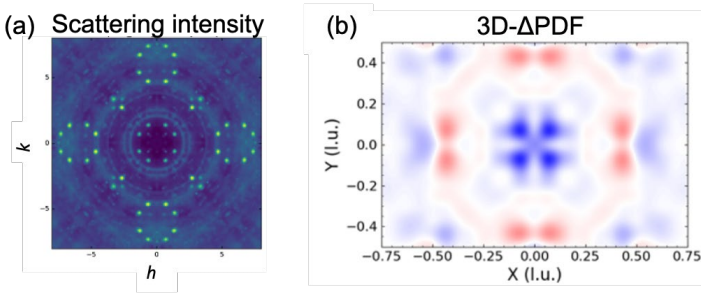

Fig. 3: (a) Diffuse scattering from $Cu_{2-x}Se$ in the high temperature, superionic phase measured on CORELLI. (b) The 3D-ΔPDF obtained from the CORELLI data show the Cu interatomic vectors.

Complex spin correlations: We plan to investigate the static and dynamic spin correlations in novel frustrated magnets. Our focus is on spins on the 'Cairo lattice', which forms a 2D pentagonal tiling with pentagons as novel elementary unit of frustration. Since there exists no Bravais lattice of pentagons, the Cairo lattice has an inherently deeper degree of complexity than systems with triangular building blocks common to most frustrated magnets. Utilizing single crystal diffuse and inelastic neutron scattering, we will investigate the various long- and short-range order that may occur on the Cairo lattice as a function of the nearest and next nearest exchange parameters in BiFe4O9, which can be modified through uniaxial stress or chemical substitution, which could lead to additional local defects and short-range ordering due to size effects. We will also investigate the evolution of the spin glass phase observed upon disordering the Cairo lattice, *e.g.* through Ga-substitution in $BiFe_{4-x}Ga_xO_9$. This provides an avenue to systematically investigate the evolution of the magnetic correlations in a geometrically frustrated material with disorder and test the recent conjecture [3] that the freezing temperature at small enough disorder should increase with increasing impurity density, as in conventional spin glasses.

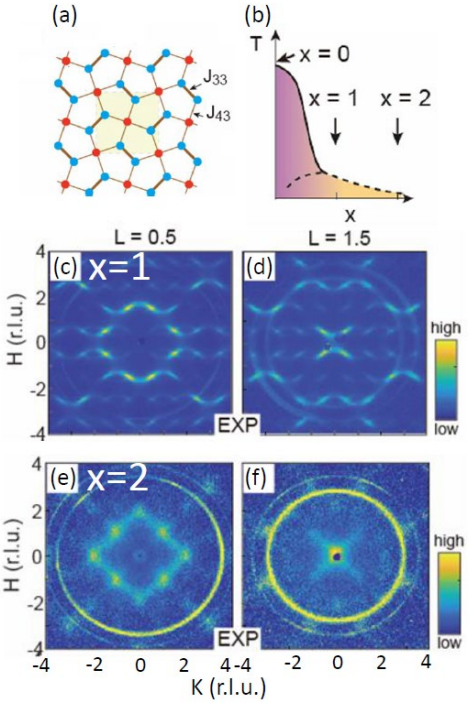

Fig. 4: (a) the Cairo lattice and (b) schematic diagram of the Néel (solid line) and spin freezing (dashed line) transition temperatures for $BiFe_{4-x}Ga_xO_9$. (c-f) diffuse scattering measured for x=1 and 2 in the (*h*,*k*,0.5) and (*h*,*k*,1.5) planes.

Intertwined order in low dimensional quantum materials: Following our previous studies of the quasi-1D chain compound KMn_6Bi_5, we plan to study the evolution of the intertwined spin and charge density waves upon diluting the intra-chain exchange interactions, through chemical substitution at the Mn site, or the inter-chain interactions by replacing K with Rb or Na. We also plan to investigate the presence of spin and/or charge correlations in various layered nickelate compounds, some of which have recently been found to exhibit superconductivity under pressure.

References

1. T. Lanigan-Atkins, X. He, M.J. Krogstad, D.M. Pajerowski, D.L. Abernathy, Guangyong Xu, Z. Xu, D.Y. Chung, M.G. Kanatzidis, S. Rosenkranz, R. Osborn, O. Delaire, *Two-Dimensional overdamped fluctuations of the soft perovskite lattice in $CsPbBr_3$*, Nat. Mater. **20**, 977 (2021).
2. Th. Proffen, R.B. Neder, *DISCUS: A program for Diffuse Scatterign and Defect-Structure Simulation*, J. Appl. Crystallogr. 30, 171 (1997).
3. S.V. Syzranov, A.P. Ramirez, *Eminuscent phase in frustrated magnets: a challenge to quantum spin liquids*, Nat. Commun. **13**, 2993 (2022).

Publications

1. R. Stadel, R. DeRose, K.M. Taddei M.J. Krogstad, P. Upreti, Z Islam, R. Woods, D. Phelan, D.Y. Chung, R. Osborn, S. Rosenkranz, O. Chmaissem, *Two-dimensional short-range chemical ordering in $Ba_{1-x}Na_xFe_2As_2$,* Phys. Rev. Mater in press (2023). arXiv:2304.07960
2. A.M. Samarakoon, J. Strempfer, Junjie Zhang, F. Ye, Y. Qiu, J.-W. Kim, H. Zheng, S. Rosenkranz, M.R. Norman, J.F. Mitchell, D. Phelan, *Bootstrapped Dimensional Crossover of a Spin Density Wave*, Phys. Rev. X **13**, 041018 (2023). DOI: 10.1103/PhysRevX.13.041018

3. E. Krivyakina, B. Poudel, Cheng Li, S. Kolesnik, B. Dabrowski, J.F. Mitchell, S. Rosenkranz, O. Chmaissem, *Redox Properties of Hexagonal and Cubic $Sr_{0.4}Ba_{0.6}Mn_{0.94}Ti_{0.06}O_{3-\delta}$ Investigated by In Situ Neutron Powder Diffraction*, Chem. Mater **35**, 5895 (2023). DOI: 10.1021/acs.chemmater.3c00693

4. Y. Li, P.G. LaBarre, D.M. Pajerowski, A.P. Ramirez, S. Rosenkranz, D. Phelan, *Neutron scattering study of fluctuating and static spin correlations in the anisotropic spin glass Fe_2TiO_5,* Phys. Rev. B **107**, 014405 (2023). DOI: 10.1103/PhysRevB.107.014405

5. Jin-Ke Bao, H. Cao, M.J. Krogstad, K.M. Taddei, C.-F. Shi, S. Cao, S.H. Lapidus, D. van Smaalen, D.Y. Chung, M.G. Kanatzidis, S. Rosenkranz, O. Chmaissem, *Spin and charge density waves in quasi-one-dimensional KMn_6Bi_5,* Phys. Rev. B **106**, L201111 (2022). DOI: 10.1103/PhysRevB.106.L201111

6. Y. Li, D. Phelan, F. Ye, H. Zheng, E. Krivyakina, A. Samarakoon, P.G. LaBarre, J. Neu, T. Siegrist, S. Rosenkranz, S.V. Syzranov, A.P. Ramirez, *Evolution of magnetic surfboards and spin glass behavior in $(Fe_{1-p}Ga_p)_2TiO_5$*, J. Phys.: Condens. Matter **35**, 475401 (2023). DOI: 10.1088/1361-648X/aceede

7. Bi-Xia Wang, M.J. Krogstad, H. Zheng, R. Osborn, S. Rosenkranz, D. Phelan, *Active and Passive Defects in Tetragonal Tungsten Bronze Relaxor Ferroelectrics*, J. Phys.: Cond. Matt. **34**, 405401 (2022). DOI: 10.1088/1361-648X/ac8261

8. R. Stadel, D.D. Khalyavin, P. Manuel, K. Yokoyama, S. Lapidus, M.H. Christensen, R. M. Fernandes, D. Phelan, D.Y. Chung, R. Osborn, S. Rosenkranz, O. Chmaissem, *Multiple Magnetic Orders in $LaFeAs_{1-x}P_xO$ Uncover Universality of Iron-Pnictide Superconductors,* Commun. Phys. **5**, 146 (2022). DOI:10.1038/ s42005-022-00911-5

9. T.B. Rawot Chhetri, T.C. Douglas, M.A. Davenport, S. Rosenkranz, R. Osborn, M.J. Krogstad, J.M. Allred, *Geometric frustration suppresses long-range structural distortions in $Nb_xV_{1-x}O_2$*, J. Phys. Chem. C **126**, 2049 – 2061 (2022). DOI: 10.1021/acs.jpcc.1c08392

10. Yaohua Liu, Huibo Cao, S. Rosenkranz, M. Frost, T. Huegle, J. Lin, P. Torres, A. Stoica, B. Chakoumakos, *PIONEER, a High-Resolution Single-Crystal Polarized Neutron Diffractometer,* Rev. Sci. Instrum. **93**, 073901(2022). DOI: 10.1063/5.0089524

Dynamics of Bottlebrush Polymers by Neutron Scattering

Gerald J. Schneider
Department of Chemistry, and Department of Physics & Astronomy, Louisiana State University, Baton Rouge, LA 70803

Keywords: bottlebrush polymers, bottlebrush dynamics, side chain dynamics, quasi-elastic neutron scattering, neutron spin echo

Research Scope

The overarching goal of this project is to gain a better understanding of the macroscopic properties of bottlebrush polymers by studying their nanoscale structure and dynamics. Bottlebrush polymers, also known as bottlebrushes, are a fascinating class of polymers that belong to the family of comb polymers (**Figure 1**). A comb polymer is called a bottlebrush once the density of side chains exceeds a certain level, defined by visibly stretching the backbone and side chains. This transition from a statistical or Gaussian coil to a spherical or elongated shape is a signature of the transition to a bottlebrush polymer.

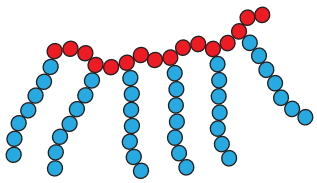

Figure 1 – Bottlebrush polymers belong to the family of comb polymers. The branched architecture has a backbone and side chains. If the number density of side chains exceeds a certain level, comb polymers are named bottlebrushes.

Materials based on bottlebrushes exhibit exceptional properties that cannot be accomplished with traditional polymers of the same chemical composition, such as:

(1) Ultralow viscosities: This makes them ideal for applications such as lubricants and coatings.
(2) Hyperelasticity: This allows them to stretch and recover their original shape without breaking.
(3) High functionality: The side chains can be functionalized with a variety of groups, making them versatile for different applications.

The design freedom to vary the backbone and side chain independently can create many opportunities. However, the massive design freedom also makes exploratory research inefficient. Therefore, we aim to gain a fundamental understanding of bottlebrushes at the nanoscale with the vision to identify a set of core parameters that allow for predicting macroscopic material properties. This will enable us to design new bottlebrush materials with specific properties for targeted applications.

Our research concentrates on the following aspects:

- **Synthesis of well-defined bottlebrush polymers**: This is essential for studying the structure-property relationships of these materials.
- **Characterization of the nanoscale structure**: using a variety of techniques, such as neutron scattering and electron microscopy, to measure the size, shape, and conformation of bottlebrush polymers.
- **Investigation of the nanoscale dynamics:** We use techniques such as neutron spin echo spectroscopy, quasi elastic neutron scattering, and nuclear magnetic resonance to study the motion of the backbone and side chains.

- **Development of theoretical models:** We use the results from our experiments to develop theoretical models that can predict the macroscopic properties of bottlebrush polymers.

By combining these approaches, we will gain a comprehensive understanding of bottlebrush polymers and their unique properties. This knowledge will enable us to design new materials with tailored properties for a wide range of applications.

Bottlebrushes present a unique challenge for material science due to their complex interplay of properties at different length and timescales at the nanoscale. While existing models can describe the macroscopic behavior of many polymers, they struggle to predict the behavior of bottlebrushes, which exhibit novel and emergent properties. Neutrons offer a powerful toolkit for addressing this challenge. Their unique combination of momentum transfer, Q, energy transfer (representing length and timescale), and isotopic sensitivity (enabling selective highlighting of specific material regions) allows us to probe bottlebrushes with unparalleled resolution. Specifically, we focused on the relaxation of the bottlebrush side chain, a crucial aspect of their overall behavior. Our work represents the first published neutron spectroscopy experiments on bottlebrushes, providing valuable insights into this promising new material class.

Recent Progress

We used neutron spin echo (NSE) to study the dynamics of PDMS-g-PDMS bottlebrush polymers in solution for the first time (**Figure 1**). By comparing the NSE results with small-angle neutron scattering (SANS) data, we observed the need for a broader length-scale range than what NSE can provide. To address this limitation, we fabricated model bottlebrushes designed to move different length-scale levels through the NSE window. This unique approach allowed us to selectively study the motion associated with different structural parts of bottlebrushes, something not previously achieved in the literature.

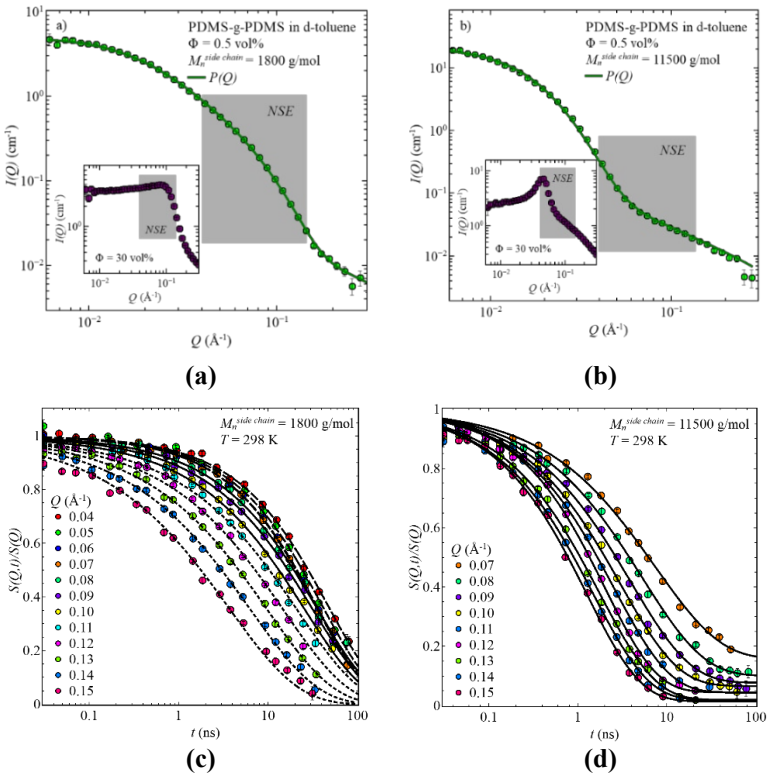

Figure 2 – **(a)** The structural region required for bottlebrush polymers is much broader than the NSE Q-window. (b) Dynamic structure factor by NSE. We used a model polymer and to move the characteristic features through the QQ-window of NSE.[2]

The distinct differences in the dynamics structure factors displayed in **Figures 2(c)** and **2(d)** are readily apparent. Notably, **Figure 2(d)** exhibits a pronounced plateau at high Fourier time, a characteristic signature of confined motion. The sample in **Figure 2(a)** and **2(c)** displays dynamics typical of cylindrical micelles, confirmed by the Q-dependence of the relaxation time and the shape parameter. Interestingly, the intermediate range exhibits a significantly stronger Q-dependence of the relaxation time than anticipated for spherical micelles. At smaller length-scales, we observe the so-called blob-region, representing internal single-chain dynamics spatially confined by neighboring chains. The dynamics at that length scale are well compatible with Zimm dynamics.

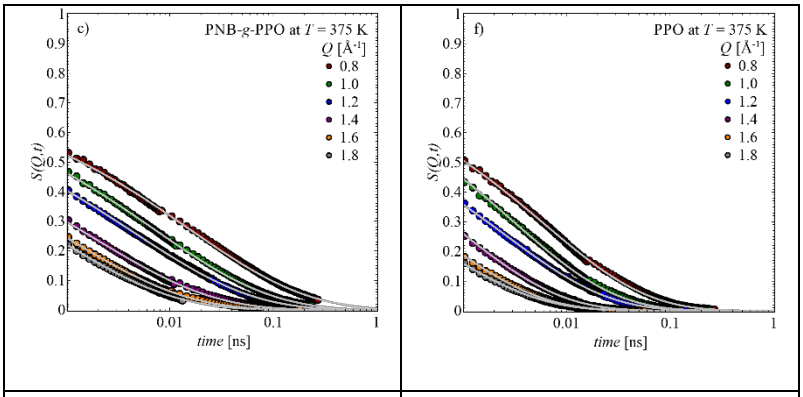

(a) (b)

Figure 3 – Quasi-elastic neutron scattering of PNB-g-PPO (a) and linear PPO (b) at $T = 375$ K.[3]

Until now, the experiments focused on systems categorized as flexible-g-flexible bottlebrush polymers. In the next step we changed the character by substituting the PDMS backbone by poly(norbornene) (PNB) which switched the character of the bottlebrush to stiff-g-flexible. Quasi-elastic neutron scattering (QENS) experiments were used to compare the segmental relaxation of bottlebrush polymers with the free, unattached side chain. As seen in **Figure 3**, the combination of three QENS spectrometers offers a time range of $t = (0.001 - 1)$ ns. Already the comparison of the intermediate scattering function, $S(Q,t)$, shows a slower decay for the bottlebrush polymer compared to the free linear chain. This is more evident, by comparing the Q-dependent relaxation times, $\langle\tau(Q)\rangle$. As shown in **Figure 4**, across all measured temperatures, the same behavior maintains, i.e., the segmental relaxation times of a linear chain attached to the backbone is longer compared to the free unattached chain. Similar results were obtained for the flexible-g-flexible system, i.e., PDMS-g-PDMS and leads to the conclusion, that the overall behavior of the segmental relaxation is not influenced by the changed character of the backbone polymer when compared with the free unattached linear side chains. [4]

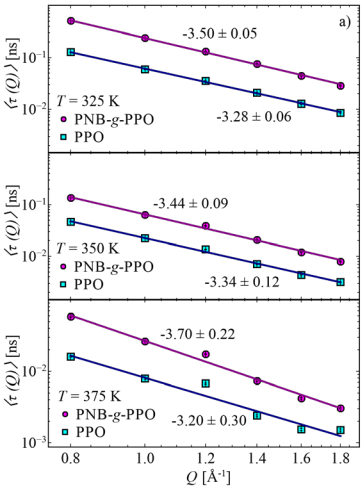

Figure 4 – Relaxation time as a function of momentum transfer.[3]

Future Plans

Continuing with the stiff-g-flexible, we performed quasi-elastic neutron scattering experiments on partially labeled samples, to investigate the segmental relaxation depending on the position within the side chain. One sample has the highlighted part on the inside to get information regarding the dynamical behavior influenced by the grafting point, whereas the second sample allows to study the dynamics of the dangling end. Comparing both samples indicates faster relaxation for the dangling end, while the inner part relaxes around 30% slower than the outer part. These results support the assumption of a gradual change of the relaxation time with increasing the distance from the branching point.

Following the stiff-g-flexible system, we investigate the side chain length dependent relaxation of the side chains for three different molecular weights by quasi-elastic neutron scattering.

From the flexible-g-flexible system, it is known that the behavior is consistent with that of linear polymer, i.e., slower segmental relaxation for longer polymer chains.[4] Simulation work from Xu et al.[5] shows a reversed behavior once the backbone character turns into stiff. However, no experimental evidence has been published yet.

Continuing with that stiff-g-flexible system, dielectric spectroscopy and rheology experiments are conducted and will be analyzed toward a joint understanding. This allows to separate the viscoelastic data into different sections, i.e., terminal region, diluted region, side chain region, and segmental region.

References

1. J. Paturej, and T. Kreer, *Hierarchical excluded volume screening in solutions of bottlebrush polymers*, Soft Matter **13**, 8534 (2017)**.**

2. K. J. Bichler, B. Jakobi, D. Honecker, L. R. Stingaciu, T. K. Weldeghiorghis, J. H. P. Collins, and G. J. Schneider, *Dynamics of Bottlebrush Polymers in Solution by Neutron Spin Echo Spectroscopy*, Macromolecules **55**, 9810 (2022)**.**

3. K. J. Bichler, B. Jakobi, A. Klapproth, T. Tominaga, R. A. Mole, and G. J. Schneider, *Side Chain Dynamics of Poly (norbornene)-g-Poly (propylene oxide) Bottlebrush Polymers*, Macromol. Rapid Commun. **44**, 2200902 (2023)**.**

4. B. Jakobi, K. J. Bichler, A. Sokolova, and G. J. Schneider, *Dynamics of PDMS-g-PDMS Bottlebrush Polymers by Broadband Dielectric Spectroscopy*, Macromolecules **53**, 8450 (2020)**.**

5. X. Xu, J. F. Douglas, and W.-S. Xu, *Influence of Side-Chain Length and Relative Rigidities of Backbone and Side Chains on Glass Formation of Branched Polymers*, Macromolecules **54**, 6327 (2021)**.**

Publications

1. K. J. Bichler, B. Jakobi, and G. J. Schneider, *Segmental Relaxation of Sequence Defined Polymers*, Journal of Physics: Condensed Matter **36**, 115101 (2024).
2. M. Wu, K. J. Bichler, B. Jakobi, A. Grzesiowski, and G. J. Schneider, *End block dynamics in unentangled polymers by dielectric spectroscopy*, J. Phys.: Condens. Matter **35**, 375101 (2023).
3. M. Wu, K. J. Bichler, B. Jakobi, and G. J. Schneider, *Uniqueness of Relaxation Times Determined by Dielectric Spectroscopy*, J. Phys.: Condens. Matter **35**, 185101 (2023).
4. K. J. Bichler, B. Jakobi, A. Klapproth, T. Tominaga, R. A. Mole, and G. J. Schneider, *Side Chain Dynamics of Poly(norbornene)-g-Poly(propylene oxide) Bottlebrush Polymers.* Macromol. Rapid Commun. **44**, 2200902 (2023).
5. K. J. Bichler, B. Jakobi, and G. J. Schneider, *Dynamics of Bottlebrush Polymers*, EPJ Web of Conferences **272**, 01002 (2022).
6. K. J. Bichler, B. Jakobi, D. Honecker, L. R. Stingaciu, T. K. Weldeghiorghis, J. H. P. Collins, and G. J. Schneider, *Dynamics of Bottlebrush Polymers in Solution by Neutron Spin Echo Spectroscopy*, Macromolecules **55**, 9810 (2022).
7. E. Mamontov, H. N. Bordallo, O. Delaire, J. Nickels, J. Peters, G. J. Schneider, J. C. Smith, and A. P. Sokolov, *Broadband Wide-Angle VElocity Selector (BWAVES) neutron spectrometer designed for the SNS Second Target Station*, EPJ Web of Conferences **272**, 02003 (2022).
8. K. J. Bichler, *Morphology and Dynamics of Bottlebrush Polymers*, Springer International Publishing (2021).
9. K. J. Bichler, B. Jakobi, V. García-Sakai, A. Klapproth, R. A. Mole, and G. J. Schneider, *Universality of the Time-Temperature Scaling Observed by Neutron Spectroscopy on Bottlebrush Polymers*, Nano Lett. **21**, 4494 (2021).
10. K. J. Bichler, B. Jakobi, and G. J. Schneider, *Dynamical Comparison of Different Polymer Architectures – Bottlebrush vs. Linear Polymer*. Macromolecules **54**, 1829 (2021).

Small Angle Neutron Scattering (SANS) Insight into Deconstruction Reaction of Complex Polymer Systems

Manjula Senanayake[a], Jialiang Zhang[a], Jingwen Luo[a], Anand Narani[a], Snehasish Mondal[a], Sai Venkatesh Pingali[b], Marcus Foston[a].
[a]Department of Energy, Environmental and Chemical Engineering, McKelvey School of Engineering, Washington University in St. Louis, Missouri 63130, United States.
[b]Neutron Scattering Division, Oak Ridge National Laboratory, Oak Ridge TN 37831, USA

Keywords: *In situ*-SANS, Biomass pretreatments, Heterogeneous catalyst**,** Plastics recycling

Research Scope

Understanding the mechanisms of polymer deconstruction, reconstruction, and functionalization is currently a topic of intense research[1]. Polymer deconstruction, reconstruction, and functionalization involve the complex coupling of chemical and physical processes that span a wide range of length and time scales. The macromolecular nature of the reaction substrate altered reaction thermodynamics, kinetics, and transport. This inherent complexity demands the development of in-situ characterization techniques and tools that are non-destructive and capable of revealing and quantitating changes in polymer substrates, reaction intermediates, and products in real time with sufficient spatial and temporal resolution under reaction conditions. In this presentation, I will highlight the on-going efforts by our group and collaborators at the Neutron Scattering Division of the Oak Ridge National Laboratory (ORNL) to advance *in-situ* small angle neutron scattering (*in-situ* SANS) as a method to provide unique insight into the polymer deconstruction reaction, in particular, those for the valorization of biomass- and plastic waste-derived polymer systems.

In-situ SANS measurements have become a critical tool in the development of complex systems and structures, enabling a deeper understanding of the underlying processes and interactions that determine material behavior and properties under realistic synthesis, processing, or operational conditions[2]. *In-situ* techniques observe, either continuously or at discrete intervals, an evolving material system often at high temperature (high-T) and/or high pressure (high-P). These *in-situ* measurements can provide unique information on changes that are often not retained upon quenching or cooling to room temperature such as phase transitions, rapid structural ordering, supercritical fluid dynamics, and reaction intermediate compositions only present at high-T and/or high-P. Moreover, even in cases where intermediate states are observable by *ex-situ* measurements, achieving the same independent variable resolution often is not possible due to limited resources and time. The ability to study materials at conditions away from standard temperature and pressure is crucial to understanding polymer deconstruction, in particular, the effect of or consequence on polymer morphology. This abstract leverage our previous experience using *in-situ* SANS to study lignocellulosic biomass during thermochemical processing[3] and catalytic depolymerization of lignin to the future projects in plastic upcycling.

Recent Progress

In-situ SANS to Study the Structural Reorganization During Pretreatment Reaction[3] : Biofuel generation from lignocellulosic biomass requires pretreatment to open the plant cell wall structure to improve enzyme access. Many different thermal, chemical and mechanical pretreatments have been extensively studied and employed. However, the most efficient and economical approach in the deconstruction of the plant cell wall via pretreatment to minimize its recalcitrant behavior for commercially viable biofuels still remains elusive. This study focused on understanding the role of noncellulosic polymers in switchgrass in altering the overall efficiency of pretreatment. The structural evolution of the matrix polymers in the plant cell wall was probed during dilute acid pretreatment (DAP) by using *in-situ* small-angle neutron scattering (*in-situ* SANS); The is the only technique that allows to observe structural changes in real time during a slow reaction. The samples studied were native switchgrass (NATV), isolated holocellulose (HOLO; lignin removed), and isolated cellulose (CELL; lignin/hemicellulose removed). The results show that aggregation was first observed at 80 °C for NATV and HOLO samples. Aggregate particles of much larger size was observed for only NATV sample at 130 °C and attributed to lignin aggregates. At higher severity of pretreatment condition of the HOLO sample, hemicellulose-derived aggregate particle sizes increased, suggesting this process was the nucleation and early-stage formation of pseudo lignin particles. Consistent with our interpretation for NATV and HOLO samples, no formation of aggregate particles was observed in CELL samples for the entire duration of the pretreatment. These results suggest that not only lignin but also hemicellulose can form aggregate particles within plant cell walls during pretreatment.

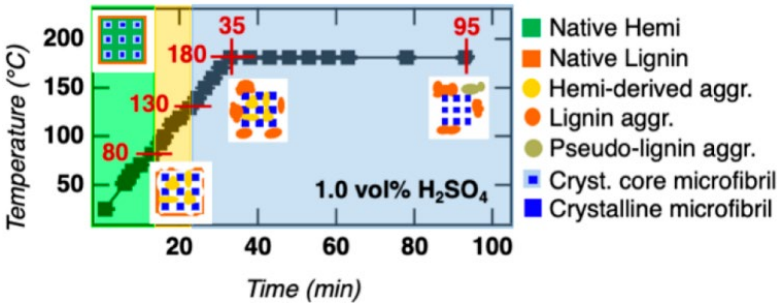

Fig. 1. Structural evolution of cellulose, hemicellulose, and cellulose at different temperatures and time in dilute acid pretreatment reaction predicted by *in-situ* SANS data analysis. **This figure was taken from *ACS Sustainable Chemistry & Engineering,* 10(1), pp.314-322.**

In-situ Neutron Scattering of the Lignin Depolymerization: Lignin (an aromatic macromolecule in biomass), the only renewable source of aromatics, is currently treated as waste and under-utilized. A more appealing and value-added use of lignin is as a precursor for the production of aromatic chemicals[4]. The depolymerization of lignin selectively into its monomers can be achieved by the appropriate combinations of solvent, catalyst, and reaction conditions. However, due to the considerable

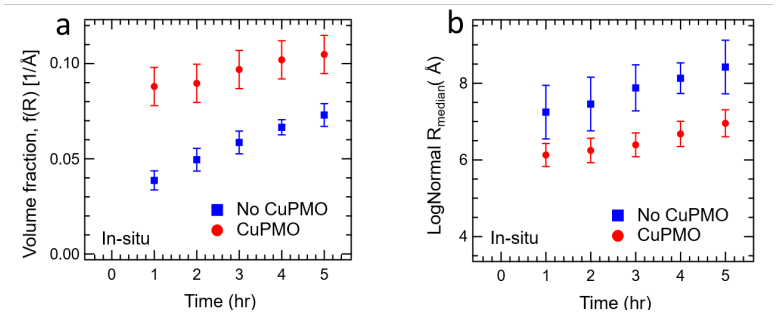

Fig. 2. The dependence of volume fraction (a), and log normal median radius (b) as a function of reaction time (blue: without CuPMO, red: with CuPMO) extracted from *in-situ* SANS data analysis.

complexity and natural variation in the molecular structure of lignin, mechanistic studies of catalytic lignin depolymerization are challenging. Beyond that, lignin depolymerization usually (1) requires high temperature (> 200 °C) and pressure (~ 80 bar); (2) involves co-existence of solid, liquid and gas phases; and (3) differs from typical catalytic reactions due to the macromolecular nature of the substrate. In this study, we have applied Small Angle Neutron Scattering (SANS) on lignin samples to probe their polymer coil size and conformational changes that occur at reaction conditions and upon interaction with copper-doped porous metal oxide catalyst. In-situ and ex-situ small angle neutron scattering (SANS) was used to study the structural changes of lignin during non-catalytic solvolysis reactions in deuterated methanol (MeOH-d_4) and reactions in the presence of a copper-containing porous metal oxide (CuPMO) catalyst and MeOH-d_4. The results indicate that at room temperature, lignin adopted a rigid and stretched conformation that becomes more spherical, flexible, and folded when heated to the reaction temperature of 250 °C. In the presence of CuPMO, the volume fraction of small lignin particles (Fig. 2a) (< 50 Å) is higher than under solvolysis conditions while the median radius (Fig. 2b) of this fraction of lignin particles is smaller. The SANS data was analyzed using a population balance model and found that two reaction processes dominate: disassembly of large lignin aggregate particles (> 50 Å) and condensation of small lignin particles (< 50 Å). The study also suggests that the cooling and quenching step in the ex-situ experiments alters the small lignin (< 50 Å) particle size distribution. This project leverages the unique high- temperature and pressure neutron cell technology at the Oak Ridge National Laboratory (ORNL).

Future Plans

In-situ SANS of the Plastic Upcycling: This project focuses on the use of porous heterogeneous catalysts in efficient plastic upcycling. Although porous heterogeneous catalysts have been shown to deconstruct polymer chains, these reactions are often non-selective because the open environment around the catalyst active sites permits non-specific interactions with indiscriminate positions along the polymer chain.

A processive mechanism of polymer deconstruction involves polymer substrate threading and confinement into a catalytic pore (Fig. 3a); and a bond breaking reaction at such active site can generate low molecular mass polymeric fragments selectively. Polyolefins, such as polyethylene (PE), and polypropylene (PP), are difficult to deconstruct by low-energy, controlled processes. Yet, in a recent effort by Tennakoon et al.[5] used of mesoporous silica ($mSiO_2$) doped with platinum nanoparticle (Pt NP) active sites enabled the processive deconstruction of PE and the tunable generation of a C_9 to C_{18} alkane product (Fig. 3b). However, the mechanism of this reaction is not clear. In this project, we will use neutron scattering to investigate (1) the mechanisms of polymer substrate infiltration into catalytic pores; (2) how polymer substrate infiltration into catalytic pores leads to processive polymer deconstruction; and (3) how catalyst pore size and surface chemistry affect polymer substrate infiltration into catalytic pores, and thus processive polymer deconstruction. The $mSiO_2$ catalyst support (i.e., SBA-15) has neutron scattering length densities (SLD) near that of silica, $\rho SiO2 = 3.47 \times 10^{-6}$ Å $^{-2}$. Based on this SLD, we will synthesize and/or purchase partially deuterated polyethylene (pdPE) at a hydrogen isotopologue mole fraction of the contrast match point for the $mSiO_2$ catalyst support. We have been awarded a proposal to the Center for Nanophase Materials Science (CNMS) at ORNL for pdPE synthesis. We will conduct the *in-situ* neutron experiments in extended-angle pressure cells (EAP) capable of reaching 300 °C. We intend to cover a range of scattering vectors of 0.008 Å^{-1} < Q < 0.7 Å^{-1}, by employing two configurations consisting of the detector sample-to-detector distances of 7 m and 1 m with neutron wavelength, λ of 4.75 Å. This broad Q range is required to study the breaking down of large PE chains into smaller fragments. We will use *in-situ* SANS to visualize plastic waste substrates in the melt, within catalyst pores, and at catalyst surfaces. $mSiO_2$ supported catalysts, known to promote threading and confinement of PE within its pores, will be studied. The results will elucidate the material design principles for heterogeneous and processive catalysts for effective plastic waste upcycling by leveraging the unique interactions of neutrons with various materials.

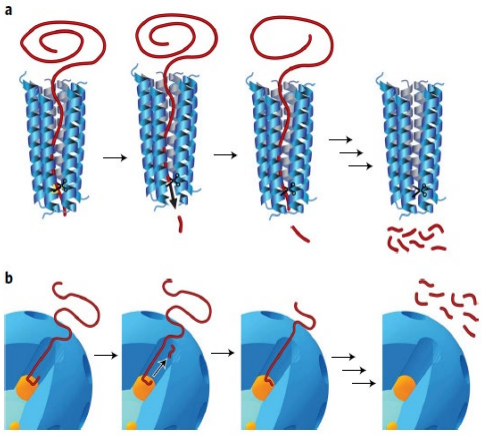

Fig. 3. Processive deconstruction of macromolecules. **(a)** The processive mechanism through which many enzymes deconstruct large macromolecules. **(b)** An analogous mechanism proposed for a Pt nanoparticles (are located at the end of nanoscale pores in $mSiO_2$.) **This figure was taken from *Nature Catalysis*, *3*(11), pp.893-901**.

References

1. Britt PF, C. G., Winey KI, Byers J, Chen E, Coughlin B, Ellison C, Garcia J, Goldman A, Guzman J, Hartwig J., Report of the Basic Energy Sciences Roundtable on Chemical Upcycling of Polymers. *USDOE Office of Science (SC)(United States)* **2019**.
2. Herrera, F.; Rumi, G.; Steinberg, P. Y.; Wolosiuk, A.; Angelomé, P. C., Small Angle Scattering Techniques for the Study of Catalysts and Catalytic Processes. *ChemCatChem* **2023,** *15* (17), e202300490.
3. Yang, Z.; Foston, M. B.; O'Neill, H.; Urban, V. S.; Ragauskas, A.; Evans, B. R.; Davison, B. H.; Pingali, S. V., Structural Reorganization of Noncellulosic Polymers Observed In Situ during Dilute Acid Pretreatment by Small-Angle Neutron Scattering. *ACS Sustainable Chemistry & Engineering* **2022,** *10* (1), 314-322.
4. Wang, H.; Pu, Y.; Ragauskas, A.; Yang, B., From lignin to valuable products–strategies, challenges, and prospects. *Bioresource Technology* **2019,** *271*, 449-461.

5. Tennakoon, A.; Wu, X.; Paterson, A. L.; Patnaik, S.; Pei, Y.; LaPointe, A. M.; Ammal, S. C.; Hackler, R. A.; Heyden, A.; Slowing, I. I.; Coates, G. W.; Delferro, M.; Peters, B.; Huang, W.; Sadow, A. D.; Perras, F. A., Catalytic upcycling of high-density polyethylene via a processive mechanism. *Nature Catalysis* **2020,** *3* (11), 893-901.

Publications

N/A

Study of Magnetic Charge Dynamics and Correlation in Artificial Magnetic Honeycomb Lattice, DOE BES Grant # DE-SC0014461

Deepak Kumar Singh, University of Missouri, Columbia, MO

Keywords: Geometrically Frustrated Magnet, Nanoengineering, Spintronics, Antiferromagnetism

Research Scope

Two-dimensional nanoengineered magnetic materials render archetypal platform to study novel scientific principle or phenomenology in disorder-free environment.[1-2] It is even more desirable in geometrically frustrated magnet where the reduction in dimensionality tends to have novel effect on magnetic properties. In the geometrically frustrated 2D honeycomb lattice, made of nanoscopic permalloy elements (typical size ~ 11 nm (length). 4 nm (width). 6-8 nm (thickness)), the underlying physics is governed by the emergent magnetic charge correlation. Despite the classical nature of the system, magnetic charge correlation and dynamics can exhibit unusual dynamic properties that are reminiscent of quantum magnetic material of atomistic origin. Understanding that property can be instrumental to the development of new science with potential for new practical implications. In the current proposal, we have discovered a new phenomenon of quasi-particle dynamics in two-dimensional magnetic honeycomb lattice that can be prevalent in any constricted nanostructured magnet. Unlike the conventional notion of domain wall dynamics as the only mechanism in nanomagnet, which requires magnetic field or electric current application, the quasi-particle kinetics are self-propelled at a temperature much below the shape-anisotropy energy barrier. The nanoscopic size quasi-particle, having the form of a vortex loop, undergoes a near-barrierless transport across the lattice, see Fig. 1. This is similar to magnetic monopole's tunneling or hopping in the monopolar regime of spin ice.[3] Besides the barrierless transport, it also exhibits temperature independent relaxation. These characteristics signifies the quantum mechanical nature of the dynamic entity. The persistent dynamic state at low temperature in 2D honeycomb lattice causes a liquid-like correlation between magnetic charges, akin to spin liquid state in bulk quantum magnet. The quasi-particle kinetics renders a new dynamic mechanism in nanomagnets, especially with constricted geometry. Since dynamic phenomena are at the core of spintronic applications in nanostructured magnet, this new finding

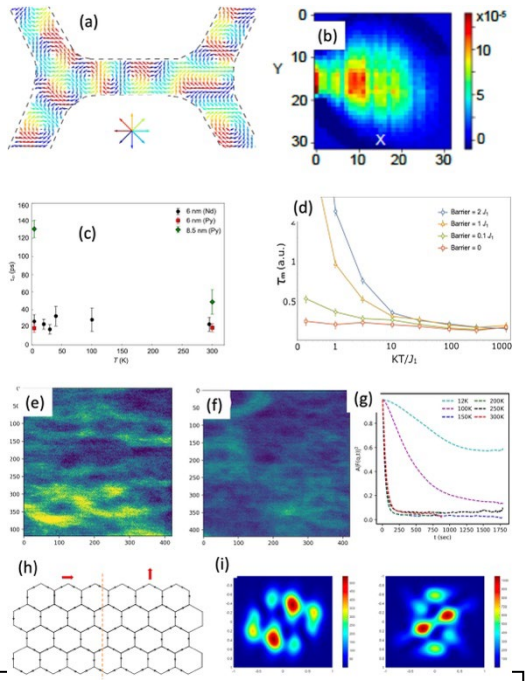

Figure 1: (a) Numerically simulated profile of vortex-type quasi-particle in nanostructured magnet. (b) NSE data showing localized excitations due to quasi-particle kinetics in 2D honeycomb lattice. (c) Temperature dependence of t. Quasi-particle dynamics is temperature independent in thin film. As thickness increases, t increases, especially at low temperature. (d) Temperature independent characteristic is only possible in the barrier-less transport, indicating quantum mechanical nature of phenomena. (e-g) XPCS data showing much slower relaxation at the macroscopic scale. (h-i) Numerical modeling of domain structures, made of several honeycomb units, explains the behavior.

can have strong implication to the spintronic device development. We have also explored and study bulk magnetic materials for spintronics research that act as guide in understanding new phenomena in 2D system.

Our research also highlights the importance of neutron spin echo (NSE) and small angle neutron scattering (SANS) in the study of novel magnetic phenomena in nanostructured magnets that have not been apparent among scientific community. Additionally, the funding allows to train graduate students and postdocs in the use of cutting-edge technologies, from nanoengineering and the synthesis of single crystal specimens to the most advanced measurement techniques of neutron scattering methods. Thus, it serves one of the main purposes of DOE-BES program in developing workforce with deep understanding of cutting-edge techniques.

Recent Progress

The nanoscopic quasi-particle is highly intriguing and extremely exciting. It not only provides us a great opportunity to understand the artificially created two-dimensional geometrically frustrated magnets from a new angle, but also generates new avenues for the technological applications in spintronic device designs and reservoir computing. In the current proposal, we have made deep inroad in understanding as well as establishing the existence of quasi-particle dynamics. To understand the nature of quasi particle, we need to perform a comprehensive set of measurements that include neutron spin echo (NSE), spin polarized neutron reflectometry (spin-PNR), SANS and X-ray Photon Correlation Spectroscopy (XPCS) on a diverse set of magnetic honeycomb lattice samples with varying geometrical and materialistic parameters. NSE and SANS measurements typically require large stacks of 2D lattice samples to increase the signal-to background ratio. Continuing the efforts in this regard, we have created a large stack of 125 macroscopic size (one sq. inch) artificial honeycomb lattice samples that were used for the NSE measurements. Detailed investigation of the dynamic properties revealed temperature independent relaxation of magnetic charge quasi-particle. The dynamic properties are robust even at T = 4 K, which is more than an order of magnitude smaller than the barrier-crossing energy (~ 75 K) for magnetization reversal due to shape anisotropy. The experimental research on the investigation of quasi-particle character of magnetic charge is complemented by theoretical calculations using quantum Monte-Carlo simulations (by Carsten Ullrich group) that suggest that such behavior can only arise in barrier-less transport of a quantum magnetic entity, see Fig. 1.

The persistent kinetics of quasi-particle causes liquid-like correlation between magnetic charges at low temperature. The liquid state is characterized by massive degeneracy of charge configurations that remain unperturbed to magnetic field application and manifest paramagnetic behavior to the lowest measurement temperature. We have performed detailed SANS measurements in applied magnetic field up to H = 10 T to understand the nature of magnetic charge liquid state at the nanoscopic level. Experimental investigation of dynamic properties in permalloy honeycomb lattice at a much longer length scale (typical domain made of 4 - 8 honeycomb units with average size of ~ 200 nm – 400 nm) using recent XPCS measurements suggest the existence of another macroscopic time scale. In addition to the persistent kinetic behavior at the nanoscopic scale, we find that multiple honeycomb units form domains that fluctuate at finite time scale of ~ few s to 400 s at T = 4 K, see Fig. 1. So, the dynamic behavior in 2D honeycomb lattice is multi-faceted and requires careful investigations.

In addition to the fundamental study, an important emphasis of our research program lies in the exploration of spintronic properties in 2D system. Previously, we had reported the discovery of magnetic diode effect in permalloy honeycomb lattice which was ascribed to the physics of magnetic charge correlation and dynamics. It showed that the magnetic charge physics provides a new venue for spintronics research and device development. We have further investigated the magnetic diode

properties as functions of temperature and magnetic field in constricted sample size, which is one of the requisites for developing practical applications. New measurements have revealed a peculiar reentrant characteristic where diode behavior is suppressed in the remnant field but reappears after thermal cycling. This new finding can be useful for the development of MRAM devices. Besides 2D material, we have also explored spintronic properties in bulk materials. In a surprising new finding, we discovered high temperature antiferromagnetism in technologically important NiSi compound with Neel temperature in excess of 700 K. Interestingly, the presence of two Ni sites with varying moments break the rotational symmetry, thus making it a non-centrosymmetric AFM compound. Also, the AFM order parameter is not fully compensated, rather a small FM component develops in the basal plane, perpendicular to the AFM order parameter. The FM and AFM order parameter exhibit distinct responses to magnetic field application directions. For example, magnetic and electrical characterizations of the system show one-step switching and the occurrence of magneto-electronic hysteresis at non-zero field values that are ascribed to the FM and AFM orders, respectively. We have also made efforts in understanding the conventional II-VI FM diluted magnetic semiconductors for the spintronics research purposes.

The research program in our group has also been very successful in training graduate students. In the current proposal, two students (George Yumnam and Jiasen Guo) have graduated with Ph.D. degree in physics. They both are currently working as the postdoctoral scholar at ORNL. Another student (Pousali Ghosh) is also expected to graduate in the summer or Fall 2024.

Future Plans

There are three central questions at the core of our research: Is the quasi-particle dynamics universal to nanomagnetic lattice? What is the nature of quasi-particle? Lastly, how does it impact the development of spintronic and reservoir computing devices?

We will take comprehensive approach of experimental and theoretical researches to address these questions. For that purpose, we will create and investigate three different nanomagnets: chemically ordered and distorted magnetic honeycomb lattice systems, and lamellar shape nanomagnetic structure using experimental techniques of NSE, XPCS, PNR, SANS and magnetic measurements. It will provide information on both static and dynamic properties. Experimental data will be used for the numerical modeling and theoretical analysis to draw a solid conclusion regarding the nature of quasi-particle. Hopefully, better understanding of the nature of quasi-particle will allow us to find suitable nobs for the tuning of spintronic properties in the artificial 2D nanomagnet. In recent times, artificial honeycomb spin ice is extensively studied to develop reservoir computer.[4] In most cases, researchers use magnetic field to tune the individual magnetic moment direction in large element size lattice that typically have disconnected structural motif. The ultra-small element and the contiguous structure in our sample allows for the electric current-based tuning of magnetic state in the 2D system. In recent preliminary measurements, we have obtained evidence in this regard. In future research, we vigorously plan to pursue this research. We will take dual approaches in this regard: first, we will perform experimental investigation using PNR measurements in current bias input conditions on samples of varying geometrical parameters and materials characteristics. Second, the experimental data will be used for machine training and testing in each case to find the optimal solution.

References

[1] S. Skjjaervo, C. Marrows, R. Stamps and L. Heyderman, Advances in artificial spin ice, *Nat. Rev. Phys.* **12**, 13 (2020).
[2] P. Schiffer and C. Nisoli, Artificial spin ice: Paths forward, *Appl. Phys. Lett*. **118**, 110501 (2021)
[3] S. Bramwell, Magnetricity near the speed of light, Nat. Phys. 8, 703 (2012).
[4] L. Heyderman, Spin ice devices from nanomagnets, *Nat. Nano*. **17**, 435 (2022)

Publications

[1] J. Guo, D. Hill, V. Lauter, L. Stingaciu, P. Zolnierczuk, C. Mazzoli, P. Ghosh, C. Ullrich and D. K. Singh, Evidence to new dynamic phenomena due to quasi particle kinetics in constricted nanomagnet, Submitted (2023)
[2] P. Ghosh, J. Guo, G. Yumnam, L. DeBeer Smith, A. Glavic, V. Lauter, L. Stingaciu, P. Zolnierczuk and D. K. Singh, A new liquid state of magnetic charge in honeycomb spin ice, *Nature Physics* (in 2nd round of review, 2023)
[3] J. Guo, P. Ghosh, D. Hill, Y. Chen, L. Stingaciu, P. Zolnierczuk, C. Ullrich and D. K. Singh, Persistent dynamics magnetic state in artificial honeycomb spin ice, *Nature Communications* 14, 5212 (2023)
[4] J. Guo, A. Sarikhani, P. Ghosh, T. Heitmann, Y. S. Hor and D. K. Singh, Chemically induced ferromagnetism at room temperature in single crystal (ZnCr)Te, *RSC Advances* 13, 8551 (2023)
[5] P. Ghosh, J. Guo, F. Ye, T. Heitmann, G. Yumnam, S. Kelley, A. Ernst, V. Dugaev and D. K. Singh, NiSi: New venue for antiferromagnetic spintronics, *Advanced Materials* 2302120 (2023)
[6] G. Yumnam, M. Nandi, P. Ghosh, A. Abdullah, M. Almasri, E. Henriksen and D. K. Singh, Field and temperature tuning of magnetic diode in permalloy honeycomb lattice, *Materials Today Advances,* 18, 100386 (2023)
[7] J. Guo and D. K. Singh, Diode type unidirectional conduction in Hall measurement of magnetic honeycomb lattice, *Physics Letters A* (2023)
[8] V. Lauter, K. Wang, T. Mewes, A. Glavic, B. Toperverg, M. Ahmadi, B. Assaf, B. Hu, M. Li, X. Liu, Y. Liu, J. Moodera, L. Rokhinson, D. K. Singh, and N. Sun, M-STAR: Magnetism second target advanced reflectometer at the Spallation Neutron Source, *Rev. Sci. Instrum*. 93, 103903 (2022)
[9] (Invited submission) J. Guo, V. Dugaev, A. Ernst, G. Yumnam, P. Ghosh and D. K. Singh, Topological monopole's gauge field induced spontaneous magnetization and anomalous Hall effect in artificial honeycomb lattice, *Natural Science* 2, e20210083 (2022)
[10] (Invited article on the 60th anniversary of the PSS journal) D. K. Singh, A. Ernst, V. Dugaev, Y. Chen and J. Gunasekera, Quantum magnetic properties and metal-to-insulator transition in chemically doped calcium ruthenate perovskite, *Physica Status Solidi B* 2100503 (2022)

Inelastic and Quasielastic Neutron Scattering Studies of Dynamics and Relaxations in Glasses

Hillary Smith, Department of Physics & Astronomy, Swarthmore College

Keywords: glasses, liquids, inelastic neutron scattering, quasielastic neutron scattering, phase transformations

Research Scope

The goal of this early-career project is to characterize the vibrational dynamics and relaxations in glass-forming liquids in the undercooled state above the glass transition, providing new insights into the nature of the glass transition. Glasses can be formed by cooling a material from its liquid state quickly enough that nucleation and growth of the crystalline phase is avoided. Figure 1(a) shows a Time-Temperature-Transformation diagram illustrating two possible cooling pathways from above the melting temperature. Figure 1(b) illustrates the temperature dependence of the volume and enthalpy of the supercooling liquid at constant pressure. The brief timescale available to probe the metastable liquid phase above the glass transition has severely limited the information that can be gained from traditional experimental tools because dynamics are rapidly changing and a thermodynamic driving force towards crystallization limits the timescale on which measurements can be performed in many glasses [1]. However, a description of the dynamics and relaxations at the glass transition and in the undercooled liquid phase in amorphous materials is critical to address fundamental questions in condensed matter physics including theories of phase transitions and states of matter [2]. This proposal will use operando inelastic neutron scattering and in situ quasielastic neutron scattering at the SNS to probe the metastable liquid phase in a range of glass-forming liquids. This project will also take advantage of event-based data collection capabilities at the SNS and develop high throughput-code for the analysis of operando INS and in situ QENS data [3]. We propose the following aims: 1) direct assessment of the vibrational entropy across the glass transition in a range of glass types; 2) investigation of the secondary relaxations and microscopic length scale dependence in the undercooled liquid phase of these glasses; 3) development codes for event-based analysis of operando INS and in situ QENS data.

Recent Progress

This early-career project started in Sept 2023. For the past three months the team has been focusing on QENS and INS data analysis and code development.

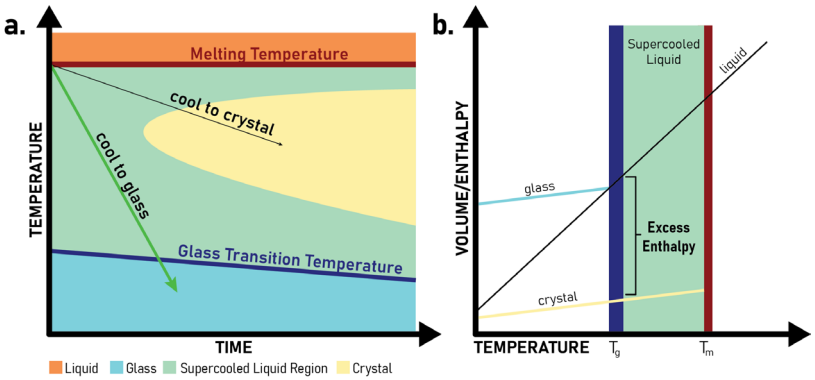

Figure 1: Overview of glass formation from the liquid phase. (a) TTT diagram with two possible cooling pathways for formation of a crystal (black) or glass (green) depending on cooling rate. (b) If a liquid forms a glass, it will have a higher volume and enthalpy than if it formed a crystal.

Characteristic Length Scales of Secondary Relaxations in Ultra-fragile Metallic Glasses

We performed in situ QENS experiments on BASIS for an ultra-fragile Pt-based metallic glass. We are assessing the temperature-dependent differences in the glass, liquid, and crystalline phases of this material. The primary goal of this investigation is to observe changes in atomic motions as the glass traverses the glass transition to the undercooled liquid phase and determine the timescale of beta relaxations in the undercooled liquid. Detailed understanding of the atomic relaxation processes in glasses is important for understanding the origins of glass formation, nucleation and growth of the crystalline phase, and the physical properties that make glasses unique. Both alpha and beta relaxations play an important role in determining bulk and microscopic properties of glassy materials. Alpha relaxations are responsible for vitrification and allow for cooperative motions of atoms at the microscopic level. Beta relaxations affect the mechanical properties of glassy solids, relate to diffusion, and affect crystallization and stability of glasses. The Q-dependence of the mean relaxation times will also reveal the characteristic relative length scale of these motions, a value that has not been reported in metallic glasses immediately above the glass transition.

The metallic glass selected for study here was first reported in 2020 and has not yet been the subject of QENS experiments. We reported *in situ* inelastic neutron scattering experiments on this glass using ARCS to assess the contribution of vibrational entropy to the specific heat absorbed as a glass transforms to a liquid [4]. Similar to our results for two Cu-based metallic glasses, we found no discontinuity in the vibrational entropy between the glass and the liquid at T_g [5]. We used a similar experimental approach to capture BASIS data for this glass, using our previous heat capacity and INS measurements as a guide. Figure 2 shows the heat capacity of $Pt_{57}Cu_{23}P_{20}$ with vertical lines indicating the onset of the glass transition, T_g, the onset of crystallization, T_x, the liquidus temperature, T_L, and the crossover temperature, T_c, estimated at twice T_g. The blue region indicates temperatures that are typically probed using QENS to study alpha relaxations in metallic glasses, beginning at T_L and extending about 250K. The green region indicates the temperature range of interest here, where we collected in situ data to probe the length scales of faster beta relaxations through the glass transition.

Analysis of our BASIS data is underway, as well as development of event-based data reduction procedures for BASIS in collaboration with computational instrument scientists.

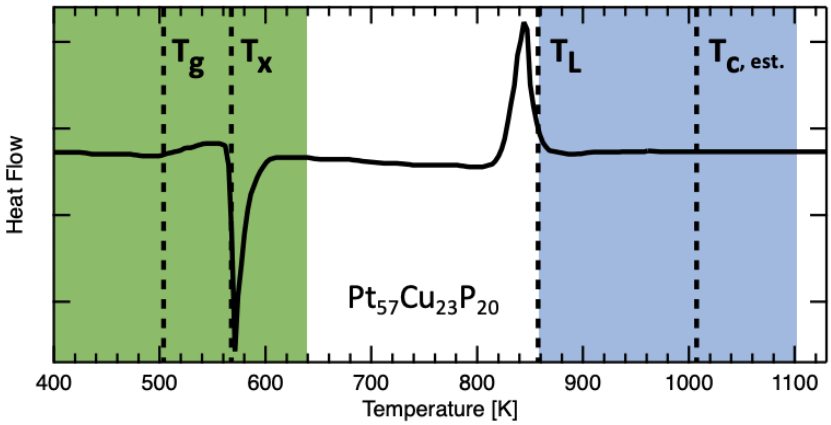

Figure 2: Heat capacity measurement for $Pt_{57}Cu_{23}P_{20}$ glass. The blue region indicates temperatures that are typically probed using QENS to study alpha relaxations in metallic glasses, beginning at T_L and extending about 250K. The green region indicates the temperature range of interest here, where we seek the length scales of faster beta relaxations through the glass transition.

Dynamics of Glassy and Liquid Selenium

We measured the dynamics in liquid and glassy selenium on ARCS using operando INS. Selenium is a chalcogenide glass that is characterized by short-range order and an atomic bonding structure that is more rigid than polymer glasses and more flexible than oxide glasses. Neutron scattering studies of Se and Se-Ge-As glasses were reported in 1989 and 1991, respectively. The high fragility of amorphous selenium results in a large, discontinuous increase in the entropy at the glass transition, in considerable excess of crystalline selenium. Phillips et al. performed the 1989 neutron scattering experiments that confirmed an earlier calorimetry report quantifying the fraction of the excess entropy that is vibrational to be about one-third. For many years these results have been the standard for describing vibrational contributions to the excess entropy at the glass transition, however, these results deserve another look, not least of which because the capabilities of modern neutron instrumentation and unequaled neutron flux at the SNS makes it possible to capture higher resolution data in a shorter period of time than ever before.

Analysis of the operando INS data on selenium is underway. Unlike traditional powder INS measurements that may produce a phonon density of states at 5-10 temperatures over 24 hours, a 4-hour operando INS measurement produces 250 diffraction patterns and 25-75 densities of states at a beam power of 1.4 MW. This output is expected to increase following the PPU project completion when data collection occurs even more quickly, making the need for high-throughput data processing codes more acute. We have written scripts that allow us to extract time and temperature- aggregated data, but this process requires development to make the code capable of large-scale processing and improve its user interface, which are part of the objectives of this project.

Future Plans

For operando INS, we are developing the necessary tools to analyze time-resolved phonon DOS for a range of amorphous materials as they traverse the glass transition. This work will provide the analysis tools necessary to post-process data that is collected while continuously heating the glass through its glass transition and subsequent crystallization. Ultimately, we seek to unify our understanding of the role of phonon dynamics at the glass transition across many types of glasses.

For in situ QENS, the necessity of long measurement times to obtain adequate signal means that we are limited in the systems that we can study. Development of analysis tools to post-process

this data is still necessary so that the long measurement data can be analyzed to determine whether the liquid went through a phase transformation (crystallization) during the measurement, and extract the liquid phase data for comparison with the glass and crystalline phases. This work will investigate the relaxations in the undercooled liquid phase of several glasses with thermodynamic stability on a timescale that is complementary to QENS data collection.

This research will impact the experimental glass communities by advancing our understanding of how the dynamics of glass-forming liquids can be used to predict properties such as glass-forming ability and stability against crystallization that are critical to engineering applications of glasses. The theoretical glass community will benefit from fresh insight into the vibrational dynamics and relaxations that are necessary to shape the description of the glass-liquid transition and Potential Energy Landscape theory.

References

1. J. Schroers, *On the formability of bulk metallic glass in its supercooled liquid state*, Acta Materialia **56,** 471 (2008).
2. F.H. Stillinger, P.G. Debenedetti, P. G. *Glass Transition Thermodynamics and Kinetics*, Annual Review of Condensed Matter Physics **4,** 263 (2013).
3. P.F. Peterson, S.I. Campbell, M.A. Reuter, R.J. Taylor, J. Zikovsky, *Event-based processing of neutron scattering data*, Nuclear Instruments and Methods in Physics Research, A **803,** 24 (2015).
4. H. L. Smith, C.N. Saunders, C. Bernal-Choban, S.H. Lohaus, C. Stoddard, L.K. Decker, J.Y.Y. Lin, J.L. Nieziela, D.L. Abernathy, J.-H. Na, M.D. Demetrious, B. Fultz, *Vibrational dynamics in the undercooled liquid of ultra-fragile metallic glasses*, Materialia **27**, 101710 (2023).
5. H.L. Smith, C.W. Li, A. Hoff, G.R. Garrett, D.S. Kim, F.C. Yang, M.S. Lucas, T. Swan-Wood, J.Y.Y. Lin, M.B. Stone, D. L. Abernathy, M.D. Demetriou, B. Fultz, *Separating the configurational and vibrational entropy contributions in metallic glasses,* Nature Physics **13,** 900 (2017).

Publications

We do not have publications to report. The project initiated three months ago.

Neutron Scattering Studies of Non-Linear Quantum Hydrodynamics and Backscattering in Low-Dimensional Systems

Paul Sokol, Indiana University, Bloomington (Principal Investigator)
Garfield Warren, Indiana University, Bloomington (Co-Investigator)
Adrian Del Maestro, University of Tennessee, Knoxville (Co-Investigator)

Keywords: 1D Luttinger physics, helium, porous materials,

Research Scope

This project aims to push the boundaries of One-Dimensional (1D) Luttinger physics by leveraging helium as a tool for exploration. With the rapid advancement of technology and the growing ability to manipulate matter at the atomic level, the significance of one-dimensional quantum many-body systems has escalated. However, comprehensive exploration of 1D behavior, especially within systems featuring tunable experimental parameters, remains a significant challenge. While certain systems like spin chains, nanotubes, and ultracold gases showcase elements of 1D behavior, they typically maintain fixed densities, limiting their capacity to delve into nonlinear quantum hydrodynamics and impeding a thorough investigation into the revolutionary aspects of 1D physics.

We have developed novel nanoengineered porous materials capable of confining helium atoms in one dimension amenable to neutron scattering studies. Our preliminary studies utilized MCM-41, a templated porous material, with pores pre-plated with Argon. The preplating of the pore reduced the pore size sufficiently that one-dimensional behavior could be observed. Preliminary neutron scattering studies, when compared to theoretical predictions (Fig 1) provide strong evidence of 1D behavior.

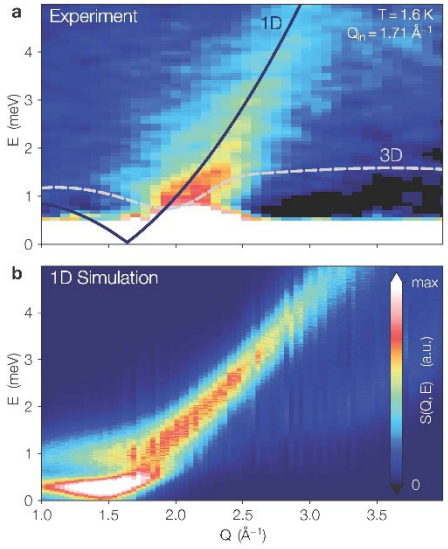

Fig 1: Inelastic scattering of a 1D quantum liquid. **a** The dynamic Structure factor, S(Q,E), from helium confined in the Ar plated pores of MCM-41. **b** the dynamic Structure factor of a purely 1D system of 4He at T=1.6 K obtained via numerical analytic continuation of the imaginary time scattering function measured via quantum Monte Carlo. From Ref . 3

This project is dedicated to fully harnessing the potential of this innovative model system. Its inherent advantage lies in the flexibility to manipulate the Luttinger liquid parameter, allowing for a spectrum from the weakly interacting dilute limit to the densely interacting concentrated limit. The research objectives encompass several key areas: 1) leveraging neutron scattering's unique capabilities to investigate both the structure and excitations within a confined, strongly interacting quantum liquid in low dimensions; 2) comprehending low-dimensional hydrodynamic transport in the quantum realm amid various types of impurities—be they fixed or mobile; 3) pioneering novel fabrication methodologies to engineer a 1D porous framework, leveraging rare earth pre-plating for unparalleled parameter tuning; 4) identifying momentum-dependent power laws within the dynamic structure factor, detected via neutron scattering, as indicative of physics surpassing the conventional Luttinger liquid paradigm; 5) scrutinizing the structure of the confined liquid, discerning the impacts of impurities and their roles

in low-dimensional particle transport; 6) investigating the conjectured emergence of a gapless topological Luttinger liquid regime owing to strong inter-pore atom interactions or spatial confinement within multiply connected pores.

Recent Progress

Commencing in September 2023, this project embarked on its initial phase with a primary emphasis on crafting a porous glass featuring pores coated with cesium. This choice stems from the established understanding that helium atoms do not adhere to a cesium surface[2]. By employing cesium-coated MCM-41, we aim to investigate one-dimensional systems that remain completely isolated from their external environment.

We have explored creating cesium-coated MCM-41 using evaporation techniques. This is challenging since cesium reacts explosively with water which presents a major safety hazard. Cesium is also a solid/liquid at room temperature with essentially zero vapor pressure. Consequently, evaporating cesium into the MCM matrix necessitates elevated temperatures, demanding precise temperature gradients to avert overfilling the pores with cesium, potential desorption of the cesium film, or destabilization of the MCM matrix. However, employing a two-zone furnace has shown promising initial success in mitigating these challenges.

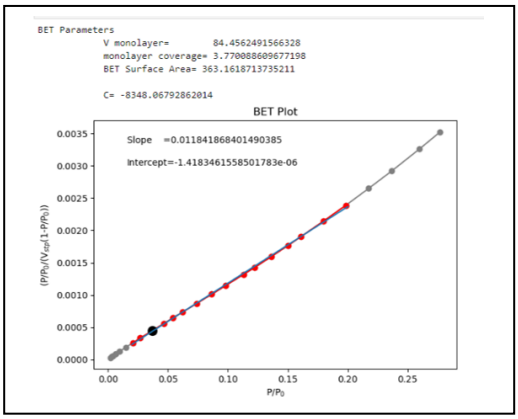

Fig 2: 4He Adsorption isotherm. Helium isotherm on cesium-plated MCM-41 carried out at 4.7 K

Subsequent characterization of the initial sample involved SAXS and nitrogen isotherm studies. These investigations revealed that the hexagonal pore structure remained unaltered following the cesium plating process at high temperatures. Nitrogen isotherms indicated a reduction in pore size and significant alterations in surface absorption potential. Helium isotherm experiments were conducted at 4 K, and Figure 2 illustrates a BET plot of the adsorption data. A notable observation was the negative intercept, suggesting a non-wetting surface. This finding is supported by preliminary theoretical calculations of helium confined inside a porous cavity in a solid cesium matrix.

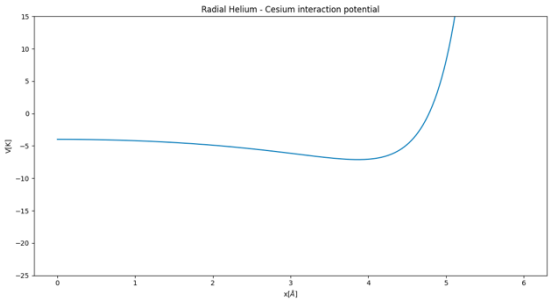

Fig 3: Confinement potential. The potential experienced by a single 4He atom confined inside an infinite cylindrical cavity carved inside solid cesium. The radius of the cylinder is R = 8 Å and the potential parameters are taken from Ref. [4].

We identified the most commonly used interaction potential between He and Cs[4] to compute the total radially symmetric confinement potential as seen in Figure 3. This potential was then included to compute the ground state wavefunction via both the standard shooting method, as well as a ground state path integral quantum Monte Carlo method. The results for the ground state radial wavefunction are in exact agreement as seen in Figure 4.

We see that the density is maximal near the center of the pore and far from the confining wall (the pore has radius 8 Å) indicating a lack of wetting behavior even inside the porous environment. This indicates that a quantum liquid of helium inside Cs coated pores should be directly tunable via density without needing to overcome strong binding (which creates solid-like behavior).

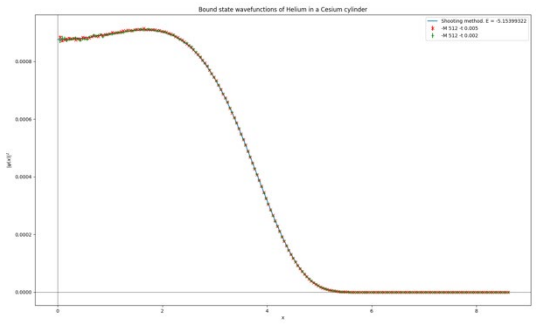

Fig 4: Ground state wavefunction. The radial wavefunction of a 4He atom confined inside a Cs nanopore with R = 8 Å defined by the potential in Fig 3. Line comes from an exact shooting method calculation and symbols are from two different ground state path integral quantum Monte Carlo simulations.

Future Plans

1) Continue our efforts to synthesize and characterize cesium-coated MCM-41. We will continue to develop evaporation-based techniques. We also plan to explore depositing cesium from a cesium-ammonia mixture. Characterization studies will include nitrogen and helium isotherms, SAXS and WAXS.
2) Carry out neutron scattering studies of the behavior of 4He in cesium-coated pores to explore the 1D Luttinger liquid behavior.
3) Move from 1-body to N-body quantum simulations inside a perfect cesium nanopore.
4) Construct an ab initio confinement potential corresponding to the microscopic cesium-coated MCM-41.
5) Investigate simple theoretical models of backscattering inside nanopores.

References

1. T. Giamarchi. *Quantum Physics in One Dimension* (Clarendon Press, Oxford, U.K., 2004). ISBN 9780198525004
2. E. Cheng, M. W. Cole, J. Dupont-Roc, W. F. Saam, and J. Treiner. "Novel wetting behavior in quantum films." Rev. Mod. Phys. 65, 557 (1993) https://doi.org/10.1103/RevModPhys.65.557
3. A. Del Maestro, N. S. Nichols, T. R. Prisk, G. Warren, and P. E. Sokol. *Experimental realization of one dimensional helium.* Nature Communications 13, 1038 (2022). https://www.nature.com/articles/s41467-022-30752-3
4. J. Treiner, *Helium mixtures on weak binding substrates*, J. Low Temp. Phys. **92**, 1 (1993). https://doi.org/10.1007/BF00681869

Publications

We do not have publications to report. The project initiated less than 3 months ago.

Revealing the molecular origin of interactions between nanocrystals

James Swan, MIT (PI)
William Tisdale, MIT (co-PI)

Program Scope

The goal of this research program is to identify and quantify the role of surface-bound molecular ligand layers in directing the self-assembly of colloidal nanocrystals into ordered superlattices. Apart from shape-driven excluded volume interactions or ligand-driven enthalpic interactions, we hypothesize that molecular organization on and around nanocrystal surfaces sensitively biases the self-assembly of particular nanocrystal superlattice morphologies. To test this hypothesis, we are using small angle scattering and molecular simulation to investigate how interactions among surface-bound ligands, solvent, and free ligands in solution control the formation of nanocrystal superlattices. The specific aims of this program are 1) to quantify molecular structure on isolated nanocrystal surfaces using small-angle neutron scattering (SANS), 2) to understand how free and bound ligands mediate nanocrystal interactions in concentrated solutions, and 3) to determine the structural organization of molecular ligands in self-assembled nanocrystal superlattices.

Recent Progress

1) Interactions between colloidal nanocrystals in concentrated solution

We used small-angle neutron scattering (SANS) to measure the solution structure factor in dispersions of fully passivated, oleate-capped PbS nanocrystals (NCs) up to concentrations of 16 v/v% (**Fig. 1**). Fitting the data by assuming an attractive square well interaction potential between NCs yielded a repulsive core diameter larger than the physical NC core diameter. This repulsive core stems from a densely packed region of the ligand-shell near the NC surface. The spatial extent of the repulsive core increases with temperature as ligand motion increases, becoming repulsive farther out in the ligand-shell, while the portion of ligand-shell outside of the repulsive region remains attractive with a strength ~1 k_BT. SANS provides a molecular interpretation of the fundamental inter-particle interactions in colloidal nanocrystal suspensions, ultimately relevant to understanding the self-organization of nanoscale materials. This work was published in *J. Phys. Chem. C* (Publication #1).

2) **Prediction of superlattice structure with large-scale patchy particle simulations**

Predictive control over the assembly of PbS nanocrystals (NCs) into ordered, oriented superlattices (SLs) and a comprehensive theoretical framework consistent with experimental observations has remained elusive. PbS NC SLs can adopt any number of configurations along the Bain path from body-centered cubic (BCC) to face-centered cubic (FCC) pathway through body-centered tetragonal (BCT) intermediates. In early work from this program, we showed that NC interactions are well-characterized by an isotropic, repulsive, densely packed ligand-shell larger than the NC core with weak attractions also present (Publication #1). Recently, we have extended that molecular understanding to parameterize a patchy particle representation of PbS NCs for large-scale Brownian dynamics (BD) simulations (Publication #2).

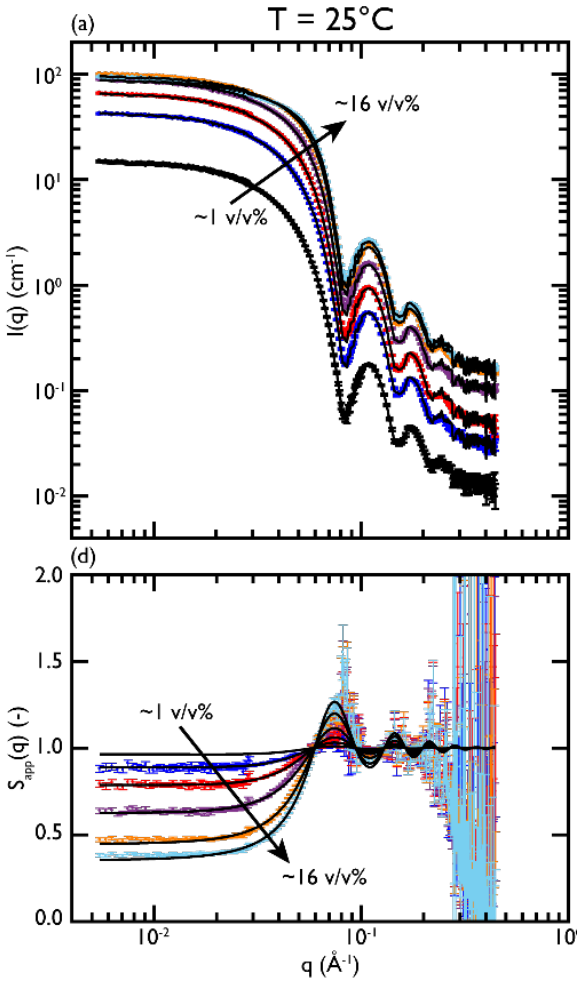

Figure 1. SANS intensity profiles (colored markers) for semi-dilute solutions of PbS NCs ($D = 6.1\,nm$, $\sigma_D \leq 3.4\%$, $\gamma = 5.8\,ligands/nm^2$, $\phi_f = 0.12$) ranging in concentration (ϕ_r = 1, 3.2, 5.6, 9.4, 14.2, and 16.5 v/v%) at 25°C. At higher concentration, the intensity at low- q falls below that of lower concentration intensity profiles, indicating the emergence of the structure factor. Comparison of the projected intensity profiles using the fit apparent structure factors are shown (black lines).

The ligand patch attractive strength is determined by comparison of the solution structure to that measured by small-angle neutron scattering (SANS) for oleate-capped PbS NCs. The patchy particle self-assembly behavior is probed using a sedimentation equilibrium methodology which returns a complete equation of state with a single simulation and allows extraction of the SL parameters and NC orientations. As the size of the repulsive ligand core increases, the lattice transitions predictably along the pathway BCC → BCT → FCC with unit cell axes lengths that perfectly match experimentally realized PbS NC SLs characterized by grazing-incidence small-angle X-ray scattering (GISAXS). Weak attractions between ligand patches, consistent with anisotropic ligand coverage on lead chalcogenide NCs, stabilize NC orientations in the SL. The nearest-neighbor spacing corresponds well with the repulsive core size. We have mapped the phase diagram across typical NC core diameters and ligand lengths and present a predictive framework that agrees with the observed SLs. This work was published in *J. Phys. Chem. C* (Publication #2).

3) Collective vibrations in nanocrystal superlattices

Colloidal nanocrystals are successfully used as nanoscale building blocks for creating hierarchical solids with structures that range from amorphous networks to sophisticated periodic superlattices. Recently, it has been observed that these superlattices exhibit collective vibrations (**Fig. 2**), which stem from the correlated motion of the nanocrystals, with their surface bound ligands acting as molecular linkers. In a recent Perspective published in *Nature Materials* (Publication #3), we described the work to date on collective vibrations in nanocrystal solids and their as-of-yet untapped potential for phononic applications. With the ability to engineer vibrations in the hypersonic regime through choice of nanocrystal and linker composition – as well as by controlling their size, shape, and chemical interactions – such superstructures offer new opportunities for phononic crystals, acoustic metamaterials, and optomechanical systems.

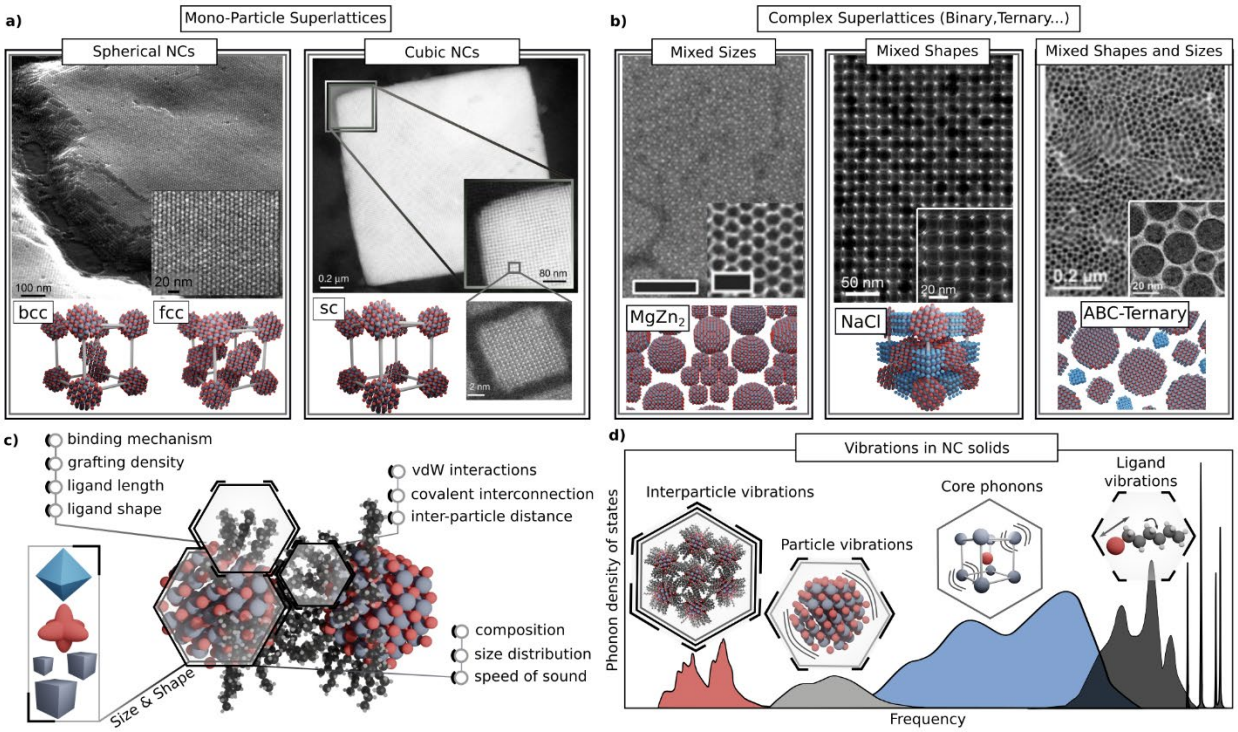

Figure 2. *Nanocrystal superlattices and their vibrations* a) Superlattices based on one nanocrystal type and size tend to order in simpler systems. b) By mixing multiple components, either different sizes, composition or anisotropic shapes, complex superlattices, e.g., binary or ternary are achieved. c) Physical parameters of the NC, the ligands and their interactions. d) Contributions to the phonon density of states by the individual components, as well as higher order contributions.

Future Plans

Recent SANS beamline trips have yielded a wealth of data regarding the organization of ligand layers on NC surfaces in solution. Experimental variables include NC size, identity of the surface ligand, identity of the solvent, and investigation of mixed ligand layers. Work is underway to analyze these data and contrast SANS information content to SAXS measurements of the same colloidal dispersions, which is a more frequently performed experiment.

In parallel, we are finalizing a manuscript predicting the orientation of faceted NCs within SLs based solely on maximizing the conformational entropy of surface ligands. This model is capable of predicting many experimental observations in the NC SL literature and solves several old mysteries in the field.

Publications supported by DE-SC0021025 (2021-2023)

1. "Repulsive, Densely Packed Ligand-Shells Mediate Interactions between PbS Nanocrystals in Solution"
   S.W. Winslow, Y. Liu, J.W. Swan, W.A. Tisdale;
   J. Phys. Chem. C. 125, 8014-8020 (2021).
2. "Prediction of PbS Nanocrystal Superlattice Structure with Large-Scale Patchy Particle Simulations"
   S.W. Winslow, W.A. Tisdale, J.W. Swan;
   J. Phys. Chem. C. 126, 14264-14274 (2022).
3. "Nanocrystal Phononics"
   M. Jansen, W.A. Tisdale, V. Wood;
   Nature Materials 22, 161-169 (2023).

Neutron Scattering Studies of Magnetic Quantum Materials

John M. Tranquada, Genda Gu, and Igor A. Zaliznyak
Condensed Matter Physics & Materials Science Division, Brookhaven National Laboratory, Upton, NY 11973
Keywords: antiferromagnetism, Dirac fermions, multi-analyzer spectrometer

Research Scope

We combine neutron scattering techniques, exploratory synthesis, and crystal growth to address key questions associated with strong interactions in quantum materials. In particular, how can we properly understand itinerant antiferromagnetism? To what extent can it be understood in terms of conventional band theory vs. spatial modulations of spin and charge? Can one exploit the interaction of spin-polarized itinerant states with local magnetic moments to obtain novel quantum behaviors, topological states, and unprecedented responses to external stimuli? Advanced synthesis techniques are used to grow high-quality crystals of interesting materials. We exploit the latest neutron-scattering technologies available at national neutron user facilities, such as the Spallation Neutron Source and the High Flux Isotope Reactor, to obtain direct information on spin correlations and atomic displacements necessary to provide transformative answers to these questions. One such technology, in whose development we have actively participated, is time-of-flight, polarized, inelastic neutron spectroscopy. Complementary characterizations and theoretical analysis are performed in collaboration with other groups in the Condensed Matter Physics and Materials Science Division, especially using the National Synchrotron Light Source II and the Center for Functional Nanomaterials.

Recent Progress

We highlight a few examples.

Coupling of magnetism and Dirac fermions in $YbMnSb_2$. The compound $YbMnSb_2$ is an example of a class of 112 ternary pnictides; it contains alternating layers of antiferromagnetic Mn and semimetallic Sb. We have used inelastic neutron scattering to measure the magnetic excitations in single-crystal samples [1]. The data exhibit considerable broadening of the spin waves at low temperature, $T \approx 5.5$ K $<< T_N$, which is consistent with substantial spin-fermion coupling in this material. By fitting the measured spin-wave spectra to the Heisenberg model with easy-axis anisotropy and with a finite spin-wave lifetime (damping), we found that the intralayer exchange couplings are similar to those previously observed in $YbMnBi_2$ [2]; however, both the interlayer coupling and the damping parameter (associated with spin-fermion

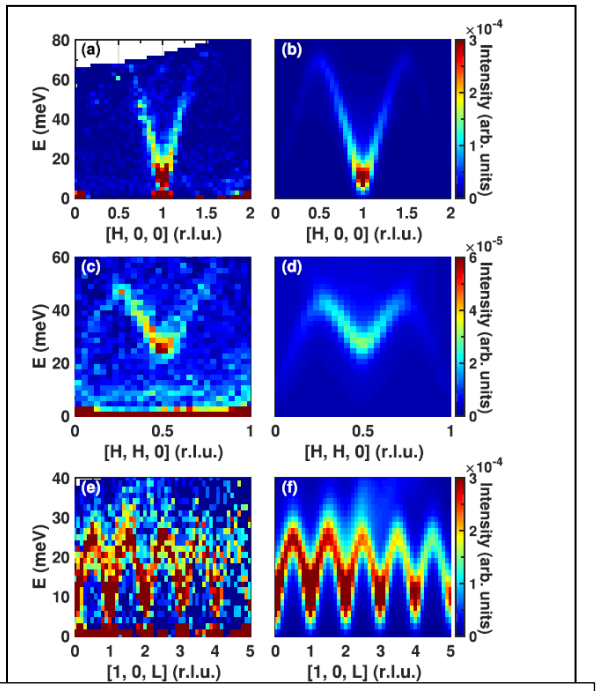

Figure 1. Measured and fitted spin-wave spectra of $YbMnSb_2$. The INS spectra were measured on SEQUOIA with Ei = 100 meV at T = 5.5(5) K along three symmetry directions: (a) [H, 0, 0], (c) [H,H, 0], and (e) [1, 0, L]. (b), (d), and (f) are the INS spectra calculated for a slightly damped spin-wave corrected for the instrument resolution.

coupling) are about twice as large as in $YbMnBi_2$. This suggests that Dirac electrons are involved in the interlayer spin coupling and might also participate in all magnetic interactions between Mn^{2+} ions. While developing a theoretical description of such a Ruderman-Kittel-Kasuya-Yosida (RKKY)-type coupling via Dirac electrons presents a challenge for the future, our results provide experimental guidance for such theories and an input for predictive theory of the magneto-transport phenomena in this regime.

Magnetism and electronic phase transition in $CaMnBi_2$. Another antiferromagnetic 112 compound of interest is $CaMnBi_2$. An electronic transition, evidenced by a resistivity anomaly, is observed at $T^* \sim 50$ K. It has been proposed that a suitable canting of the magnetic moments could yield a ferrimagnetic response, in which the degeneracy of the Dirac dispersion in the Bi layers would be broken. To test this possibility, we have carried out neutron (polarized and unpolarized) and x-ray diffraction measurements on single crystals of $CaMnBi_2$ [3]. Our measurements reveal a coupled magnetic and structural transition at $T^* = 46(1)$ K. We find that $CaMnBi_2$ undergoes a structural transition from tetragonal to orthorhombic symmetry, with a doubling of the unit cell along the c-axis. While the magnetic symmetry allows for a ferromagnetic canting within each MnBi layer, the net moment in such case alternates in sign along the c axis, so that there is no field in the semi-metallic Bi layers; furthermore, the neutron diffraction data indicate that the canting is barely discernible. The measured superlattice peak intensities and the distortion parameter indicate a continuous second order phase transition, suggesting a single underlying order parameter. The refined pattern of atomic displacements indicates either Mn-Mn (Fig. 2b), or Bi-Bi (Fig. 2c) in-plane bond-order modulation; the distortion breaks a mirror symmetry such that, in combination with antiferromagnetism, the product of parity and time-reversal symmetries is broken. The impact on the Hall effect remains to be investigated.

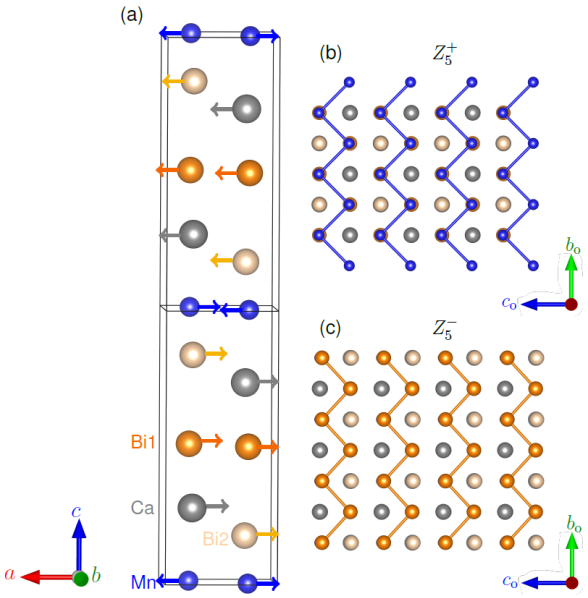

Figure 2. Tetragonal P4/*nmm* crystal structure of $CaMnBi_2$ containing two unit cells along the *c*-axis, which is equivalent to a unit cell of the lower-symmetry orthorhombic P*nmm* lattice below T*, (a). Arrows illustrate the displacements of each atom along the *a*-axis of P4/*nmm*. Two possible displacement patterns in the lower-symmetry orthorhombic phase with zig-zag-like bond order wave formation in the Mn (b) or Sb (c) layer.

HODACA: Inverse Rowland type multi-analyzer spectrometer for a continuous reactor-based neutron source. In the traditional setup of a crystal-analyzer spectrometer at a continuous (*e.g.*, reactor-based) neutron source, a single analyzer-detector channel is used, which limits the angular acceptance measured by the detector at one time to 1 degree or less. This limitation severely curtails the throughput of continuous-source triple-axis instruments compared to the time-of-flight spectrometers at pulsed spallation sources, which have detector banks simultaneously covering a large range of scattering angles. The development of multi-analyzer setups for crystal spectrometers at continuous sources, such as MACS at NCNR, or CAMEA at PSI, addresses this deficiency and allows to increase the instrument efficiency by orders of magnitude. Along these lines, Zaliznyak has recently proposed an inverse Rowland inelastic spectrometer (IRIS) setup. The first such instrument (Fig. 3) has been built recently at JRR-3 in Japan, in collaboration between Zaliznyak and T. Masuda's group at ISSP, University of Tokyo [4]. This instrument is currently being commissioned and tuned up for optimal performance. Having learned from this initial experience, further optimization of the design will be developed both for JRR-3 and for possible application at HFIR.

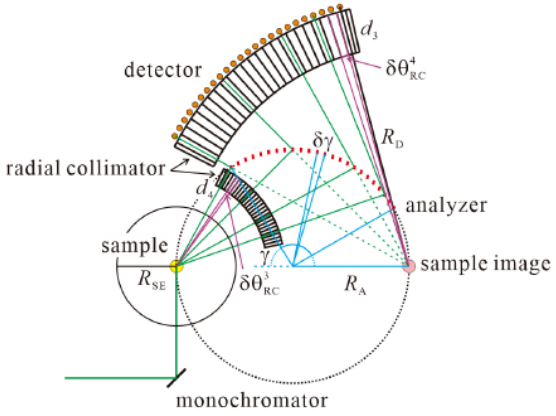

Figure 3. Schematic of the Inverse Rowland Inelastic Spectrometer (IRIS) setup implemented at HODACA spectrometer at JRR-3.

Future Plans

Here we mention just a couple of our future projects.

We have previously studied $FeSb_2$ because of its impressive thermoelectric properties, but another aspect involves magnetism. Zaliznyak has used neutron scattering to search for magnetic scattering from iron moments at various temperatures but has found no signal. Alternatively, one can obtain antiferromagnetism by partially substituting Cr for Fe; we have unpublished neutron scattering results for $Fe_{0.5}Cr_{0.5}Sb_2$ demonstrating the emergent antiferromagnetism. It has been proposed that in a compound where the structural unit cell is the same size as the antiferromagnetic unit cell, it is possible that the magnetism may be described by distinct spin up and spin down bands, corresponding to "altermagnetism". Such a state has been proposed for $Fe_{0.75}Cr_{0.25}Sb_2$. We will test for and characterize any magnetic order or correlations in a crystal of this composition using neutron scattering.

When charge carriers are doped into a strongly-correlated antiferromagnet, they often segregate into periodically-modulated charge stripes that are intertwined with spin stripes. In such a state, there are no extra electronic degrees of freedom to screen the charge modulation. Instead, the ionic lattice must participate in screening [5], but we do not have a complete picture of this screening. We have collaborated with Prof. Dmitry Reznik (Univ. Colorado, Boulder) and his student Tyler Sterling on extensive measurements of phonons in $La_{1.75}Sr_{0.25}NiO_4$ using ARCS (SNS). We are working on extracting new insights from this dataset, especially from constant-energy slices plotted in the 2D reciprocal lattice for a NiO_2 plane. The phonon behavior complements the dynamic magnetic response previously studied.

References

1. Xiao Hu, A. Sapkota, Z. Hu, A. T. Savici, A. I. Kolesnikov, J. M. Tranquada, C. Petrovic, I. A. Zaliznyak. *Coupling of magnetism and Dirac fermions in $YbMnSb_2$*. Phys. Rev. B **107**, L201117 (2023).
2. A. Sapkota, L. Classen, M. B. Stone, A. T. Savici, V. O. Garlea, Aifeng Wang, J. M. Tranquada, C. Petrovic, I. A. Zaliznyak. *Signatures of coupling between spin waves and Dirac fermions in $YbMnBi_2$*. Phys. Rev. B **101**, 041111(R) (2019).
3. A. Sapkota, Xiao Hu, M. Matsuda, G. Y. Xu, J. M. Wilde, A. Kreyssig, P. C. Canfield, C. Petrovic, J. M. Tranquada, and I. A. Zaliznyak (in preparation).
4. H. Kikuchi, S. Asai, T. J. Sato, T. Nakajima, L. Harriger, I. Zaliznyak, T. Masuda. *A new inelastic neutron spectrometer HODACA*. J. Phys. Soc. Japan (in review, 2023)
5. J. Sears, Y. Shen, M. J. Krogstad, H. Miao, E. S. Bozin, I. K. Robinson, G. D. Gu, R. Osborn, S. Rosenkranz, J. M. Tranquada, and M. P. M. Dean, *Structure of charge density waves in $La_{1.875}Ba_{0.125}CuO_4$*, Phys. Rev. B **107**, 115125 (2023).

Publications (10 out of 88)

1. Xiao Hu, Aashish Sapkota, Zhixiang Hu, Andrei T. Savici, Alexander I. Kolesnikov, John M. Tranquada, Cedomir Petrovic, and Igor A. Zaliznyak, "Coupling of magnetism and Dirac fermions in $YbMnSb_2$," Phys. Rev. B **107**, L201117 (2023).
2. Andrei T. Savici, Martyn A. Gigg, Owen Arnold, Roman Tolchenov, Ross E. Whitfield, Steven E. Hahn, Wenduo Zhou, and Igor A. Zaliznyak, "Efficient data reduction for time-of-flight neutron scattering experiments on single crystals," J. Appl. Cryst. **55**, 1514–1527 (2022).
3. Xiao Hu, A. Sapkota, V. O. Garlea, G. D. Gu, I. A. Zaliznyak, and J. M. Tranquada, "Spin canting and lattice symmetry in La_2CuO_4," Phys. Rev. B **107**, 094413 (2023).
4. Jieming Sheng, Le Wang, Andrea Candini, Wenrui Jiang, Lianglong Huang, Bin Xi, Jize Zhao, Han Ge, Nan Zhao, Ying Fu, Jun Ren, Jiong Yang, Ping Miao, Xin Tong, Dapeng Yu, Shanmin Wang, Qihang Liu, Maiko Kofu, Richard Mole, Giorgio Biasiol, Dehong Yu, Igor A. Zaliznyak, Jia-Wei Mei, and Liusuo Wu, "Two-dimensional quantum universality in the spin-1/2 triangular-lattice quantum antiferromagnet $Na_2BaCo(PO_4)_2$," Proc. Natl. Acad. Sci. U.S.A. **119**, e2211193119 (2022).
5. Yangmu Li, A. Sapkota, P. M. Lozano, Zengyi Du, Hui Li, Zebin Wu, Asish K. Kundu, R. J. Koch, Lijun Wu, B. L. Winn, Songxue Chi, M. Matsuda, M. Frontzek, E. S. Bozin, Yimei Zhu, I. Bozovic, Abhay N. Pasupathy, Ilya K. Drozdov, Kazuhiro Fujita, G. D. Gu, I. A. Zaliznyak, Qiang Li, and J. M. Tranquada, "Strongly overdoped $La_{2-x}Sr_xCuO_4$: Evidence for Josephson-coupled grains of strongly correlated superconductor," Phys. Rev. B **106**, 224515 (2022).
6. Zhendong Jin, Yangmu Li, Zhigang Hu, Biaoyan Hu, Yiran Liu, Kazuki Iida, Kazuya Kamazawa, Matthew B. Stone, Alexander I. Kolesnikov, Douglas L. Abernathy, Xiangyu Zhang, Haiyang Chen, Yandong Wang, Chen Fang, Biao Wu, Igor A. Zaliznyak, John M. Tranquada, and Yuan Li, "Magnetic molecular orbitals in MnSi," Science Advances **9**, eadd5239 (2023).
7. Machteld E. Kamminga, Kristine M. L. Krighaar, Astrid T. Rømer, Lise Ø. Sandberg, Pascale P. Deen, Martin Boehm, Genda D. Gu, John M. Tranquada, and Kim Lefmann, "Evolution of magnetic stripes under uniaxial stress in $La_{1.885}Ba_{0.115}CuO_4$ studied by neutron scattering," Phys. Rev. B **107**, 144506 (2023).
8. Xintong Li, Yuchen Gu, Yue Chen, V. Ovidiu Garlea, Kazuki Iida, Kazuya Kamazawa, Yangmu Li, Guochu Deng, Qian Xiao, Xiquan Zheng, Zirong Ye, Yingying Peng, I. A. Zaliznyak, J. M. Tranquada, and Yuan Li, "Giant Magnetic In-Plane Anisotropy and Competing Instabilities in $Na_3Co_2SbO_6$," Phys. Rev. X **12**, 041024 (2022).
9. Qianheng Du, Yilin Wang, Yuan Wei, Robert Joseph Koch, Lijun Wu, Wenliang Zhang, Teguh Citra Asmara, Zhixiang Hu, Emil S. Bozin, Yimei Zhu, Thorsten Schmitt, Gabriel Kotliar, and Cedomir Petrovic, "Cascade of Spin-State Transitions in the Intermetallic Marcasite FeP_2," Chem. Mater. **34**, 2025–2033 (2022).
10. Aifeng Wang, Ana Milosavljevic, A. M. Milinda Abeykoon, Valentin Ivanovski, Qianheng Du, Andreas Baum, Eli Stavitski, Yu Liu, Nenad Lazarevic, Klaus Attenkofer, Rudi Hackl, Zoran Popovic, and Cedomir Petrovic, "Suppression of Superconductivity and Nematic Order in $Fe_{1-y}Se_{1-x}S_x$ ($0 \le x \le 1$; $y \le 0.1$) Crystals by Anion Height Disorder," Inorganic Chemistry **61**, 11036–11045 (2022).

Diffuse Neutron Scattering Studies of Far-from-equilibrium Topological Defects

Priya Vashishta, University of Southern California

Keywords: Far-from-equilibrium; Kibble-Zurek mechanism; Barium titanate; Yttrium manganite

Program Scope

Symmetry-breaking phase transitions are ubiquitous in nature. Sir Tom Kibble theorized in the 1970s that in the early universe symmetry breaking may have led to the formation of topological defects such as point-like monopoles, cosmic strings or planar domain walls.[1] The defect-formation model, developed originally for cosmology, has found remarkably fruitful applications in condensed matter physics and has become an important addition to the general theory of far-from-equilibrium systems. There is good evidence from disparate systems that a rapid phase transition leads to the formation of a random tangle of defects. Defects form as the cooling or quenching process begins and small regions of local order appear within the disordered medium. These regions form a mosaic of causally disconnected domains of local order and the regions grow until they encounter each other. Yet, we do not fully understand how the rate at which a system passes through a phase transition affects the number of defects formed. Where it has been possible to check the dependence of the defect density on the quench rate of the transition, the results have been consistent in most cases with the power-law behavior.

The goal of this joint simulation and experimental study is to investigate far-from-equilibrium physics of rapidly quenched multiferroic manganites and SpinIce materials that combines kinematic constraints, emerging topological defects, and Kibble-Zurek mechanisms. We will use Reactive and Quantum Dynamics simulations and Monte Carlo method along with Neural Network Quantum Molecular Dynamics to compute diffuse neutron scattering for rapid thermal and magnetic field quenched systems and investigate classification and analysis of defects created in far-from-equilibrium processes. We are doing Diffuse Neutron Scattering experiments at Spallation Neutron Source (SNS), Oak Ridge National Laboratory (ORNL), on multiferroic manganites in collaboration with Despina Louca, University of Virginia.

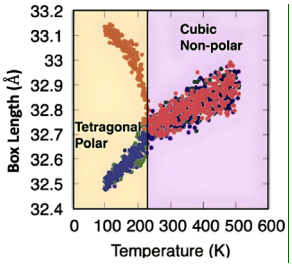

Fig. 1: Variation of molecular dynamics box length of BTO system under cubic to tetragonal phase transformation.

Recent Progress

Kibble-Zurek Scaling of Nonequilibrium Phase Transition in Barium Titanate: The KZ scaling has been studied theoretically using spin models[2] and macroscopic partial differential equations.[3] More microscopic models such as coarse-grained molecular dynamics (MD) simulations have also been applied.[3] Recently, large-scale atomistic MD simulations on $PbTiO_3$ perovskite based on a neural-network force field demonstrated KZ-like defect structures under optical quenching instead of temperature quenching. In this work we investigate atomistic processes leading to defect creation and KZ scaling during temperature quenching.[4] We will use large scale reactive molecular dynamics (RMD) simulations to demonstrate KZ scaling upon rapid temperature quenching in barium titanate $BaTiO_3$ (BTO). For our MD simulations, we will use validated reactive force field (ReaxFF) for ferroelectric perovskite BTO developed by van Duin's group.[5] BTO has two crystal structures that concern us in the thermal quenching process. The high temperature phase of BTO is cubic and non-ferroelectric while the tetragonal phase exhibits finite electric polarization because of the asymmetry along c-direction. We have carried out RMD simulations to validate that the ReaxFF force-field correctly describes these two phases of BTO, see Fig. 1. Simulation results are shown in Figs. 2-5.

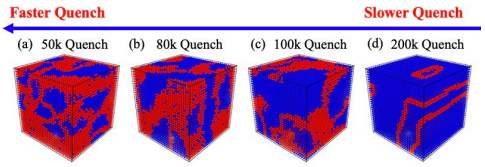

Fig. 3: Real-space defect structure in quenched BTO. The state of the Ti atom is shown from a fast 50k-step quench on the left (a) to a slow 200k-step quench in the right (d). The +1 and -1 states are colored in red and blue, respectively.

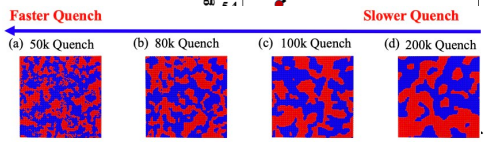

Fig. 4: Slices of the three-dimensional structures shown in Fig. 3 for quenched BTO.

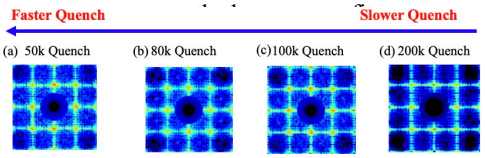

Fig. 5: Computed diffuse scattering in (001) plane for ferroelectric BTO quenched at four different rates – (a) 50k quench – fastest, (b) 80k quench, (c) 100k quench and (d) 200k quench – slowest.

Inelastic Neutron Scattering (INS) Study of Phonon Density of States of Iodine Oxides and First-Principles Calculations: Iodine oxides I_2O_y (y = 4,5,6) crystallize into atypical structures that fall in-between molecular- and framework-base types and exhibit high reactivity in ambient environment, a property highly desired in the so called "agent defeat materials." INS experiments were performed to determine the phonon density-of-states of the I_2O_5 and I_2O_6 samples. First principles calculations were carried out for I_2O_4, I_2O_5 and I_2O_6 to predict their thermodynamic properties and phonon density-of-states (Figs. 6 and 7). Comparison of the INS data with the Raman and infrared measurements as well as the first-principles calculations sheds light on their distinctive, anisotropic thermo-mechanical properties.

The crystal structures of anhydrous I_2O_5 and I_2O_6 over the temperature range of 4-300 K were investigated by neutron powder diffraction using the POWGEN diffractometer at the Spallation Neutron Source (SNS).[6] Inelastic neutron scattering (INS) was carried out at low temperature (10 K) using the chopper spectrometer, ARCS, also at SNS.[7] To achieve the best energy resolution in the whole vibrational spectra of I_2O_y, $\Delta E/E_i \approx$ 1-3%, we used the incident energies of E_i = 20, 45, 85 and 150 meV, selected by the Fermi chopper. Iodine and oxygen atoms mainly scatter neutrons coherently, therefore neutron scattering had to be averaged over a large range of neutron momentum transfer to obtain the vibrational density of states of polycrystalline samples.

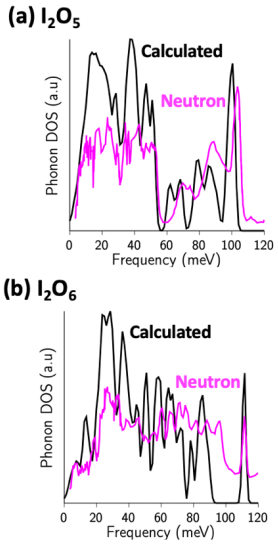

Fig. 6: The experimentally measured and calculated neutron-weighted phonon densities of states for (a) I_2O_5 and (b) I_2O_6 normalized to the same integrated area.

The simulations account for the crystal structures as well as the lattice dynamics of I_2O_y systems reasonably well, notwithstanding the 10-15% energy shifts of high-energy modes which is caused by the compromise between inter- and intra-molecular interactions due to the vdW correction.

Neutron Scattering, Nuclear Quantum Effects and Neural Networks: The Delicate Case of the Ammonia Vibrational Spectrum: We are doing INS measurement of vibrational properties of ammonia along the solid-to-liquid phase transition with high enough resolution for direct comparisons to *ab-initio* simulations, which is critically lacking in the literature. Theoretical analysis reveals the essential role of nuclear quantum effects (NQEs) for correctly describing the intermolecular spectrum as well as high energy intramolecular N-H stretching modes. This is achieved by training neural network models using *ab-initio* path-integral molecular dynamics (PIMD) simulations, (Fig. 8). Our results not only establish the role of NQEs in ammonia but also provide general computational frameworks to study complex molecular systems with NQEs.

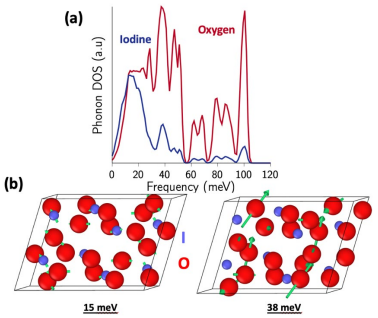

Fig. 7: Calculated phonon densities of states for (a) I_2O_5 decomposed by atom type. Low (high) frequency modes are characterized by vibrations of primarily iodine (oxygen) atoms. (b) Atomic displacements (in green) corresponding to eigenvectors of these modes in I_2O_5 reflect this atom decomposition.

NQE-induced anharmonicity is expected to be quite common in molecular solids/liquids, especially in systems with "flexible" groups such as -OH, -CH_3, -NH_2. Significant discrepancies between simulated peak positions (harmonic approximation) and measured ones have been observed in many related systems, including ice, amino acids, drugs, *etc*. Interpretation of the discrepancies, when comparing theory and experiment, can be complicated and potentially misleading. With the recent explosion of machine-learning-based interatomic potentials, evaluation of NQEs in large spatiotemporal simulations at near DFT accuracy is possible, as demonstrated in a recent study of water/ice where NQEs are found to have a crucial contribution to the stability of ice Ih. The framework presented here is anticipated to serve as a guide for proper analysis of INS experiments in the future. The major goal of spectral analysis is not to make a model that can replicate the spectrum but to have a model that can simulate the spectrum based on the correct physics and thus also have extrapolation power by capturing the fundamental interactions and nuclear quantum dynamics.

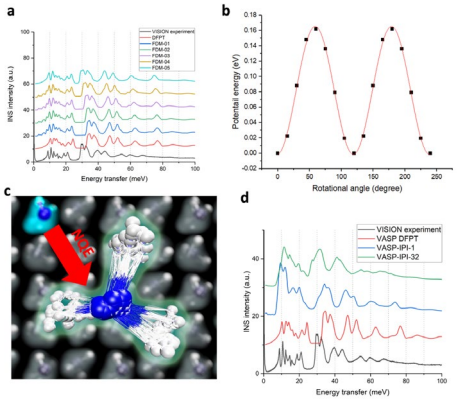

Fig. 8: Evaluation of nuclear quantum effects with DFT. (a) INS spectra of solid ammonia simulated with various step sizes using the finite displacement methods (e.g., FDM-01 means a step size of 0.1 Å). The drifting librational band is an indication of its anharmonicity. (b) Potential energy profile of NH_3 rotation in solid ammonia. The energy barrier is determined to be 167 meV and the associated NH_3 quantum rotor has an excitation energy ($n = 0 \rightarrow 1$) of 32 meV. (c) Illustration of PIMD simulation. (d) INS spectra of solid ammonia from DFPT, *ab initio* PIMD (1-bead and 32-bead TRPMD), and VISION experiment. The PIMD simulation with 32 beads reproduces the experimentally observed peak positions very well.

Future Plans

Diffuse Neutron Scattering Experiment for rapidly quenched $YMnO_3$ Crystals and Neural Network Quantum Dynamics Simulations for Determining Kibble-Zurek (KZ) scaling behavior. *To test scaling behavior of the KZ model in describing non-equilibrium phase transitions in manganite materials, we propose to perform diffuse neutron scattering experiments using CORELLI at SNS. We will investigate the scaling properties in far-from-equilibrium phase transformations of thermally quenched manganite $InMnO_3$.* Manganites are of the form $AMnO_3$ (A = In, Sm, Er, Y etc.) and have crystal structures shown in Fig. 9a. These materials have a potential energy landscape that forms a buckled Mexican hat that hosts a nonpolar phase at its center, and polar and antipolar phases at the minima and maxima of its brim (Fig. 9b). A 2-D order parameter couples to a ferroelectric displacement with polarization along the *c* axis. This coupling is responsible for the minima in the brim of the Mexican hat and stabilizes the ground state.

Single crystals with different quenched rate have been prepared for diffuse scattering. Based on the neutron attenuation length of 5 mm at wavelength of 1 Å for $YMnO_3$, optimized sample volume of 30-60 mm^3 (mass between 200-400 milligram) are chosen for diffraction.

Crystalline samples of manganite are synthesized by Yan, Jiaqiang, Materials Science Division of ORNL. Samples have been subjected to thermal quench by Professor Despina Louca at University of Virginia. We have prepared thermally quenched samples at eight different quench rates. It is known that the quenched samples are stable and maintain their disorder for a duration of months to years.

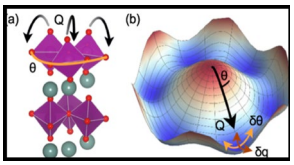

Fig. 9: $YMnO_3$. (a) Oxygen-manganese bipyramidal tilt (black arrows) and phase (orange) motions are proposed to be related to the Higgs and Goldstone modes respectively. (b) The potential in the hexagonal manganites approximates to the Mexican hat potential (top).

The thermally quenched samples will be pre-aligned in the (H, 0, L) scattering plane to simultaneously probe the evolution of the short-range correlation within and perpendicular to the basal plane. Since all elements have good neutron cross sections, we will use 360-degree rotation (3-degree step) along the vertical axis, with 5-10 mins at each rotation angle to obtain good counting statistics. Eight single crystals with different quenched rate will be collected at 300 K to perform systematic comparison. A low background close-cycle-refrigerator (CCR) with base temperature of 5 K will be used for the data collection.

We are also planning Diffuse Neutron Scattering experiments at Spallation Neutron Source (SNS), Oak Ridge National Laboratory (ORNL on SpinIces, $Dy_2Ti_2O_7$ in collaboration with Alan Tennant, University of Tennessee and ORNL.

INS Experiments and NNQMD Simulations for Ammonia-Water mixtures is also planned. Validation of the computed vibrational density of states with measured INS data, will be essential for informing exchange-correlation used in DFT based quantum simulations of water-ammonia systems as well as in the development of reactive and ML forcefields. This experiment will provide much needed data for the development of models to describe complex hydrogen bonding dynamics in mixed polar solvents, which is needed in the development of sustainable energy technologies.

References

1. T. W. B. Kibble, Phys Today **60**, 47 (2007).

2. W. H. Zurek, U. Dorner and P. Zoller, Phys Rev Lett **95**, 105701 (2005).

3. Z. Bradač, S. Kralj and S. Žumer, Phys Rev E **65**, 021705 (2002).

4. T. Linker, K. Nomura, A. Aditya, S. Fukshima, R. K. Kalia, A. Krishnamoorthy, A. Nakano, P. Rajak, K. Shimmura, F. Shimojo and P. Vashishta, Science Adv **8**, eabk2625 (2022).

5. D. Akbarian, *et al*., Phys Chem Chem Phys **21**, 18240 (2019).

6. A. Huq, J. P. Hodges, O. Gourdon and L. Heroux, Z Kristall Proc **1**, 127 (2011).

7. D. L. Abernathy, *et al*., Rev Sci Instrum **83**, 015114 (2012).

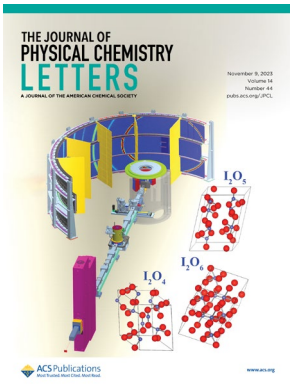

Cover of Journal of Physical Chemistry Letters (Nov. 9, '23).

Publications Resulting from Work Supported by the DOE Grant over the Previous Two Years

1. "Inelastic neutron scattering study of phonon density of states of iodine oxides and first-principles calculations," A. I. Kolesnikov, A. Krishnamoorthy, K. Nomura, Z. Wu, D. L. Abernathy, A. Huq, G. E. Granroth, K. O. Christe, R. Haiges, R. K. Kalia, A. Nakano, and Priya Vashishta, J Phys Chem Lett **14**, 10080 (2023); *journal cover*.

2. “Kibble-Zurek scaling of nonequilibrium phase transition in barium titanate,” N. Baradwaj, A. Krishnamoorthy, K. Nomura, A. Nakano, R. K. Kalia, and P. Vashishta, Appl Phys Lett, in press (2023).

3. “Neutron scattering, nuclear quantum effects and neural networks: the delicate case of the ammonia vibrational spectrum,” T. M. Linker, A. Krishnamoorthy, L. L. Daemen, A. J. Ramirez-Cuesta, K. Nomura, A. Nakano, Y. Q. Cheng, W. R. Hicks, A. I. Kolesnikov, and P. D. Vashishta, Nature Commun, under review.

Neutron Diffraction Study of Magnetic Structures in Heavy Lanthanides under Extreme Conditions

Yogesh K. Vohra, Department of Physics, University of Alabama at Birmingham (UAB)

Keywords: Neutron Diffraction, Lanthanides, Magnetic Structures, Extreme Conditions

Research Scope

The application of pressure causes electron transfer from the extended s-band to a more compact d-band due to a relative rise in the s-band energy with increasing pressure in lanthanide elements. This s-d electron transfer drives the structural phase transitions in lanthanides and leads to *hcp→Sm-phase→dhcp→fcc→distroted fcc (hR24)* crystal structure sequence with increasing pressure. The changes in electronic structure driving structural phase transitions under pressure in lanthanides are well recognized; however, their role in the onset of magnetic ordering temperatures and magnetic structures is unknown. We have investigated magnetic ordering in the heavy lanthanide Terbium (Tb) and Erbium (Er) under high pressures and low temperatures using a large-volume diamond anvil cell at the SNAP beamline at the Spallation Neutron Source, Oak Ridge National Laboratory.

Recent Progress

The lanthanide elements share many common physical and chemical properties, owing to the progressive filling of the inner *4f* electron shell from lanthanum to lutetium. Upon compression, their structural and magnetic properties are heavily influenced by s→d-band electron transfer and delocalization of the 4f-shell at ultra-high pressures [1]. While high pressure x-ray diffraction experiments have confirmed a common sequence of close-packed structures for the lanthanides (with notable exceptions Eu and Yb), magnetic structure determinations at high pressure continue to be challenging due to the lack of direct methods, e.g., neutron diffraction.

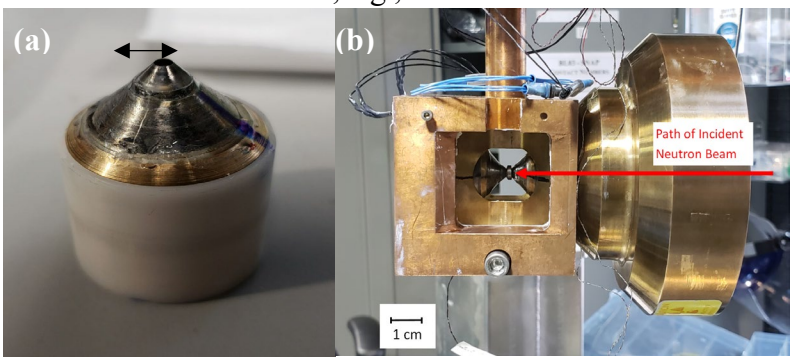

Figure 1. (a) Large diamond single crystal (6 mm girdle diameter) grown by chemical vapor deposition for neutron diffraction studies to 50 GPa and 10 K. (b) Large-volume diamond anvil cell used for experiments at SNAP beamline, Spallation Neutron Source, Oak Ridge National Laboratory. The path of the incident neutron beam is indicated by a red arrow. The large-volume cell is mounted on the cold head of the cryo-refrigerator.

Early studies of magnetic ordering in lanthanides at high pressure used indirect means, e.g., electrical transport and/or magnetic susceptibility measurements. A study of six heavy lanthanides using ac-magnetic susceptibility measurements found that magnetic transition temperatures decrease with increasing pressure [2]. With magnetic susceptibility signals disappearing by 10-20 GPa [2], many of the higher-pressure lanthanide phases remained unexplored. Advances in large-volume diamond anvil cells (DACs) at neutron diffraction facilities (Fig. 1) offer the most direct route to study the

magnetic properties of lanthanides at high pressure [3]. For neutron diffraction studies, we combine multi-frame neutron diffraction data collection (collected at wavelengths nominally centered at λ = 6.4 Å and 2.1 Å) with a large-volume diamond anvil cell at the Spallation Neutron Source, Oak Ridge National Laboratory. Diamond anvils (6 mm in diameter and 6 mm in height) with 1 mm diameter culets are employed to reach a maximum pressure of 30 GPa at 10 K. The neutron diffraction study of the dhcp phase for Tb at 20 GPa (Fig. 2) revealed magnetic peaks that can be assigned a propagation vector **k** = (1/2, 0, 1/2), and a magnetic ordering temperature that is consistent with the magnetostriction effect observed with x-ray diffraction.

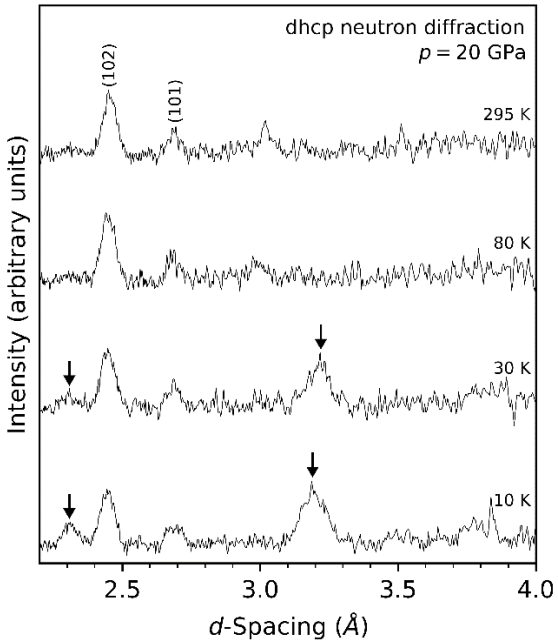

Figure 2. Neutron diffraction patterns for Tb at 20 GPa and various temperatures between 10 K and 295 K. The onset of magnetic transition is marked by the appearance of two new magnetic peaks at 3.194 Å and 2.311 Å as indicated by the downward pointing arrows. The magnetic peaks are assigned to a propagation vector $\boldsymbol{k} = (\frac{1}{2}, 0, \frac{1}{2})$.

We have combined earlier measurements with this study to create a magnetic phase diagram for various high-pressure phases of Tb, which is summarized in Fig. 3. Earlier electrical transport measurements [4], magnetic susceptibility measurements [5, 6], and neutron diffraction measurements [7] on Tb have established that the ferromagnetic Curie temperature T_C in the *hcp* phase decreases linearly with pressure. The electrical transport measurements by Lim et al. [4] indicate a minimum in magnetic ordering temperature at a pressure of 18 GPa, followed by an increase in magnetic ordering temperature up to 50 GPa. The two antiferromagnetic transitions observed by Kozlenko et al. [8] at 50 K and 110 K for the *α-Sm* phase are also included in Fig. 3. Our data for the *dhcp* and *hR24* phases are plotted with symbols: black for x-ray diffraction studies showing splitting, and red for the neutron diffraction study showing the emergence of the AFM2 phase with propagation vector $\boldsymbol{k}_{\mathrm{AFM2}} = (\frac{1}{2}, 0, \frac{1}{2})$. We did not observe any splitting in the high-pressure *oF16* phase of Tb observed above 53 GPa.

In summary, we report on the first observations of magnetostriction in Tb under high pressures and low temperatures. The magnetostriction results in a spontaneous strain that is easily detectable as splitting of prominent diffraction peaks in the high pressure and low temperature structural data obtained with x-ray diffraction. This offers a novel and convenient way for measuring magnetic ordering temperatures for the high-pressure phases of Tb. Magnetic ordering in the *dhcp* phase was also confirmed by neutron diffraction data that showed magnetic peaks corresponding to a

propagation vector **k** = (1/2, 0, 1/2) and a magnetic ordering temperature consistent with the observation of magnetostriction. The fact that no splitting is observed in the *oF16* phase in Tb at 70 GPa suggests that the collapsed phase of heavy lanthanide had a significant decrease in magnetic moment of 4*f*-shell due to band broadening at ultrahigh compression. Our study, when combined with those of Kozlenko et al. [8] and Lim et al. [4], shows that magnetic ordering temperature increases monotonically with pressure through the *α-Sm*, *dhcp*, and *hR24* phases.

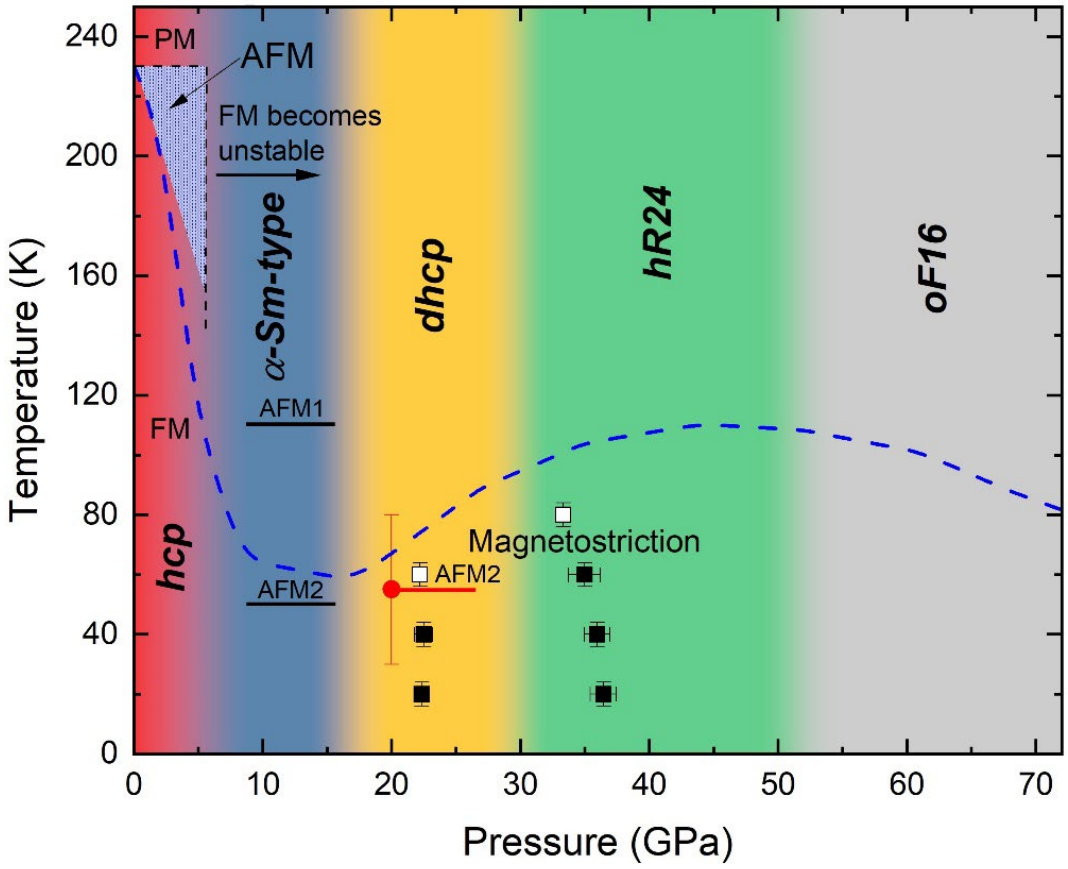

Figure 3. A comprehensive display of magnetic ordering temperatures for various high-pressure phases of Tb up to 70 GPa. PM: paramagnetic; AFM: antiferromagnetic (helical); FM: ferromagnetic; AFM1: propagation vector $\boldsymbol{k}_{\mathrm{AFM1}} = (0,0,\frac{1}{2})$; AFM2: propagation vector $\boldsymbol{k}_{\mathrm{AFM2}} = (\frac{1}{2},0,\frac{1}{2})$. Filled squares mark data points with magnetostrictive splitting, and open squares mark data points with no splitting. The AFM2 transition in the *dhcp* phase observed with neutron diffraction is marked with the red circle. The dashed blue line represents the magnetic ordering temperatures determined by the electrical transport measurements of Lim et al. [4].

Future Plans

The neutron diffraction data on heavy lanthanide Er has been collected up to a pressure of 30 GPa and 10 K at the SNAP beamline at SNS and the magnetic structure refinements are being completed and the results being prepared for publication. We plan to employ first-principles dynamical mean-field theory (DMFT) calculations to study magnetism of heavy lanthanides under high pressure and low temperature. The calculations will be based on a fully self-consistent, all-electron density functional theory (DFT)+DMFT method as implemented in the EDMFTF code. The theoretical results are being prepared for comparison and discussion of corresponding high-pressure neutron scattering experiments.

References

1. G. K. Samudrala, Y. K. Vohra, Chapter 257 - structural properties of lanthanides at ultra-high pressure, in: J.-C. G. Bu¨nzli, V. K. Pecharsky (Eds.), Including Actinides, Vol. 43 of Handbook on the Physics and Chemistry of Rare Earths, Elsevier, 2013, pp. 275–319.
2. D. D. Jackson, V. Malba, S. T. Weir, P. A. Baker, Y. K. Vohra, High-pressure magnetic susceptibility experiments on the heavy lanthanides Gd, Tb, Dy, Ho, Er, and Tm, Phys. Rev. B **71**, 184416 (2005).
3. C. S. Perreault, Y. K. Vohra, A. M. dos Santos, J. J. Molaison, Magnetic structure of antiferromagnetic high-pressure phases of dysprosium, Journal of Magnetism and Magnetic Materials **545**, 168749 (2022).
4. J. Lim, G. Fabbris, D. Haskel, J. S. Schilling, Anomalous pressure dependence of magnetic ordering temperature in tb revealed by resistivity measurements to 141 GPa: Comparison with Gd and Dy, Phys. Rev. **B 91**, 174428 (2015).
5. W. C. Koehler, H. R. Child, E. O. Wollan, J. W. Cable, Some magnetic structure properties of terbium and of terbium-yttrium alloys, Journal of Applied Physics **34 (4,)** 1335 (1963).
6. M. Mito, Y. Kimura, K. Yamakata, M. Ohkuma, H. Chayamichi, T. Tajiri, H. Deguchi, M. Ishizuka, Relationship of magnetic ordering and crystal structure in the lanthanide ferromagnets Gd, Tb, Dy, and Ho at high pressures, Phys. Rev. **B 103**, 024444 (2021).
7. S. A. Thomas, J. M. Montgomery, G. M. Tsoi, Y. K. Vohra, G. N. Chesnut, S. T. Weir, C. A. Tulk, A. M. dos Santos, Neutron diffraction and electrical transport studies on magnetic ordering in terbium at high pressures and low temperatures, High Pressure Research **33 (3)**, 555–562 (2013).
8. D. P. Kozlenko, V. Y. Yushankhai, R. Hayn, M. Richter, N. O. Golosova, S. E. Kichanov, E. V. Lukin, B. N. Savenko, Pressure-induced structural transition and antiferromagnetism in elemental terbium, Phys. Rev. Mater. **5**, 034402 (2021).

Publications

1. Matthew P. Clay, Raimundas Sereika, Wenli Bi, Yogesh K. Vohra, “Magnetic ordering in terbium at high pressures and low temperatures”, Journal of Magnetism and Magnetic Materials **580**, 170935 (2023). https://doi.org/10.1016/j.jmmm.2023.170935. OSTI ID: 1985815

Orbitally-Active Platforms for Novel Magnetism and Entangled Electronic States

Stephen D. Wilson

Materials Department, University of California, Santa Barbara, Santa Barbara CA 93427

Keywords: Triangular lattice, quantum disorder, Kitaev materials, quantum magnetism

Research Scope

Our program focuses on the synthesis and neutron-scattering based study of key members of geometrically frustrated magnets built from atoms with orbitally-active electronic wave functions. In triangular and related lattices, geometric frustration combined with the ability to tailor spin-orbit entangled wave functions on their magnetic sites renders a rich physical landscape with theoretically predicted novel ground states and unconventional phase behaviors. These new states range from new forms of quantum spin liquid states, to intertwined multipolar orders, to new settings for anisotropic Kitaev exchange, as well as other magnetic states defined by extensive degeneracies and quantum fluctuations. **Figure 1** illustrates some of the key lattice motifs and structure types targeted in our work, primarily comprised of layered triangular lattice compounds and diamond lattice variants. In each structure type, magnetic moments that derive from a spin-orbit entangled wave function are chosen in order to encode anisotropies capable of destabilizing long-range magnetic order and promoting the formation of a quantum disordered state. This program focuses on the growth of new powder and single crystal specimens in these classes of compounds and on the exploration of their magnetic ground states with neutron scattering-based techniques. Our goal is to understand and engineer the interactions that stabilize quantum disorder and quantum spin liquid ground states in these highly frustrated magnetic materials.

Figure 1: Lattice structures and geometrically frustrated lattice motifs explored under this award. The S_{eff}=1/2 and J_{eff}=1/2 wave functions created by strongly spin-orbit coupled lanthanide and transition metal ions and their local connectivity are noted in the right panels.

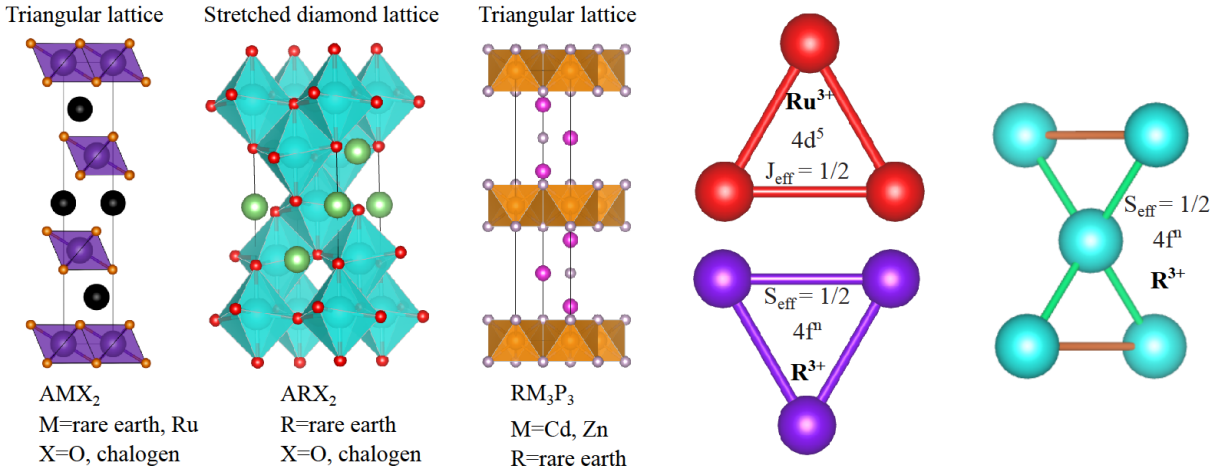

Recent Progress

Our recent progress has centered around two classes of triangular lattice compounds: the first are based on S_{eff}=1/2 moments born from the 4*f* orbitals of Ln^{3+} ions, and the second are based on J_{eff}=1/2 moments born from the 4*d* orbitals of the Ru^{3+} transition metal ion. Quantum disordered states were stabilized in both classes of materials; in particular within the $RbCeO_2$ and $NaRuO_2$ classes of compounds. Specific advances and insights gained into the materials are described in detail below.

Quantum disorder in $NaRuO_2$: One mechanism for engineering strong quantum fluctuations in a triangular lattice is to design strong, bond-directional anisotropic exchange terms in the magnetic Hamiltonian. These so called "Kitaev" exchange terms can be created and amplified in real materials via networks of J_{eff}=1/2 moments whose wave functions are built from spin-orbit entangled t_{2g} orbitals. These moments, when connected via 90° exchange pathways, realize strong Kitaev exchange terms and near vanishing, competing Heisenberg interaction terms. As a result, edge-sharing lattices built from strongly spin-orbit coupled d^5 transition metal ions in an octahedral environment are sought for stabilizing the theorized Kitaev spin liquid states.

Triangular lattices built from Ru^{3+} ions are a promising avenue for realizing a quantum disordered state via this mechanism, and we developed stoichiometric specimens of the material $NaRuO_2$ to test this conjecture [1,2]. Our results demonstrate a quantum disordered state that seemingly forms close to a ferromagnetic instability (**Figure 2**). *Ab initio* models and quantum chemistry calculations predict a ferromagnetic ground state and the presence of a strong antiferromagnetic Kitaev exchange term; however, when accounting for longer-range exchange terms (as is expected for extended 4*d* orbitals), a quantum spin liquid regime is also predicted to manifest in the phase diagram [3,4]. $NaRuO_2$'s quantum disordered ground state can be perturbed via engineering chemical disorder in the form of in-plane, nonmagnetic Na defects placed onto Ru-sites. This defect engineering forces the formation of a spin glass state at low temperature [2], whose freezing temperature increases with increased impurity density. Our result provides a valuable diagnostic wherein the dynamic magnetism that forms in the chemically stoichiometric $NaRuO_2$ compound can be driven into conventional freezing behavior via the introduction of extrinsic chemical disorder.

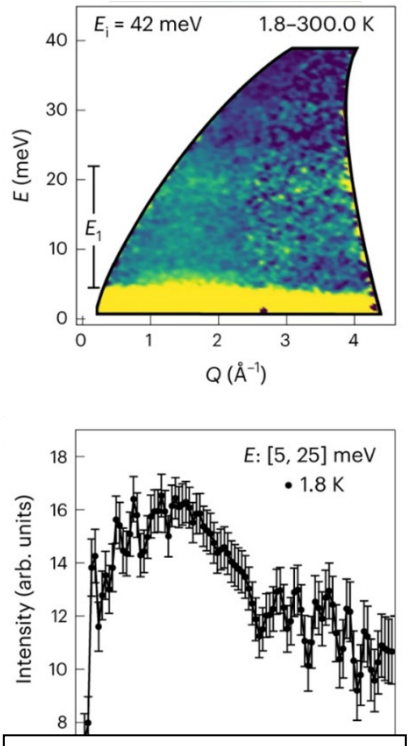

Figure 2: Spin dynamics measured in $NaRuO_2$ on SEQUOIA. Continuum excitations are observed at **q**=0 type positions, consistent with a nearby ferromagnetic instability.

Quantum disorder in $RbCeO_2$: Our previous work discovered the presence of a field-tunable quantum disordered state in $NaYbO_2$ [5], a material whose fundamental building blocks are layers of Yb^{3+} triangular lattice moments (with a single hole in the *f*-shell) and whose J=7/2 states split until an S_{eff}=1/2 ground state doublet. A broad family of these Yb-based compounds are now known to exhibit spin-liquid like ground states with examples such as $NaYbS_2$, $NaYbSe_2$, $KYbSe_2$, etc. One recent focus has been to explore whether comparable states can be realized in the single-electron cousins to this family, built from Ce^{3+} ions. Curiously, our own prior work and existing literature on $ACeX_2$ (A=alkali metal, X=O, S) compounds demonstrated that these materials have a propensity to form long-range order, unlike their Yb counterparts. To explore this in a controlled way, we synthesized and studied an entire series of $RbCeX_2$ variants with variable anion compositions (*X*=O, S, Se, Te).

We were able to create the full series of RbCeX_2 compounds (**Figure 3**), stabilizing the oxide phase $RbCeO_2$ for the first time. Curiously, we found that all variants showed signs of conventional magnetic order or spin freezing below ≈1 K, with the exception of the oxide. Instead, in $RbCeO_2$, the trigonal distortion of the oxygen octahedra about the Ce^{+3} ion is greatly enhanced, leading to substantially smaller Ce-Ce distances and a dramatically amplified antiferromagnetic exchange field. The result is a doubling of the mean-field strength determined via the Curie-Weiss Θ_w temperature and the vanishing of conventional freezing behavior. Inelastic neutron scattering data determined that the ground state multiplet remained unchanged across the RbCeX_2 series, though the crystal electric field splitting increased dramatically for the oxide. The picture is then one of strong antiferromagnetic exchange promoting more energetic spin fluctuations capable of destabilizing long-range magnetic order or conventional spin freezing.

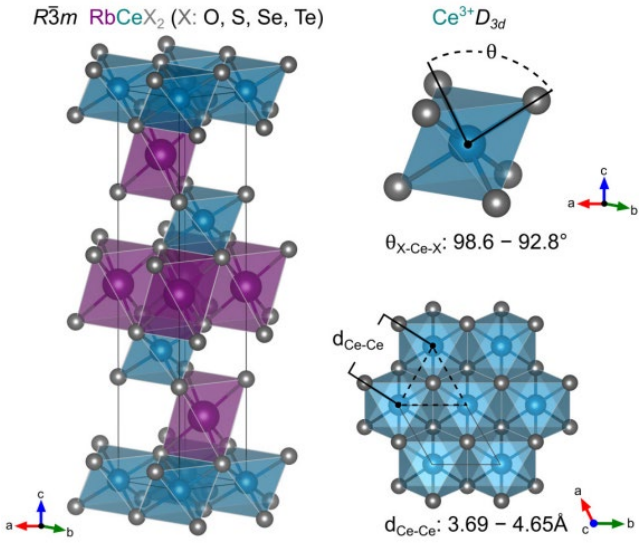

Figure 3: Crystal structure of the RbCeX_2 (X=O, S, Se, Te) series explored within this project.

Future Plans

Our future work will focus on the neutron-scattering based exploration of the quantum disordered ground states in $NaYbO_2$, $RbCeO_2$, and $NaRuO_2$ and related compounds. We are refining crystal growth methods for creating large volume samples of these compounds for more in-depth neutron scattering study; studies under applied magnetic field and chemical perturbation will be used to better isolate the underlying Hamiltonians of these compounds. An additional direction we are pursuing is the growth and study of members of the RM_3P_3 family where R are lanthanide sites capable of realizing S_{eff}=1/2 ground state wave functions and M are transition metal sites. An ideal triangular lattice network of R-sites forms in these compounds, and unlike their rare-earth delafossite cousins, these RM_3P_3 compounds are dopable semiconductors. We view this as a promising future direction for interfacing charge carriers with the highly frustrated (potentially quantum disordered) network of R-site ions. Experiments are currently underway in both crystal growth and neutron scattering-based characterization of these compounds. We also plan to explore the more three-dimensional, diamond-like lattice that forms in $AROO_2$ compounds. Our recent work has suggested there are substantial fluctuation effects remnant in R=Yb based variants of this materials class and we plan to explore the origins of this via neutron scattering based measurements.

References

1. 1. Brenden R. Ortiz, Paul M. Sarte, Alon Hendler Avidor, Aurland Hay, Eric Kenney, Alexander I. Kolesnikov, Daniel M. Pajerowski, Adam A. Aczel, Keith M. Taddei, Craig M. Brown, Chennan Wang, Michael J. Graf, Ram Seshadri, Leon Balents, and Stephen D. Wilson "Quantum disordered ground state in the triangular-lattice magnet $NaRuO_2$" *Nature Physics* **19**, 943 (2023).

2. Brenden R. Ortiz, Paul M. Sarte, Alon H. Avidor, and Stephen D. Wilson, “Defect control in the Heisenberg-Kitaev candidate material $NaRuO_2$” *Physical Review Materials* **6**, 104413 (2022).
3. Pritam Bhattacharyya, Nikolay A. Bogdanov, Satoshi Nishimoto, Stephen D. Wilson, and Liviu Hozoi “$NaRuO_2$: Kitaev-Heisenberg exchange in triangular-lattice setting” *npj Quantum Materials* **8**, 52 (2023).
4. Aleksandar Razpopov, David A. S. Kaib, Steffen Backes, Leon Balents, Stephen D. Wilson, Francesco Ferrari, Kira Riedl, and Roser Valentí “A $j_{\text{eff}} = 1/2$ Kitaev material on the triangular lattice: the case of $NaRuO_2$” *npj Quantum Materials* **8**, 36 (2023).
5. Mitchell Bordelon, Chunxiao Liu, Eric Kenney, Tom Hogan, Lorenzo Posthuma, Marzieh Kavand, Yuanqi Lyu, Mark Sherwin, N. P. Butch, Craig Brown, M. J. Graf, Leon Balents, and Stephen D. Wilson, “Field-tunable quantum disordered ground state in the triangular lattice antiferromagnet $NaYbO_2$” *Nature Physics* **15**, 1058 (2019).

Publications (10 most relevant publications supported by BES in the past two years)

1. Kristina Michelle Nuttall, Christiana Z. Suggs, Henry E. Fischer, Mitchell M. Bordelon, Stephen D. Wilson, and Benjamin A. Frandsen "Quantitative investigation of the short-range magnetic correlations in the candidate quantum spin liquid $NaYbO_2$" *Physical Review B* **108**, L140411 (2023).
2. Pritam Bhattacharyya, Nikolay A. Bogdanov, Satoshi Nishimoto, Stephen D. Wilson, and Liviu Hozoi "$NaRuO_2$: Kitaev-Heisenberg exchange in triangular-lattice setting" *npj Quantum Materials* **8**, 52 (2023).
3. Eli Zoghlin, Matthew B. Stone, and Stephen D. Wilson, "Refined spin-wave model and multimagnon bound states in Li_2CuO_2" *Physical Review B* **108**, 064408 (2023). (Editor's suggestion)
4. Aleksandar Razpopov, David A. S. Kaib, Steffen Backes, Leon Balents, Stephen D. Wilson, Francesco Ferrari, Kira Riedl, and Roser Valentí "A $j_{\text{eff}} = 1/2$ Kitaev material on the triangular lattice: the case of $NaRuO_2$" *npj Quantum Materials* **8**, 36 (2023).
5. Brenden R. Ortiz, Paul M. Sarte, Alon Hendler Avidor, Aurland Hay, Eric Kenney, Alexander I. Kolesnikov, Daniel M. Pajerowski, Adam A. Aczel, Keith M. Taddei, Craig M. Brown, Chennan Wang, Michael J. Graf, Ram Seshadri, Leon Balents, and Stephen D. Wilson "Quantum disordered ground state in the triangular-lattice magnet $NaRuO_2$" *Nature Physics* **19**, 943 (2023).
6. Eric M. Kenney, Mitchell M. Bordelon, Chennan Wang, Hubertus Luetkens, Stephen D. Wilson, and Michael J. Graf "Novel magnetic ordering in $LiYbO_2$ probed by muon spin relaxation" *Physical Review B* **106**, 144401 (2022).
7. Brenden R. Ortiz, Paul M. Sarte, Ganesh Pokharel, Michael Garcia, Marcos Marmolejo, and Stephen D. Wilson, "Traversing the pyrochlore stability diagram: Microwave-assisted synthesis and discovery of mixed B-site Ln_2InSbO_7 Family" *Physical Review Materials* **6**, 094403 (2022).
8. Brenden R. Ortiz, Paul M. Sarte, Alon H. Avidor, and Stephen D. Wilson, "Defect control in the Heisenberg-Kitaev candidate material $NaRuO_2$" *Physical Review Materials* **6**, 104413 (2022).
9. Brenden R. Ortiz, Mitchell M. Bordelon, Pritam Bhattacharyya, Ganesh Pokharel, Paul M. Sarte, Lorenzo Posthuma, Thorben Petersen, Mohamed S. Eldeeb, Garrett E. Granroth, Clarina R. Dela Cruz, Stuart Calder, Douglas L. Abernathy, Liviu Hozoi, and Stephen D. Wilson "Electronic and structural properties of $RbCeX_2$ (X_2: O_2, S_2, SeS, Se_2, TeSe, Te_2" *Physical Review Materials* **6**, 084402 (2022).
10. Yun-Yi Pai, Claire E. Marvinney, Ganesh Pokharel, Jie Xing, Haoxiang Li, Xun Li, Michael Chilcote, Matthew Brahlek, Lucas Lindsay, Hu Miao, Athena S. Sefat, David Parker, Stephen D. Wilson, Jason S. Gardner, Liangbo Liang, and Benjamin J. Lawrie" Angular-Momentum Transfer Mediated by a Vibronic-Bound-State" *Advanced Science* 2304698 (2023).

Unraveling Emergent Quantum States in Magnetic Topological Materials using High Pressure Neutron Scattering

Weiwei Xie, Chemistry, Michigan State University

Keywords: High pressure, neutron scattering, novel quantum materials

Research Scope

This proposal aims to uncover novel quantum phenomena under high pressure and understand the pressure effects on the atomic electronic interactions in magnetic topological materials. To achieve this goal, we will heavily utilize and advance High-Pressure Neutron Scattering (HP-NS) techniques for systematically direct determination of the magnetic structures and electronic interactions, which are hardly obtained by the conventional high-pressure analytical methods, such as high-pressure laser and synchrotron X-ray probes. Our work will be at the intersection of chemistry and physics. Magnetic topological materials are a new class of quantum material in which the interplay of intrinsically magnetic and topological properties stabilizes new quantum states of matter. On the atomic lattice of quantum materials, the interactions of the four fundamental degrees of freedom--lattice, charge, orbital, and spin--formulate an ever-expanding array of electronic orders that cooperate or compete in a dynamically intertwined fashion. In specific, the program initially targets materials with layered trigonal 122-type compounds, AMn_2M_2 (A= Ca, Sr and Eu; M= As, Sb and Bi), based on the magnetic element Mn and topological-state-originating heavy metals such as Bi, in which the interplay of crystal symmetry, spin dimensionality and hybridization controls spin states and quasiparticle coherence. We will be able to probe the polymorphism in both crystal and magnetic structures, electron-electron interactions, dynamical characteristics on the nanosecond timescale, and sub-nanometer spatial information on the motions in magnetic quantum materials. Such high-resolution information at high pressure is heretofore unavailable and will allow us to address the long-standing questions relevant to the interactions among spin, charge, lattice and orbitals in quantum materials under high pressure, with the ultimate aim of designing and synthesizing materials for quantum technological goals.

Recent Progress

1. Incommensurate Magnetic Orders detected using High Pressure Neutron Diffraction

To investigate the magnetic behavior of $CaMn_2Bi_2$ in extreme conditions, we first applied the high-pressure neutron diffraction at Oak Ridge National Lab- SNAP to study the magnetic structure in $CaMn_2Bi_2$.[1] In contrast to antiferromagnetic ordering on Mn atoms reported at ambient pressure, our results reveal that at high pressure, incommensurate spiral spin order emerges due to the interplay between magnetism on the Mn atoms and strong spin-orbit coupling on the Bi atoms: sinusoidal spin order is observed at pressures as high as 7.4 GPa. First-principles calculations with noncollinear spin orientation demonstrate band crossing behavior near the Fermi level as a result of strong hybridization between the *d*-orbitals of Mn and the *p*-orbitals of Bi atoms. Competing antiferromagnetic order is observed at different temperatures in the partially frustrated lattice. Theoretical models are developed to investigate spin dynamics. This research provides a unique toolbox for conducting experimental and theoretical magnetic and spin dynamics studies on magnetic quantum materials via high pressure neutron diffraction.

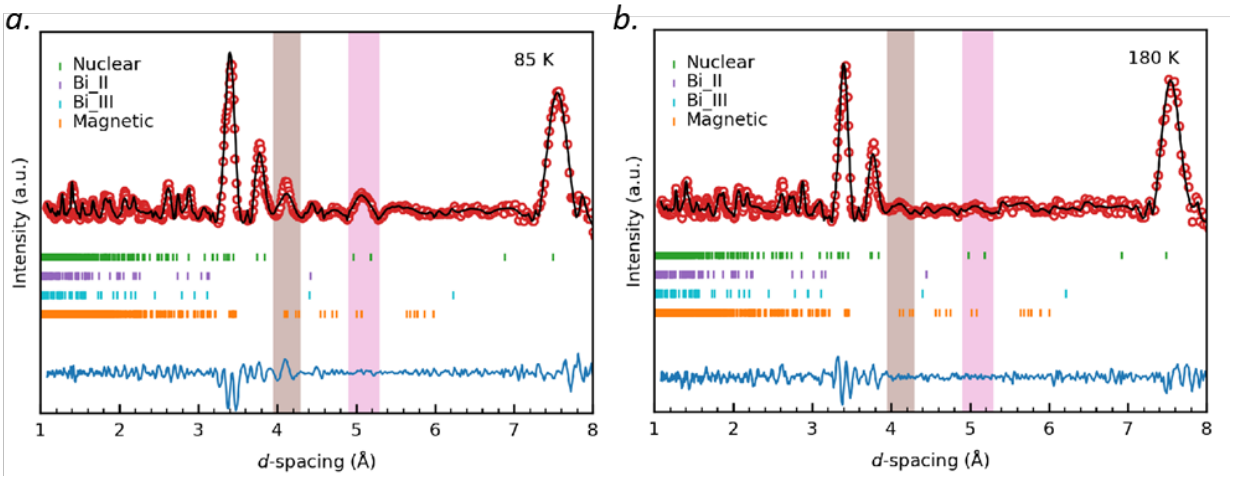

Figure 1. The NPD refinements of $CaMn_2Bi_2$ at ~6.9 GPa at temperatures of 85 K (*a*) and 180 K (*b*), The theoretical Bragg peak positions are indicated for the $CaMn_2Bi_2$ nuclear peaks (green), Bi II (purple), Bi III (teal) and the $CaMn_2Bi_2$ magnetic peaks (orange). The magnetic peak regions are highlighted in brown and pink for visual purposes.

2. Novel Quantum Materials with Frustrated Magnetism in the New Pyrochlore Lattice.[2,3]

Three-dimensionally (3D) frustrated magnets generally exist in the magnetic diamond and pyrochlore lattices, in which quantum fluctuations suppress magnetic orders and generate highly entangled ground states. $LiYbSe_2$ in a previously unreported pyrochlore lattice was discovered from LiCl flux growth. Distinct from the quantum spin liquid (QSL) candidate $NaYbSe_2$ hosting a perfect triangular lattice of Yb^{3+}, $LiYbSe_2$ crystallizes in the cubic pyrochlore structure with space group *Fd*-3*m* (No. 227). The Yb^{3+} ions in $LiYbSe_2$ are arranged on a network of corner-sharing tetrahedra, which is particularly susceptible to geometrical frustration. According to our temperature-dependent magnetic susceptibility measurements, the dominant antiferromagnetic interaction in $LiYbSe_2$ is expected to appear around 8 K. However, no long-range magnetic order is detected in thermomagnetic measurements above 70 mK. Specific heat measurements also show magnetic correlations shifting with applied magnetic field with a degree of missing entropy that may be related to the slight mixture of Yb^{3+} on the Li site. Such magnetic frustration of Yb^{3+} is rare in pyrochlore structures. Thus, $LiYbSe_2$ shows promise in intrinsically realizing disordered quantum states like QSL in pyrochlore structures.

3. High Pressure Study on $LiYbSe_2$ with the New Pyrochlore Lattice.[4]

We performed a high-pressure study on $LiYbSe_2$. The crystal structural evolution of $LiYbSe_2$ under hydrostatic pressure was studied by performing XRD experiments at room temperature up to 15 GPa. The cubic pyrochlore structure with the space group F*d*-3*m* is maintained under pressures up to Pa.

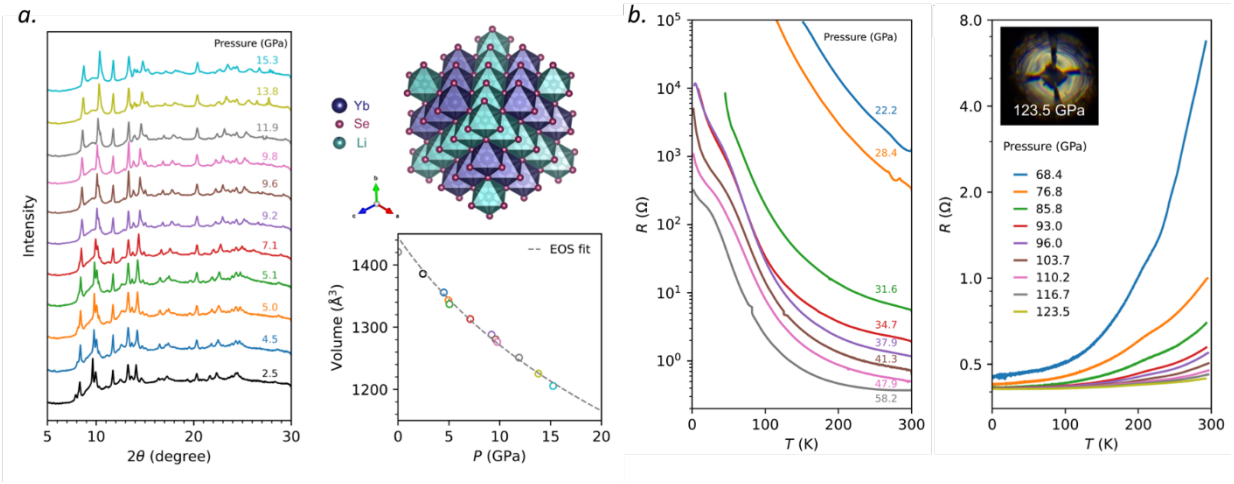

Fig. 2. (a) High pressure XRD data taken at room temperature and pressure dependence and second-order Birch-Murnaghan EOS fit of the unit cell volume of $LiYbSe_2$ up to 15.3 GPa; (b) Temperature dependence of resistance of $LiYbSe_2$ up to 123.3 GPa.

To study the electrical transport properties and explore potential superconductivity which may arise from suppressing the frustrated magnetism in $LiYbSe_2$, the temperature dependence of resistance R of $LiYbSe_2$ between 2 and 300 K under various pressures up to 123.5 GPa was measured. The results are shown in **Fig. 2**. At lower pressure range (< 22 GPa), the resistance is too large to be measured in the Physical Property Measurement System (PPMS). Starting from 22.2 GPa, the resistance can be detected. From 22.2 to 58.2 GPa, $LiYbSe_2$ shows semiconductor-like behavior in the whole temperature range. The resistance was measured with the pressure applied up from 68.4 GPa to 123.5 GPa. A very weak drop (< 0.5% drop) in resistance was observed starting at around 3.0 K from 96 GPa. The potential phase transition temperature is slightly suppressed with pressure from 3.0 K at 96 GPa to around 2.5 K at 116.7 GPa. However, to detect the local structure and bonding vibration under high pressure at room temperature (300 K), we applied Raman spectra under high pressure shown in **Fig. 3*a***. At ~5.6 GPa, a small peak at 207 cm^{-1} appears. It moves to lower frequency under pressurization, merging with Mode 2 at about 200 cm^{-1} and 8.6 GPa. The observation indicates that the hidden phase may be related to spin-phonon interactions which may be clearly detected by neutron diffraction under high pressure. Moreover, the disappearance of two-in and two-out spin freezing at low temperature in $LiYbSe_2$ may be understood by high pressure neutron scattering study.

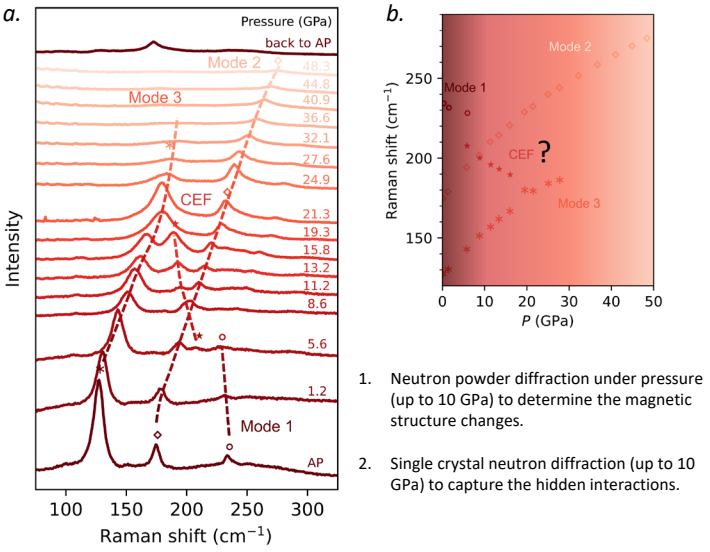

1. Neutron powder diffraction under pressure (up to 10 GPa) to determine the magnetic structure changes.
2. Single crystal neutron diffraction (up to 10 GPa) to capture the hidden interactions.

Fig. 3. (a) High pressure Raman spectra of $LiYbSe_2$ (b) Evolution of Raman vibration modes up to 48 GPa.

Future Plans

1. Considering the potential existence of diverse quantum spin liquid (QSL) states, there is a compelling interest in categorizing these states. Although the resolution of this issue remains

incomplete, it is evident that the range of feasible states is substantial, possibly extending to infinity. Diverse numerical methodologies have been employed to investigate potential QSL phases within theoretical models, including the imposition of an external magnetic field. In this study, we propose to utilize physical pressure as a tuning parameter to scrutinize electronic interactions within the $LiYbSe_2$ compound up to 10 GPa using neutron scattering to illustrate the possible hidden phases. Our objective is to systematically classify the distinct QSL states using high pressure neutron diffraction within $LiYbSe_2$ and, moreover, to garner insights that may contribute to the comprehension of analogous QSL systems.

2. We will expand our high-pressure neutron scattering study to Kagome metals with flat bands to explore possible new magnetic phase under high pressure using neutron scattering. Using various measurements such as advanced muon-spin rotation spectroscopy, an unexpected hidden magnetism of the charge order was detected. Thus, we propose to utilize high pressure to suppress the charge density wave in $SmNi_6Al_6$ recently discovered in our lab, and induce other exotic quantum phenomena, such as superconductivity or magnetic ordering on Ni or Sm. Our objective is to study the magnetic and structure phase diagram of $SmNi_6Al_6$ under high pressure using neutron diffraction.

3. We will also expand our high-pressure study to other frustrated systems, for example, square net lattice to understand the superconductivity and magnetism in the system, especially nickelates. Thus, we propose to study the magnetic and superconducting properties of bulk $R_{3-d}A_dNi_2O_{7-x}$ under high pressure to examine the superconductivity and other magnetic behaviors in the system using neutron scattering.

References

1. M. Marshall, H. Wang, A.M. Dos Santos, B. Haberl, W. Xie. *Incommensurate Spiral Spin Order in $CaMn_2Bi_2$ Observed via High-Pressure Neutron Diffraction*. Inorganic Chemistry, in press, (2023). https://doi.org/10.1021/acs.inorgchem.3c02379
2. R.S. Dissanayaka Mudiyanselage, H. Wang, O. Vilella, M. Mourigal, G. Kotliar, W. Xie. *$LiYbSe_2$: Frustrated Magnetism in the Pyrochlore Lattice.* Journal of the American Chemical Society, **144**, 11933-11937 (2022). https://doi.org/10.1021/jacs.2c02839
3. R. S. Dissanayaka Mudiyanselage, T. Klimczuk, D. Ni, R. J. Cava, W. Xie. "*Chemical Pressure Tuning Magnetism from Pyrochlore to Triangular Lattices*" Inorganic Chemistry, **61**, 18010-18018 (2022). https://doi.org/10.1021/acs.inorgchem.2c02232
4. H. Wang, L. Shi, S. Huyan, G.C. Jose, B. Lavina, S.L. Bud'ko, W. Bi, P.C. Canfield, J. Cheng, W. Xie. *Insulator to Metal Transition, Spin-Phonon Coupling, and Potential Magnetic Transition Observed in Quantum Spin Liquid Candidate $LiYbSe_2$ under High Pressure*. arXiv preprint arXiv:2312.00270 (2023).
5. J.L.G. Jimenez, C. Melnick, K.P. Koirala, R. Adler, F. Wang, M. Berrada, B. Chen, L. Wang, D. Walker, G. Kotliar, W. Xie. *Tetragonal Kondo Insulator $EuCd_2Sb_2$ Discovered via High Pressure High Temperature Synthesis.* Advanced Functional Materials, 2303612 (2023). https://doi.org/10.1002/adfm.202303612

Publications

1. Marshall, M., Wang, H., Dos Santos, A.M., Haberl, B., Xie, W.* Incommensurate Spiral Spin Order in $CaMn_2Bi_2$ Observed via High-Pressure Neutron Diffraction. *Inorg. Chem.* In press, 2023. (Selected as the Cover)
2. Jimenez, J.L.G., Melnick, C., Koirala, K.P., Adler, R., Wang, F., Berrada, M., Chen, B., Wang, L., Walker, D., Kotliar, G., Xie, W.* Tetragonal Kondo Insulator $EuCd_2Sb_2$ Discovered via High Pressure High Temperature Synthesis. *Adv. Funct. Mater.* 2023, 2303612.

3. Wang, H., Xu, X., Ni, D., Walker, D., Li, J., Cava, R.J. Xie, W.* Impersonating a Superconductor: High-Pressure $BaCoO_3$, an Insulating Ferromagnet. . *J. Am. Chem. Soc.* 2023, 145, 21203-21206.
4. Wang, H., Marshall, M., Wang, Z., Plumb, K.W., Greenblatt, M., Zhu, Y., Walker, D., Xie, W. Non-Centrosymmetric Sr_2IrO_4 Obtained Under High Pressure. *Inorg. Chem.* 2023, 62, 5, 2161–2168.
5. Hu, Y., Wu, X., Yang, Y., Gao, S., Plumb, N.C., Schnyder, A.P., Xie, W., Ma, J., Shi, M. Tunable topological Dirac surface states and van Hove singularities in kagome metal GdV_6Sn_6. *Sci. Adv.* 2022, 8(38), eadd2024.
6. Dissanayaka Mudiyanselage, R. S.; Wang, H.; Vilella, O.; Mourigal, M.; Kotliar, G.; Xie, W.* $LiYbSe_2$: Frustrated Magnetism in the Pyrochlore Lattice. *J. Am. Chem. Soc.* 2022, 144, 11933-11937. (Selected as the Cover)
7. Marshall, M., Wang, F., Klimczuk, T., Dissanayaka Mudiyanselage, R.S., Greenblatt, M., Walker, D., Xie, W.* $Eu_2Mg_3Bi_4$: Competing Magnetic Orders on a Buckled Honeycomb Lattice. *Chem. Mater.*, 2022, 34, 3902-3909.
8. Ma, J., Nie, S., Gui, X. et al. Multiple mobile excitons manifested as sidebands in quasi-one-dimensional metallic $TaSe_3$. *Nat. Mater.* 2022, 21, 423-429.
9. Marshall, M., Xie, W.* Crystal Defect Doping on Antiferromagnetic Topological Insulator Candidate $EuMg_2Bi_2$. *J. Phys. Chem. C* 2021, 126, 737-742.
10. Marshall, M., Pletikosić, I., Yahyavi, M., Tien, H.J., Chang, T.R., Cao, H., Xie, W.* Magnetic and electronic structures of antiferromagnetic topological material candidate $EuMg_2Bi_2$. *J. Applied Phys.* 2021, 129(3), 035106.

Project title: Exotic Magnetic Orders and Dynamics in Chiral Magnets

PI: Junjie Yang, Department of Physics, New Jersey Institute of Technology, NJ 07102

Keywords: polarized neutron scattering, magnetic chirality, multiferroic, Hall effect, domain

Program Scope

The breaking of fundamental symmetries such as space inversion, mirror symmetry, and time reversal symmetries invariably leads to intriguing phenomena in chiral magnets.[1-3] When we introduce chemical substitutions into chiral magnets, we have the potential to significantly alter magnetic interactions and anisotropy. The intricate correlations between these modified structural features and the resulting changes in magnetic behavior can give rise to entirely new magnetic orders. The effects of chemical substitution in chiral magnets remain relatively understudied. Thus, it becomes imperative to elucidate the role of chemical substitution in these materials, as it provides an effective avenue for tailoring their physical properties. Within the chiral lattice framework of the parent compounds, chemical substitutions hold the potential to introduce diverse magnetic anisotropies and fine-tune the competitive magnetic interactions. These alterations pave the way for the emergence of novel physics in chemically-substituted chiral magnets. The goal of this project is to unveil the intricate correlations between chemical substitution, chiral crystal structures, magnetic interactions, and the emergence of exotic magnetic orders in substituted chiral magnets, through a series of neutron scattering experiments.

Recent Progress

We have made progress along several avenues. In our previous investigations, we noted that the Mn substitution in $Ni_{3-x}Mn_xTeO_6$ can induce the chiral helical magnetic structure.[3] Furthermore, our refinement unveiled partial ionic ordering of Mn ions, sparking our interest in exploring the relationship between this ionic ordering and magnetic structures in $Ni_{3-x}Mn_xTeO_6$. To delve deeper into this question, we synthesized both quenched and annealed $Ni_{2.2}Mn_{0.8}TeO_6$. The quenched variant was rapidly cooled to liquid nitrogen immediately after synthesis, while the annealed counterpart was subjected to a gradual cooling process at a rate of 10 °C/hour. Both the quenched and annealed specimens exhibit an identical crystal structure to the parent compound Ni_3TeO_6. In Fig. 1(A), the magnetic moment versus temperature (*M-T*) curves illustrate noteworthy differences between the two samples. The quenched sample displays a single magnetic transition occurring at 72 K, whereas the annealed sample exhibits two distinct

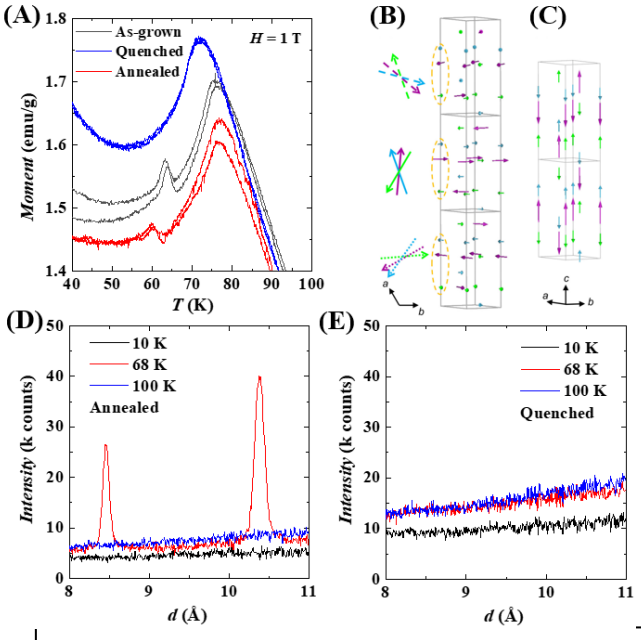

Figure 1. (A) The *M-T* cuvres of $Ni_{2.2}Mn_{0.8}TeO_6$ samples. (B) The helical magnetic structure of $Ni_{2.2}Mn_{0.8}TeO_6$. (C) The collinear magnetic structure of $Ni_{2.2}Mn_{0.8}TeO_6$. (D)-(E) Neutron powder diffraction patterns for annealed and quenched $Ni_{2.2}Mn_{0.8}TeO_6$.

magnetic transitions, one at 77 K and another at 60 K. Our neutron powder diffraction findings, obtained through measurements conducted at POWGEN, shed further light on it. Fig. 1(B) and 1(C) reveal that the annealed sample showcases a pair of incommensurate magnetic peaks at 68 K. In contrast, the quenched sample does not exhibit these incommensurate magnetic peaks. These compelling results strongly suggest that the Mn ionic ordering plays a pivotal role in favoring the emergence of the intermediate helical magnetic structure phase, thus providing valuable insights into the intricate interplay between ionic ordering and magnetic behavior in $Ni_{3-x}Mn_xTeO_6$.

In our prior research endeavors, we made a noteworthy observation concerning the $NiCo_2TeO_6$ compound, wherein it also led to the emergence of a chiral helical magnetic structure. Notably, our polarized neutron diffraction investigations on the as-grown crystal shed light on the dominance of one helical magnetic domain with a ratio of 2.5:1. To obtain a crystal with a single chiral domain, we employed a novel approach involving single crystal growth under a 1000 V voltage. Capitalizing on the interlock between polarity and chirality, we harnessed the influence of external voltage to induce a monopolar domain, thereby achieving a monochiral domain state. As depicted in Fig. 2(A), the crystal grown under the voltage undergoes magnetic ordering at 52 K. Employing unpolarized neutron diffraction at the HB-2C, we unveiled the helical magnetic structure characterized by a magnetic propagation vector of (0, 0, 1.27), as illustrated in Fig. 2(B)-(C). Furthermore, polarized neutron diffraction data acquired at HB1 confirmed the presence of a left-handed magnetic chirality within the single-domain crystal, as shown in Fig. 2(D) and 2(E). Fig. 2(F) offers a comprehensive view of the helical magnetic structure, while the inset of Fig. 2(E) presents a polarized optical microscope image of the crystal. Remarkably, with the polarizer and analyzer oriented at an angle of 81°, the entire crystal exhibits uniform darkness without any discernible bright-dark contrast, thus indicating the crystal's single-chiral domain nature.

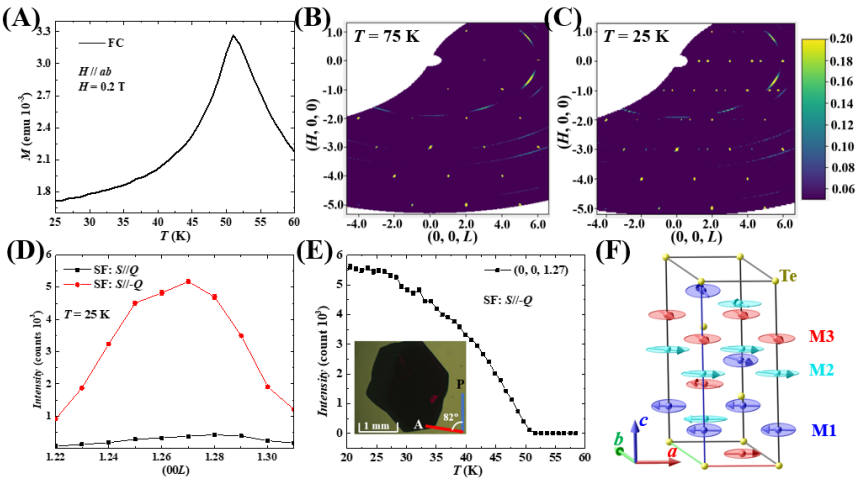

Figure 2. (A) The *M*-*T* cuvres of $NiCo_2TeO_6$. (B)-(C) Neutron diffraction patterns at 75 K and 25 K. (D) Polarized neutron diffraction patterns at (0, 0, 1.27) peak. (E) Order parameter vs tempeature measured at (0, 0, 1.27). (F) Helical magnetic structure of $NiCo_2TeO_6$.

We have undertaken a comprehensive investigation into the chiral $Co_{1/3}TaS_2$. Our neutron diffraction verifies the lattice structure to be of the chiral $P6_322$. The magnetic behavior, as depicted in Fig. 3(A), reveals a magnetic ordering temperature of 42 K. Notably, this magnetic transition is characterized by a moment jump along the *c*-axis, signifying the presence of a net magnetic moment.

Of particular interest are our Hall effect measurements, which unveil an Anomalous Hall effect (AHE), as depicted in Fig. 3(B). This effect is associated with a weak ferromagnetic hysteresis behavior. It's worth noting that these findings diverge significantly from recent reports on $Co_{1/3}TaS_2$, which exhibited the propagation vectors of (0.5, 0.5, 0) and (0.5, 0, 0).[4] Our neutron diffraction carried out at HB1A, yield results that indicate three equivalent magnetic propagation vectors: (1/3, 0, 0), (0, 1/3, 0), (1/3, -1/3, 0), and one unique vector (0, 0, 0.075). These vectors are indicative of a magnetic structure in our $Co_{1/3}TaS_2$ that differs significantly from previous findings. A plausible magnetic structure is depicted in Fig. 3(F), illustrating a toroidal moment and a net moment along the *c*-axis within a single layer. Moreover, the spins within the *ab* plane rotate along the *c*-axis, giving rise to the (0, 0, 0.075) vector.

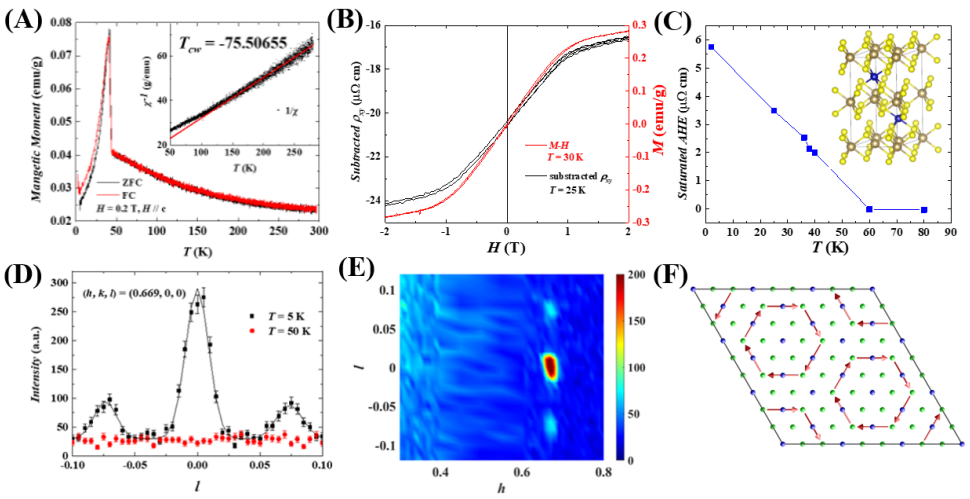

Figure 3. (A) The *M*-*T* cuvres of $Co_{1/3}TaS_2$. (B) AHE signal (black curve) and magnetic moment (red) vs magnetic field. (C) AHE signal vs tempeature. The inset show the chiral lattice structure. (D)-(E) The magnetic peaks measured at 5 K for $Co_{1/3}TaS_2$. (F) The toroidal magnetic structure in one layer of $Co_{1/3}TaS_2$.

We have made an intriguing discovery in a new chiral magnetic system, $ReFe(SO_4)_2$.[5] It's worth noting that $ReFe(SO_4)_2$ demonstrates a high ferro-rotational transition temperature at 300 °C. Through the utilization of the high-pressure hydrothermal method, we have successfully reduced the growth temperature to 210°C. Under these conditions, the grown crystals exhibit a single-domain character. In Fig. 4(A), the *M*-*T* curves indicate spin order below 4 K. Subsequent neutron diffraction experiments have unveiled a helical magnetic structure with a propagation vector of (1/3, 1/3, 0.43). Importantly, this helical magnetic structure results in the emergence of polarization along the *c*-axis, as depicted in Fig. 4(B). The presence of the ferro-rotational lattice with polarization along the *c*-axis results in a chiral lattice structure. Furthermore, it suggests that the lattice chirality can be controlled by the electric field. Significantly, since the magnetic chirality is intimately linked to the chiral lattice structure, altering the lattice chirality can also impact the magnetic chirality. Our polarized neutron diffraction experiments, conducted at the HB1 spectrometer, confirm this intricate relationship. Fig. 4(C) depicts the intensity differences, $I_x^{\mp}$ and $I_x^{\pm}$, at the (1/3, 1/3, 2.43) peak for a crystal subjected to a +1.75 kV/cm electric field, suggesting the presence of a single-domain magnetic configuration. Fig. 4(D) provides a complementary view, showing $I_x^{\mp}$ and $I_x^{\pm}$ for the (1/3, 1/3, 2.43) peak when the crystal is exposed to a -1.75 kV/cm electric field. Remarkably, the negative electric field effectively reverses the handedness of the magnetic chirality.

Future Plans

We will continue our efforts to understand the physics of chiral magnets. With the acquisition of high-quality single-domain $NiCo_2TeO_6$ crystals, we are poised to conduct polarized inelastic neutron scattering experiments on these co-aligned crystals. This endeavor aims to validate the existence of potential non-reciprocal spin waves. Despite our progress, the microscopic origins of the unusual magnetic structure observed in our $Co_{1/3}TaS_2$ remain enigmatic. To unravel this mystery, we plan to co-align single crystals and conduct inelastic neutron scattering experiments, to elucidate the spin waves and extract the exchange coupling constants. These insights will be instrumental in uncovering the microscopic underpinnings of the magnetic structure and the associated AHE. Upon obtaining single-domain $Co_{1/3}TaS_2$ crystals, we will extend our research to include polarized inelastic neutron scattering experiments. Furthermore, the $RbFe(SO_4)_2$ system serves as an excellent platform for investigating electric-field-controlled spin waves. We will co-align single-domain crystals and conduct polarized inelastic neutron scattering experiments under the electric field, to uncover the potential for electric-field-controlled non-reciprocal spin waves.

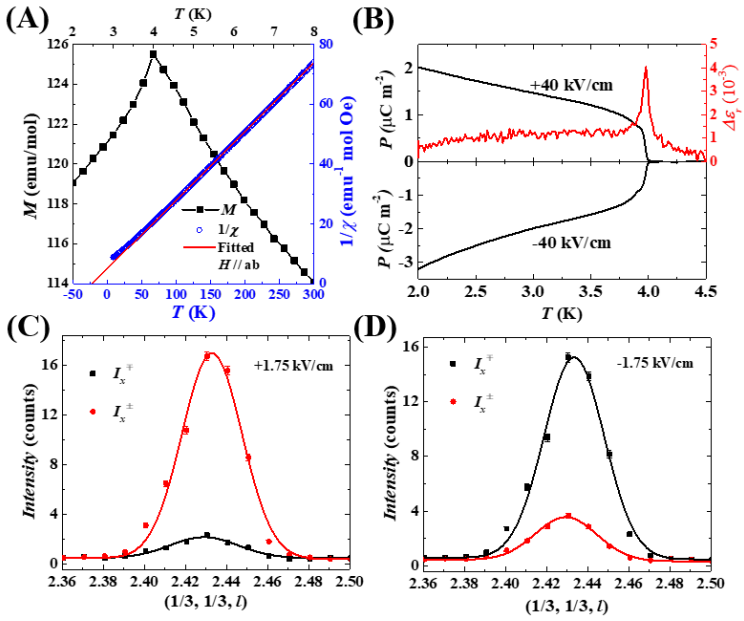

Figure 4. (A) The *M-T* cuvres of $ReFe(SO_4)_2$. (B) The polarization (black) and dielectric constant (red) vs temperature. (C)-(D) Polarized neutron diffraction patterns under positive electric field and negative electric field, respectively.

The broken space inversion symmetry observed in all of our chiral magnetic crystals opens up avenues for the manifestation of the Spin-Orbit Coupling (SOC) effect. This SOC phenomenon not only can induce exotic magnetic orders but also gives rise to novel neutron spin-orbit scattering processes. An illustrative example is the Schwinger scattering observed in polar and chiral crystals. Neutron spin-orbit scattering, in comparison to Schwinger scattering, offers a considerably richer array of possibilities. Its manifestations can vary significantly depending on the experimental setup and the orientation of the crystals under investigation. This versatile phenomenon can also lead to the emergence of polarity-induced spin selectivity effects or chirality-induced spin selectivity for neutrons. Our forthcoming research endeavors will focus on neutron spin-orbit scattering in noncentrosymmetric magnets, including the chiral magnets that are central to our current project. This exploration promises to uncover further insights into the intricate interplay of SOC, crystal symmetry, and magnetic behavior in these unique materials.

References

1. Cheong, S. W., SOS: symmetry-operational similarity. npj Quantum Mater. 4 (1), 2019.
2. Mühlbauer, S.; Binz, B.; Jonietz, F.; Pfleiderer, C.; Rosch, A.; Neubauer, A.; Georgii, R.; Böni, P., Skyrmion lattice in a chiral magnet. Science, 323 (5916), 915-919, 2009.

3 Kim, J.W.; Yang, J.J.; Won, C.J.; Kim, K; Kim, B; Obeysekera, D; Lee, D.W.; Cheong, S.-W, “Helical versus collinear antiferromagnetic order tuned by magnetic anisotropy in polar and chiral $(Ni,Mn)_3TeO_6$”, Phys. Rev. Materials. 5, 094405, 2021.

4. H. Takagi, R. Takagi, S. Minami, T. Nomoto, K. Ohishi, M.-T. Suzuki, Y. Yanagi, M. Hirayama, N. D. Khanh, K. Karube, H. Saito, D. Hashizume, R. Kiyanagi, Y. Tokura, R. Arita, T. Nakajima & S. Seki, “Spontaneous topological Hall effect induced by non-coplanar antiferromagnetic order in intercalated van der Waals materials”, Nature Physics, 19, 961, 2023.

5. Rachel Owen, Elizabeth Drueke, Charlotte Albunio, Austin Kaczmarek, Wencan Jin, Dimuthu Obeysekera, Sang-Wook Cheong, Junjie Yang, Steven Cundiff, and Liuyan Zhao, “Second-order nonlinear optical and linear ultraviolet-visible absorption properties of the type-II multiferroic candidates RbFe(AO4)2 (A=Mo,Se,S)”, Phys. Rev. B 103, 054104, 2021.

Publications

1. Min Gyu Kim , Andi Barbour, Wen Hu, Stuart B. Wilkins , Ian K. Robinson , Mark P. M. Dean, Junjie Yang, Choongjae Won , Sang-Wook Cheong , Claudio Mazzoli, Valery Kiryukhin, “Real-space observation of fluctuating antiferromagnetic domains”, Science Advances, 8, eabj9493, 2022

2. Kai Du, Fei-Ting Huang, Kasun Gamage, Junjie Yang, Maxim Mostovoy, Sang-Wook Cheong, “Strain-Control of Cycloidal Spin Order in a Metallic Van der Waals Magnet”, Advanced Materials, 35, 2303750, 2023,

3. Shinichiro Yano, Chin-Wei Wang, Junjie Yang, “The Magnetic Structural Analysis of Two-dimensional Triangular Heisenberg Antiferromagnetic Yb0.42Sc0.58FeO3”, New Physics: Sae Mulli, 73, 1, 2023

Universality of Collective Density Fluctuations in Liquids at and away from Equilibrium – An Integrated Inelastic Neutron Scattering, Theoretical, and Computational Study

Professor Yang Zhang (YZ), Department of Nuclear Engineering and Radiological Sciences, Department of Materials Science and Engineering, Department of Robotics, Applied Physics Program, University of Michigan

Keywords: Liquid Dynamics, Glasses, Neutron Spin Echo, Quasi-Elastic Neutron Scattering (QENS), Neural-Network Forcefield

Research Scope

Liquids, including complex fluids, as one of the three phases of matter, are ubiquitous on earth and are prototypical disordered condensed matter. However, the physics of liquids is far from being completely understood and therefore excluded by Landau and Lifshitz from their Course of Theoretical Physics. As the mediate phase between non-structured gases and ordered solids, liquids possess intriguing complexities that are absent on either extreme counter phase, especially when they are driven away from equilibrium. Despite decades of studies, the physics of liquids still keeps surprising us and challenges our understanding of condensed matter, emergent phenomena, and complex systems. Furthermore, numerous soft and biological materials of amazing far-from-equilibrium complexity seem to share many intriguing features of liquids. Therefore, quantitative descriptions of the structure and dynamics of liquids and liquid-like matter will likely impact a wide range of disciplines.

Among the many interesting properties of liquids, the nature of collective dynamics in liquids remains elusive because of both the presence of strong interactions and the absence of translational invariance. Our research activities center around the understanding of collective density fluctuations (or collective modes), which include both phonon-like excitations and collective relaxations, in the Q-dependent generalized hydrodynamic regime in liquids and liquid-like matter both at and away from equilibrium. We perform systematic studies of the fast collective dynamics of a variety of liquids characterized by different fragilities and interactions (ionic, metallic, hydrogen-bonded, van der Waals) using synergistically integrated coherent neutron scattering experiments, a ViscoElastic Hydrodynamics theory we have been developing, and Molecular Dynamics (MD) simulations and our analysis package LiquidLib. The transformative knowledge of the collective dynamics in liquids is important to understand and ultimately control the transport of mass, energy, and charge in liquids, both at and away from thermal equilibrium, which may will likely impact a wide range of disciplines.

Recent Progress

1. Using a combination of the new wide-angle neutron spin-echo **(WASP)** at ILL and the time-of-flight direct geometry chopper spectrometer **AMATERAS** at J-PARC, we measured the collective relaxation dynamics of a model fragile glass-forming liquid CKN covering a wide Q range and time range. The results show, for the first time experimentally, temperature independent dynamic heterogeneity with more Arrhenius-like behavior at the local length scales. (*Nature*

Communications, 13, 2092 (2022). This is world's first wide-angle neutron spin-echo (WASP) paper to our knowledge.

The relaxation behavior of glass formers exhibits spatial heterogeneity and dramatically changes upon

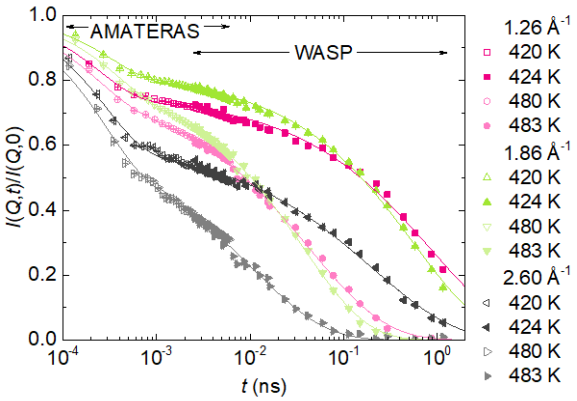

Figure 1. ISF of CKN covering a broad time window at three representative Q's: (1.26, 1.86 and 2.60) Å^{-1}. The data presented by open symbols from 0.1 ps to 6 ps are Fourier deconvoluted time-of-flight spectra measured on AMATERAS, those presented by solid symbols from 2.6 ps to 1.2 ns are the WASP data. The AMATERAS data are measured at T = 420 K and 480 K, and the WASP data are at T = 424 K and 483 K. These two sets of data match in the overlapping time range without any artificial adjustment.

cooling towards the glass transition. However, the underlying mechanisms of the dynamics at different microscopic length scales are not fully understood. Employing the recently developed wide-angle neutron spin-echo spectroscopy technique, we measured the Q-dependent coherent intermediate scattering function of a prototypical ionic glass former $Ca_{0.4}K_{0.6}(NO_3)_{1.4}$, in the highly viscous liquid state. In contrast to the structure modulated dynamics for $Q < 2.4$ Å^{-1}, i.e., at and below the structure factor main peak, for $Q > 2.4$ Å^{-1}, beyond the first minimum above the structure factor main peak, the stretching exponent exhibits no temperature dependence and concomitantly the relaxation time shows smaller deviations from Arrhenius behavior. This finding indicates a change in the dominant relaxation mechanisms around a characteristic length of $2\pi/(2.4$ Å$^{-1}) \approx 2.6$ Å, below which the relaxation process exhibits a temperature independent distribution and more Arrhenius-like behavior. The results show, for the first time experimentally, that the temperature independent dynamic heterogeneity with more Arrhenius-like behavior at the local length scales. The method also demonstrates that Q-dependent coherent scattering is more than a simple two-point time-correlation function and therefore can provide some sort of experimental measurement of the dynamic heterogeneity.

2. Using both neutron spin echo, we discovered an unusual non-monotonic temperature-dependence of the stretching exponent β as the prototypical network ionic liquid $ZnCl_2$ is supercooled. MD simulations using neural-network forcefield revealed that this unusual dynamic behavior is due to the competition between dynamic and chemical heterogeneity. (JPCL 2021 [1] and new WASP + simulation paper to be submitted shortly)

Molten zinc chloride ($ZnCl_2$), a prototypical AX_2-type tetrahedral network liquid, displays unique physical and thermodynamic properties and possesses a propensity for glass formation. These features make $ZnCl_2$ an intriguing material for fundamental research, with particular attention given to its relaxation dynamics. Recently, Luo et al. reported an increase in the stretch exponent β in molten $ZnCl_2$ from T_m+85 K to T_m+35 K using neutron-spin echo (NSE) spectroscopy. This discovery stands in sharp contrast to other glass forming systems. In this study, we conducted molecular dynamics simulations using a neural network forcefield (NNFF) from 900 K to 500 K and found a non-monotonic temperature dependence of β. A window of increasing β from 800 K to 650 K was identified and attributed to the decrease in the diversity of chemical motifs. We believe that this suppression of "Chemical Heterogeneity" leads to a decrease in the overall dynamical heterogeneity

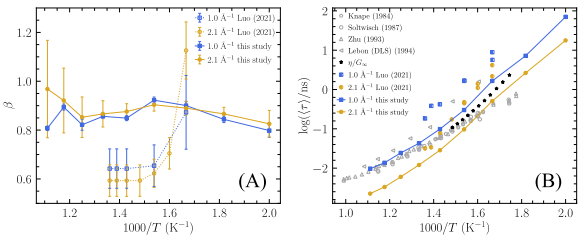

Figure 2. (A) The non-monotonic temperature dependence of β fitted from the simulated $F(Q,t)$ in this study (solid lines) and the experimental $F(Q,t)$ measured by Luo (dotted lines). Regime I and III was denoted as the "Dynamical Heterogeneity" dominated (DH-dominated) regime while regime II was referred to as the "Chemical Heterogeneity" dominated (CH-dominated) regime. (B) The comparisons of the logrithmic average relaxation time $\log(\langle\tau\rangle)$ as functions of inverse temperature.

over a certain temperature window, which may contribute to a better understanding of the structural relaxation of other tetrahedral network liquids.

3. Using algebraic topology tools Morse-Smale complex and sublevelset persistence homology, we are able to provide topology-based interpretations to the autoencoder-learned collective variables (CVs). These collective CVs provide minimal number of parameters to describe the dynamics of liquids. We used a series of n-alkanes as an example [2,3]. (submitted to PRL)

Dimensionality reduction often serves as the first step towards a minimalist understanding of physical systems as well as the accelerated simulations of them. In particular, neural network-based nonlinear dimensionality reduction methods, such as autoencoder, have shown promising outcomes in uncovering collective variables (CVs). However, the physical meaning of these CVs remain largely elusive. In this work, we constructed a framework that 1) determines the optimal number of CVs needed to capture the essential molecular motions using an ensemble of hierarchical autoencoders, and 2) provides topology-based interpretations to the autoencoder-learned CVs with Morse-Smale complex and sublevelset persistence homology. This approach was exemplified using a series of n-alkanes and can be regarded as a general method.

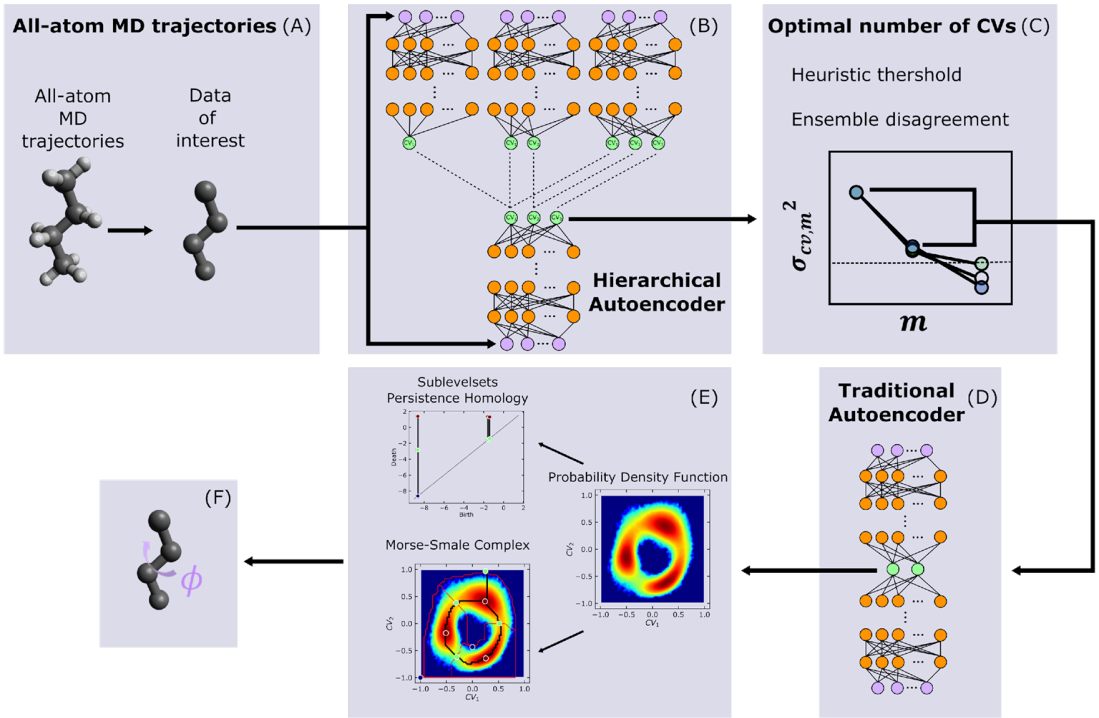

Figure 3. Framework of topology-based interpretation of autoencoder-leaned collective variables. (A) All-atom MD trajectories. (B) Architecture of a hierarchical autoencoder (HAE). (C) Determination of the optimal number of CVs. (D) Traditional autoencoder with the optimal number of CVs. (E) Sublevelset persistent homology and Morse-Smale complex decomposition of the autoencoder-learned CV space. (F) Automatically extracted transition pathways.

4. We continue to develop and maintain ***LiquidLib®*** for computing various weighted statistical quantities of liquids and liquid-like systems from classical and *ab initio* molecular dynamics trajectories, which can be directly compared with both elastic and inelastic neutron scattering experiments. Up to date, *LiquidLib®* has >330 users worldwide.

Future Plans

We will use a combination of several INS/QENS/NSE spectrometers to cover a wide dynamic/time range and wave vector transfer range. We will measure the Q dependence, "dispersion relation" if you wish, collective dynamics of the representative model liquid systems over a wide temperature range. Specifically, the near future plans will be centered around CKN and $ZnCl_2$ which are the two ends of the spectrum of fragility.

1. To expand our pervious WASP work on CKN, which summarized the slow relaxation of CKN, we have also measured the fast dynamics of CKN using AMATERAS at J-PARC. The paper was reviewed at PNAS. The reviewers raised significant questions that can only be addressed with new experimental data. Since the last report, we have performed another experiment using AMATERAS. We are analyzing the data and preparing to resubmit the paper.
2. The WASP experiment on $ZnCl_2$ at ILL was delayed due to the availability of the special furnace for the spin echo experiment. Finally, we were able to perform the experiment in September 2023. While waiting, we have performed MD simulations with neural-network forcefields we developed for $ZnCl_2$. We are currently wrapping up the paper.
3. Continue to develop functionalities and maintain LiquidLib.

References

1. P. Luo, Y. Zhai, J. Leao, M. Kofu, K. Nakajima, A. Faraone, **Y Z*,** "Neutron spin echo studies of the structural relaxation of liquid ZnCl2 at the structure factor primary peak and pre-peak", *J. Phys. Chem. Lett.* 12(1), 392 (2021)
2. K. Yang, Z. Cai, A. Jaiswal, M. Tyagi, J. S. Moore, **Y. Zhang*,** "Dynamic odd-even effect in liquid n-alkanes near melting points", *Angew. Chem. Int. Ed.* 55(45), 14090 (2016)
3. J. Mirth, Y. Zhai, J. Bush, E. G. Alvarado, H. Jordan, M. Heim, B. Krishnamoorthy, M. Pflaum, A. Clark, **Y Z***, H. Adams, "Representations of energy landscapes by sublevelset persistent homology: an example with n-alkanes", *J. Chem. Phys.* 154, 114114 (2021)

Publications

1. S.-C. Lee, **Y Z***, "Interpretation of autoencoder-learned collective variables using Morse-Smale complex and sublevelset persistence homology: an application on molecular trajectories", submitted to *Phys. Rev. Lett.*
2. C. Do, R. Ashkar, C. Boone, W.-R. Chen, G. Ehlers, P. Falus, A. Faraone, J. Gardner, V. Graves, T. Huegle, R. Katsumata, D. Kent, J. Lin, W. McHargue, B. Olsen, Y. Wang, D. Wilson, Y Z, "EXPANSE: a time-of-flight expanded angle neutron spin echo spectrometer at the second target station of the spallation neutron source", *Rev. Sci. Instrum.* 93, 075107 (2022)
3. G. Sala, M. Mourigal, C. Boone, N. Butch, A. Christianson, O. Delaire, A. DeSantis, C. Hart, R. P. Hermann, T. Huegle, D. Kent, J. Lin, M. Lumsden, M. Manley, D. Quirinale, M. Stone, Y Z, "CHESS: the future direct geometry spectrometer at the second target station", *Rev. Sci. Instrum. 93, 065109* (2022)
4. P. Luo, Y. Zhai, P. Falus, V. Garcia-Sakai, M. Hartl, M. Kofu, K. Nakajima, A. Faraone, **Y Z*,** "Q-dependent collective relaxation dynamics of glass-forming liquid $Ca_{0.4}K_{0.6}(NO_3)_{1.4}$ investigated by wide-angle neutron spin-echo", *Nature Commun.* 13, 2092 (2022)
5. Y. Zhai, P. Luo, J. Waller, J. L. Self, L. W. Harriger, **Y Z*,** A. Faraone, "Dynamics of molecular associates in methanol/water mixtures", *Phys. Chem. Chem. Phys.* 24, 2287 (2022)

Author Index

Banerjee, Arnab, 15
Bates, Frank S., 133
Billinge, Simon J. L., 20
Birol, Turan, 22, 28, 32, 83, 255
Bockstaller, Michael R., 36
Broholm, Collin, 41
Cheong, Sang-Wook, 42
Chmaissem, Omar, 187
Choi, Joshua J., 112
Christianson, Andrew, 47
Dai, Pengcheng, 52
Delaire, Olivier, 57, 60
Eskildsen, Morten, 64
Fernandes, Rafael, 22, 28, 32, 83
Foston, Marcus, 197
Frandsen, Benjamin, 69
Fultz, Brent, 73
Gilbert, Dustin, 78
Greven, Martin, 8, 22, 28, 32, 83, 87, 173, 255
Gu, Genda, 217
Gu, Xiaodan, 92
Haravifard, Sara, 97
Helgeson, Matthew, 98
Hermann, R. P., 103, 106, 107, 250
Karim, Alamgir, 36
Ke, Xianglin, 108
Kiryukhin, Valery, 42
Lee, Seung-Hun, 112
Lee, Young, 115
Leighton, Chris, 8, 22, 28, 32, 83, 87, 255
Li, Chen, 118
Li, Mingda, 123, 128
Lodge, Timothy P., 133
Louca, Despina, 138
Luo, Jingwen, 197
Manley, 103, 107
Matyjaszewski, Krzysztof, 36
May, Steven, 144
McChesney, Jessica, 183
Mondal, Snehasish, 197
Moulé, Adam, 148
Mourigal, Martin, 152
Nakatsuji, Satoru, 41
Narani, Anand, 197
Olsen, Bradley D., 157
Osborn, Raymond, 187
Phelan, Daniel, 187
Pingali, Sai Venkatesh, 197
Pitenis, Angela, 162
Plumb, Kemp, 163
Pozzo, Lilo D., 166
Reznik, Dmitry, 170
Richards, Jeffrey J., 174
Rodriguez, Efrain E., 180
Rosenkranz, Stephan, 183, 187
Schneider, Gerald J., 192
Senanayake, Manjula, 197
Singh, Deepak Kumar, 202
Sirenko, Andrei, 42
Smith, Hillary, 206
Sokol, Paul, 210
Sun, Chengjun, 183
Swan, James, 213
Tranquada, John M., 217
Vashishta, Priya, 222
Vohra, Yogesh K., 228
Wilson, Stephen D., 232
Xie, Weiwei, 237
Yang, Junjie, 242
Zaliznyak, Igor A., 217
Zhang, Jialiang, 197
Zhang, Yang, 247

Participant List

Name	Organization	Email
Jared Allred	The University of Alabama	jmallred@ua.edu
Arnab Banerjee	Purdue University	arnabb@purdue.edu
Kipton Barros	Los Alamos National Laboratory	kbarros@lanl.gov
Frank Bates	University of Minnesota	bates001@umn.edu
Cristian Batista	University of Tennessee	cbatist2@utk.edu
Simon Billinge	Columbia University	sb2896@columbia.edu
Turan Birol	University of Minnesota	tbirol@umn.edu
Michael Bockstaller	Carnegie Mellon University	bockstaller@cmu.edu
Collin Broholm	Johns Hopkins University	broholm@jhu.edu
Katherine Brown	U. S. Department of Energy	katherine.brown@science.doe.gov
Claudia Cantoni	U. S. Department of Energy	claudia.cantoni@science.doe.gov
Andrew Christianson	Oak Ridge National Laboratory	christiansad@ornl.gov
Pengcheng Dai	Rice University	pdai@rice.edu
Adrian Del Maestro	University of Tennessee, Knoxville	Adrian.DelMaestro@utk.edu
Olivier Delaire	Duke University	olivier.delaire@duke.edu
Morten Eskildsen	University of Notre Dame	eskildsen@nd.edu
Michael Fitzsimmons	U. S. Department of Energy	michael.fitzsimmons@science.doe.gov
Marcus Foston	Washington University in St. Louis	mfoston@wustl.edu
Benjamin Frandsen	Brigham Young University	benfrandsen@byu.edu
Brent Fultz	California Institute of Technology	btf@caltech.edu
Dustin Gilbert	University of Tennessee	dagilbert@utk.edu
Martin Greven	University of Minnesota	greven@umn.edu
Xiaodan Gu	University of Southern Mississippi	xiaodan.gu@usm.edu
Sara Haravifard	Duke University	sara.haravifard@duke.edu
Matthew Helgeson	University of California, Santa Barbara	helgeson@ucsb.edu
Raphael Hermann	Oak Ridge National Laboratory	hermannrp@ornl.gov
Ronald Jones	National Institute of Standards and Technology	ronald.jones@nist.gov
Alamgir Karim	University of Houston	akarim4@uh.edu
Xianglin Ke	Michigan State University	kexiangl@msu.edu
Helen Kerch	U. S. Department of Energy	helen.kerch@science.doe.gov
Valery Kiryukhin	Rutgers University	vkir@physics.rutgers.edu
Seunghun Lee	University of Virginia	shlee@virginia.edu
Young Lee	Stanford University	youngsl@stanford.edu
Chris Leighton	University of Minnesota	leighton@umn.edu
Mingda Li	Massachusetts Institute of Technology	mingda@mit.edu
Chen Li	University of California, Riverside	chenli@ucr.edu
Timothy Lodge	University of Minnesota	lodge@umn.edu
Despina Louca	University of Virginia	louca@virginia.edu
Michael Manley	Oak Ridge National Laboratory	manleyme@ornl.gov
Andrew May	Oak Ridge National Laboratory	mayaf@ornl.gov
Steven May	Drexel University	smay@drexel.edu
Tim Mewes	U. S. Department of Energy	tim.mewes@science.doe.gov
Claudia Mewes	U. S. Department of Energy	claudia.mewes@science.doe.gov
Adam Moule	University of California, Davis	amoule@ucdavis.edu
Martin Mourigal	Georgia Institute of Technology	mourigal@gatech.edu
Bradley Olsen	Massachusetts Institute of Technology	bdolsen@mit.edu
Raymond Osborn	Argonne National Laboratory	rosborn@anl.gov
Michael (Mick) Pechan	U. S. Department of Energy	michael.pechan@science.doe.gov
Daniel Phelan	Argonne National Laboratory	dphelan@anl.gov
Angela Pitenis	University of California, Santa Barbara	apitenis@ucsb.edu
Kemp Plumb	Brown University	kemp_plumb@brown.edu
Lilo Pozzo	University of Washington	dpozzo@uw.edu
William Ratcliff	National Institute of Standards and Technology	william.ratcliff@nist.gov

Dmitry Reznik	University of Colorado, Boulder	dmitry.reznik@colorado.edu
Jeffrey Richards	Northwestern University	jeffrey.richards@northwestern.edu
Efrain Rodriguez	University of Maryland	efrain@umd.edu
Stephan Rosenkranz	Argonne National Laboratory	srosenkranz@anl.gov
Paul Sammak	U. S. Department of Energy	paul.sammak@science.doe.gov
Gerald Schneider	Louisiana State University	gjschneider@lsu.edu
Viviane Schwartz	U. S. Department of Energy	viviane.schwartz@science.doe.gov
Andrew Schwartz	U. S. Department of Energy	andrew.schwartz@science.doe.gov
Athena Sefat	U. S. Department of Energy	athena.sefat@science.doe.gov
Manjula Senanayake	Washington University in St. Louis	manju@wustl.edu
Deepak Singh	University of Missouri, Columbia	singhdk@missouri.edu
Andrei Sirenko	New Jersey Institute of Technology	sirenko@njit.edu
Hillary Smith	Swarthmore College	hsmith3@swarthmore.edu
Paul Sokol	Indiana University	pesonol@indiana.edu
Jonathan Taylor	Oak Ridge National Laboratory	taylorjw@ornl.gov
William Tisdale	Massachusetts Institute of Technology	tisdale@mit.edu
John Tranquada	Brookhaven National Laboratory	jtran@bnl.gov
Patrick Underhill	Rensselaer Polytechnic Institute	underp3@rpi.edu
Priya Vashishta	University of Southern California	priyav@usc.edu
Yogesh Vohra	University of Alabama, Birmingham	ykvohra@uab.edu
Jiajia Wen	SLAC National Accelerator Laboratory	jwen11@stanford.edu
Stephen Wilson	University of California, Santa Barbara	stephendwilson@ucsb.edu
Lane Wilson	U. S. Department of Energy	lane.wilson@science.doe.gov
Weiwei Xie	Michigan State University	xieweiwe@msu.edu
Zhewei Xie	Massachusetts Institute of Technology	oxie@mit.edu
Junjie Yang	New Jersey Institute of Technology	jyang@njit.edu
Igor Zaliznyak	Brookhaven National Laboratory	zaliznyak@bnl.gov
Yang Zhang	University of Michigan	yzyz@umich.edu
Mikhail Zhernenkov	U. S. Department of Energy	mikhail.zhernenkov@science.doe.gov